High-Resolution Direction Finding in Multi-Dimensional Scenarios

by

Jacek Jachner

Bachelor of Engineering, McGill University (1981)
Master of Science, Massachusetts Institute of Technology (1983)

Submitted to the
Department of Electrical Engineering and Computer Science
in partial fulfillment of the requirements for the degree of

Doctor of Science

at the

MASSACHUSETTS INSTITUTE OF TECHNOLOGY

September 1993

Author _____
Department of Electrical Engineering and Computer Science
September 1, 1993

Certified by _____
Harry B. Lee
Atlantic Aerospace Electronics Corporation
Thesis Supervisor

Certified by _____
Alan V. Oppenheim
Professor, Department of Electrical Engineering and Computer Science
Thesis Supervisor

Accepted by _____
Frederic R. Morgenthaler
Chairman, Department Committee on Graduate Students

High-Resolution Direction Finding in Multi-Dimensional Scenarios

by

Jacek Jachner

Submitted to the Department of Electrical Engineering and Computer Science
on September 1, 1993, in partial fulfillment of the
requirements for the degree of
Doctor of Science

Abstract

There has been strong recent interest in high resolution techniques for reliably resolving closely-spaced sources and estimating their directions. The performance of candidate techniques has, until recently, been assessed empirically in most publications. Several recent contributions have facilitated analytical performance assessment for scenarios with a single unknown direction parameter for each source (1-D). However, many practical geolocation applications require estimating multiple position-location parameters for each source (e.g. azimuth, elevation and possibly range). This thesis generalizes many of the 1-D results to scenarios with multiple parameters (multi-D).

The main results of the thesis are analytical expressions, valid for closely spaced sources in multi-D scenarios, for the eigenstructure of the data covariance matrix, for the singular value decomposition of its matrix factor, for the Cramér Rao lower bound on directional variance, and for detection and resolution thresholds. The expressions make explicit the impact of scenario parameters such as maximum source separation, source configuration, source powers and correlations, and sensor array geometry.

The multi-D results herein in some ways parallel the prior 1-D results, but also differ in interesting and significant ways. For a given number of closely-spaced sources, we find for multi-D scenarios, in relation to 1-D scenarios, that 1) the direction finding (DF) problem is much better conditioned, 2) the Cramér Rao variance lower bounds are much lower, and 3) the source detection and resolution problems are easier.

The thesis provides an analytical framework for the direction finding problem in multi-D scenarios, which should facilitate the assessment of candidate DF techniques, help quantify the numerical-accuracy and hardware-alignment issues associated with implementing high-resolution techniques, facilitate beamformer design and provide insight helpful to the development of improved DF algorithms for multi-D scenarios.

Thesis Supervisor: Harry B. Lee
Title: Atlantic Aerospace Electronics Corporation

Thesis Supervisor: Alan V. Oppenheim
Title: Professor, Department of Electrical Engineering and Computer Science

Acknowledgements

I wish to thank my thesis supervisors, Dr. Harry Lee and Prof. Alan Oppenheim for their support and encouragement in the course of my Doctoral studies. I am sincerely grateful to Al for providing the initial inputs to my studies, and for his guidance throughout my program. His constant support and commitment has contributed greatly to the success of my endeavour.

I would like to express my deep appreciation to Harry for introducing me to the thesis topic, for his nurturing technical guidance and for his many insightful contributions. His intellectual abilities, uncompromising high standards, friendship and altruistic interest in my personal development, have contributed greatly to my life, and to this thesis. Recognizing a time of need, and giving generously the gifts of time, interest and compassion, Harry has fulfilled the full meaning of 'teacher' and 'mentor'. To his wife Barbara, always cheerful and welcoming, I am grateful for letting me share Harry's time during the long months spent reviewing this work, and the many late night technical discussions.

I would also like to thank Profs. Al Willsky and Art Baggeroer for serving as thesis readers, and for their stimulating technical comments which helped shape the development of this work.

My special thanks go to Marilyn Pierce at the EECS Graduate Office, for all her kind help and attention during my stay at MIT. I thank all the friends I made at the MIT Digital Signal Processing Group and at Atlantic Aerospace Electronics Corporation (AAEC), especially Dr. Michael Wengrovitz, whose stimulating energy and passionate dedication have been an inspiration. I gratefully recognize the financial support for this work provided by the Natural Sciences and Engineering Research Council (Canada), the Fonds FCAR (Quebec), Bell Northern Research and AAEC.

To my wife Donna, I express by deepest gratitude for bringing joy when it was most needed, support and encouragement throughout. I thank her for many interesting technical discussions, as our years together have often revolved around our educational pursuits in our shared career choice. She has brightened my life with her wonderfully eclectic qualities of beauty and elegance, kindness and humor, reason and technical

ability, and with her passionate love of all things living, including our companions Hook, Wuzzy and Rooda. I look forward with anticipation to share every day of the rest of our lives, to conquer new challenges, to attain new heights.

To Ben and Olga Fagen, I express my thanks for their affection, unwavering trust and support in my long quest, and for their most precious gift of all, their daughter Donna.

I also thank my large extended family, grandmother Teresa and aunt Urszula in particular, for all their kind thoughts, wishes and prayers of encouragement.

Finally, I express my heartfelt thanks to my mother Jadwiga, for her selfless love and dedication to her sons in the face of a difficult life, for inspiring the dream and setting my sights on the highest mountain. Her university studies, began at life threatening risk at the underground Warsaw Polytechnic during the war, were concluded as the first woman engineer to graduate at the Université de Louvain. I now echo her celebratory graduation telegram to her mother, and send "Zdobyłem Szczyt".

Contents

List of Figures

Chapter 1

Introduction

Determining the direction of propagating signals incident upon a sensor array, in the challenging case when the separation between signal sources is small, has been a topic of strong interest over the last two decades. Numerous *High Resolution* direction finding techniques have been proposed with the purpose of reliably resolving closely-spaced sources and estimating their directions [1]-[5]. The performance of the candidate techniques in terms of bias, variance, detection and resolution thresholds has, until recently, been assessed only empirically [4], [6]-[8]. Such empirical assessment is not entirely satisfactory since it is scenario dependent and does not provide insight into fundamental performance limitations.

Several recent contributions have facilitated analytical performance assessment for closely-spaced sources, and made explicit the impact upon performance of scenario parameters such as sensor array geometry, source configuration, source powers and correlations, and maximum source separation $\delta\omega$. Available analytical results for closely-spaced sources include estimator bias and variance expressions for specific direction finding (DF) algorithms [9], [10], Cramér Rao bound expressions for the minimum directional variance attainable with any unbiased algorithm [11], eigenstructure expressions for the data covariance matrix that is central to DF algorithms [12], and expressions for the detection and resolution thresholds [13]. These analytical formulations have generally been obtained for scenarios with a single unknown direction parameter for each source (1-D scenarios). Many practical direction finding

applications involve two or more unknown direction parameters for each source (e.g. azimuth, elevation, and in some applications also range). Corresponding analytical results for multi-D scenarios are not currently available.

The purpose of this thesis is to generalize many of the analytical results recently developed for 1-D direction finding scenarios to multi-D scenarios. Thesis results for closely-spaced sources in multi-D include expressions for the eigenstructure of the data covariance matrix, for the Cramér Rao lower bound on directional variance, and for the detection and resolution thresholds. The multi-D results developed herein in some ways parallel the prior 1-D results, but also differ from the 1-D results in interesting and significant ways. For a given number of closely-spaced sources, we find for multi-D scenarios, in relation to 1-D scenarios, that 1) the DF problem is much better conditioned, 2) the Cramér Rao variance lower bounds are much lower, and 3) the source detection and resolution problems are easier.

1.1 Recent Developments in Spatial Spectrum Estimation

Many of the techniques proposed for estimating the direction of closely-spaced sources were originally proposed for estimating the frequency spectrum of time series. Since sampling of a function in time is analogous to sampling of a function in space, estimating the frequency of sinusoids in noise is similar to estimating the direction of plane waves in noise. It is at times convenient to represent the unknown plane wave direction as a *spatial frequency* ω for 1-D scenarios, or as *spatial frequency vector* $\vec{\omega}$ for multi-D scenarios. The following discussion reviews recent developments in spectrum estimation in the context of estimating spatial frequency vector $\vec{\omega}$ [7], [8].

In a typical direction finding scenario, an array of sensors observes signals propagating from a number of sources. The sensor array is characterized by the *generic arrival vector* $\vec{a}(\vec{\omega})$, which is the ideal (noise-free) array response to a unit amplitude, zero phase signal with spatial frequency $\vec{\omega}$. It is assumed that $\vec{a}(\vec{\omega})$ is known for all $\vec{\omega}$. The function $\vec{a}(\vec{\omega})$ sometimes is called the *array manifold.*

The sensor array data typically consists of N snapshot vectors $\vec{y}(t)$, where the i^{th} element $y_i(t)$ denotes the output of the i^{th} sensor at sampling time t, with $t = 1, \cdots N$. The data is assumed to be a linear combination of generic arrival vectors for each of the sources present, scaled by the respective signal amplitude, with additive noise. Specifically, the data model addressed in this thesis is of the form

$$\vec{y}(t) = \sum_{j=1}^{M} \vec{a}(\vec{\omega}_j) x_j(t) + \vec{\epsilon}(t) \tag{1.1}$$

where $\vec{\omega}_1 \cdots \vec{\omega}_M$ denote the (unknown) source spatial frequencies for each of M sources present, $x_j(t)$ denotes the complex amplitude of the j^{th} source, and $\vec{\epsilon}(t)$ is a vector of additive, uncorrelated white noise (e.g. sensor noise). The (spatial) frequency estimation problem is to identify the $\vec{\omega}_1$, $\cdots$ $\vec{\omega}_M$ from the snapshot vectors $\vec{y}(1)$, $\cdots$ $\vec{y}(N)$ and the known array manifold $\vec{a}(\vec{\omega})$.

To obtain the benefits of averaging, most practical spectral estimation algorithms average outer products of the snapshot vectors to compute a *sample data covariance matrix* $\hat{R}$. For large data sets (as $N \rightarrow \infty$), the sample data covariance matrix converges with probability one to the *asymptotic data covariance matrix* R. That is

$$\hat{R} \triangleq \frac{1}{N} \sum_{t=1}^{N} \vec{y}(t) \vec{y}(t)^h \tag{1.2}$$

$$R \triangleq E\{\vec{y}(t) \vec{y}(t)^h\} \tag{1.3}$$

and

$$\lim_{N \rightarrow \infty} \hat{R} = R \tag{1.4}$$

To obtain spatial frequency estimates, the sample data covariance $\hat{R}$ is transformed to generate a non-negative spectrum function $S(\vec{\omega})$. The domain of this function is the set of all possible spatial frequencies $\vec{\omega}$; the values of $\vec{\omega}$ at spectrum peaks (maxima) are interpreted as estimates of source spatial frequencies.

Table 1.1 lists the spectrum functions $S(\vec{\omega})$ used by a number of popular algo-

Spectral Estimation Algorithm	Spectrum Function
Conventional Beamscan	$S_{CBS}(\vec{\omega}) = \frac{\vec{a}(\vec{\omega})^h \hat{R} \vec{a}(\vec{\omega})}{\vec{a}(\vec{\omega})^h \vec{a}(\vec{\omega})}$
Maximum Entropy Method	$S_{MEM}(\vec{\omega}) = \frac{\text{constant}}{\left\| \vec{a}(\vec{\omega})^h \, (\hat{R}^{-1})_{\text{first column}} \right\|^2}$
Maximum Likelihood Method	$S_{MLM}(\vec{\omega}) = \frac{\vec{a}(\vec{\omega})^h \vec{a}(\vec{\omega})}{\vec{a}(\vec{\omega})^h \, \hat{R}^{-1} \, \vec{a}(\vec{\omega})}$
MUSIC	$S_{MUSIC}(\vec{\omega}) = \frac{\vec{a}(\vec{\omega})^h \vec{a}(\vec{\omega})}{\vec{a}(\vec{\omega})^h \, \hat{E}_N \hat{E}_N^h \, \vec{a}(\vec{\omega})}$
MinNorm	$S_{MinNorm}(\vec{\omega}) = \frac{\vec{a}(\vec{\omega})^h \vec{a}(\vec{\omega})}{\vec{a}(\vec{\omega})^h \, \hat{E}_N \vec{t} \, \vec{t}^h \hat{E}_N^h \, \vec{a}(\vec{\omega})}$

$\hat{E}_N$ = columns of $\hat{E}_N$ are selected (noise-space) eigenvectors of $\hat{R}$

$\vec{t}$ = selected to minimize the norm of $\vec{t}^h \hat{E}^h \hat{E}_N \vec{t}$ subject to first element of $\hat{E}_N \vec{t}$ being equal to 1

Table 1.1: Spectrum Functions of Representative Spectrum Estimation Techniques

rithms. In each case, the algorithm operates on the covariance matrix $\hat{R}$ with the generic arrival vector $\vec{a}(\vec{\omega})$ to generate the spectral value for direction $\vec{\omega}$.

The Conventional Beamscan (CBS) method is the classic direction finding algorithm and actually provides the best possible estimate of the spatial frequency $\vec{\omega}$ of a single source received in the presence of (spatially) white noise [7]. Unfortunately, the CBS method is not optimal in the presence of multiple sources, and breaks down completely if two or more sources are closely-spaced.

The CBS method is analogous to classical time-series matched-filtering, (and also

analogous to Fourier spectral analysis of time series). The value of spectrum $S_{CBS}(\vec{\omega})$ is large when the vector $\vec{a}(\vec{\omega})$ equals one signal component $\vec{a}(\vec{\omega}_j)$ (i.e. when $\vec{\omega}$ equals the spatial frequency vector of one of the sources). For a scenario with a single source at $\vec{\omega}_1$ and spatially white noise, the value of $\vec{\omega}$ at the peak of the $S_{CBS}(\vec{\omega})$ spectrum is an optimum, unbiased estimator of $\vec{\omega}_1$. For large data sets ($\hat{R} \rightarrow R$), the peak of the $S_{CBS}(\vec{\omega})$ spectrum is exactly at $\vec{\omega}_1$. The width of the $S_{CBS}(\vec{\omega})$ peak is independent of the data set size N; the width as measured between the 3 dB attenuation points is commonly designated as the *Rayleigh beamwidth.*

For scenarios with more than one source, the $S_{CBS}(\vec{\omega})$ spectrum consists of the sum of individual spectra of each of the sources. As a consequence, the spectral peak frequencies in scenarios with multiple sources may not have means equal to the source locations $\vec{\omega}_j$, not even as $\hat{R} \rightarrow R$; thus the CBS estimator is *biased.* Furthermore if two sources are spaced closer than one Rayleigh beamwidth, the $S_{CBS}(\vec{\omega})$ spectrum typically exhibits only one peak (in the vicinity of the two source spatial frequencies). Therefore the CBS method typically does not resolve sources separated by less that one Rayleigh beamwidth.

A large number of DF techniques has been developed in the past two decades to overcome the resolution limitations of Conventional Beamscan. These so-called *High Resolution* techniques can resolve sources with spacing less than the Rayleigh beamwidth given favorable conditions (e.g. large data set ($N \rightarrow \infty$), high signal-to-noise ratio (SNR), accurate array calibration, etc.)

Early High Resolution DF techniques were based upon classical methods of spectrum estimation, but made no use of any information about the underlying propagating signal process. Representative early High Resolution techniques include Maximum Entropy Method (MEM) attributed to Burg [1] and the Maximum Likelihood Method (MLM) technique attributed to Capon [2] with spectrum functions $S_{MEM}(\vec{\omega})$ and $S_{MLM}(\vec{\omega})$ as in Table 1.1. Under favorable conditions, these spectral estimators resolve sources within a Rayleigh beamwidth, but the direction estimates (the spectral peak locations) obtained with these methods typically are biased even for large data sets (as $\hat{R} \rightarrow R$).

Over the last decade a new class of High Resolution techniques has been introduced, including MinNorm [3], [4], MUSIC [5] and related *Eigenvector* techniques based upon the eigenanalysis of the covariance matrix $\hat{R}$. For large data sets ($\hat{R} \rightarrow R$), subject to data model assumptions, MinNorm and MUSIC provide asymptotically unbiased estimates of the source spatial frequencies regardless of signal-to-noise ratios and frequency separation of the sources.

In contrast to classical spectral methods, eigenvector techniques assume (require) that the direction finding scenario consist of spatially discrete signal sources, that the number of sources be less than the number of sensors, and that the noise be uncorrelated and white (or pre-whitened). Under these conditions, the covariance matrices $\hat{R}$, R can be decomposed into orthogonal "signal" and "noise" vector subspaces. Eigenvector direction finding techniques exploit the property that the generic arrival vectors $\vec{a}(\vec{\omega}_1), \cdots, \vec{a}(\vec{\omega}_M)$ for each of the sources lie within the "signal" vector subspace of the asymptotic covariance matrix R, and therefore are perpendicular to the corresponding "noise" vector subspace. The denominators of the spectrum functions $S_{MUSIC}(\vec{\omega})$ and $S_{MinNorm}(\vec{\omega})$ in Table 1.1 involve the projection of $\vec{a}(\vec{\omega})$ onto vectors in the noise subspace of $\hat{R}$. Whenever $\vec{\omega}$ equals a source spatial frequency, the denominator tends to zero as $\hat{R} \rightarrow R$, and therefore the spectrum functions peaks are asymptotically unbiased estimators of source spatial frequency.

1.2 Closely-Spaced Sources

The performance of High Resolution direction finding techniques is roughly comparable when sources are well separated. Performance differences become evident in the stressful case when sources are closely-spaced. Therefore the ability of a High Resolution technique to resolve closely-spaced sources, and to accurately estimate their parameters, has become a standard test in the literature of the "power" of the technique.

The spatial spectra of the Maximum Entropy and of the Maximum Likelihood estimation algorithms depend upon the inverse of sample covariance matrix $\hat{R}$; the

spectra of the so-called eigenvector techniques such as MinNorm and MUSIC depend upon selected eigenvectors of $\hat{R}$. (See Table 1.1). Therefore the performance of these algorithms depends strongly on the eigenstructure of matrix $\hat{R}$. Under the data model assumptions, the sample covariance matrix $\hat{R}$ converges with probability one for large data sets (as $N \rightarrow \infty$) to the asymptotic form

$$R = R_S + \sigma^2 I \tag{1.5}$$

where matrix term R_S reflects the spatial covariance contribution due to the incident signals, and $\sigma^2 I$ reflects the additive, uncorrelated and spatially white sensor noise. For closely spaced sources, signal covariance matrix R_S is ill-conditioned with the result that direction estimates are very sensitive to hardware errors and finite data sets.

Analytical expressions for the eigenstructure of the sample covariance matrix $\hat{R}$, if available, would facilitate the analysis of the statistical properties of the directional spectra of Table 1.1, and hence facilitate performance analysis of the candidate DF algorithms for closely-spaced sources. The eigenstructure of the sample covariance matrix $\hat{R}$ can be expressed in terms of the eigenstructure of the asymptotic covariance matrix R using classical perturbation theory results [9], [19]. Thus the eigenstructure of $\hat{R}$ can be determined if the eigenstructure of R is available. The eigenstructure of R is straightforwardly related to that of the signal component R_S of (1.5). Thus the eigenstructure problem for closely-spaced sources is essentially that of identifying the eigenstructure of asymptotic signal covariance component R_S.

Direct analytical expressions for the eigenvalues and eigenvectors of R_S are not available for general scenarios with more than 1 or 2 sources, due to the difficulty in explicitly solving the polynomial characteristic equation of order greater than 2. Thus, until recently, assessment of High Resolution estimator performance in terms of bias, variance and resolution threshold has been largely empirical [4], [6], [7]. Such empirical assessments leave unanswered important design questions; specifically they

- are scenario dependent,

- do not establish fundamental performance limitations.

A recent contribution by Lee [12] developed an approach that facilitates analytical identification of the eigenstructure of R_S for closely spaced sources in scenarios with a single unknown direction parameter for each source (1-D scenarios). The results are summarized in the next section.

Another useful tool for performance analysis is the Cramér Rao (CR) bound. The CR bound provides a lower bound upon the variance achievable by any unbiased estimator [20]. Therefore the CR bound is commonly used as a yardstick to measure the directional accuracy of candidate DF algorithms. Analytical expressions for the CR bound applicable to DF scenarios, if available, would indicate whether existing High Resolution techniques are near-optimum, and potentially lead to new techniques which remedy any identified shortcomings.

Development of analytical results for the covariance matrix eigenstructure and the CR bound for closely-spaced sources has been a recent focus of interest [9]-[14]. The work reported thus far has been for 1-D scenarios. The results are summarized below.

1.3 Available Analytical Results (1-D)

An important early contribution by Kaveh and Barabell [9] analyzed the statistical properties of the MUSIC and MinNorm algorithms. Using a first order approximation of the MUSIC spectral bias, the authors determine an expression for the minimum (threshold) signal-to-noise ratio (SNR) at which MUSIC is able to reliably resolve two closely-spaced equal-power uncorrelated sources observed by a uniform linear array.

Lee and Wengrovitz [10], [14] extended these results to arbitrary arrays, to beam-space pre-processing, and to two (possibly) correlated sources of (possibly) unequal powers. The authors also identified the beamforming pre-processor which minimizes the MUSIC resolution threshold.

Lee [12] derived explicit expressions for the eigenstructure of asymptotic signal covariance R_S in (1.5) for the problem of M closely-spaced sources in 1-D scenarios. The author showed that for closely-spaced sources, the eigenstructure of R_S decomposes

so that eigenvalues and eigenvectors can be determined by straightforward linear algebra operations, without eigenanalysis. Specifically, if the number of sources M is less than the number of sensors, and if we denote the maximum source separation as $\delta\omega$, the ordered non-zero eigenvalues of R_S as $\lambda_1(\delta\omega) \geq \cdots \geq \lambda_M(\delta\omega)$, and the associated eigenvectors as $\vec{e}_i(\delta\omega)$, $i = 1, \cdots M$, then example results of [12] are

1) Non-zero eigenvalues $\lambda_i(\delta\omega)$ of R_S converge as $\delta\omega \rightarrow 0$ to limiting eigenvalues $\lambda_i \delta\omega^{2(i-1)}$, where λ_i are positive constants and $i = 1, \cdots M$.

2) Eigenvectors $\vec{e}_i(\delta\omega)$ of R_S converge as $\delta\omega \rightarrow 0$ to constant vectors $\vec{e}_i$, corresponding to the generic arrival vector $\vec{a}(\omega)$ and its derivatives, suitably orthonormalized.

3) Limiting condition number of R_S is $\frac{\lambda_1}{\lambda_M}\delta\omega^{-2(M-1)}$.

4) Remarkably, the quantities λ_i and $\vec{e}_i$ are calculable via linear algebra operations; solving a characteristic equation is not required.

Thus for closely spaced sources in 1-D, the eigenanalysis of R_S decomposes completely into explicit expressions for each eigenvalue and eigenvector.

Lee and Li [13] addressed the problem of detecting the number of sources in a cluster of M closely-spaced sources. Using the foregoing eigenvalue results, they argued that the SNR threshold $\mathcal{E}_D$ at which so-called Normal Algorithms can reliably estimate the number of sources in 1-D scenarios is proportional to $\delta\omega^{-2(M-1)}$. That is

$$\mathcal{E}_D \simeq \frac{K_D}{\delta\omega^{2(M-1)}} \tag{1.6}$$

where K_D is a suitable constant.

Lee [11] extended general results on the CR bound due to Stoica and Nehorai [15] to the case of closely-spaced sources. Explicit formulae for the CR lower bound on the variance of unbiased (1-D) spatial frequency estimates were derived for closely-spaced sources. The variance bound on the spatial frequency estimate $\hat{\omega}_j$ for the j^{th} source

was found to be

$$\mathrm{Var}\{\widehat{\omega}_j\} \;\geq\; \frac{1}{N \cdot \mathrm{SNR}_j} \frac{b_j}{\delta\omega^{2(M-1)}} + \mathcal{O}(\delta\omega^{-2(M-1)+1}) \tag{1.7}$$

for small frequency separation $\delta\omega$, where N denotes the data set size, SNR_j the signal-to-noise ratio for the j^{th} source, M the number of sources, and b_j is a suitable constant that depends upon the other scenario parameters of sensor array geometry, source configuration, source powers and correlations. Lee used these results to argue that the SNR resolution threshold $\mathcal{E}_R$ for any unbiased estimator in 1-D scenarios is proportional to $\frac{1}{N}\delta\omega^{-2M}$. That is

$$\mathcal{E}_R \;\simeq\; \frac{K_R}{N \cdot \delta\omega^{2M}} \tag{1.8}$$

where K_R is a suitable constant.

Results of the form (1.6)-(1.8) are quite useful in that they make explicit the dependence of performance metrics $\mathcal{E}_D$, $\mathrm{Var}\{\widehat{\omega}_j\}$ and $\mathcal{E}_R$ upon the source separation factor $\delta\omega$. For example, Eq. (1.8) indicates for a 1-D scenario with $M = 3$ sources that reducing $\delta\omega$ by a factor of 10 *increases the resolution threshold SNR by 60 dB for any sensor array and relative source configuration.*

1.4 Thesis Objective

The purpose of this thesis is to generalize many of the foregoing results for 1-D direction finding scenarios to multi-D scenarios. The two principal issues addressed in the thesis are 1) the eigenstructure of the asymptotic signal covariance matrix R_S, and 2) the Cramér Rao bound on spectral estimate variance, for closely-spaced sources in multi-D. Major results include the following.

Building upon the work of Lee [12] for 1-D scenarios, analytical expressions are developed that facilitate identification of R_S eigenstructure for M closely-spaced sources in multi-D scenarios. The approach used herein differs from that used by Lee for 1-D

scenarios [12] in that covariance matrix R_S is factored as

$$R_S = BB^h \tag{1.9}$$

where rectangular matrix B has Taylor series in source separation parameter $\delta\omega$. The thesis identifies explicit expressions for the small $\delta\omega$ Singular Value Decomposition (SVD) of the rectangular matrix B, building upon classical eigenstructure results of Kato [17] and Coderch, Willsky, Sastry, and Castanon [18]. The eigenstructure of R_S for small $\delta\omega$ then follows immediately from (1.9). The SVD results are not only important enabling tools for the multi-D eigenstructure problem, but also may themselves constitute important results for other applications.

The properties of R_S eigenstructure for multi-D scenarios identified herein often parallel those for 1-D scenarios, but also diverge in interesting and significant ways. Example thesis results for non-degenerate multi-D scenarios with M closely-spaced sources are

1) Non-zero eigenvalues $\lambda_i(\delta\omega)$ of R_S converge as $\delta\omega \rightarrow 0$ to limiting eigenvalues $\lambda_i\, \delta\omega^{2k_i}$, where λ_i are positive constants, and $k_i \in \{0, \cdots m\}$, for all $i = 1, \cdots M$ and with $m < M - 1$. Typically there are multiple limiting eigenvalues proportional to $\delta\omega^{2k}$ for each $k = 0, \cdots m$; the group of limiting eigenvalues proportional to $\delta\omega^{2k}$ is designated as the k^{th} *eigenvalue shell.*

2) Eigenvectors $\vec{e}_i(\delta\omega)$ of R_S associated with each eigenvalue shell converge as $\delta\omega \rightarrow 0$ to constant limiting subspaces spanned by the generic arrival vector and its partial derivatives, suitably orthonormalized.

3) Limiting condition number of R_S is $\frac{\lambda_1}{\lambda_M}\delta\omega^{-2m}$. Thus parameter m determines condition number sensitivity to maximum source spacing $\delta\omega$.

4) Eigenvalues of R_S that exhibit the behavior $\lambda_i\delta\omega^{2k}$ as $\delta\omega \rightarrow 0$, have as multipliers λ_i the non-zero eigenvalues of a constant low-rank matrix $R_{2k,0}$. Furthermore as $\delta\omega \rightarrow 0$, the associated eigenvectors of R_S span the column space of $R_{2k,0}$.

Matrix $R_{2k,0}$ is independent of $\delta\omega$, and is straightforwardly calculable via linear algebra operations.

Thus in multi-D, the eigenanalysis of R_S decomposes into a sequence of much simpler shell problems; the k^{th} shell problem involves eigenanalysis of the constant low-rank matrix $R_{2k,0}$. Nevertheless, eigenanalysis is not required to determine the span of limiting eigenvectors associated with each $R_{2k,0}$, nor to determine conditioning sensitivity parameter m. For 1-D scenarios, $k_i = i-1$, $m = M-1$ and matrices $R_{2k,0}$ have rank 1, whereupon thesis results simplify to those of [12]. For non-degenerate multi-D scenarios, typically $m < M-1$, and thus R_S conditioning for small $\delta\omega$ is much improved relative to 1-D settings.

A major contribution of the thesis is to identify simple explicit expressions for the matrices $R_{2k,0}$ for typical multi-D direction finding scenarios.

The eigenvalue results are used to extend the 1-D SNR detection threshold results of Lee and Li [13]. Based upon classical eigenstructure perturbation theory, the thesis argues that the minimum SNR at which any eigenvalue based detection algorithm can reliably estimate the number of sources in multi-D scenarios is proportional to $\delta\omega^{-2m}$. It is further argued that the minimum data set size N for reliable detection in multi-D scenarios is proportional to $\delta\omega^{-4m}$. That is

$$\mathcal{E}_D \simeq \frac{K'_D}{\sqrt{N}\cdot\delta\omega^{2m}} \tag{1.10}$$

$$\mathcal{N}_D \simeq \frac{(K'_D)^2}{(\mathrm{SNR})^2\cdot\delta\omega^{4m}} \tag{1.11}$$

for large N and small $\delta\omega$, where $\mathcal{E}_D$ denotes the SNR detection threshold, $\mathcal{N}_D$ the data set size N detection threshold, and K'_D is a suitable constant. Since typically $m < M-1$, we conclude from (1.6) and (1.10) that for small $\delta\omega$, the detection threshold SNR typically is much smaller (more favorable) in multi-D than in 1-D scenarios.

The second part of the thesis extends the general results on the CR bound in multi-D due to Yau and Bresler [16], to develop CR bound expressions for closely-spaced sources in multi-D which parallel those of Lee [11] in 1-D scenarios. For unbiased

estimators in typical multi-D scenarios, the variance bound on $\widehat{\omega}_{ij}$, the i^{th} component of spatial frequency vector $\vec{\omega}_j$ for the j^{th} source, is shown to satisfy

$$\mathrm{Var}\{\widehat{\omega}_{ij}\} \;\geq\; \frac{1}{N \cdot \mathrm{SNR}_j} \frac{b_{ij}}{\delta\omega^{2(\chi-1)}} + \mathcal{O}(\delta\omega^{-2(\chi-1)+1}) \tag{1.12}$$

for small frequency separation $\delta\omega$, where N denotes the data set size, SNR_j the signal-to-noise ratio for the j^{th} source, $\chi \in \{m, m+1\}$ depends only on the number of sources M and scenario dimensionality. The constants b_{ij} depend upon the other scenario parameters of sensor array geometry, source configuration, source powers and correlations. Significantly the value of χ in typical multi-D scenarios is less the number of sources M; therefore for a given number of sources, the CR variance bound typically is much smaller (more favorable) in multi-D than in 1-D scenarios.

Building upon the results of Lee in [11], the thesis uses the multi-D CR bound results to argue that the minimum SNR at which any unbiased estimator can reliably resolve M sources in multi-D scenarios is proportional to $\delta\omega^{-2\chi}$. It is further argued that the minimum data set size N for reliable detection in multi-D scenarios is also proportional to $\delta\omega^{-2\chi}$. That is

$$\mathcal{E}_R \;\simeq\; \frac{K'_R}{N \cdot \delta\omega^{2\chi}} \tag{1.13}$$

$$\mathcal{N}_R \;\simeq\; \frac{K'_R}{\mathrm{SNR} \cdot \delta\omega^{2\chi}} \tag{1.14}$$

for large N and small $\delta\omega$, where $\mathcal{E}_R$ denotes the SNR resolution threshold, $\mathcal{N}_R$ the data set size N resolution threshold, and K'_R is a suitable constant. Since typically $\chi < M$, we conclude from (1.8) and (1.13) that for small $\delta\omega$, the resolution threshold SNR typically is much smaller (more favorable) in multi-D than in 1-D scenarios.

Thesis analysis is facilitated by identification of structural conditions characteristic of a large class of DF scenarios, designated herein as *non-degenerate*. For such scenarios, the eigenstructure conditioning parameter m, and the CR bound parameter χ, are as small as possible for the given number of sources M. For *degenerate* scenarios the direction estimation problem typically becomes more difficult; that is,

the numerical conditioning of R_S typically degrades, the CR bound on directional variance typically increases, and the detection and resolution thresholds typically increase. Analysis leads to identification of sufficient conditions for non-degenerate scenarios, and identification of practically important sensor geometries and source configurations that result in degenerate scenarios.

1.5 Organization

The thesis is organized as follows.

The problem addressed in this thesis is detailed in Chapter 2, including the data model assumptions and notation conventions, the classical perturbation theory relation between $\hat{R}$ and R, and the prior CR bound expressions for 1-D and multi-D scenarios. The thesis analysis approach is introduced, as well as the example DF scenarios that are used in numerical simulations throughout the chapters to illustrate theoretical results.

Prior results on the eigenstructure of perturbed matrices are reviewed in Chapter 3, including the eigenstructure of R_S identified by Lee [12] for closely-spaced sources in 1-D scenarios, and the eigenstructure results of Kato [17] and Coderch et al. [18] for any perturbed Hermitian matrix.

New results on the singular value decomposition (SVD) of perturbed rectangular matrices are derived in Chapter 4, which extend the eigenstructure results of [17], [18]. A particularly simple formulation for the small perturbation SVD structure is developed for non-degenerate matrices that satisfy side conditions typically present in DF scenarios.

In Chapter 5, the eigenstructure of R_S for closely-spaced sources is identified from the SVD structure of its factor B. A reasonably complete characterization of the eigenstructure of R_S for small source separations is obtained for non-degenerate scenarios, including the limiting eigenvalues, the limiting eigenvectors, the limiting numerical conditioning and the limiting span of R_S.

The eigenstructure results are applied in Chapter 6 to identify the minimum

(threshold) SNR and data set size N necessary for reliable estimation (detection) of the number of sources M by any algorithm based upon consideration of the sample eigenvalues of $\hat{R}$.

The eigenstructure of R_S for degenerate scenarios is addressed in Chapter 7. Expressions are developed that facilitate eigenstructure identification for two classes of practically important degenerate scenarios, which arise from degenerate sensor array geometry or degenerate source configuration.

Chapter 8 lays the foundation for CR bound analysis by reviewing the available CR bound expressions, and relating them to the MUSIC null spectrum. The thesis approach to CR bound analysis is introduced, and sufficient conditions for non-degenerate CR bounds are defined.

Explicit expressions for CR bounds on spatial frequency variance in multi-D scenarios are derived in Chapter 9, and illustrative examples are presented.

The CR bound results are applied in Chapter 10 to identify the minimum (threshold) SNR and data set set size N necessary for reliable resolution of closely spaced sources by any unbiased direction estimation algorithm.

A discussion of thesis results is presented in Chapter 11.

Chapter 2

Problem Addressed

In order to lay the foundation for the forthcoming analysis, this chapter introduces a motivating direction finding problem in Section 2.1, the data model assumptions and notation conventions in Section 2.2, the classical perturbation theory relation between the eigenstructure of sample and asymptotic covariance matrices $\widehat{R}$ and R in Section 2.3, and the available CR bound expressions for 1-D and multi-D DF scenarios in Section 2.4. The thesis analysis approach for closely-spaced sources is presented in Section 2.5. Section 2.6 introduces example scenarios that are used in numerical simulations throughout the thesis to illustrate theoretical results.

2.1 The Direction Finding Problem

In a typical direction finding (DF) scenario, an array of sensors observes signals propagating from one or more spatially discrete sources. The problem of interest is to determine the spatial location, or direction, of the sources by comparing the signals observed at the collection of sensors with array calibration data.

A DF scenario is designated as *one-dimensional* (1-D) if only one unknown real scalar direction parameter is to be determined for each source. An example 1-D DF scenario is illustrated in Figure 2-1; a uniform linear array of three sensors observes signals from a single source. To simplify discussion of the example scenario, we make the following assumptions:

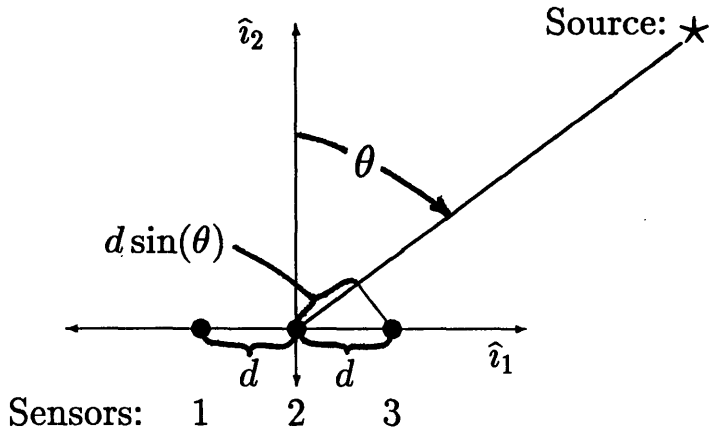

Figure 2-1: Example 1-D Direction Finding Scenario

far-field source: the source-to-sensor distances are assumed to be large relative to the sensor-to-sensor spacing, (or equivalently, that the propagating signal consists of *plane waves*),

monochromatic source: the transmitted signal is a sinusoid at a single, constant temporal frequency f,

identical omni-directional sensors: the complex gain response of each of the sensors is unity in all directions.

The direction finding problem is to estimate the off-broadside direction of arrival angle θ.

The key feature of propagating signals that can be exploited in direction finding is that the signal waveform emitted by a source is received at a sensor with a propagation delay that depends upon the source-to-sensor distance. In Figure 2-1, the source signal received at sensor 2 is delayed relative to that received at sensor 3 and advanced relative to that received at sensor 1 (since sensor 3 is closer and sensor 1 is farther from the source than sensor 2). Under the far-field assumption, the incremental source-to-sensor distance in Figure 2-1 between sensors 2 and 3, and between sensors 1 and 2, is essentially $d\sin(\theta)$, where d is inter-sensor spacing and θ is the off-broadside angle. For a given uniform sensor spacing d and uniform propagation speed in the medium

c, the signal at sensor 2 is delayed (advanced) relative to that at sensor 3 (sensor 1) by a time δt, where

$$\delta t = \frac{d\sin(\theta)}{c} \tag{2.1}$$

Under the monochromatic source assumption, signal delay results in signal phase shift. In the example scenario of Figure 2-1, if $x(t)$ denotes the noise-free source signal as might (ideally) be received at sensor 2 at time t, then $x(t)\cdot e^{j2\pi f\delta t}$ denotes the (phase-advanced) noise-free signal received at sensor 3 at time t (assuming identical omni-directional sensors, and negligible magnitude attenuation between sensors for a far-field source).

In reality, the source signals cannot be received noise-free. If $\epsilon_i(t)$ denotes the additive noise at the i^{th} sensor at time t, and $y_i(t)$ the source signal as received at the i^{th} sensor with additive sensor noise, then for a far-field, monochromatic source and identical omni-directional sensors in Figure 2-1, the received signals can be modeled as

$$\begin{aligned} y_1(t) &= x(t)\cdot e^{-jd\cdot\omega} + \epsilon_1(t) \\ y_2(t) &= x(t) + \epsilon_2(t) \\ y_3(t) &= x(t)\cdot e^{jd\cdot\omega} + \epsilon_3(t) \end{aligned} \tag{2.2}$$

where d is the intersensor distance, and ω denotes the quantity

$$\omega = \frac{2\pi f}{c}\sin(\theta) \tag{2.3}$$

Due to the appearance of ω in the complex phasors in (2.2), ω is commonly designated as the *spatial frequency* of the source in 1-D scenarios. For constant source temporal frequency f, and constant, uniform propagation speed c, ω in (2.3) depends only on the direction of arrival angle θ of the source. Therefore, the direction finding problem is often alternately stated as the problem of estimating spatial frequency ω.

A direction finding scenario in which there are two or more unknown direction

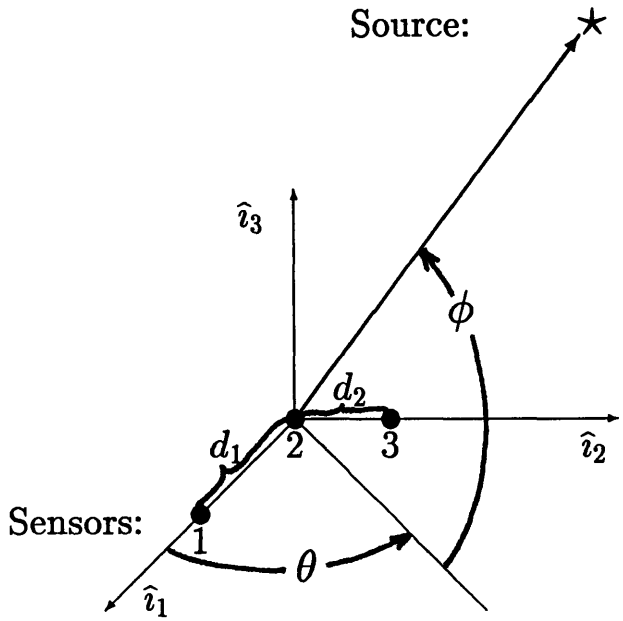

Figure 2-2: Example Multi-D Direction Finding Scenario

parameters for each source is designated as *multi-dimensional* (multi-D). An example two-dimensional (2-D) scenario is illustrated in Figure 2-1; a triangular array of three sensors observes a single far-field signal source. The sensor coordinates in the sensor plane are $(d_1, 0)$, $(0, 0)$ and $(0, d_2)$. The source direction is measured by two parameters: θ measures azimuth angle in the sensor plane from the $\hat{i}_1$ axis, and ϕ measures elevation angle from the $\hat{i}_1$, $\hat{i}_2$ plane. The problem here is to estimate the two angular direction parameters of azimuth θ and elevation ϕ for the far-field source.

If we assume in Figure 2-2 that the source is far-field and monochromatic, and that the sensors are identical, unit gain in all directions (isotropic) and that noise is additive, then analogously to equations (2.2) for 1-D, the received signals in Figure 2-2 can be modeled as

$$\begin{aligned} y_1(t) &= x(t) \cdot e^{jd_1\omega_1} + \epsilon_1(t) \\ y_2(t) &= x(t) + \epsilon_2(t) \\ y_3(t) &= x(t) \cdot e^{jd_2\omega_2} + \epsilon_3(t) \end{aligned} \tag{2.4}$$

where at time t, $x(t)$ is the noise-free signal at sensor 2, $\epsilon_i(t)$ is the additive noise at the i^{th} sensor, and $y_i(t)$ is the signal at the i^{th} sensor with additive noise. The parameters ω_1 and ω_2 denote the quantities

$$\begin{aligned} \omega_1 &= \frac{2\pi f}{c}\cos(\theta)\cos(\phi) \\ \omega_2 &= \frac{2\pi f}{c}\sin(\theta)\cos(\phi) \end{aligned} \tag{2.5}$$

where f is the (monochromatic) source temporal frequency, c is the (uniform) propagation speed in the medium, θ is source azimuth angle, and ϕ is source elevation angle. Due to the appearance of ω_1, ω_2 in the complex phasors in (2.4), ω_1 is designated as the *spatial frequency* component along the $\hat{\imath}_1$ axis, and ω_2 as the *spatial frequency* component along the $\hat{\imath}_2$ axis. For convenience, the scalar spatial frequency components are collected into a single real *spatial frequency vector* $\vec{\omega}$. That is,

$$\vec{\omega} = [\omega_1, \omega_2]^t \tag{2.6}$$

For constant source temporal frequency f, and constant propagation speed c, $\vec{\omega}$ depends only on the direction of arrival angles θ and ϕ of the source. Therefore, the multi-D direction finding problem is often alternately stated as the problem of estimating spatial frequency vector $\vec{\omega}$.

To compactly represent the data model (2.4), it is convenient to adopt the vector notation

$$\vec{y}(t) = \vec{a}(\vec{\omega})x(t) + \vec{\epsilon}(t) \tag{2.7}$$

where $x(t)$ is the noise-free signal at a reference sensor at time t, and

$$\begin{aligned} \vec{y}(t) &= [y_1(t), y_2(t), y_3(t)]^t \\ \vec{a}(\vec{\omega}) &= \left[e^{jd_1\omega_1},\ 1,\ e^{jd_2\omega_2}\right]^t \\ \vec{\epsilon}(t) &= [\epsilon_1(t), \epsilon_2(t), \epsilon_3(t)]^t \end{aligned} \tag{2.8}$$

The data vector $\vec{y}(t)$ is commonly designated the vector *snapshot* of sensor outputs at time t. The vector $\vec{a}(\vec{\omega})$ is a function of spatial frequency vector $\vec{\omega}$, but is independent of the transmitted signal $x(t)$. Thus $\vec{a}(\vec{\omega})$ represents the generic array response to a unit amplitude signal arriving with spatial frequency vector $\vec{\omega}$, and is commonly designated the *generic arrival vector* for spatial frequency $\vec{\omega}$.

2.2 Data Model

The data model addressed in this thesis is the *narrowband* source model, which generalizes the example data model (2.7) of the previous section to multiple sources, and relaxes the simplifying assumptions of far-field, monochromatic sources and identical, isotropic sensors.

In a multi-D direction finding scenario with $\mathcal{D}$ unknown real scalar spatial frequencies $\omega_1, \cdots, \omega_{\mathcal{D}}$ to be determined for each source, it is convenient to collect the scalar parameters into a real spatial frequency vector $\vec{\omega}$. That is

$$\vec{\omega} \;=\; [\omega_1, \cdots \omega_{\mathcal{D}}]^t \tag{2.9}$$

In a multi-D scenario with M sources, we assume that source directions are specified by parameter vectors $\vec{\omega}_1, \cdots \vec{\omega}_M$. The $\vec{\omega}_1, \cdots \vec{\omega}_M$ are to be estimated from observation data across an array of W sensors. The observed data consists of N vector snapshots of the assumed form

$$\vec{y}(t) \;=\; A \cdot \vec{x}(t) + \vec{\epsilon}(t) \qquad t = 1, \cdots N \tag{2.10}$$

At sample index t, $\vec{y}(t)$ is a noisy (complex) W element observed data vector, $\vec{x}(t)$ is an M element vector of source complex amplitudes, and $\vec{\epsilon}(t)$ is a W element vector of additive complex noise. A is a constant matrix having special form

$$A \;=\; [\vec{a}(\vec{\omega}_1), \cdots \vec{a}(\vec{\omega}_M)] \qquad (W \times M) \tag{2.11}$$

where $\vec{a}(\vec{\omega})$ is the generic arrival vector for signals with spatial frequency $\vec{\omega}$. Typically the i^{th} element of vector $\vec{a}(\vec{\omega})$ reflects the magnitude and phase observed at the i^{th} sensor in response to a unit amplitude signal with spatial frequency $\vec{\omega}$.

In the data model (2.10), (2.11) the sources need not be monochromatic, but are assumed to be *narrowband* with a center frequency f. Specifically, it is assumed that the coherence length of the source modulating waveform is much larger than the maximum sensor-to-sensor separation. Under the narrowband assumption signal delay is essentially equivalent to complex phase shift.

The data model (2.10), (2.11) also supports generic arrival vectors $\vec{a}(\vec{\omega})$ for sources that are not far-field, and for sensors that are not identical and that do not have isotropic response. Nevertheless to simplify the discussion, scenarios with far-field sources and identical, isotropic sensors will be used in all examples in this thesis. The following example illustrates the structure of the generic arrival vector $\vec{a}(\vec{\omega})$ for a simple 2-D scenario used repeatedly in thesis examples.

Example 2.1 : Consider a 2-D direction estimation problem consisting of a planar array of identical unit-gain, isotropic sensors observing signals from a cluster of far-field sources. The data model for this scenario takes the form (2.10), (2.11). The generic arrival vector for a planar array of W unit gain isotropic sensors is

$$\vec{a}(\vec{\omega}) \;=\; \left[e^{j\vec{r}_1^t\vec{\omega}},\; e^{j\vec{r}_2^t\vec{\omega}},\; \cdots,\; e^{j\vec{r}_W^t\vec{\omega}}\right]^t \tag{2.12}$$

where $\vec{r}_i = [r_{1i}, r_{2i}]^t$ is the location of the i^{th} sensor in sensor plane, and $\vec{\omega}$ is the projection of the source direction onto the sensor plane defined as

$$\vec{\omega} \;=\; \frac{2\pi f}{c}\begin{bmatrix}\cos\theta\cos\phi\\ \sin\theta\cos\phi\end{bmatrix} \tag{2.13}$$

where θ measures azimuth angle in the sensor plane from the $\hat{\imath}_1$ axis, and ϕ measures elevation angle from the $\hat{\imath}_1, \hat{\imath}_2$ plane as illustrated in Figure 2-2.

2.2.1 Assumptions

The vectors $\vec{a}(\vec{\omega})$, $\vec{x}(t)$ and $\vec{\epsilon}(t)$ in data model (2.10), (2.11) are assumed to satisfy the following conditions:

$\vec{a}(\vec{\omega})$:

A1. the number W of sensors is greater than the number M of sources, i.e. $W > M$,

A2. matrix A is a $W \times M$ matrix of the form (2.11), with columns $\vec{a}(\vec{\omega}_1), \cdots \vec{a}(\vec{\omega}_M)$.

A3. matrix A has linearly independent columns, provided $\vec{\omega}_i \neq \vec{\omega}_j$ for $i \neq j$.

A4. the elements of $\vec{a}(\vec{\omega})$ are bounded and possess partial derivatives of all orders with respect to the elements of $\vec{\omega}$, within a convex region of $\vec{\omega}$ space that includes all source spatial frequency vectors $\vec{\omega}_1, \cdots, \vec{\omega}_M$.

$\vec{x}(t)$:

X1. the sequence of source amplitude vectors $\vec{x}(t)$, $t = 1 \cdots N$ is fixed for all realizations of the data sequence $\vec{y}(t)$,

X2. the *sample* source amplitude cross-power matrix

$$\hat{P} \triangleq \sum_{t=1}^{N} \vec{x}(t)\vec{x}(t)^h \qquad (M \times M) \tag{2.14}$$

is Hermitian positive definite.

X3. for large data sets (as $N \to \infty$), $\hat{P}$ converges with probability one to the asymptotic source amplitude cross-power matrix

$$P \triangleq E\left\{\vec{x}(t)\vec{x}(t)^h\right\} \qquad (M \times M) \tag{2.15}$$

which also is Hermitian positive definite.

$\vec{\epsilon}(t)$:

E1. the noise vector $\vec{\epsilon}(t)$ varies randomly across the ensemble of data vectors $\vec{y}(t)$. Specifically, the $\vec{e}(t)$ for $t = 1 \cdots N$, are samples of a zero-mean complex Gaussian random process with

$$\begin{aligned} E\left\{\vec{\epsilon}(t)\vec{\epsilon}(s)^h\right\} &= \begin{cases} \sigma^2 I & t = s \\ 0 & t \neq s \end{cases} \\ E\left\{\vec{\epsilon}(t)\vec{\epsilon}(s)^t\right\} &= 0 \end{aligned} \tag{2.16}$$

Following [15], [11], we designate the data model defined by (2.10), (2.11) and the assumptions **X1-X3, E1** as the conditional model. The unconditional model (or stochastic model) differs from the foregoing in that assumptions **X1-X3** are replaced by assumptions that allow $\vec{x}(t)$ also to vary randomly across the ensemble of data vectors [15].

2.2.2 Notation

We use the following conventional notation:

$(\cdot)^t$	transpose,
$(\cdot)^*$	complex conjugate,
$(\cdot)^h$	Hermitian transpose (conjugate transpose),
$(\cdot)^{-1}$	conventional inverse,
$(\cdot)^+$	pseudo inverse,
$\lvert\cdot\rvert$	matrix determinant,
$\lVert\cdot\rVert$	2-norm,
$I_{q\times q}$	$q \times q$ identity matrix,
$1_{p\times q}$	$p \times q$ matrix of ones,
$A \odot B$	Schur-Hadamard product (See Appendix A),
$A \otimes B$	Kronecker product (See Appendix A),

$\widehat{z}$	unbiased estimate of parameter z,
$E\{\cdot\}$	Expectation,
$\mathrm{Cov}\{\widehat{\vec{\psi}}\}$	matrix $E\{(\widehat{\vec{\psi}}-\vec{\psi})(\widehat{\vec{\psi}}-\vec{\psi})^h\}$,
$A > B$	$A-B$ is positive definite,
$A \geq B$	$A-B$ is non-negative definite,
$\triangleq$	"is defined to be",
$A = \mathcal{O}(\epsilon^p)$	the elements of A are of order ϵ^p,
$A = o(\epsilon^p)$	the elements of A are of order ϵ^q, $q > p$,
$X \subseteq Y$	the elements in set X are contained in set Y.

Projection matrices play a fundamental role in our results. To simplify the discussion, we introduce the following additional notation.

$Q_{[Z]}$	$\triangleq$	ZZ^+	projection matrix onto the column space of Z,
$Q_{[Z^h]}$	$\triangleq$	$Z^h(Z^h)^+ = Z^+Z$	projection matrix onto the row space of Z,
$P_{[Z]}$	$\triangleq$	$I - Q_{[Z]}$	projection matrix onto the column nullspace of Z,
$P_{[Z^h]}$	$\triangleq$	$I - Q_{[Z^h]}$	projection matrix onto the row nullspace of Z.

2.3 Eigenstructure of $\widehat{R}$

To obtain the benefits of averaging, many practical direction finding algorithms compute the *sample data covariance matrix*

$$\widehat{R} \triangleq \frac{1}{N}\sum_{t=1}^{N}\vec{y}(t)\vec{y}(t)^h \qquad (W \times W) \tag{2.17}$$

For the assumed data vector (2.10), with assumptions **X1-X3**, **E1**, the sample covariance matrix $\widehat{R}$ converges as $N \to \infty$ with probability one to the *asymptotic data covariance matrix*

$$R \triangleq E\left\{\vec{y}(t)\vec{y}(t)^h\right\} = R_S + \sigma^2 I \qquad (W \times W) \tag{2.18}$$

where R_S is the *asymptotic signal (noise-free) covariance matrix*

$$R_S \triangleq APA^h \qquad (W \times W) \qquad (2.19)$$

with matrices A, P as in (2.11), (2.15). It follows from (2.19) and assumption **X3** that R_S is Hermitian non-negative definite.

The data covariance matrices $\hat{R}$, R play a fundamental role in direction finding. Many direction finding techniques generate a non-negative *spectrum* function from the sample data covariance matrix $\hat{R}$ (recall Table 1.1). The values of $\vec{\omega}$ at the peaks of the spectrum function are taken to be estimates of the source spatial frequency vectors. The spectrum functions for High Resolution algorithms typically depend upon the inverse of $\hat{R}$, or upon selected eigenvectors of $\hat{R}$. Therefore, the performance of direction finding techniques in terms of bias, variance, detection and resolution thresholds depends critically upon the eigenstructure of $\hat{R}$, or of the corresponding asymptotic matrix R, for large data set size N.

From assumptions **A1-A3** and **X3**, matrix R_S of (2.19) has M non-zero eigenvalues; therefore the eigenvalues and eigenvectors of R in (2.18) can be partitioned as follows. Let $\bar{\lambda}_1 \geq \bar{\lambda}_2 \geq \cdots \geq \bar{\lambda}_M$ and $\bar{\vec{e}}_1 \cdots \bar{\vec{e}}_M$ denote respectively the M largest eigenvalues of R, and the corresponding (signal-space) eigenvectors. Let $\bar{\lambda}_{M+1} = \cdots = \bar{\lambda}_W = \sigma^2$ and $\bar{\vec{e}}_{M+1} \cdots \bar{\vec{e}}_W$ denote respectively the remaining eigenvalues and corresponding (noise-space) eigenvectors. Finally let $\bar{E}$ denote the complete matrix of eigenvectors

$$\bar{E} \triangleq \left[\bar{E}_S,\ \bar{E}_N\right]$$
$$\bar{E}_S \triangleq \left[\bar{\vec{e}}_1 \ldots \bar{\vec{e}}_M\right] \quad , \quad \bar{E}_N \triangleq \left[\bar{\vec{e}}_{M+1} \ldots \bar{\vec{e}}_W\right] \qquad (2.20)$$

The corresponding eigenstructure of the sample covariance matrix $\hat{R}$ is denoted using modifier $\hat{}$ in place of $\bar{}$, and can be similarly partitioned. Thus let $\hat{\lambda}_1 \geq \hat{\lambda}_2 \geq \cdots \geq \hat{\lambda}_M$ and $\hat{\vec{e}}_1 \cdots \hat{\vec{e}}_M$ denote respectively the M largest eigenvalues of $\hat{R}$, and the corresponding (signal-space) eigenvectors. Let $\hat{\lambda}_{M+1} \geq \cdots \geq \hat{\lambda}_W$ and $\hat{\vec{e}}_{M+1} \cdots \hat{\vec{e}}_W$

denote respectively the remaining eigenvalues and corresponding (noise-space) eigenvectors. Finally let $\hat{E}$ denote the complete matrix of eigenvectors

$$\hat{E} \triangleq \left[\hat{E}_S,\ \hat{E}_N\right] \tag{2.21}$$

$$\hat{E}_S \triangleq \left[\hat{\vec{e}}_1 \ldots \hat{\vec{e}}_M\right] \quad , \quad \hat{E}_N \triangleq \left[\hat{\vec{e}}_{M+1} \ldots \hat{\vec{e}}_W\right] \tag{2.22}$$

To quantify performance of candidate DF algorithms, it is desirable to have available a model of the eigenstructure of the sample data covariance matrix $\hat{R}$. The sample quantities can be expressed as the sum of the asymptotic values and random perturbations as follows

$$\hat{\lambda}_i = \bar{\lambda}_i + \mu_i \tag{2.23}$$

$i = 1 \cdots W$ and

$$\hat{\vec{e}}_i = \bar{\vec{e}}_i + \vec{\eta}_i \tag{2.24}$$

for $i = 1 \cdots M$, where the signal space eigenvalues are assumed to be distinct.

If the eigenstructure of the asymptotic covariance matrix R is available, then classical statistical results provide expressions for the mean and variance of the eigenvalue and eigenvector sampling errors μ_i and $\vec{\eta}_i$, in terms of the asymptotic eigenvalues $\bar{\lambda}_i$ and eigenvectors $\bar{\vec{e}}_i$. Drawing upon results of [9] for the eigenvalues and eigenvectors of the sample covariance matrix $\hat{R}$ of a complex Gaussian process, the asymptotic (large N) first and second order statistics of μ_i and $\vec{\eta}_i$ are

$$E\{\mu_i\} = o(1/N) \tag{2.25}$$

$$E\{\mu_i \mu_j\} = \frac{\bar{\lambda}_i^2}{N}\delta_{ij} + o(1/N) \tag{2.26}$$

$$E\{\vec{\eta}_i\} = \left(-\frac{\bar{\lambda}_i}{2N}\sum_{\substack{k=1 \\ k\neq i}}^{W} \frac{\bar{\lambda}_k}{(\bar{\lambda}_i - \bar{\lambda}_k)^2}\right)\bar{\vec{e}}_i + o(1/N) \tag{2.27}$$

$$E\{\vec{\eta}_i\vec{\eta}_j^h\} = \frac{\bar{\lambda}_i}{N}\sum_{\substack{k=1\\k\neq i}}^{W}\frac{\bar{\lambda}_k}{(\bar{\lambda}_i-\bar{\lambda}_k)^2}\bar{\vec{e}}_k\bar{\vec{e}}_k^h\delta_{ij} + o(1/N) \quad (2.28)$$

$$E\{\vec{\eta}_i\vec{\eta}_j^t\} = \frac{\bar{\lambda}_i\bar{\lambda}_j}{N(\bar{\lambda}_i-\bar{\lambda}_j)^2}\bar{\vec{e}}_j\bar{\vec{e}}_i^t(1-\delta_{ij}) + o(1/N) \quad (2.29)$$

where δ_{ij} is the Kronecker delta and $o(1/N)$ denotes terms of order $1/N^q$ with $q > 1$. If the eigenvalues $\bar{\lambda}_i$ and $\bar{\vec{e}}_i$ of R were available, then the statistical properties of the eigenstructure of $\hat{R}$ could be ascertained from the classical perturbation results (2.25)-(2.29).

For the data model addressed, we recall from (2.18) that matrix R takes the form

$$R = R_S + \sigma^2 I \quad (2.30)$$

where R_S reflects the covariance contribution of the M source signals, and σ^2 is the variance of the additive noise. Due to the uncorrelated and white structure of the noise component of R, the eigenstructure of R is simply obtained from that of R_S. The eigenvalues of R are those of R_S incremented by the constant σ^2. The signal-space eigenvectors of R (columns of $\bar{E}_S$ in (2.20)) associated with the i^{th} largest eigenvalue of R are the eigenvectors of R_S associated with the i^{th} largest non-zero eigenvalue of R_S. The noise-space eigenvectors of R (columns of $\bar{E}_N$) are the eigenvectors of R_S associated with the zero eigenvalue of R_S.

Therefore, identification of the eigenstructure of R_S is a fundamental enabling step for obtaining analytical expressions for the performance of candidate direction finding algorithms for closely-spaced sources. Reference [12] introduced simple expressions for the eigenstructure of R_S for closely-spaced sources in 1-D scenarios. A major result of this thesis is to derive analogous simple formulations for the eigenstructure of R_S applicable to multi-D scenarios.

2.4 Cramér Rao Bounds

The Cramér-Rao (CR) lower bound on the variance of unbiased direction estimates provides a useful benchmark for assessing estimation accuracy of direction finding algorithms [15]. The CR bound also can provide insight into the performance impact of individual scenario parameters such as sensor array geometry, source configuration, source powers and correlations [11].

Evaluation of the CR bound generally requires inverting the applicable Fisher Information matrix $\mathcal{F}$ of dimension equal to the number of unknown (real and imaginary) model parameters. In the Conditional signal model specified by Assumptions **X1-X2** and **E1**, the unknown parameters are not only the source spatial frequency vectors $\vec{\omega}_1, \cdots, \vec{\omega}_M$ of interest, but also the noise variance σ^2 and the complex signal amplitude vector sequence $\vec{x}(1), \cdots \vec{x}(N)$. These latter unknowns are essentially nuisance parameters for the DF problem, which enlarge $\mathcal{F}$ and make direct calculation of $\mathcal{F}^{-1}$ exceedingly cumbersome.

The CR bound of present interest is that on the covariance of the spatial frequency vectors. This bound is given by a submatrix of $\mathcal{F}^{-1}$. Since only a submatrix of $\mathcal{F}^{-1}$ is required, it is useful for both analytical and numerical work to have available an explicit formulation for the applicable submatrix of $\mathcal{F}^{-1}$. Such formulations have been developed by Stoica and Nehorai for 1-D scenarios [15], and extended by Yau and Bresler to multi-D scenarios [16].

For 1-D scenarios, the CR bound on sample frequency covariances takes the form

$$E\left\{\left(\vec{\hat{\Omega}} - \vec{\Omega}\right)\left(\vec{\hat{\Omega}} - \vec{\Omega}\right)^h\right\} \geq B_C \tag{2.31}$$

where $A \geq B$ means that the matrix $A - B$ is non-negative definite, and

$$\vec{\Omega} \triangleq [\omega_1, \omega_2, \cdots, \omega_M]^t \tag{2.32}$$

$$\vec{\hat{\Omega}} \triangleq [\hat{\omega}_1, \hat{\omega}_2, \cdots, \hat{\omega}_M]^t \tag{2.33}$$

$\hat{\omega}_j$ denotes an unbiased estimate of the spatial frequency ω_j for the j^{th} source ($j =$

$1 \cdots M$). The matrix B_C is

$$B_C = \frac{\sigma^2}{2N} \left\{ \mathrm{Re}\left[H \odot \hat{P}^T \right] \right\}^{-1} \tag{2.34}$$

where

$$H \triangleq D^h \left[I - A(A^h A)^{-1} A^h \right] D \tag{2.35}$$

$$D \triangleq \left[\vec{d}(\omega_1), \vec{d}(\omega_2), \cdots \vec{d}(\omega_M) \right] \tag{2.36}$$

$$\vec{d}(\omega_j) \triangleq \left. \frac{d\vec{a}(\omega)}{d\omega} \right|_{\omega=\omega_j} \tag{2.37}$$

Vector $\vec{a}(\omega)$ is the generic arrival vector for (scalar) spatial frequency ω, matrix A is the source arrival matrix (2.11) and $\hat{P}$ is the sample source amplitude covariance matrix (2.14). The result (2.31), (2.34) is valid for 1-D scenarios under the conditional signal model assumptions **X1-X3** and **E1**. The result is due to Stoica and Nehorai [15].

For multi-D scenarios, the CR bound applicable to the parameter vectors $\vec{\omega}_1 \cdots \vec{\omega}_M$ also takes the form (2.31), this time with

$$\vec{\Omega} \triangleq [\omega_{11} \cdots \omega_{\mathcal{D}1} \cdots \omega_{1M} \cdots \omega_{\mathcal{D}M}]^t \tag{2.38}$$

$$\hat{\vec{\Omega}} \triangleq [\hat{\omega}_{11} \cdots \hat{\omega}_{\mathcal{D}1} \cdots \hat{\omega}_{1M} \cdots \hat{\omega}_{\mathcal{D}M}]^t \tag{2.39}$$

$\hat{\omega}_{ij}$ denotes an unbiased estimate of i^{th} element of $\vec{\omega}_j$, ($i = 1 \cdots \mathcal{D}, j = 1 \cdots M$). Compact expressions for B_C in multi-D scenarios, again under the conditional signal model assumptions **X1-X3** and **E1**, have been identified by Yau and Bresler [16]. The detailed expression of [16] for B_C in multi-D is given in Section 8.2.3.

A shortcoming of the B_C expressions of [15] and [16] is that the dependence of B_C upon the scenario parameters such as sensor array geometry, source configuration, source powers and correlations remains implicit. For the case of closely-spaced sources in 1-D direction finding scenarios, simple explicit expressions have been developed by Lee [11] in terms of the maximum source separation $\delta\omega$ and the foregoing scenario

parameters. These expressions provide great insight into the dependence of the CR bound upon scenario elements, and facilitate derivation of fundamental performance metrics such as the minimum (threshold) SNR at which closely-spaced sources are resolvable. At present no analogous results for Multi-D scenarios are available in the literature. The second major result of this thesis is to derive analogous explicit expressions for B_C for closely-spaced sources in multi-D scenarios.

2.5 Analysis Approach

The main results of this thesis are obtained by identifying the eigenstructure of R_S, and identifying expressions for the CR bound B_C, as source spacing becomes small. Extending the approach of [11], [12] for 1-D scenarios, we express the spatial frequency vector for the j^{th} source as

$$\vec{\omega}_j = \vec{\omega}_0 + \delta\omega \cdot \vec{q}_j \tag{2.40}$$

$j = 1, \cdots M$, where $\vec{\omega}_0$ is a nearby fixed reference vector, $\delta\omega$ is a variable real scale factor, and

$$\vec{q}_j = [q_{1j}, \cdots q_{Dj}]^t \tag{2.41}$$

is a normalized offset vector with constant real elements. The $\vec{q}_j$ are normalized so that $\delta\omega$ equals the maximum separation $\|\vec{\omega}_j - \vec{\omega}_i\|$ between pairs of vectors $\vec{\omega}_1, \cdots \vec{\omega}_M$. That is,

$$\delta\omega = \max_{j,i} \|\vec{\omega}_j - \vec{\omega}_i\| \tag{2.42}$$

The analysis strategy is to examine the structure of R_S and of the Cramér Rao bound B_C as scaling factor $\delta\omega \rightarrow 0$, while the $\vec{q}_i$ are held constant. The leverage in the representation (2.40) is that it replaces the M variable spatial vectors $\vec{\omega}_1 \cdots \vec{\omega}_M$ by a single variable scalar parameter $\delta\omega$, thereby greatly simplifying analysis. The

condition $\delta\omega \rightarrow 0$ corresponds to the coalescing of all source parameter vectors to the reference vector $\vec{\omega}_0$, while the relative (normalized) source configuration remains unchanged.

Example 2.2 : To illustrate the analysis strategy, consider the 2-D problem of estimating a 2-element spatial frequency vector $\vec{\omega}_j = [\omega_{xj}, \omega_{yj}]^t$ for each source $(j = 1, 2, 3)$ in a cluster of 3 far-field sources in the triangular configuration illustrated in Figure 2-3A. To implement the analysis approach, we express each source spatial frequency vector as in (2.40). We define a reference vector $\vec{\omega}_0$ in the vicinity of the source spatial frequency vectors, a scalar parameter $\delta\omega$ to be the maximum source separation, which in Figure 2-3A is

$$\delta\omega \;=\; \|\vec{\omega}_1 - \vec{\omega}_3\| \tag{2.43}$$

and finally define normalized offset vectors $\vec{q}_1$, $\vec{q}_2$, $\vec{q}_3$ to satisfy (2.40). The normalized source configuration are illustrated in Figure 2-3B. As $\delta\omega \rightarrow 0$, the actual source configuration in Figure 2-3A coalesces to the reference direction $\vec{\omega}_0$, but the normalized configuration in Figure 2-3B remains fixed.

2.5.1 Factoring Matrix R_S

For the data model addressed, we recall from (2.19) that matrix R_S is Hermitian positive definite and takes the form

$$R_S \;\triangleq\; APA^h \qquad (W \times W) \tag{2.44}$$

with matrices A, P as in (2.11), (2.15). It is helpful in our analysis to express R_S as an outer product of matrix factors B. That is

$$R_S \;=\; BB^h \tag{2.45}$$

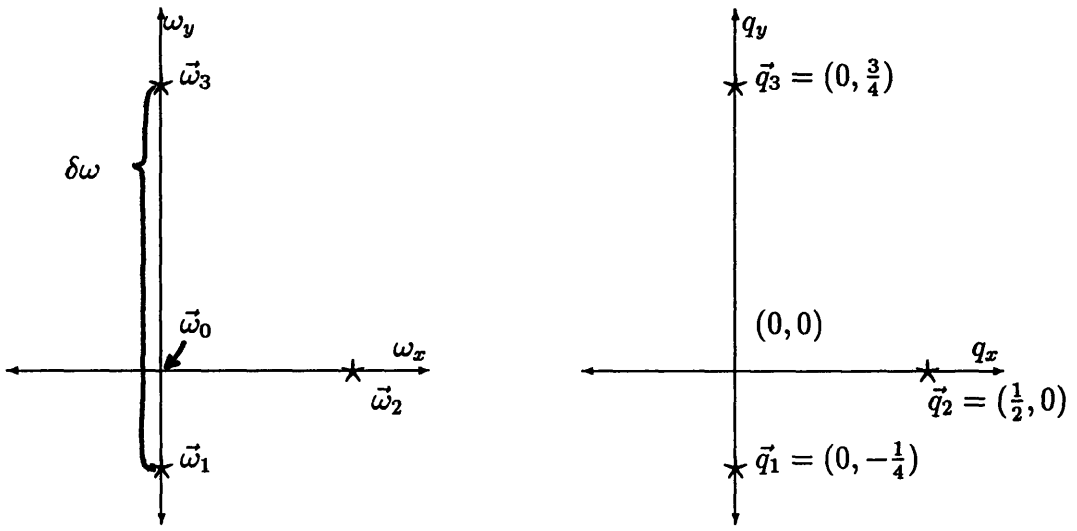

A. Actual Source Configuration **B.** Normalized Source Configuration

Figure 2-3: Actual and Normalized Source Configurations for a 2-D DF Scenario

where

$$B \triangleq A\Pi \qquad (W \times M) \tag{2.46}$$

and Π is a square full-rank factor of P such that

$$P = \Pi\,\Pi^h \tag{2.47}$$

A non-unique decomposition (2.47) exists since P is Hermitian positive definite by assumption **X2**. With the representation (2.40), B is a function of the variable scale factor $\delta\omega$, the reference frequency $\vec{\omega}_0$, the normalized offset vectors $\vec{q}_1 \cdots \vec{q}_M$ and the constant matrix P. Our interest is to identify the limiting eigenstructure of (2.45) as $\delta\omega \to 0$.

The thesis approach to eigenanalysis of R_S is to first identify the limiting form of the SVD of matrix B as $\delta\omega \to 0$. The limiting SVD of B is simplified by structural conditions satisfied by B for typical direction finding scenarios. Once expressions for the limiting SVD of B are identified, the limiting eigenstructure of R_S follows straightforwardly from (2.45).

2.5.2 Taylor Series Representations

Taylor series representations are central to our analysis of the closely-spaced source problem. To facilitate identification of the small $\delta\omega$ structure of covariance matrix R_S and of CR bound B_C in subsequent chapters, this section constructs the Taylor series of the generic arrival vector $\vec{a}(\vec{\omega})$, and of the associated matrix A of (2.11) and matrix B of (2.46).

Following our analysis approach of (2.40), we express the spatial frequency vector $\vec{\omega}$ as

$$\vec{\omega} \;=\; \vec{\omega}_0 + \delta\omega\ \vec{q} \tag{2.48}$$

where $\vec{\omega}_0$ is the reference vector, $\delta\omega$ is the scaling factor that satisfies (2.42), and $\vec{q}$ is a *normalized spatial frequency vector.* To explicitly denote dependence on the terms of (2.48), we express the Taylor series of the generic arrival vector $\vec{a}(\vec{\omega})$ about the reference vector $\vec{\omega}_0$ as

$$\vec{a}(\vec{\omega}) \;=\; \sum_{p=0}^{\infty} \delta\omega^p \dot{A}_p \cdot \vec{\gamma}_p(\vec{q}) \tag{2.49}$$

where the columns of $\dot{A}_p$ are the p^{th} order spatial derivatives of $\vec{a}(\vec{\omega})$ at $\vec{\omega}_0$ with respect to the elements of $\vec{\omega} = [\omega_1, \omega_2, \cdots \omega_D]^t$. That is,

$$\dot{A}_p \;\triangleq\; \left[\frac{\partial^p \vec{a}(\vec{\omega})}{\partial\omega_1^p}, \frac{\partial^p \vec{a}(\vec{\omega})}{\partial\omega_1^{p-1}\partial\omega_2}, \cdots, \frac{\partial^p \vec{a}(\vec{\omega})}{\partial\omega_D^p}\right]_{\vec{\omega}=\vec{\omega}_0} \qquad (W \times \bar{n}_p) \tag{2.50}$$

where $\bar{n}_p$ is the number of p^{th} order spatial derivatives. Vector $\vec{\gamma}_p(\vec{q})$ is $\bar{n}_p \times 1$ and depends only on the normalized direction offset vector $\vec{q}$. The $\dot{A}_p$ and $\vec{\gamma}_p(\vec{q})$ are constant with $\delta\omega$; $\dot{A}_p$ is typically complex, while $\vec{\gamma}_p(\vec{q})$ is always real.

To illustrate (2.49), consider a 2-D application with $\vec{\omega} = [\omega_x, \omega_y]^t$, and $\vec{q} = [q_x, q_y]^t$. The $p = 0, 1, 2, 3$ terms in (2.49) are

$$\dot{A}_0 \;=\; [\vec{a}(\vec{\omega}_0)]$$

$$\begin{aligned}
\dot{A}_1 &= \left[\vec{a}^{(1,0)}(\vec{\omega}_0),\, \vec{a}^{(0,1)}(\vec{\omega}_0)\right] \\
\dot{A}_2 &= \left[\vec{a}^{(2,0)}(\vec{\omega}_0),\, \vec{a}^{(1,1)}(\vec{\omega}_0),\, \vec{a}^{(0,2)}(\vec{\omega}_0)\right] \\
\dot{A}_3 &= \left[\vec{a}^{(3,0)}(\vec{\omega}_0),\, \vec{a}^{(2,1)}(\vec{\omega}_0),\, \vec{a}^{(1,2)}(\vec{\omega}_0),\, \vec{a}^{(0,3)}(\vec{\omega}_0)\right]
\end{aligned} \tag{2.51}$$

with arrival vector partial derivatives denoted as

$$\vec{a}^{(p_x,p_y)}(\vec{\omega}_0) \triangleq \left[\frac{\partial^{p_x+p_y}\vec{a}(\vec{\omega})}{\partial\omega_x^{p_x}\partial\omega_y^{p_y}}\right]_{\vec{\omega}=\vec{\omega}_0} \tag{2.52}$$

For 2-D Taylor series, the number of p^{th} order partial derivatives is

$$\bar{n}_p = p+1 \tag{2.53}$$

(i.e. $\bar{n}_0 = 1$, $\bar{n}_1 = 2$, $\bar{n}_2 = 3$, $\bar{n}_3 = 4, \cdots$). The associated vectors that depend on $\vec{q}$ are

$$\vec{\gamma}_0(\vec{q}) = [1]\,, \quad \vec{\gamma}_1(\vec{q}) = \begin{bmatrix} q_x \\ q_y \end{bmatrix}, \quad \vec{\gamma}_2(\vec{q}) = \begin{bmatrix} q_x^2/2 \\ q_x q_y \\ q_y^2/2 \end{bmatrix}, \quad \vec{\gamma}_3(\vec{q}) = \begin{bmatrix} q_x^3/6 \\ q_x^2 q_y/2 \\ q_x q_y^2/2 \\ q_y^3/6 \end{bmatrix} \tag{2.54}$$

The general expression for $\vec{\gamma}_p(\vec{q})$ for 2-D scenarios is

$$\vec{\gamma}_p(\vec{q}) \triangleq \left[c_{0,p}q_x^p,\; c_{1,p}q_x^{p-1}q_y^1,\; \cdots,\; c_{p,p}q_y^p\right]^t \tag{2.55}$$

where

$$c_{i,p} \triangleq \binom{p}{i}\frac{1}{p!} \tag{2.56}$$

$i = 0, \cdots p$, and the first factor of (2.56) is the binomial coefficient.

Expressions analogous to (2.51) and (2.54) can be written for Taylor series of any dimensionality.

The Taylor series of the generic signal vector at each of the source spatial frequencies $\vec{\omega}_1, \cdots \vec{\omega}_M$ is simply (2.49) with corresponding $\vec{q}_1, \cdots \vec{q}_M$. Therefore the Taylor series for matrix A in (2.11) follows directly from (2.49):

$$\begin{aligned} A &= [\vec{a}(\vec{\omega}_1), \cdots \vec{a}(\vec{\omega}_M)] \\ &= \sum_{p=0}^{\infty} \delta\omega^p \dot{A}_p \Gamma_p \end{aligned} \tag{2.57}$$

where matrix $\dot{A}_p$ is as in (2.50), and Γ_p is a constant real $\bar{n}_p \times M$ matrix of the form

$$\Gamma_p \triangleq [\vec{\gamma}_p(\vec{q}_1), \cdots \vec{\gamma}_p(\vec{q}_M)] \tag{2.58}$$

For 2-D scenarios, with $\vec{q}_j = [q_{xj}, q_{yj}]^t$

$$\begin{aligned} \Gamma_0 &= [1, \quad \cdots \quad 1] \\ \Gamma_1 &= \begin{bmatrix} q_{x1}, & \cdots & q_{xM} \\ q_{y1}, & \cdots & q_{yM} \end{bmatrix} \\ \Gamma_2 &= \begin{bmatrix} q_{x1}^2/2, & \cdots & q_{xM}^2/2 \\ q_{x1}q_{y1}, & \cdots & q_{xM}q_{yM} \\ q_{y1}^2/2, & \cdots & q_{yM}^2/2 \end{bmatrix} \\ \Gamma_3 &= \begin{bmatrix} q_{x1}^3/6, & \cdots & q_{xM}^3/6 \\ q_{x1}^2 q_{y1}/2, & \cdots & q_{xM}^2 q_{yM}/2 \\ q_{x1} q_{y1}^2/2, & \cdots & q_{xM} q_{yM}^2/2 \\ q_{y1}^3/6, & \cdots & q_{yM}^3/6 \end{bmatrix} \end{aligned} \tag{2.59}$$

The matrix factor B of R_S is defined in (2.46) in terms of matrix A and constant matrix Π. Since matrix A has Taylor series (2.57), it follows that matrix B also has Taylor series of the form

$$B = A\Pi = \sum_{p=0}^{\infty} \delta\omega^p \dot{A}_p \Gamma_p \Pi \qquad (W \times M) \tag{2.60}$$

with $\dot{A}_p$ as in (2.50), Γ_p as in (2.58) and Π as in (2.47).

2.5.3 Sufficient Conditions for Non-Degenerate Scenarios

Analysis in this thesis is simplified by identification of structural conditions satisfied in typical (i.e. *non-degenerate*) DF scenarios. This section defines these conditions.

Recall from (2.57) that for closely spaced sources, matrix A has a Taylor series of the form

$$A = \sum_{p=0}^{\infty} \delta\omega^p \dot{A}_p \Gamma_p \qquad (W \times M) \tag{2.61}$$

where $\dot{A}_p$ is a constant $W \times \bar{n}_p$ matrix as in (2.50), and Γ_p is a constant $\bar{n}_p \times M$ matrix as in (2.58). The number $\bar{n}_p$ is the number of p^{th} order partial derivatives of the generic arrival vector function $\vec{a}(\vec{\omega})$ with respect to the elements of $\vec{\omega}$.

Reference to (2.51) shows that $\dot{A}_0$ has rank of unity, and successive $\dot{A}_p$ have small and increasing ranks. As a consequence, successive terms of (2.61) are of low and slowly increasing rank, and a number of such terms typically must be included in a partial sum to obtain a full-rank approximation of A. To characterize the minimum number of such terms we define integer parameter m as follows:

Definition of m: Integer m is the smallest number such the partial Taylor sum formed by the successive terms $p = 0, \cdots m$ of (2.61) has full rank.

Provided Conditions **C1-C3** (detailed subsequently) are satisfied, m is determined by the relationship

$$\sum_{p=0}^{m-1} \bar{n}_p < M \leq \sum_{p=0}^{m} \bar{n}_p \tag{2.62}$$

If Conditions **C1-C3** are not all satisfied, m may not be determined by (2.62); in such cases, alternate determining relations are defined in Chapter 7.

Conditions **C1-C3** sufficient for (2.62) to determine m are the following:

C1. The generic arrival vector $\vec{a}(\vec{\omega})$ and its partial derivatives at $\vec{\omega} = \vec{\omega}_0$ up to order $m-1$ with respect to the elements of $\vec{\omega}$ are linearly independent. That is, matrices $\dot{A}_p$ have full rank $\bar{n}_p$ for $p = 0 \cdots m-1$, and the columns of $\dot{A}_p$

are linearly independent from the vector space spanned by the columns of the sequence $\dot{A}_0, \cdots, \dot{A}_{p-1}$ for $p = 1 \cdots m-1$. Specifically,

$$\begin{aligned} \text{Rank}\{\dot{A}_0\} &= \bar{n}_0 \\ \text{Rank}\{P_{[\dot{A}_0, \cdots \dot{A}_{p-1}]} \dot{A}_p\} &= \bar{n}_p \qquad \text{for } p = 1 \cdots m-1 \end{aligned} \tag{2.63}$$

where $P_{[Z]}$ is the notation for the projection onto the nullspace of the columns of Z as defined in Section 2.2.2.

C2. The matrices Γ_p have full rank $\bar{n}_p$ for $p = 0 \cdots m-1$, and the rows of Γ_p are linearly independent from the space spanned by the rows of the sequence $\Gamma_0, \cdots, \Gamma_{p-1}$ for $p = 1 \cdots m-1$. Specifically

$$\begin{aligned} \text{Rank}\{\Gamma_0\} &= \bar{n}_0 \\ \text{Rank}\{\Gamma_p P_{[\Gamma_0^h, \cdots \Gamma_{p-1}^h]}\} &= \bar{n}_p \qquad \text{for } p = 1 \cdots m-1 \end{aligned} \tag{2.64}$$

where $P_{[Z^h]}$ is the notation for the projection onto the nullspace of the rows of Z as defined in Section 2.2.2.

C3. For $p = m$, the component of the product $\dot{A}_m \Gamma_m$ which has columns orthogonal to those of the sequence $\dot{A}_0, \cdots, \dot{A}_{m-1}$ *and* has rows orthogonal to those of the sequence $\Gamma_0, \cdots, \Gamma_{m-1}$ has sufficient rank to complete the rank of A. That is,

$$\text{Rank}\{P_{[\dot{A}_0, \cdots \dot{A}_{m-1}]} \dot{A}_m \Gamma_m P_{[\Gamma_0^h, \cdots, \Gamma_{m-1}^h]}\} = M - \sum_{p=0}^{m-1} \bar{n}_p \tag{2.65}$$

Conditions **C1-C2** are central the simplified SVD analysis of matrix A. Condition **C3** is sufficient to guarantee that m determined by (2.62) is such that the partial Taylor series consisting of terms of order $p = 0$ through $p = m$, does in fact have full rank M.

Condition **C1** depends upon the array geometry and sensor directional response, and is independent of source configuration or source powers and correlations. Condition **C2** depends only upon the normalized source coordinates $\vec{q}_j$ $(j = 1 \cdots M)$. Thus

C2 depends only upon normalized source configuration, and is independent of the array geometry, sensor directional response, or source powers and correlations.

Note that Conditions **C1-C3** assume (require) that matrix A have more columns than rows ($W > M$), and that matrix A be full rank ($= M$). These pre-requisites are satisfied under thesis Assumptions **A1-A3**.

Thesis analysis of the eigenstructure of R_S and of the CR bound B_C for closely spaced sources exploits Conditions **C1**, **C2** and **C3**. Additional Conditions are defined in Chapter 8 to facilitate CR bound analysis; these additional conditions are simply Conditions **C1-C3** applied to a augmented matrix which includes matrix A and additional columns.

For convenience, scenarios which satisfy Conditions **C1**, **C2** and **C3**, are designated as *non-degenerate scenarios.* Examples show that Conditions **C1-C3** are satisfied for typical DF scenarios.

Furthermore, scenarios which satisfy only one of Conditions **C1** or **C2**, are designated as *partially degenerate scenarios.* Partially degenerate scenarios are of second-order interest in DF applications, and are addressed in the thesis primarily to contrast with non-degenerate scenarios. Completely degenerate scenarios for which none of the conditions are satisfied are of third-order interest in DF applications, and hence are not addressed in this thesis.

Example scenarios are presented in the next section to illustrate non-degenerate and partially degenerate scenarios.

2.6 Example Direction Finding Scenarios

We introduce three example direction finding scenarios which will be used in numerical simulations to illustrate thesis results. All three examples build upon the 2-D scenario of Example 2.1 which addressed a planar array of identical, unit-gain isotropic sensors observing a cluster of far-field sources. Example 2.3 is a non-degenerate scenario for which Conditions **C1-C3** are satisfied. Examples 2.4 and 2.5 are partially degenerate scenarios which respectively satisfy Condition **C1** or **C2**.

Each example involves a planar array of $W = 16$ unit-gain, isotropic sensors, and $M = 6$ far-field sources clustered near to the array broadside.

The generic arrival vector takes the form

$$\vec{a}(\vec{\omega}) \;=\; \left[e^{j\vec{r}_1^t\vec{\omega}},\; e^{j\vec{r}_2^t\vec{\omega}},\; \cdots,\; e^{j\vec{r}_W^t\vec{\omega}}\right]^t \tag{2.66}$$

where $\vec{r}_i = [r_{xi}, r_{yi}]^t$ is the location of the i^{th} sensor in sensor plane. The reference parameter vector $\vec{\omega}_0$ is taken to be at array broadside (elevation angle $\phi = 90°$). From (2.13) we have

$$\vec{\omega}_0 \;=\; [0,\; 0]^t \tag{2.67}$$

Matrices $\dot{A}_0$, $\dot{A}_1$, $\dot{A}_2$ and $\dot{A}_3$ of (2.51) then are

$$\dot{A}_0 = \begin{bmatrix} 1 \\ \vdots \\ 1 \end{bmatrix},\; \dot{A}_1 = j\cdot\begin{bmatrix} r_{x1} & r_{y1} \\ \vdots & \vdots \\ r_{xW} & r_{yW} \end{bmatrix},\; \dot{A}_2 = -1\cdot\begin{bmatrix} r_{x1}^2 & r_{x1}r_{y1} & r_{y1}^2 \\ \vdots & \vdots & \vdots \\ r_{xW}^2 & r_{xW}r_{yW} & r_{yW}^2 \end{bmatrix}$$

$$\dot{A}_3 = -j\cdot\begin{bmatrix} r_{x1}^3 & r_{x1}^2 r_{y1} & r_{x1}r_{y1}^2 & r_{y1}^3 \\ \vdots & \vdots & \vdots & \vdots \\ r_{xW}^3 & r_{xW}^2 r_{yW} & r_{xW}r_{yW}^2 & r_{yW}^3 \end{bmatrix} \tag{2.68}$$

The three example scenarios are defined as follows.

Example 2.3 : For this example, the array and source geometries are as follows.

Array: Sensors in a sparse grid per Figure 2-4A,

Sources: Sources clustered around broadside in a "double chevron" configuration per Figure 2-5A.

It can be verified that the columns of $\dot{A}_0$, $\dot{A}_1$, $\dot{A}_2$, and $\dot{A}_3$ in (2.68) are all linearly independent for this sensor array. Similarly, the rows of Γ_0, Γ_1, Γ_2 given by (2.59) with $M = 6$ are all linearly independent for this source configuration. Thus the partial Taylor sum of A with terms $p = 0, 1, 2$ is full rank $M = 6$,

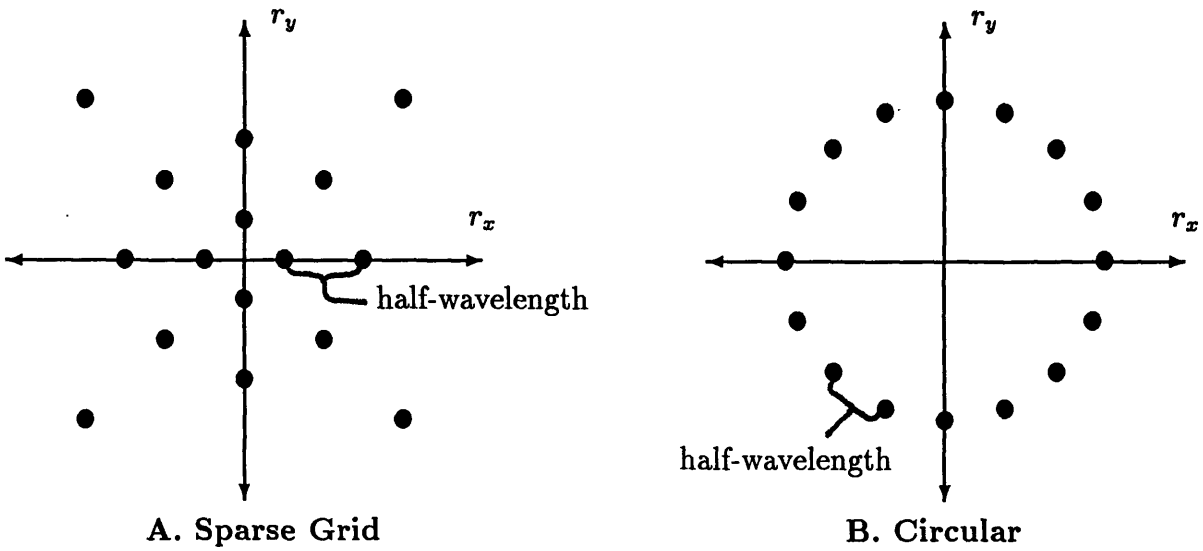

Figure 2-4: Example Planar Sensor Array Geometries

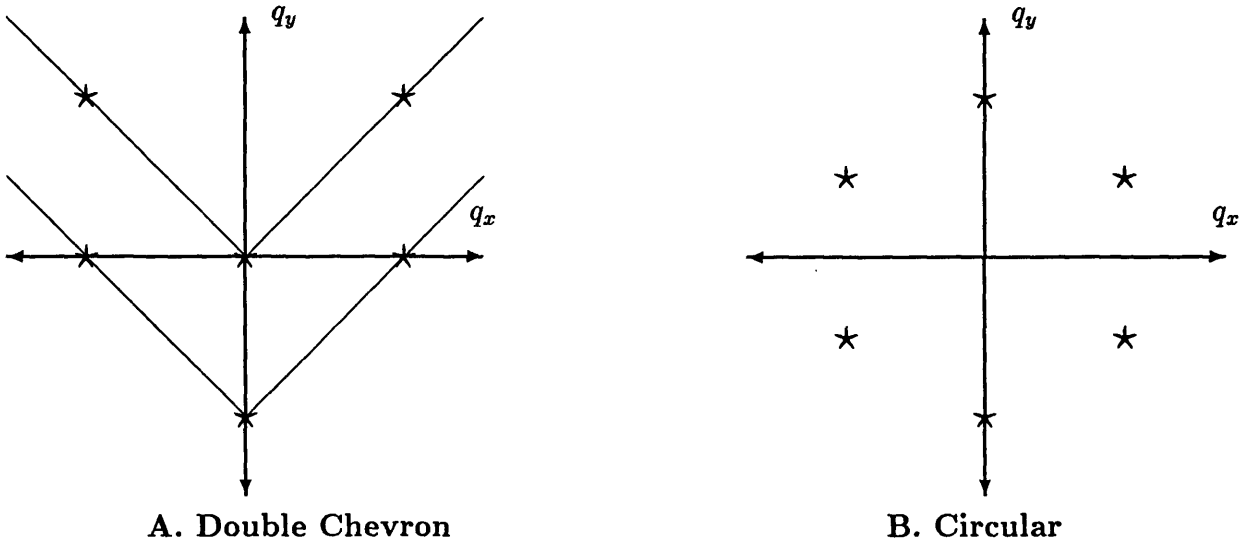

Figure 2-5: Example Far-Field Source Normalized Configurations

and thus $m = 2$. Consequently, Conditions **C1, C2, C3** are all satisfied with $m = 2$; this is an example of a non-degenerate scenario.

Example 2.4 : For this example, the array and source geometries are as follows.

Array: Sensors in a sparse grid per Figure 2-4A,

Sources: Sources clustered around broadside in a circular configuration per Figure 2-5B.

The sensor array is unchanged from Example 2.3, hence the columns of $\dot{A}_0$, $\dot{A}_1$, $\dot{A}_2$, $\dot{A}_3$ are again all linearly independent. The rows of Γ_0, Γ_1, and Γ_2 are given by (2.59) with $M = 6$. It is clear from the figure that the rows of Γ_0, Γ_1, and Γ_2 *are not linearly independent* for this source configuration since the normalized source parameters satisfy the circle equation

$$q_{xj}^2 + q_{yj}^2 \;=\; c \tag{2.69}$$

wtih constant c for all $j = 1 \cdots M$, and the rows of Γ_0 and Γ_2 are linearly dependent. The additional Γ_3 term is required to fully span the row space of matrix A. In this example the partial Taylor sum of A with terms $p = 0, 1, 2$ is not full rank, but the sum over $p = 0, 1, 2, 3$ is full rank $M = 6$, and thus $m = 3$. Consequently, Condition **C1** is satisfied, but Conditions **C2, C3** are not. This is an example of a partially degenerate scenario which satisfies Condition **C1** only. We designate the scenario as *source configuration degenerate.*

Example 2.5 : For this example, the array and source geometries are as follows.

Array: Sensors in a circular geometry per Figure 2-4B,

Sources: Sources clustered around broadside in a "double chevron" configuration per Figure 2-5A.

The source configuration is unchanged from Example 2.3, hence the rows of Γ_0, Γ_1, and Γ_2 are all linearly independent. For this sensor array, the columns of

$\dot{A}_0$, $\dot{A}_1$ and $\dot{A}_2$ *are not linearly independent* since the sensor location parameters satisfy the circle equation

$$r_{xi}^2 + r_{yi}^2 \;=\; c' \tag{2.70}$$

with constant c' for all $i = 1 \cdots W$, and the columns of $\dot{A}_0$ and $\dot{A}_2$ are linearly dependent. The additional $\dot{A}_3$ term is required to fully span the column space of matrix A. In this example the partial Taylor sum of A with terms $p = 0, 1, 2$ is again not full rank, but the sum over $p = 0, 1, 2, 3$ is full rank $M = 6$, and thus $m = 3$. Consequently, Condition **C2** is satisfied, but Conditions **C1, C3** are not. This is an example of a partially degenerate scenario which satisfies Condition **C2** only. We designate the scenario as *array geometry degenerate.*

Chapter 3

Prior Results on Eigenstructure of Perturbed Matrices

This chapter reviews prior results on eigenstructure of perturbed matrices which are relevant to identifying the eigenstructure of asymptotic signal covariance matrix R_S for closely-spaced sources in multi-D direction finding scenarios. For the data model addressed, matrix R_S is Hermitian of the form

$$R_S = APA^h \qquad W \times W \tag{3.1}$$

where A is the matrix (2.11) of generic arrival vectors for each of the sources, P is the Hermitian positive definite asymptotic source amplitude cross-power matrix (2.15), and W denotes the number of sensors.

Recently published work by Lee [12] has shown that for closely spaced sources in 1-D direction finding scenarios, the limiting eigenstructure of R_S, as source separation $\delta\omega \rightarrow 0$, can be determined simply without eigenanalysis. For example, for a typical 1-D scenario with M sources and fewer sources than sensors ($M < W$), each of the M non-zero limiting eigenvalues of R_S is shown to be proportional to a different power of $\delta\omega^2$, from $\delta\omega^0$ to $\delta\omega^{2(M-1)}$. The proportionality constant for each limiting eigenvalue is determined by straightforward linear algebra operations. The corresponding limiting eigenvectors are shown to be the generic signal vector and its

spatial derivatives in the source cluster direction, suitably orthonormalized. Thus the eigendecomposition of R_S for closely spaced sources in 1-D scenarios is reduced to simple linear algebra operations. In addition, the dependence of eigenvalues and eigenvectors of R_S on scenario parameters such as maximum source spacing $\delta\omega$ is made explicit. Unfortunately, the approach used to derive the results of [12] exploits simplifications unique to 1-D scenarios, and thus extension of the approach to multi-D scenarios is not readily apparent.

Fundamental results regarding the eigenvalues and eigenvectors of square matrices with Taylor series in any small perturbation factor ϵ have been developed by Kato [17], and extended by Coderch, Willsky, Sastry, and Castanon [18]. The authors show that the limiting (as $\epsilon \rightarrow 0$) eigenvalues and the span of the corresponding eigenvectors can be identified by eigenanalysis of a sequence of low rank, constant matrices, designated as *limiting eigenmatrices* herein. In principle, this approach is applicable to identifying the eigenstructure of R_S for closely spaced sources in multi-D scenarios, with the identification $\epsilon = \delta\omega$. Unfortunately, in order to determine the limiting eigenmatrices for the general eigenstructure problem addressed in [17], [18], the authors derive expressions which are implicit and quite complex (compared to the intuitively simple 1-D R_S eigenstructure results of [12]). The complexity of these results typically precludes an explicit analytical identification of the number of limiting eigenvalues proportional to each power of $\delta\omega$, or of the span of the corresponding eigenvectors.

The thesis objective with regard to the eigenstructure of R_S is to obtain simple and explicit multi-D results, analogous to the 1-D results of [12], which make explicit the dependence of R_S eigenstructure on scenario parameters in multi-D direction finding scenarios. This chapter reviews the prior eigenstructure results of [12], and of [17], [18]. Chapters 4-7 build upon these prior results to derive simple expressions for the eigenstructure of R_S in multi-D scenarios.

3.1 Eigenstructure of R_S in 1-D [12]

The eigenstructure of a number of common covariance matrices has been identified by Lee [12] for M closely spaced signals with scalar frequency parameters. The limiting eigenstructures, as signal spacing $\delta\omega \rightarrow 0$, are remarkably simple. The results of [12] applicable to covariance matrix R_S in 1-D direction finding scenarios are outlined below.

Reference [12] considers square matrices of the form

$$R_1 \triangleq APA^h \qquad (W \times W) \tag{3.2}$$

where P is a constant $M \times M$ Hermitian positive definite matrix, A is of the form (2.11), satisfies assumptions **A1-A4**, and Conditions **C1-C3** with $m = M - 1$. The signal frequencies are represented by scalar frequency parameters $\omega_1 \cdots \omega_M$ as follows:

$$\omega_j = \omega_0 + q_j \delta\omega \tag{3.3}$$

$j = 1 \cdots M$. Here ω_0 denotes a fixed reference frequency, the q_j are normalized offsets such that $q_1 < q_2 < \cdots q_M$ with $q_1 = -1/2$ and $q_M = +1/2$, and $\delta\omega$ is a variable scale parameter corresponding to the separation of the extreme frequencies. The paper analyzed the eigenstructure of (3.2) as the multiplier $\delta\omega \rightarrow 0$. Representation (3.3) facilitates analysis of the eigenstructure of R_1 since the problem is reduced to one with a single variable parameter $\delta\omega$. The condition $\delta\omega \rightarrow 0$ corresponds to coalescing the signal frequencies about the reference frequency ω_0.

Reference [12] identifies explicit expressions for the eigenstructure of R_1 in terms of the coefficients of the Taylor series of A. Following the notation in Section 2.5.2, matrix A has a Taylor series in $\delta\omega$ about ω_0 of the form

$$A = \sum_{p=0}^{\infty} \delta\omega^p A_p \tag{3.4}$$

where

$$A_p = \dot{A}_p \Gamma_p \tag{3.5}$$

with

$$\dot{A}_p = \left. \frac{d^p \vec{a}(\omega)}{d\omega^p} \right|_{\omega=\omega_0} \tag{3.6}$$

$$\Gamma_p = [q_1^p/p!, \cdots q_M^p/p!] \tag{3.7}$$

for $p = 0, 1 \cdots$, where $\vec{a}(\omega)$ is the generic arrival vector function of ω, and $q_1, \cdots q_M$ are the normalized frequency offsets in (3.3).

The R_1 eigenstructure results of [12] are as follows:

E1. The non-zero ordered eigenvalues $\lambda_1(\delta\omega) \geq \lambda_2(\delta\omega) \geq \cdots \geq \lambda_M(\delta\omega)$ of matrix (3.2) are asymptotically (as $\delta\omega \rightarrow 0$) proportional to *non-negative even integer* powers of $\delta\omega$. That is

$$\lim_{\delta\omega \to 0} \left\{ \frac{\lambda_i(\delta\omega)}{\lambda_i \cdot \delta\omega^{2(i-1)}} \right\} = 1 \tag{3.8}$$

$i = 1, \cdots M$, where λ_i is the positive constant

$$\lambda_i = \frac{\left| \left[\Gamma_0^h, \cdots \Gamma_i^h\right]^h P \left[\Gamma_0^h, \cdots \Gamma_i^h\right] \right|}{\left| \left[\Gamma_0^h, \cdots \Gamma_{i-1}^h\right]^h P \left[\Gamma_0^h, \cdots \Gamma_{i-1}^h\right] \right|} \frac{\left| \left[\dot{A}_0 \cdots \dot{A}_i\right]^h \left[\dot{A}_0 \cdots \dot{A}_i\right] \right|}{\left| \left[\dot{A}_0 \cdots \dot{A}_{i-1}\right]^h \left[\dot{A}_0 \cdots \dot{A}_{i-1}\right] \right|} \tag{3.9}$$

where $\dot{A}_p$ and Γ_p are the factors (3.6), (3.7) of Taylor series matrix coefficients A_p in (3.5). P is the asymptotic source amplitude cross-power matrix (2.15). Notation $|\cdot|$ represents matrix determinant. (See Equations (3), (71) of [12]).

E2. The corresponding eigenvectors $\vec{e}_1(\delta\omega), \vec{e}_2(\delta\omega), \cdots \vec{e}_M(\delta\omega)$ of matrix (3.2) have the limiting form

$$\lim_{\delta\omega \to 0} \vec{e}_i(\delta\omega) = \vec{e}_i \tag{3.10}$$

where the $\vec{e}_i$ are constant vectors corresponding to the generic arrival vector $\vec{a}(\omega)$ and its derivatives, suitably orthonormalized. Specifically,

$$\begin{aligned} \vec{e}_0 &= c_0 \dot{A}_0 \\ \vec{e}_i &= c_i P_{[\dot{A}_0 \cdots \dot{A}_{i-1}]} \dot{A}_i \qquad\qquad i = 1 \cdots M \end{aligned} \tag{3.11}$$

where c_i are normalizing constants so that $\vec{e}_i^h \vec{e}_i = 1$, and $P_{[Z]}$ denotes the column nullspace projection defined in Section 2.2.2. (See Equations (4), (54) of [12]).

Remarkably the quantities λ_i and $\vec{e}_i$ in (3.9) and (3.11) are calculated via linear algebra operations; eigenanalysis and the associated polynomial rooting are *not required.* The identified eigenstructure, together with classical perturbation techniques, provides a powerful tool for analyzing the performance of High Resolution techniques in 1-D scenarios.

Unfortunately, the simple results **E1** and **E2** apply only to 1-D scenarios. For multi-D scenarios, matrices $\dot{A}_i$ have more than one column and Γ_i have more than one row. It is not immediately clear how to extend the analysis to multi-D scenarios.

3.2 Eigenstructure of Arbitrary Hermitian Perturbed Matrices [17], [18]

Fundamental results regarding the perturbation of linear operators have been developed by Kato [17] including results for eigenvalues and eigenvectors of perturbed square matrices. The eigenvalue perturbation results of [17] have been simplified by Coderch et al. [18]. Results of [17], [18] relevant to analysis in this thesis are outlined below.

Reference [18] considers a square matrix $A_0(\epsilon)$ with Taylor series about $\epsilon = 0$

$$A_0(\epsilon) = \sum_{p=0}^{\infty} \epsilon^p A_{0,p} \tag{3.12}$$

where $A_{0,p}$ are known constant matrices, independent of variable parameter ϵ. For

present purposes, we consider the results applicable to *Hermitian* matrices $A_0(\epsilon)$, (for which $A_0(\epsilon)^h = A_0(\epsilon)$), which form a sub-class of the more general matrices addressed in [17], [18].

The analysis in [17], [18] derives the following result:

R1. For any Hermitian $A_0(\epsilon)$ with Taylor series in ϵ, each non-zero eigenvalue $\lambda_i(\epsilon)$ is asymptotically (as $\epsilon \rightarrow 0$) proportional to a *non-negative integer* power of ϵ. That is,

$$\lim_{\epsilon \rightarrow 0} \left\{ \frac{\lambda_i(\epsilon)}{\lambda_i \cdot \epsilon^{k_i}} \right\} = 1 \tag{3.13}$$

for suitable constants λ_i and $k_i \in \{0, 1 \cdots\}$, for all $i = 1, \cdots,$ rank$\{A_0(\epsilon)\}$. (See text following Eq (4.10) of [18]).

For convenience, we designate the $\lambda_i \epsilon^{k_i}$ as *limiting eigenvalues* of $A_0(\epsilon)$. Limiting eigenvalues of $A_0(\epsilon)$ proportional to ϵ^0 (i.e. constant) as $\epsilon \rightarrow 0$ can be identified directly from (3.12) as the constant non-zero eigenvalues of leading Taylor series term $A_{0,0}$.

To characterize the remaining limiting eigenvalues of $A_0(\epsilon)$, the development in [17], [18] recursively defines a sequence of constant Hermitian matrices $A_{k,0}$ and establishes the results:

R2. The non-zero eigenvalues of $A_{k,0}$ are the constants λ_i in limiting eigenvalues of $A_0(\epsilon)$ of the form $\lambda_i \epsilon^k$. (See Part 3 of Proposition 4.4 of [18]).

R3. The column space of $A_{k,0}$ is spanned by the limiting eigenvectors of $A_0(\epsilon)$ associated with the group of limiting eigenvalues proportional to ϵ^k as $\epsilon \rightarrow 0$. (See Section 4.1, Chapter II of [17]).

The essence of these results is that:

- eigenvalues of $A_0(\epsilon)$ that tend to non-zero constants as $\epsilon \rightarrow 0$, have as limiting values the non-zero eigenvalues of $A_{0,0}$. The corresponding limiting eigenvectors of $A_0(\epsilon)$ are the principal eigenvectors of $A_{0,0}$ [assuming distinct eigenvalues],

- eigenvalues of $A_0(\epsilon)$ that exhibit the behavior $\lambda_i\epsilon^1$ as $\epsilon \rightarrow 0$, have as multipliers λ_i the non-zero eigenvalues of $A_{1,0}$. The corresponding limiting eigenvectors of $A_0(\epsilon)$ are the principal eigenvectors of $A_{1,0}$ [assuming distinct eigenvalues],

- etc.

Accordingly, if the $A_{k,0}$ were readily available, straightforward analysis of the low-rank constant $A_{k,0}$ would reveal the limiting eigenvalues and the limiting span of the eigenvectors of $A_0(\epsilon)$, [or the limiting eigenvectors of $A_0(\epsilon)$ directly, assuming distinct eigenvalues]. For convenience, we designate the $A_{k,0}$ as the *limiting eigenmatrices* of $A_0(\epsilon)$.

Unfortunately for many matrices $A_0(\epsilon)$, the expressions for the $A_{k,0}$ in terms of the constant matrices $A_{0,p}$ which appear in the Taylor series (3.12) are quite complex. Reference [17] derives very complicated, recursive formulations using function theory that identify the limiting eigenmatrices $A_{k,0}$ for all $k > 0$. Reference [18] builds upon the results of [17] to derive the following simplified recursive expressions for $A_{k,0}$ for $k = 0, 1, 2, 3$, in terms of the matrix coefficients $A_{0,p}$ in the Taylor series of a Hermitian matrix $A_0(\epsilon)$:

$$\begin{aligned}
A_{0,0} &= A_{0,0} \\
A_{1,0} &= P_0 A_{0,1} P_0 \\
A_{2,0} &= P_1 P_0 \left(A_{0,2} - A_{0,1} A_{0,0}^{+} A_{0,1} \right) P_0 P_1 \\
A_{3,0} &= P_2 P_1 P_0 \left(A_{0,3} - A_{0,1} A_{0,0}^{+} A_{0,2} - A_{0,2} A_{0,0}^{+} A_{0,1} \right. \\
&\quad + A_{0,1} A_{0,0}^{+} A_{0,1} A_{0,0}^{+} A_{0,1} - A_{0,2} (P_0 A_{0,1} P_0)^{+} A_{0,2} \\
&\quad + A_{0,2} (P_0 A_{0,1} P_0)^{+} A_{0,1} A_{0,0}^{+} A_{0,1} + A_{0,1} A_{0,0}^{+} A_{0,1} (P_0 A_{0,1} P_0)^{+} A_{0,2} \\
&\quad \left. - A_{0,1} A_{0,0}^{+} A_{0,1} (P_0 A_{0,1} P_0)^{+} A_{0,1} A_{0,0}^{+} A_{0,1} \right) P_0 P_1 P_2
\end{aligned} \tag{3.14}$$

(Proposition 4.12 of [18], with a sign correction). The $A_{0,p}$ are the known matrix coefficients of Taylor series (3.12), while the P_k, defined *recursively* as

$$P_k \triangleq I - A_{k,0} A_{k,0}^{+} \tag{3.15}$$

are projections onto the null space of the limiting eigenmatrices. The definition of $A_{k,0}$ used in [17], [18] and an outline of the derivation of expressions (3.14) is presented in Appendix B.

Although the foregoing results theoretically characterize the limiting eigenstructure of Hermitian $A_0(\epsilon)$, they do not provide much insight into the limiting eigenstructure. For example, reference to the expression for $A_{3,0}$ in (3.14) reveals little about:

- the rank of $A_{3,0}$, and, therefore, the number of eigenvalues of $A_0(\epsilon)$ which satisfy (3.13) with $k_i = 3$.
- the vector space spanned by the corresponding eigenvectors.

Furthermore, even the simplified expressions (3.14) for $A_{k,0}$ rapidly become complicated as k increases. Expressions for $k > 3$ are not provided in References [17], [18] and are extremely laborious to derive from the recursive approach of Reference [17]. Finally, it is not immediately clear how to simplify these expressions to obtain the simple R_S eigenstructure of [12] for 1-D direction finding scenarios.

A major result of this thesis is the identification of very simple expressions for limiting eigenmatrices $A_{k,0}$ whenever $A_0(\epsilon)$ satisfies conditions which are characteristic of R_S in typical multi-D direction finding scenarios (specifically Conditions **C1**, **C2** and **C3** of Chapter 2). The multi-D expressions derived herein extend the simple, explicit expressions obtained for 1-D by Lee in [12] to multi-D DF scenarios.

Chapter 4

SVD of Perturbed Matrices

The limiting eigenstructure results of References [17], [18] apply to square Hermitian matrices $A_0(\epsilon)$ with Taylor series in ϵ. This chapter develops analogous results for the SVD structure of rectangular matrices $B_0(\epsilon)$ with Taylor series in ϵ, including non-Hermitian or non-diagonalizable square matrices. The SVD results developed in this chapter facilitate identification of the limiting eigenstructure of asymptotic signal covariance matrix R_S. They also may have use in other applications.

Recall from Section 2.5.1 that R_S can be factored as

$$R_S = BB^h \qquad (W \times W) \tag{4.1}$$

in terms of rectangular matrix B with Taylor series

$$B = \sum_{p=0}^{\infty} \delta\omega^p B_p \qquad (W \times M) \tag{4.2}$$

where $\delta\omega$ is a scalar measure of the maximum angular separation between the sources, and the Taylor series matrix coefficients B_p are identified in (2.60). If the SVD of B can be identified, then the eigenstructure of R_S follows immediately from (4.1). From (4.1) and the definition of the SVD, the non-zero eigenvalues of R_S are the squares of the non-zero singular values of B, and the eigenvectors of R_S are the corresponding left singular vectors (defined subsequently) of B. Thus identification of

the limiting SVD of rectangular matrix B is an important enabling step for identifying the eigenstructure of covariance R_S.

To parallel the notation of the eigenstructure analysis of [18], this chapter assumes that the matrix of interest is $B_0(\epsilon)$ and can be expressed as a Taylor series

$$B_0(\epsilon) \triangleq \sum_{p=0}^{\infty} \epsilon^p B_{0,p} \qquad (W \times M) \tag{4.3}$$

where $B_{0,p}$ are known constant matrices, independent of variable parameter ϵ.

Any rectangular matrix possesses a singular value decomposition (SVD) [21, Appendix A]. For matrix $B_0(\epsilon)$, the SVD takes the form

$$B_0(\epsilon) = U(\epsilon)\,\Sigma(\epsilon)\,V(\epsilon)^h \qquad (W \times M) \tag{4.4}$$

where the columns of $W \times W$ unitary matrix $U(\epsilon)$ are orthonormal eigenvectors of $B_0(\epsilon)B_0(\epsilon)^h$, the columns of $M \times M$ unitary matrix $V(\epsilon)$ are orthonormal eigenvectors of $B_0(\epsilon)^h B_0(\epsilon)$, and the only non-zero entries of the $W \times M$ matrix $\Sigma(\epsilon)$ are the *singular values* on the main diagonal, defined as positive square roots of nonzero eigenvalues of $B_0(\epsilon)B_0(\epsilon)^h$. For convenience, this thesis refers to the columns of $U(\epsilon)$ as the *left singular vectors* and to the columns of $V(\epsilon)$ as the *right singular vectors* of $B_0(\epsilon)$.

Analysis in this chapter identifies the limiting singular values and corresponding singular vectors of $B_0(\epsilon)$ as $\epsilon \to 0$. The results represent an extension of Kato-Coderch eigenstructure results to the SVD problem. Side conditions are identified which enormously simplify the SVD results; these conditions are satisfied in typical direction finding scenarios. The SVD results not only provide a convenient tool for the R_S eigenstructure problem, but may also themselves constitute important results for other applications.

The development in this chapter begins in Section 4.1 with the identification of simplifying side conditions. Section 4.2 specializes the prior eigenstructure results of [17], [18] to the Hermitian matrices that arise in the SVD of $B_0(\epsilon)$, namely the inner and outer products of matrices $B_0(\epsilon)$ with Taylor series in ϵ. These specialized results,

together with the prior limiting eigenstructure results of [17], [18], form the basis for analysis of the limiting SVD of $B_0(\epsilon)$ in Section 4.3. Section 4.4 develops an enabling property that characterizes the limiting SVD of any matrix $B_0(\epsilon)$ with Taylor series in ϵ. Section 4.5 then exploits this characterization to develop remarkably simple expressions for the limiting SVD of matrices $B_0(\epsilon)$ that satisfy all the identified side conditions. Section 4.6 similarly develops somewhat more complicated expressions for the limiting SVD of matrices $B_0(\epsilon)$ that satisfy some, but not all side conditions. The SVD results are summarized in Section 4.7, and illustrative examples are presented in Section 4.8.

4.1 Simplifying Conditions

This section defines side conditions which greatly simplify the SVD analysis. The side conditions generalize Conditions **C1-C3** of Section 2.5.3 to an arbitrary matrix $B_0(\epsilon)$.

As a first step, we denote the rank of $B_0(\epsilon)$ for small, but non-zero ϵ as

$$\mathcal{R} \triangleq \text{Rank}\,\{B_0(\epsilon)\} \tag{4.5}$$

We recall that $B_0(\epsilon)$ has Taylor series (4.3). To characterize the minimum number of terms of (4.3) required for a partial Taylor sum to have rank $\mathcal{R}$, we define integer parameter $\tilde{m}$ as follows:

Definition of $\tilde{m}$: Integer $\tilde{m}$ is the smallest number such the partial Taylor sum formed by the successive terms $p = 0, \cdots \tilde{m}$ of (4.3) has full rank.

Provided Conditions I-III (detailed subsequently) are satisfied, $\tilde{m}$ is determined by the relationship

$$\sum_{p=0}^{\tilde{m}-1} \text{Rank}\,\{B_{0,p}\} \;<\; \mathcal{R} \;\leq\; \sum_{p=0}^{\tilde{m}} \text{Rank}\,\{B_{0,p}\} \tag{4.6}$$

where $B_{0,p}$ are the matrix coefficients of the Taylor series (4.3). If Conditions I-III

are not all satisfied, $\tilde{m}$ may not be determined by (4.6); in such cases, alternate determining relations are defined Section 4.6.

For convenience, we denote

$$C_{p-1} \triangleq [B_{0,0}, \cdots B_{0,p-1}] \tag{4.7}$$

$$R_{p-1} \triangleq \left[B^h_{0,0}, \cdots B^h_{0,p-1}\right] \tag{4.8}$$

to respectively aggregate the columns and rows of the Taylor series matrix coefficient sequence $B_{0,0}, \cdots B_{0,p-1}$.

Conditions I-III sufficient for (4.6) to determine $\tilde{m}$ are the following:

$$\textbf{I.} \quad \text{Rank}\{P_{[C_{p-1}]}B_{0,p}\} = \text{Rank}\{B_{0,p}\} \qquad \text{for } p = 1, \cdots \tilde{m}-1 \tag{4.9}$$

$$\textbf{II.} \quad \text{Rank}\{B_{0,p}\, P_{[R_{p-1}]}\} = \text{Rank}\{B_{0,p}\} \qquad \text{for } p = 1, \cdots \tilde{m}-1 \tag{4.10}$$

$$\textbf{III.} \quad \text{Rank}\{P_{[C_{\tilde{m}-1}]}B_{0,\tilde{m}}\, P_{[R_{\tilde{m}-1}]}\} = \mathcal{R} - \sum_{p=0}^{\tilde{m}-1} \text{Rank}\{B_{0,p}\} \tag{4.11}$$

where matrix $P_{[C_{p-1}]}$ denotes the projection away from the vector space spanned by the columns of the Taylor series matrix coefficient sequence $B_{0,0}, \cdots B_{0,p-1}$, namely

$$P_{[C_{p-1}]} \triangleq I - [B_{0,0},\, B_{0,1},\, \cdots B_{0,p-1}]\,[B_{0,0},\, B_{0,1},\, \cdots B_{0,p-1}]^+ \tag{4.12}$$

for $p \geq 1$. Similarly $P_{[R_{p-1}]}$ denotes the projection away from the vector space spanned by the rows of the sequence $B_{0,0}, \cdots B_{0,p-1}$, namely

$$\begin{aligned} P_{[R_{p-1}]} &\triangleq I - \left[B^h_{0,0},\, B^h_{0,1},\, \cdots B^h_{0,p-1}\right]\left[B^h_{0,0},\, B^h_{0,1},\, \cdots B^h_{0,p-1}\right]^+ \\ &= I - \begin{bmatrix} B_{0,0} \\ B_{0,1} \\ \vdots \\ B_{0,p-1} \end{bmatrix}^+ \begin{bmatrix} B_{0,0} \\ B_{0,1} \\ \vdots \\ B_{0,p-1} \end{bmatrix} \end{aligned} \tag{4.13}$$

for $p \geq 1$.

We interpret Condition I-III as follows.

- Condition I specifies that the *column space* of Taylor series matrix coefficient $B_{0,p}$ is *linearly independent* from those of prior coefficients $B_{0,0}, \cdots B_{0,p-1}$, for $p = 0 \cdots \tilde{m} - 1$.

- Similarly, Condition II specifies that the *row space* of $B_{0,p}$ is *linearly independent* from those of $B_{0,0}, \cdots B_{0,p-1}$, for $p = 0 \cdots \tilde{m} - 1$.

- Finally, Condition III specifies that the component of Taylor series matrix coefficient $B_{0,\tilde{m}}$ which has *orthogonal columns and rows* from those of prior coefficients $B_{0,0}, \cdots B_{0,\tilde{m}-1}$, has sufficient rank to complete the span of $B_0(\epsilon)$.

Conditions I and II are central to the simplified SVD analysis. Condition III is sufficient to guarantee that $\tilde{m}$ determined by (4.6) is such that the partial Taylor series of $B_0(\epsilon)$ consisting of terms of order $p = 0$ through $p = \tilde{m}$, does in fact have rank $\mathcal{R}$. We will find that whenever Conditions I, II and III are satisfied, the limiting SVD of $B_0(\epsilon)$ as $\epsilon \rightarrow 0$ is entirely determined by the terms of (4.3) from $B_{0,0}$ to $B_{0,\tilde{m}}$; subsequent terms only add higher order effects.

Note that Conditions I-III do not place any restriction on the size or rank of $B_0(\epsilon)$. Specifically, Conditions I-III may be satisfied by arbitrarily sized matrices $B_0(\epsilon)$ (i.e. $M < W$, $M = W$ or $M > W$), with partial rank or full rank (i.e. $\mathcal{R} \leq \min\{M, W\}$).

We designate matrices $B_0(\epsilon)$ that satisfy Conditions I-III as *non-degenerate matrices.* We designate matrices $B_0(\epsilon)$ that satisfy only one of Conditions I or II as *partially degenerate matrices.*

Analysis in the next sections develops a partial characterization of the limiting SVD of any matrix $B_0(\epsilon)$ for small ϵ. Section 4.4 then identifies a simple and explicit characterization of the limiting SVD of non-degenerate $B_0(\epsilon)$. Section 4.5 further identifies a more complicated characterization of the limiting SVD of partially degenerate $B_0(\epsilon)$.

4.2 Specialization of Prior Eigenstructure Results

The point of departure of our SVD analysis are the prior results of [17], [18] for the limiting eigenstructure of Hermitian matrices $A_0(\epsilon)$. Since the SVD of $B_0(\epsilon)$ is defined in terms of the eigendecomposition of $B_0(\epsilon)B_0(\epsilon)^h$ and $B_0(\epsilon)^h B_0(\epsilon)$, this section specializes the results of [17], [18] for Hermitian $A_0(\epsilon)$ which are products of matrices $B_0(\epsilon)$ with Taylor series in ϵ. Specifically, we examine the limiting eigenstructure of matrices $A_0(\epsilon)$ that satisfy

Condition IV. Matrices $A_0(\epsilon)$ are the outer product

$$A_0(\epsilon) \;=\; B_0(\epsilon)B_0(\epsilon)^h \qquad (W \times W) \tag{4.14}$$

of rectangular matrix $B_0(\epsilon)$ with Taylor series

$$B_0(\epsilon) = \sum_{p=0}^{\infty} \epsilon^p B_{0,p} \qquad (W \times M) \tag{4.15}$$

where $B_{0,p}$ are constant low-rank rectangular matrices, independent of ϵ. Clearly $A_0(\epsilon)$ is Hermitian and has a Taylor series in ϵ.

Matrices $A_0(\epsilon)$ that satisfy Condition IV are outer products of matrices $B_0(\epsilon)$, and the $B_0(\epsilon)$ have Taylor series in ϵ. The first result derived characterizes eigenvalues of such $A_0(\epsilon)$ more precisely than prior result **R1** of Section 3.2.

Lemma 4.1 : If matrix $A_0(\epsilon)$ satisfies Condition IV, then each non-zero eigenvalue $\lambda_i(\epsilon)$ of $A_0(\epsilon)$ is asymptotically (as $\epsilon \to 0$) proportional to non-negative *even* powers of ϵ. That is,

$$\lim_{\epsilon \to 0} \left\{ \frac{\lambda_i(\epsilon)}{\lambda_i \cdot \epsilon^{2k_i}} \right\} \;=\; 1 \tag{4.16}$$

for suitable constants λ_i and $k_i \in \{0, 1 \cdots\}$, for all $i = 1, \cdots,$ Rank$\{A_0(\epsilon)\}$.

Proof: See Appendix C.

It follows from Lemma 4.1 and result **R2** that for $A_0(\epsilon)$ which satisfy Condition IV, the odd-order limiting eigenmatrices satisfy

$$A_{2k+1,0} = 0 \tag{4.17}$$

for $k = 0, 1 \cdots$.

In addition, for $A_0(\epsilon)$ that satisfy Condition IV, the even-order limiting eigenmatrices $A_{2k,0}$ can be characterized by:

Lemma 4.2 : If matrix $A_0(\epsilon)$ satisfies Condition IV, then each even-order limiting eigenmatrix $A_{2k,0}$ can be expressed as

$$A_{2k,0} = B_{k,0} B_{k,0}^h \tag{4.18}$$

with a suitable matrix $B_{k,0}$ for each $k = 0, 1 \cdots$.

Proof: Matrix A can be expressed as an outer product of a suitable matrix B if and only if matrix A is Hermitian and has non-negative eigenvalues [21]. Therefore any matrix $A_0(\epsilon)$ that satisfies Condition IV has non-negative eigenvalues for any ϵ, and specifically the limiting eigenvalues of $A_0(\epsilon)$ are non-negative. It follows from result **R2** that the even-ordered limiting eigenmatrices $A_{2k,0}$ also have non-negative eigenvalues. Since limiting eigenmatrices of Hermitian $A_0(\epsilon)$ are by construction also Hermitian, $A_{2k,0}$ can be expressed as in (4.18) as the outer product of a suitable matrix $B_{k,0}$.

It can be straightforwardly verified that expressions (3.14) derived in [18] satisfy (4.17), (4.18) whenever $A_0(\epsilon)$ satisfies Condition IV.

Note that Lemma 4.2 provides only the form of the limiting eigenmatrix matrices of $B_0(\epsilon) B_0(\epsilon)^h$. The structure of the matrix factors $B_{k,0}$ is not defined, and the $B_{k,0}$ that satisfy (4.18) are not unique. In the following section, we define a structure for matrices $B_{k,0}$ that not only satisfy (4.18), and also characterize the limiting SVD of $B_0(\epsilon)$.

Relations (4.17) and (4.18) together outline the structure of all limiting eigenmatrices $A_{k,0}$ ($k = 0, 1 \cdots$) whenever $A_0(\epsilon)$ satisfies Condition IV. Since by definition the SVD of $B_0(\epsilon)$ depends on the eigenstructure of Hermitian matrices $B_0(\epsilon)B_0(\epsilon)^h$ and $B_0(\epsilon)^h B_0(\epsilon)$ that satisfy Condition IV, the results of Lemmas 4.1 and 4.2 together with the prior limiting eigenstructure results [17], [18] form the basis of our analysis of the limiting SVD of $B_0(\epsilon)$ in the next section.

4.3 Limiting Singular Matrices of $B_0(\epsilon)$

This section further characterizes the constant matrices $B_{k,0}$, and shows that the limiting SVD of $B_0(\epsilon)$ as $\epsilon \to 0$ can be characterized in terms of the SVDs of the $B_{k,0}$. The $B_{k,0}$ matrices play a role for $B_0(\epsilon)$ analogous to that played by the constant matrices $A_{k,0}$ in characterizing the eigenstructure of $A_0(\epsilon)$ as $\epsilon \to 0$. (Recall Section 3.2). The $B_{k,0}$ are therefore designated the *limiting singular matrices* of $B_0(\epsilon)$.

4.3.1 Definition of $B_{k,0}$

As a first step, we characterize the singular values of $B_0(\epsilon)$ as $\epsilon \to 0$ by the result:

S1. For any $B_0(\epsilon)$ with Taylor series in ϵ, each non-zero singular value $\sigma_i(\epsilon)$ is asymptotically (as $\epsilon \to 0$) proportional to non-negative *integer* powers of ϵ. That is,

$$\lim_{\epsilon \to 0} \left\{ \frac{\sigma_i(\epsilon)}{\sigma_i \cdot \epsilon^{k_i}} \right\} = 1 \tag{4.19}$$

for suitable constants σ_i and $k_i \in \{0, 1 \cdots\}$, for all $i = 1, \cdots,$ Rank$\{B_0(\epsilon)\}$.

Proof: By definition, the singular values of $B_0(\epsilon)$ are the square roots of the eigenvalues of a corresponding square matrix $A_0(\epsilon) = B_0(\epsilon)B_0(\epsilon)^h$ that satisfies Condition IV. Proof of the result is immediate from Lemma 4.1, with $\sigma_i = \sqrt{\lambda_i}$.

Result **S1** is the SVD analog of the prior eigenvalue result **R1**. For convenience, we designate $\sigma_i \epsilon^{k_i}$ as a *limiting singular value* of $B_0(\epsilon)$. Furthermore, we designate the group of limiting singular values proportional to ϵ^k as the k^{th} *limiting singular*

value shell. The limiting singular values of $B_0(\epsilon)$ in shell $k = 0$ (i.e. constant as $\epsilon \to 0$) can be identified directly from Taylor series (4.15) as the constant non-zero singular values of the leading term $B_{0,0}$.

To identify the remaining limiting singular values, we exploit result **S1** to group the singular values of $B_0(\epsilon)$ according to the power of ϵ of the limiting singular value. We express the matrix $\Sigma(\epsilon)$ in (4.4) as

$$\Sigma(\epsilon) \;=\; \sum_{k=0}^{\bar{m}} \Sigma_k(\epsilon) \tag{4.20}$$

where the only non-zero entries of $\Sigma_k(\epsilon)$ are on the main diagonal, and are the singular values of $B_0(\epsilon)$ proportional to ϵ^k as $\epsilon \to 0$. Thus if the i^{th} main diagonal element of $\Sigma(\epsilon)$ is proportional to ϵ^{k_i} as $\epsilon \to 0$, then it is equal to the i^{th} main diagonal element of $\Sigma_{k_i}(\epsilon)$ and furthermore the i^{th} main diagonal element of all other $\Sigma_k(\epsilon)$, $k \neq k_i$, is zero. Since $B_0(\epsilon)$ has rank $\mathcal{R}$, there can be at most $\mathcal{R}$ non-trivial terms in the sum (4.20); $\bar{m}$ denotes the index of the last non-trivial term in (4.20). By construction,

$$\sum_{k=0}^{\bar{m}} \text{Rank}\{\Sigma_k(\epsilon)\} \;=\; \text{Rank}\{B_0(\epsilon)\} \;=\; \mathcal{R} \tag{4.21}$$

The SVD (4.4) of $B_0(\epsilon)$ can then be expressed as the series

$$\begin{aligned} B_0(\epsilon) \;&=\; U(\epsilon)\left(\sum_{k=0}^{\bar{m}} \Sigma_k(\epsilon)\right) V(\epsilon)^h \\ &=\; \sum_{k=0}^{\bar{m}} \epsilon^k \tilde{B}_k(\epsilon) \end{aligned} \tag{4.22}$$

where

$$\tilde{B}_k(\epsilon) \;\triangleq\; U(\epsilon)\frac{1}{\epsilon^k}\Sigma_k(\epsilon)V(\epsilon)^h \tag{4.23}$$

are low-rank matrices whose column, row spaces are respectively spanned by the columns of $U(\epsilon)$, $V(\epsilon)$ associated with the non-zero entries of $\Sigma_k(\epsilon)$.

The expansion of $B_0(\epsilon)$ in series (4.22) differs from Taylor series (4.15) in that

1. Eq. (4.22) represents $B_0(\epsilon)$ as a finite sum, whereas the Taylor series typically involves an infinite number of terms.

2. The matrix coefficients $\tilde{B}_k(\epsilon)$ typically are non-constant with ϵ, aggregating many of the Taylor series components.

3. The column spaces of $\tilde{B}_k(\epsilon)$, $\tilde{B}_j(\epsilon)$, with $k \neq j$, are orthogonal, since they consist of non-overlapping column sets of unitary matrix $U(\epsilon)$.

4. The row spaces of $\tilde{B}_k(\epsilon)$, $\tilde{B}_j(\epsilon)$, with $k \neq j$, are similarly orthogonal.

The question arises as to the behavior of the matrix coefficients $\tilde{B}_k(\epsilon)$ as $\epsilon \to 0$; specifically, do the $\tilde{B}_k(\epsilon)$ converge to constant matrices as $\epsilon \to 0$?

A preliminary observation is that the matrices (4.23) do not "blow up" as $\epsilon \to 0$ since (4.19) shows that the factor $(1/\epsilon^k)\Sigma_k(\epsilon) \to \Sigma_k$ as $\epsilon \to 0$, where Σ_k is a constant diagonal matrix, and the columns of $U(\epsilon)$ and $V(\epsilon)$ have unit norm.

To further address the convergence question, we note that the $\tilde{B}_k(\epsilon)$ are by construction related to the eigenstructure of the products $B_0(\epsilon)B_0(\epsilon)^h$ and $B_0(\epsilon)^h B_0(\epsilon)$ by the properties

P1. The eigenvalues of $B_0(\epsilon)B_0(\epsilon)^h$ (or equivalently of $B_0(\epsilon)^h B_0(\epsilon)$) proportional to ϵ^{2k} as $\epsilon \to 0$, are equal to the squares of the non-zero singular values of $\tilde{B}_k(\epsilon)$, multiplied by ϵ^{2k}.

P2. The associated eigenvectors of $B_0(\epsilon)B_0(\epsilon)^h$ span the column space of $\tilde{B}_k(\epsilon)$.

P3. The associated eigenvectors of $B_0(\epsilon)^h B_0(\epsilon)$ span the row space of $\tilde{B}_k(\epsilon)$.

Therefore the small ϵ properties of matrix coefficients $\tilde{B}_k(\epsilon)$ can be inferred from the eigenstructure properties identified in [17], [18]. Specifically, Appendix D shows that the matrices $\tilde{B}_k(\epsilon)$ have Taylor series in ϵ. That is

Lemma 4.3 : If $B_0(\epsilon)$ has Taylor series in ϵ, then matrices $\tilde{B}_k(\epsilon)$ also have Taylor series in ϵ.

Thus, non-withstanding the denominator factor ϵ in (4.23), matrices $B_0(\epsilon)$ have limiting values as $\epsilon \rightarrow 0$.

We now define the limiting singular matrices $B_{k,0}$:

Definition of $B_{k,0}$: Limiting singular matrix $B_{k,0}$ is the order ϵ^0 (or constant) Taylor series term of $\tilde{B}_k(\epsilon)$. That is

$$B_{k,0} \triangleq \lim_{\epsilon \rightarrow 0} \tilde{B}_k(\epsilon) \tag{4.24}$$

$k = 0, 1, \cdots$.

The $B_{k,0}$ exist since $\tilde{B}_k(\epsilon)$ has a Taylor series in ϵ per Lemma 4.3.

The $B_{k,0}$ defined above satisfy expression (4.18) for the limiting eigenmatrices of $B_0(\epsilon)B_0(\epsilon)^h$, since by definition of the SVD,

1. The non-zero eigenvalues of $B_{k,0}B_{k,0}^h$ are the constants λ_i in the limiting eigenvalues of $B_0(\epsilon)B_0(\epsilon)^h$ of the form $\lambda_i \epsilon^{2k}$. (From property **P1** as $\epsilon \rightarrow 0$, and (4.24)).

2. The column space of $B_{k,0}B_{k,0}^h$ is spanned by limiting eigenvectors of $B_0(\epsilon)B_0(\epsilon)^h$ associated with the group of limiting eigenvalues proportional to ϵ^{2k} as $\epsilon \rightarrow 0$. (From property **P2** as $\epsilon \rightarrow 0$, and (4.24)).

Therefore $B_{k,0}B_{k,0}^h$ satisfies properties **R2, R3**, and can be used as in (4.18) to determine the limiting eigenstructure of $B_0(\epsilon)B_0(\epsilon)^h$.

In the next section, we show that the $B_{k,0}$ can also be used to determine the limiting SVD of $B_0(\epsilon)$.

4.3.2 Limiting SVD of $B_0(\epsilon)$ Determined by the $B_{k,0}$

As a next step in relating the SVDs of $B_0(\epsilon)$ and of $B_{k,0}$, we note the following $B_{k,0}$ properties:

S2. The non-zero singular values of $B_{k,0}$ are the constants σ_i in limiting singular values of $B_0(\epsilon)$ of the form $\sigma_i \epsilon^k$.

S3. The column, row spaces of $B_{k,0}$ are respectively spanned by the left, right singular vectors of $B_0(\epsilon)$ associated with the group of limiting singular values proportional to ϵ^k as $\epsilon \to 0$.

(Both properties follow from construction (4.23) of $\tilde{B}_k(\epsilon)$ in terms of the SVD of $B_0(\epsilon)$, and by definition (4.24) of $B_{k,0}$ as the limiting value of $\tilde{B}_k(\epsilon)$).

Accordingly, if one could readily determine the $B_{k,0}$ from the matrix coefficients $B_{0,p}$ of the Taylor series (4.3) for $B_0(\epsilon)$, then straightforward analysis of the (low-rank constant) $B_{k,0}$ would reveal the limiting singular values and the limiting span of the associated vectors of $B_0(\epsilon)$.

Analysis so far has shown that limiting singular matrices $B_{k,0}$ exist for any $B_0(\epsilon)$ with Taylor series in ϵ. Moreover, the SVD's of the $B_{k,0}$ specify the limiting structure of $B_0(\epsilon)$ as $\epsilon \to 0$. However we have not shown how to determine the $B_{k,0}$ from the Taylor series matrix coefficients $B_{0,p}$. Expressions for $B_{k,0}$ in terms of $B_{0,p}$ are developed in the following sections.

4.4 Partial Identification of the $B_{k,0}$

This section derives a property which partially identifies the limiting singular matrix $B_{k,0}$ in terms of the Taylor series matrix coefficients $B_{0,p}$. Section 4.5 exploits this property together with Conditions I-III to derive simple explicit formulae for the $B_{k,0}$ in terms of the Taylor series coefficients $B_{0,k}$ of non-degenerate $B_0(\epsilon)$. Section 4.6 also uses this property together with either one of Conditions I or II to identify more complex formulae for $B_{k,0}$ of partially degenerate $B_0(\epsilon)$.

The property of interest is:

Lemma 4.4 : For any $B_0(\epsilon)$ with Taylor series in ϵ, limiting singular matrices $B_{k,0}$ have the recursive structure

$$B_{k,0} = \begin{cases} B_{0,0} & k = 0 \\ P_{[B_{0,0}]} B_{0,1} P_{[B^h_{0,0}]} & k = 1 \\ P_{[B_{0,0},\cdots B_{k-1,0}]} \left(B_{0,k} + F_{k-1}\right) P_{[B^h_{0,0},\cdots B^h_{k-1,0}]} & k = 2, \cdots \end{cases} \tag{4.25}$$

where $B_{0,k}$ is the matrix coefficient of the k^{th} order term in the Taylor series of $B_0(\epsilon)$, and $P_{[B_{0,0},\cdots B_{k-1,0}]}$, $P_{[B^h_{0,0},\cdots B^h_{k-1,0}]}$ respectively denote projections onto the column, row nullspace of limiting singular matrix sequence $B_{0,0},\cdots B_{k-1,0}$. That is

$$P_{[B_{0,0},\cdots B_{k-1,0}]} \triangleq I - [B_{0,0},\cdots,B_{k-1,0}][B_{0,0},\cdots,B_{k-1,0}]^+ \tag{4.26}$$

$$\begin{aligned} P_{[B^h_{0,0},\cdots B^h_{k-1,0}]} &\triangleq I - [B^h_{0,0},\cdots,B^h_{k-1,0}][B^h_{0,0},\cdots,B^h_{k-1,0}]^+ \\ &= I - \begin{bmatrix} B_{0,0} \\ \vdots \\ B_{k-1,0} \end{bmatrix}^+ \begin{bmatrix} B_{0,0} \\ \vdots \\ B_{k-1,0} \end{bmatrix} \end{aligned} \tag{4.27}$$

Matrix F_{k-1} $(k = 2,\cdots)$ is a suitable rectangular matrix with properties:

a) the column space of F_{k-1} is contained in that of Taylor series matrix coefficient sequence $B_{0,1},\cdots B_{0,k-1}$.

b) the row space of F_{k-1} is contained in that of Taylor series matrix coefficient sequence $B_{0,1},\cdots B_{0,k-1}$,

Proof: See Appendix E.

To illustrate the form of F_{k-1} that satisfies properties a) and b) of Lemma 4.4, we may write

$$F_{k-1} = [B_{0,1},\cdots,B_{0,k-1}]\, G_{k-1} \begin{bmatrix} B_{0,1} \\ \vdots \\ B_{0,k-1} \end{bmatrix} \tag{4.28}$$

for $k = 2,\cdots$, where G_{k-1} is an appropriate matrix. Note that the matrices $B_{l,0}$ which appear in (4.26) and (4.27) are the matrices which we seek to identify whereas matrices $B_{0,l}$ which appear in (4.28) are the known matrix coefficients of the Taylor series. In general, $B_{l,0} \neq B_{0,l}$ so that the projection matrices $P_{[B_{0,0},\cdots B_{k-1,0}]}$ and $P_{[B^h_{0,0},\cdots B^h_{k-1,0}]}$ do not necessarily annihilate F_{k-1}.

The SVD result (4.25) can be compared with the eigenstructure result (3.14) of Reference [18] for $A_0(\epsilon)$, by imposing the requirement

$$B_0(\epsilon) \;=\; A_0(\epsilon) \;=\; \text{Hermitian} \tag{4.29}$$

which cause the SVD and eigendecomposition to coincide. In this case, the matrices (3.14) take the form (4.25) with

$$\begin{aligned} F_1 &= -A_{0,1}A_{0,0}^{+}A_{0,1} \\ F_2 &= -A_{0,1}A_{0,0}^{+}A_{0,2} - A_{0,2}A_{0,0}^{+}A_{0,1} \\ &\quad + A_{0,1}A_{0,0}^{+}A_{0,1}A_{0,0}^{+}A_{0,1} - A_{0,2}(P_0A_{0,1}P_0)^{+}A_{0,2} \\ &\quad + A_{0,2}(P_0A_{0,1}P_0)^{+}A_{0,1}A_{0,0}^{+}A_{0,1} + A_{0,1}A_{0,0}^{+}A_{0,1}(P_0A_{0,1}P_0)^{+}A_{0,2} \\ &\quad - A_{0,1}A_{0,0}^{+}A_{0,1}(P_0A_{0,1}P_0)^{+}A_{0,1}A_{0,0}^{+}A_{0,1} \\ &= [A_{0,1}\ ,\ A_{0,2}]\,G_2 \begin{bmatrix} A_{0,1} \\ A_{0,2} \end{bmatrix} \end{aligned} \tag{4.30}$$

with

$$G_2 = \begin{bmatrix} [A_{0,0}^{+}A_{0,1}A_{0,0}^{+} - A_{0,0}^{+}A_{0,1}(P_0A_{0,1}P_0)^{+}A_{0,1}A_{0,0}^{+}] & [-A_{0,0}^{+} + A_{0,0}^{+}A_{0,1}(P_0A_{0,1}P_0)^{+}] \\ [-A_{0,0}^{+} + (P_0A_{0,1}P_0)^{+}A_{0,1}A_{0,0}^{+}] & -(P_0A_{0,1}P_0)^{+} \end{bmatrix} \tag{4.31}$$

Note that Lemma 4.4 characterizes the limiting singular matrix $B_{k,0}$ as orthogonal to $B_{j,0}$, for $k \neq j$, and explicitly identifies one component associated with Taylor series matrix coefficient $B_{0,k}$. This is sufficient to explicitly identify the first two limiting matrices $B_{0,0}$ and $B_{1,0}$. Lemma 4.4 does not however fully identify the $B_{k,0}$ for $k > 1$ since the structure of G_{k-1} in (4.28) is not specified.

Lemma 4.4 is important since it *characterizes* $B_{k,0}$ *for any* matrix $B_0(\epsilon)$, and *for any* $k = 0, 1, \cdots$. The following section shows that in the non-degenerate case when $B_0(\epsilon)$ satisfies Conditions I-III, the lemma is sufficient to identify a simple explicit expression for all the $B_{k,0}$.

4.5 Explicit $B_{k,0}$ Expressions for Non-Degenerate $B_0(\epsilon)$

This section specializes the $B_{k,0}$ characterization of the previous section to matrices $B_0(\epsilon)$ that satisfy Conditions I-III. For such non-degenerate matrices, remarkably simple and explicit $B_{k,0}$ expressions are derived.

The first two limiting singular matrices $B_{0,0}$, and $B_{1,0}$ were explicitly identified in Lemma 4.4. Under the simplifying conditions, the explicit identification can be extended to $B_{k,0}$, $k > 1$, as follows.

Theorem 4.1 : If $B_0(\epsilon)$ has a Taylor series in ϵ, and satisfies Conditions I and II, then

$$\textbf{1)} \qquad P_{[B_{0,0},\cdots B_{k-1,0}]} = P_{[C_{k-1}]} \tag{4.32}$$

$$\textbf{2)} \qquad P_{[B^h_{0,0},\cdots B^h_{k-1,0}]} = P_{[R_{k-1}]} \tag{4.33}$$

$$\textbf{3)} \qquad B_{k,0} = P_{[C_{k-1}]} B_{0,k} P_{[R_{k-1}]} \tag{4.34}$$

for $k = 1 \cdots \tilde{m}$, where C_{k-1} and R_{k-1} are as defined in (4.7) and (4.8) in terms of the Taylor series coefficients $B_{0,0}, \cdots B_{0,k-1}$.

Proof: The proof is by induction.

Obviously (4.32), (4.33) are satisfied for $k = 1$. Reference to (4.25) shows that (4.34) also is satisfied for $k = 1$.

To complete the induction we show that if (4.32)-(4.34) hold for $k = j$, then (4.32)-(4.34) hold for $k = j + 1$. Thus we assume

$$\textbf{1)} \qquad P_{[B_{0,0},\cdots B_{j-1,0}]} = P_{[C_{j-1}]} \tag{4.35}$$

$$\textbf{2)} \qquad P_{[B^h_{0,0},\cdots B^h_{j-1,0}]} = P_{[R_{j-1}]} \tag{4.36}$$

$$\textbf{3)} \qquad B_{j,0} = P_{[C_{j-1}]} B_{0,j} P_{[R_{j-1}]} \tag{4.37}$$

and show

$$\textbf{1)} \qquad P_{[B_{0,0},\cdots B_{j,0}]} = P_{[C_j]} \tag{4.38}$$

$$\textbf{2)} \qquad P_{[B^h_{0,0},\cdots B^h_{j,0}]} = P_{[R_j]} \tag{4.39}$$

$$\textbf{3)} \qquad B_{j+1,0} = P_{[C_j]} B_{0,j} P_{[R_j]} \tag{4.40}$$

for $1 \leq j \leq \tilde{m} - 1$.

The first projection matrix of interest is

$$\begin{aligned} P_{[B_{0,0},\cdots B_{j-1,0},\, B_{j,0}]} &= P_{[C_{j-1},\,(P_{[C_{j-1}]} B_{0,j} P_{[R_{j-1}]})]} \\ &= P_{[C_{j-1},\,(B_{0,j} P_{[R_{j-1}]})]} \end{aligned} \tag{4.41}$$

It follows from Condition II of (4.10) that

$$\text{Column Space}\{B_{0,j} P_{[R_{j-1}]}\} = \text{Column Space}\{B_{0,j}\} \tag{4.42}$$

for $j \leq \tilde{m} - 1$. Therefore

$$P_{[C_{j-1},\,(B_{0,j} P_{[R_{j-1}]})]} = P_{[C_{j-1},\,B_{0,j}]} = P_{[C_j]} \tag{4.43}$$

Substitution of (4.43) into (4.41) establishes (4.38).

A parallel argument using Condition I of (4.9) in the place of (4.10) establishes (4.39).

Finally use of (4.38), (4.39) in (4.25) establishes (4.40).

Theorem 4.1 presents a remarkably simple characterization of the limiting singular matrices $B_{k,0}$ whenever $B_0(\epsilon)$ satisfies both Conditions I and II. Specifically,

- The vector spaces spanned by the columns, rows of limiting singular matrix sequence $B_{0,0}, \cdots B_{k-1,0}$ *are equal to* those spanned by the columns, rows of Taylor series matrix coefficient sequence $B_{0,0}, \cdots B_{0,k-1}$.

- The limiting singular matrix $B_{k,0}$ is simply the component of the k^{th} order Taylor series matrix coefficient $B_{0,k}$ that is orthogonal to the vector spaces spanned by rows and columns of Taylor series matrix coefficients of lower order.

The rank and span properties of the limiting SVD of non-degenerate $B_0(\epsilon)$ can be easily inferred from Theorem 4.1, as shown below.

4.5.1 Rank of $B_{k,0}$ for Non-Degenerate $B_0(\epsilon)$

For non-degenerate $B_0(\epsilon)$, we use Theorem 4.1 to show that the rank of limiting singular matrix $B_{k,0}$ is simply equal to that of Taylor series matrix coefficient $B_{0,k}$, for $k = 0 \cdots \tilde{m} - 1$, but not necessarily for $k = \tilde{m}$. Specifically,

Lemma 4.5 : If $B_0(\epsilon)$ has a Taylor series in ϵ, and satisfies Conditions I and II, then

$$\text{Rank}\{B_{k,0}\} = \begin{cases} \text{Rank}\{B_{0,k}\} & k = 0, \cdots \tilde{m} - 1 \\ \text{Rank}\{P_{[C_{\tilde{m}-1}]} B_{0,\tilde{m}} P_{[R_{\tilde{m}-1}]}\} & k = \tilde{m} \end{cases} \tag{4.44}$$

Proof: From (4.25) of Lemma 4.4, the result is trivial for $k = 0$.

For $k > 0$, from (4.34) of Theorem 4.1, we have

$$\text{Rank}\{B_{k,0}\} = \text{Rank}\{P_{[C_{k-1}]} B_{0,k} P_{[R_{k-1}]}\} \tag{4.45}$$

for $k = 1, \cdots \tilde{m}$. Relation (4.9) of Condition I states that pre-multiplication of $B_{0,k}$ by $P_{[C_{k-1}]}$ does not affect rank for $k = 1, \cdots \tilde{m} - 1$. Similarly, relation (4.10) of Condition II states that post-multiplication of $B_{0,k}$ by $P_{[R_{k-1}]}$ does not affect rank for $k = 1, \cdots \tilde{m} - 1$. Hence (4.45) simplifies to (4.44) whenever Conditions I and II are both satisfied.

For convenience we denote as n_k the number of limiting singular values of $B_0(\epsilon)$ proportional to ϵ^k. From result **S2**, n_k is equal to the rank of limiting singular matrix

$B_{k,0}$. Thus we define

$$n_k \triangleq \text{Rank}\{B_{k,0}\} \tag{4.46}$$

Using Lemma 4.5 we identify n_k to be the rank of Taylor series matrix coefficient $B_{0,k}$, for $k = 0 \cdots \tilde{m} - 1$, subject to Conditions I and II. Condition III specifies the rank of $B_{\tilde{m},0}$, hence also $n_{\tilde{m}}$. Therefore we have

Corollary 4.1 : If $B_0(\epsilon)$ has a Taylor series in ϵ, and satisfies all Conditions I-III, then the number n_k of limiting singular values of $B_0(\epsilon)$ proportional to ϵ^k equals the rank of the k^{th} order Taylor series matrix coefficient $B_{0,k}$, for $k = 0, \cdots \tilde{m}-1$. Furthermore the sum of n_k from $k = 0$ to $k = \tilde{m}$ equals the rank $\mathcal{R}$ of $B_0(\epsilon)$. Specifically

$$n_k = \text{Rank}\{B_{0,k}\} \qquad \text{for } k = 0, \cdots \tilde{m} - 1 \tag{4.47}$$

and

$$\sum_{k=0}^{\tilde{m}} n_k = \text{Rank}\{B_0(\epsilon)\} = \mathcal{R} \tag{4.48}$$

It follows from (4.48) and (4.21) that $B_{k,0} = 0$ for $k > \tilde{m}$. Therefore for non-degenerate matrices $B_0(\epsilon)$ with Conditions I-III all satisfied, Theorem 4.1 identifies explicit expressions for the limiting singular matrices $B_{0,0}, \cdots B_{\tilde{m},0}$ that characterize the *entire* limiting SVD of $B_0(\epsilon)$.

4.5.2 Limiting Singular Vectors for Non-Degenerate $B_0(\epsilon)$

We now identify the vector spaces spanned by the singular vectors of $B_0(\epsilon)$. From result **S3**, the column, row spaces of limiting singular matrices $B_{k,0}$ respectively define the span of the left, right singular vectors of $B_0(\epsilon)$ associated with the group of limiting singular values proportional to ϵ^k. The column, row spaces of $B_{k,0}$ for non-degenerate $B_0(\epsilon)$ are identified in terms of Taylor series coefficients $B_{0,p}$ as follows:

Lemma 4.6 : If $B_0(\epsilon)$ has a Taylor series in ϵ, and satisfies Conditions I and II, then

a) Column Space$\{B_{k,0}\}$ =

$$\begin{cases} \text{Column Space}\{B_{0,k}\} & k = 0 \\ \text{Column Space}\{P_{[C_{k-1}]}B_{0,k}\} & k = 1, \cdots \tilde{m} - 1 \\ \text{Column Space}\{P_{[C_{\tilde{m}-1}]}B_{0,\tilde{m}}P_{[R_{\tilde{m}-1}]}\} & k = \tilde{m} \end{cases} \quad (4.49)$$

b) Row Space$\{B_{k,0}\}$ =

$$\begin{cases} \text{Row Space}\{B_{0,k}\} & k = 0 \\ \text{Row Space}\{B_{0,k}P_{[R_{k-1}]}\} & k = 1, \cdots \tilde{m} - 1 \\ \text{Row Space}\{P_{[C_{\tilde{m}-1}]}B_{0,\tilde{m}}P_{[R_{\tilde{m}-1}]}\} & k = \tilde{m} \end{cases} \quad (4.50)$$

Proof: We begin with proof of Assertion a). From Lemma 4.4 and Theorem 4.1 we have

$$\text{Column Space}\{B_{k,0}\} = \begin{cases} \text{Column Space}\{B_{0,k}\} & k = 0 \\ \text{Column Space}\{P_{[C_{k-1}]}B_{0,k}P_{[R_{k-1}]}\} & k = 1, \cdots \tilde{m} \end{cases} \quad (4.51)$$

Condition II states that the rank of $B_{0,k}$ is unaffected by post-multiplication by $P_{[R_{k-1}]}$, for $k = 1, \cdots \tilde{m} - 1$. It follows that the rank of $P_{[C_{k-1}]}B_{0,k}$ is also unaffected by post-multiplication by $P_{[R_{k-1}]}$, for $k = 1, \cdots \tilde{m} - 1$. Therefore the span of the columns of $P_{[C_{k-1}]}B_{0,k}$ is not reduced by post-multiplication by $P_{[R_{k-1}]}$, and we have

$$\text{Column Space}\{P_{[C_{k-1}]}B_{0,k}P_{[R_{k-1}]}\} = \text{Column Space}\{P_{[C_{k-1}]}B_{0,k}\} \quad (4.52)$$

for $k = 1 \cdots \tilde{m} - 1$. Use of (4.52) in (4.51) gives (4.49).

Proof of Assertion b) is analogous, using Theorem 4.1 and Condition I to identify the row space of $B_{k,0}$.

The span of the singular vectors of $B_0(\epsilon)$ associated with limiting singular values proportional to ϵ^k is easy to identify whenever $B_0(\epsilon)$ satisfies Conditions I and II.

Specifically from result **S3** and Lemma 4.6 we have

Corollary 4.2 : If $B_0(\epsilon)$ has a Taylor series in ϵ, and satisfies Conditions I and II, then

a) the limiting left singular vectors of $B_0(\epsilon)$ associated with limiting singular values proportional to ϵ^k span the column space of

i) $B_{0,0}$ for $k = 0$,

ii) $P_{[C_{k-1}]}B_{0,k}$ for $k = 1, \cdots \tilde{m} - 1$,

iii) $P_{[C_{\tilde{m}-1}]}B_{0,\tilde{m}}P_{[R_{\tilde{m}-1}]}$ for $k = \tilde{m}$.

b) the limiting right singular vectors of $B_0(\epsilon)$ associated with limiting singular values proportional to ϵ^k span the row space

i) $B_{0,0}$ for $k = 0$,

ii) $B_{0,k}P_{[R_{k-1}]}$ for $k = 1, \cdots \tilde{m} - 1$,

iii) $P_{[C_{\tilde{m}-1}]}B_{0,\tilde{m}}P_{[R_{\tilde{m}-1}]}$ for $k = \tilde{m}$.

Thus whenever $B_0(\epsilon)$ satisfies Conditions I and II, the space of the limiting singular vectors associated with limiting singular values proportional to ϵ^k is easily identified from the column, row spaces of Taylor series matrix coefficient $B_{0,k}$ suitably orthogonalized with respect to the vector spaces spanned by prior Taylor series matrix coefficients $B_{0,0}$, $B_{0,1}, \cdots, B_{0,k-1}$.

The entire limiting column and row spaces of $B_0(\epsilon)$ are, from result **S3**, the spaces spanned by all the columns and rows, respectively, of all non-trivial limiting singular matrices $B_{0,0}, \cdots B_{\tilde{m},0}$. Extending the nullspace projection results of Theorem 4.1, we obtain

Lemma 4.7 : If $B_0(\epsilon)$ has a Taylor series in ϵ, and all three Conditions I-III are satisfied, then

1)
$$P_{[B_{0,0},\cdots B_{\tilde{m},0}]} = P_{[\overline{B}_0]} \tag{4.53}$$

where

$$\overline{B}_0 = \left[B_{0,0}, \cdots, B_{0,\tilde{m}-1}, (B_{0,\tilde{m}} P_{[R_{\tilde{m}-1}]})\right] \quad (4.54)$$

2) $$P_{[B^h_{0,0},\cdots B^h_{\tilde{m},0}]} = P_{[\overline{\overline{B}}_0]} \quad (4.55)$$

where

$$\overline{\overline{B}}_0 = \left[B^h_{0,0}, \cdots B^h_{0,\tilde{m}-1}, (B^h_{0,\tilde{m}} P_{[C_{\tilde{m}-1}]})\right] \quad (4.56)$$

Proof: From (4.32)-(4.34) of Theorem 4.1, with $k = \tilde{m}$

$$P_{[B_{0,0},\cdots B_{\tilde{m}-1,0}]} = P_{[C_{\tilde{m}-1}]} \quad (4.57)$$

$$P_{[B^h_{0,0},\cdots B^h_{\tilde{m}-1,0}]} = P_{[R_{\tilde{m}-1}]} \quad (4.58)$$

$$B_{\tilde{m},0} = P_{[C_{\tilde{m}-1}]} B_{0,\tilde{m}} P_{[R_{\tilde{m}-1}]} \quad (4.59)$$

The first projection matrix of interest is

$$\begin{aligned} P_{[B_{0,0},\cdots B_{\tilde{m}-1,0},\, B_{\tilde{m},0}]} &= P_{[C_{\tilde{m}-1},\, (P_{[C_{\tilde{m}-1}]} B_{0,\tilde{m}} P_{[R_{\tilde{m}-1}]})]} \\ &= P_{[C_{\tilde{m}-1},\, (B_{0,\tilde{m}} P_{[R_{\tilde{m}-1}]})]} \end{aligned} \quad (4.60)$$

which is (4.53).

The second projection matrix is

$$\begin{aligned} P_{[B^h_{0,0},\cdots B^h_{\tilde{m}-1,0},\, B^h_{\tilde{m},0}]} &= P_{[R_{\tilde{m}-1},\, (P_{[R_{\tilde{m}-1}]} B^h_{0,\tilde{m}} P_{[C_{\tilde{m}-1}]})]} \\ &= P_{[R_{\tilde{m}-1},\, (B^h_{0,\tilde{m}} P_{[C_{\tilde{m}-1}]})]} \end{aligned} \quad (4.61)$$

which is (4.55).

Note that the post factors $P_{[R_{\tilde{m}-1}]}$ and $P_{[C_{\tilde{m}-1}]}$ in (4.54) and (4.56) limit the ranks of matrices $\overline{B}_0$ and $\overline{\overline{B}}_0$ to $\mathcal{R}$.

Thus the limiting projections onto the null-space of the columns and rows of $B_0(\epsilon)$ are remarkably easy to express. From result **S3** and Lemma 4.7, we obtain:

Corollary 4.3 : If $B_0(\epsilon)$ has a Taylor series in ϵ, and satisfies all Conditions I-III, then

$$\text{a)} \qquad \lim_{\epsilon \to 0} P_{[B_0(\epsilon)]} = \lim_{\epsilon \to 0} \left(I - B_0(\epsilon) B_0(\epsilon)^+ \right) = P_{[\overline{B}_0]} \tag{4.62}$$

$$\text{b)} \qquad \lim_{\epsilon \to 0} P_{[B_0(\epsilon)^h]} = \lim_{\epsilon \to 0} \left(I - B_0(\epsilon)^+ B_0(\epsilon) \right) = P_{[\overline{\overline{B}}_0]} \tag{4.63}$$

where $\overline{B}_0$, $\overline{\overline{B}}_0$ are defined in (4.54), (4.56).

Theorem 4.1 and Corollaries 4.1-4.3 are important tools for analysis of the limiting structure of perturbed rectangular matrices. As will be seen in Chapter 8, application of Corollary 4.3 is a key enabling step for identifying the CR bound for multi-D DF scenarios with closely spaced sources.

4.5.3 Specialization to Eigenstructure of Non-Degenerate Hermitian $B_0(\epsilon)$

The above SVD results can be compared with the eigenstructure result (3.14) derived in Reference [18] for $A_0(\epsilon)$, by imposing the requirement

$$B_0(\epsilon) = A_0(\epsilon) = \text{Hermitian} \tag{4.64}$$

which cause the SVD and eigendecomposition to coincide, and by assuming that Conditions I and II are satisfied by the Taylor series coefficients $A_{0,0}, A_{0,1}, A_{0,2}, A_{0,3}$ of $A_0(\epsilon)$.

In this case, products of the projection matrices P_j defined in (3.15) take the form (4.32) with

$$\begin{aligned} P_0 &= P_{[A_{0,0}]} \\ P_0 P_1 &= P_{[A_{0,0},\, A_{0,1}]} = P_1 P_0 \\ P_0 P_1 P_2 &= P_{[A_{0,0},\, A_{0,1},\, A_{0,2}]} = P_2 P_1 P_0 \end{aligned} \tag{4.65}$$

and therefore the expressions (3.14) reduce to

$$\begin{aligned} A_{0,0} &= A_{0,0} \\ A_{1,0} &= P_{[A_{0,0}]} A_{0,1} P_{[A_{0,0}]} \\ A_{2,0} &= P_{[A_{0,0},\, A_{0,1}]} A_{0,2} P_{[A_{0,0},\, A_{0,1}]} \\ A_{3,0} &= P_{[A_{0,0},\, A_{0,1},\, A_{0,2}]} A_{0,3} P_{[A_{0,0},\, A_{0,1},\, A_{0,2}]} \end{aligned} \tag{4.66}$$

which is consistent with result (4.34) of Theorem 4.1. The rank and span properties of $A_0(\epsilon)$ follow from Corollaries 4.1-4.3.

4.6 $B_{k,0}$ Expressions for Partially Degenerate $B_0(\epsilon)$

This section identifies expressions for the limiting singular matrices $B_{k,0}$ applicable to matrices $B_0(\epsilon)$ which satisfy only one of Conditions I or II. In such cases, the identified $B_{k,0}$ expressions are more complex than in the non-degenerate case, but nonetheless generalize the SVD results of Section 4.5 to partially degenerate matrices $B_0(\epsilon)$.

We recall that $\tilde{m}$ is defined as the minimum number such that the partial sum of terms $p = 0 \cdots \tilde{m}$ of the Taylor series terms of $B_0(\epsilon)$ has rank equal to $\mathcal{R}$, the rank of $B_0(\epsilon)$. For degenerate scenarios for which Conditions I-III *are not all satisfied* parameter $\tilde{m}$ is *not necessarily given by* (4.6). For partially degenerate scenarios, we identify $\tilde{m}$ as follows:

Condition I satisfied: Provided Conditions I and IIIr (detailed subsequently) are satisfied, $\tilde{m} = \tilde{m}_r$, where $\tilde{m}_r$ is defined by

$$\text{Rank}\left\{\left[B^h_{0,0},\, \cdots,\, B^h_{0,\tilde{m}_r-1}\right]\right\} < \mathcal{R} \leq \text{Rank}\left\{\left[B^h_{0,0},\, \cdots,\, B^h_{0,\tilde{m}_r}\right]\right\} \tag{4.67}$$

Condition II satisfied: Provided Conditions II and IIIc (detailed subsequently) are

satisfied, $\tilde{m} = \tilde{m}_c$, where $\tilde{m}_c$ is defined by

$$\text{Rank}\,\{[B_{0,0}, \cdots, B_{0,\tilde{m}_c-1}]\} < \mathcal{R} \leq \text{Rank}\,\{[B_{0,0}, \cdots, B_{0,\tilde{m}_c}]\} \quad (4.68)$$

Conditions I and II as defined in (4.9), (4.10) are central to the simplified SVD analysis of partially degenerate matrices. Conditions IIIr, IIIc are modified versions of Condition III defined as follows.

IIIr. $$\text{Rank}\{P_{[C_{\tilde{m}-1}]} B_{0,\tilde{m}} P_{[R_{\tilde{m}-1}]}\} = \mathcal{R} - \text{Rank}\left\{\left[B^h_{0,0}, \cdots, B^h_{0,\tilde{m}_r-1}\right]\right\} \quad (4.69)$$

IIIc. $$\text{Rank}\{P_{[C_{\tilde{m}-1}]} B_{0,\tilde{m}} P_{[R_{\tilde{m}-1}]}\} = \mathcal{R} - \text{Rank}\,\{[B_{0,0}, \cdots, B_{0,\tilde{m}_c-1}]\} \quad (4.70)$$

Condition IIIr or IIIc is sufficient to guarantee that $\tilde{m}$ determined by (4.67) or (4.68) is such that the partial Taylor series consisting of terms of order $p = 0$ through $p = \tilde{m}$, does in fact have rank $\mathcal{R}$. We will find that whenever Conditions I and IIIr, or II and IIIc are satisfied, the limiting SVD of $B_0(\epsilon)$ as $\epsilon \to 0$ is entirely determined by the terms of (4.3) from $B_{0,0}$ to $B_{0,\tilde{m}}$; subsequent terms only add higher order effects.

To identify $B_{k,0}$ expressions for partially degenerate $B_0(\epsilon)$, the point of departure is again the partial identification of the $B_{k,0}$ of Lemma 4.4. The first two limiting singular matrices $B_{0,0}$ and $B_{1,0}$ were explicitly identified in Lemma 4.4. Under simplifying Condition II, identification can be extended to $B_{k,0}$, $k > 1$, as follows.

Theorem 4.2 : If $B_0(\epsilon)$ has a Taylor series in ϵ, and Condition II is satisfied, then

1) $$P_{[B_{0,0},\cdots B_{k-1,0}]} = P_{[C_{k-1}]} \quad (4.71)$$

2) $$P_{[B^h_{0,0},\cdots B^h_{k-1,0}]} = P_{[R'_{k-1}]} \quad (4.72)$$

where

$$R'_{k-1} = \left[B^h_{0,0}, (B^h_{0,1} P_{[C_0]}) \cdots (B^h_{0,k-1} P_{[C_{k-2}]})\right] \quad (4.73)$$

3) $$B_{k,0} = P_{[C_{k-1}]} B_{0,k} P_{[R'_{k-1}]} \quad (4.74)$$

for $k = 1 \cdots \tilde{m}_c$, where C_{k-1} is as defined in (4.7) in terms of the Taylor series coefficient sequence $B_{0,0}, \cdots, B_{0,k-1}$.

Proof: The proof is by induction. The proof parallels that of Theorem 4.1 up to (4.42), with R_{j-1}, R_j replaced by R'_{j-1}, R'_j in (4.36)-(4.41).

Equation (4.42) is replaced by

$$\text{Column Space}\{B_{0,j}P_{[R'_{j-1}]}\} = \text{Column Space}\{B_{0,j}\} \tag{4.75}$$

for $j = 1, \cdots \tilde{m}_c - 1$. This relationship does not follow immediately from Condition II of (4.10), but is implied by it and can be supported as follows. Reference to (4.73) shows that

$$\text{Column Space}\{R'_{j-1}\} \subseteq \text{Column Space}\{R_{j-1}\} \tag{4.76}$$

so that

$$\text{Column Space}\{P_{[R'_{j-1}]}\} \supseteq \text{Column Space}\{P_{[R_{j-1}]}\} \tag{4.77}$$

Therefore

$$\begin{aligned} \text{Column Space}\{B_{0,j}P_{[R'_{j-1}]}\} &\supseteq \text{Column Space}\{B_{0,j}P_{[R_{j-1}]}\} \\ &= \text{Column Space}\{B_{0,j}\} \end{aligned} \tag{4.78}$$

the last line following from (4.42). But

$$\text{Column Space}\{B_{0,j}P_{[R'_{j-1}]}\} \subseteq \text{Column Space}\{B_{0,j}\} \tag{4.79}$$

Eq. (4.75) follows from (4.78) and (4.79), and enables simplification of the counterpart of Eq. (4.41) to the counterpart of Eq. (4.43), which establishes (4.71) for $k = j + 1$, $k = 1, \cdots \tilde{m}_c$.

The matrix R'_{j-1} (in place of R_{j-1}) results from the fact that the simplifying step parallel to Eq. (4.39) is no longer possible, which leads to (4.72) for $k = j + 1$.

Finally use of (4.71) for $k = j + 1$ in (4.25) establishes (4.74) for $k = j + 1$.

Theorem 4.2 expresses the limiting singular matrices $B_{k,0}$ explicitly in terms of the Taylor series terms $B_{0,p}$, and their column aggregates C_p, when Condition II is satisfied. The expressions are more complicated than the expressions obtained for non-degenerate scenarios in Theorem 4.1, due to the structure of R'_{k-1} in (4.73).

Nonetheless we have the following characterization whenever Condition II is satisfied.

- The vector space spanned by the *columns* of limiting singular matrix sequence $B_{0,0}, \cdots B_{k-1,0}$ is equal to that spanned by the columns of Taylor series matrix coefficient sequence $B_{0,0}, \cdots B_{0,k-1}$.

- The limiting singular matrix $B_{k,0}$ is the component of the k^{th} order Taylor series matrix coefficient $B_{0,k}$ that is orthogonal to the vector space spanned by the columns, and by the subspace defined by R'_{k-1} of that spanned by the rows, of Taylor series matrix coefficients of lower order.

for $k = 0 \cdots \tilde{m}_c$. (From (4.71)-(4.74) of Theorem 4.2).

It is straightforwardly verified that Theorem 4.2 identifies explicit expressions for the limiting singular matrices $B_{0,0}, \cdots B_{0,\tilde{m}_c}$ that characterize the entire limiting SVD of $B_0(\epsilon)$, if Conditions II and IIIc are satisfied.

Clearly, a result parallel to Theorem 4.2 is available when Condition I is satisfied. That is

Theorem 4.3 : If $B_0(\epsilon)$ has a Taylor series in ϵ, and Condition I is satisfied, then

$$\textbf{1)} \qquad P_{[B_{0,0},\cdots B_{k-1,0}]} = P_{[C'_{k-1}]} \tag{4.80}$$

where

$$C'_{k-1} = \left[B_{0,0},\ (B_{0,1}P_{[R_0]}) \cdots (B_{0,k-1}P_{[R_{k-2}]})\right] \tag{4.81}$$

$$\textbf{2)} \qquad P_{[B^h_{0,0},\cdots B^h_{k-1,0}]} = P_{[R_{k-1}]} \tag{4.82}$$

$$\textbf{3)} \qquad B_{k,0} = P_{[C'_{k-1}]}B_{0,k}P_{[R_{k-1}]} \tag{4.83}$$

for $k = 1 \cdots \tilde{m}_r$, where R_{k-1} is as defined in (4.8) in terms of the Taylor series coefficients $B_{0,0}, \cdots B_{0,k-1}$.

Proof: The proof parallels that of Theorem 4.2.

Theorem 4.3 expresses the limiting singular matrices $B_{k,0}$ explicitly in terms of the Taylor series terms $B_{0,p}$, and their column aggregates C'_p, when Condition I is satisfied. The expressions are again more complicated than the expressions obtained for non-degenerate scenarios in Theorem 4.1, due to the structure of C'_{k-1} in (4.81).

Nonetheless we have the following characterization whenever Condition I is satisfied.

- The vector space spanned by the *rows* of limiting singular matrix sequence $B_{0,0}, \cdots B_{k-1,0}$ is equal to that spanned by the rows of Taylor series matrix coefficient sequence $B_{0,0}, \cdots B_{0,k-1}$.

- The limiting singular matrix $B_{k,0}$ is the component of the k^{th} order Taylor series matrix coefficient $B_{0,k}$ that is orthogonal to the vector space spanned by the rows, and by the subspace defined by C'_{k-1} of that spanned by the columns, of Taylor series matrix coefficients of lower order.

for $k = 0 \cdots \tilde{m}_r$. (From (4.80)-(4.83) of Theorem 4.3).

It is straightforwardly verified that Theorem 4.3 identifies explicit expressions for the limiting singular matrices $B_{0,0}, \cdots B_{0,\tilde{m}_r}$ that characterize the entire limiting SVD of $B_0(\epsilon)$, if Conditions I and IIIr are satisfied.

In the non-degenerate case, Corollary 4.1 explicitly identified the number n_k of limiting singular values in each singular value shell of $B_0(\epsilon)$. We now develop bounding relations for n_k applicable to partially degenerate matrices $B_0(\epsilon)$.

Corollary 4.4 : If $B_0(\epsilon)$ satisfies either set of Conditions I and IIIr, or II and IIIc, then the number n_k of limiting singular values of $B_0(\epsilon)$ proportional to ϵ^k is less than or equal to the rank of the k^{th} order Taylor series matrix coefficient $B_{0,k}$. That is

$$\begin{aligned} n_k &= \text{Rank}\{B_{0,0}\} && k = 0 \\ n_k &\leq \text{Rank}\{B_{0,k}\} && k = 1, \cdots \tilde{m} \\ n_k &= 0 && k > \tilde{m} \end{aligned} \tag{4.84}$$

where $\tilde{m} = \tilde{m}_r$ defined in (4.67) if Condition I is satisfied and $\tilde{m} = \tilde{m}_c$ defined in (4.68) if Condition II is satisfied.

Proof: The result for $k = 0$ is trivial for $k = 0$, is immediate for $k = 1 \cdots \tilde{m}$ from the applicable Theorem 4.2 or 4.3 since the rank of a product is at most the rank of any of its factors, and for $k > \tilde{m}$ follows from Condition IIIr or IIIc.

For partially degenerate matrices $B_0(\epsilon)$, Corollary 4.4 shows that the rank of Taylor series matrix coefficient $B_{0,k}$ provides an upper bound on the number n_k of limiting singular values of $B_0(\epsilon)$ proportional to ϵ^k as $\epsilon \rightarrow 0$. Reference to Corollary 4.1 shows that the bound is satisfied with equality for $k = 0 \cdots \tilde{m} - 1$ for non-degenerate matrices $B_0(\epsilon)$.

4.7 Summary of SVD Results

Thesis results so far have identified the following properties of $B_0(\epsilon)$ for small ϵ:

Shell Structure: The non-zero singular values of $B_0(\epsilon)$ can be grouped according to their ϵ dependence into sets, or *shells*. Singular values in the k^{th} shell are proportional to ϵ^k as $\epsilon \rightarrow 0$. Thus singular value energy decreases rapidly with shell number k. For non-degenerate matrices all the non-zero singular values are in shells $k = 0, \cdots \tilde{m}$, where $\tilde{m}$ satisfies (4.6).

Shell Size: For non-degenerate matrices $B_0(\epsilon)$, the number of singular values in the k^{th} shell is equal the rank of the k^{th} order Taylor series term of $B_0(\epsilon)$, except for the last shell.

Shell Problems: The SVD of $B_0(\epsilon)$ can be decomposed into a set of *shell problems*, consisting of the SVD of constant low-rank matrices $B_{k,0}$. For non-degenerate $B_0(\epsilon)$, $B_{k,0}$ is the component of the k^{th} order Taylor series term of $B_0(\epsilon)$ which is orthogonal to the column and row spaces spanned by the 0 to $(k-1)^{th}$ order Taylor series terms. Specifically $B_{k,0}$ is given by (4.32)-(4.34).

Limiting Singular Values: Limiting singular values of $B_0(\epsilon)$ converge to the non-zero singular values of $B_{k,0}$ scaled by ϵ^k.

Limiting Singular Vectors: The left (right) singular vectors associated with limiting singular values of $B_0(\epsilon)$ proportional to ϵ^k converge as $\epsilon \rightarrow 0$ to the column (row) space of $B_{k,0}$.

Degenerate Cases: In degenerate cases, the k^{th} shell ($k = 0 \cdots \tilde{m} - 1$) may have fewer singular values than the rank of the corresponding Taylor series term, i.e. shells may be *not full.* Conditions I-III are sufficient to prevent degeneracy. Expressions for limiting singular matrices $B_{k,0}$ have been identified for partially degenerate $B_0(\epsilon)$ which satisfy only one set of Conditions I and IIIr, or II and IIIc.

The foregoing SVD properties provide a reasonably complete characterization of the SVD of $B_0(\epsilon)$ for small ϵ. The SVD results are applied to identify the limiting eigenstructure of covariance matrix R_S in the following Chapters. The above results may also be useful in other applications.

4.8 SVD Examples

To illustrate the accuracy of the foregoing limiting SVD theoretical expressions, we compare the predicted limiting and exact singular values and vectors for the rectangular matrix factor B of R_S for the 2-D direction finding scenarios of Examples 2.3-2.5 of Section 2.6.

Each example involves a planar array of $W = 16$ unit-gain, isotropic sensors, and $M = 6$ far-field sources clustered near to the array broadside.

We assume that the sources are *uncorrelated* and have equal powers. Total source power is taken to be unity, so that the cross-power matrix is $P = 1/M \cdot I$.

The matrix factor B of R_S in such scenarios is of the form (2.46), that is

$$B = A\Pi$$

$$= \frac{1}{\sqrt{M}} \cdot A \tag{4.85}$$

since $\Pi = 1/\sqrt{M} \cdot I$ for M uncorrelated and equal power sources with unity total power, where A is the matrix of source generic arrival vectors. The Taylor series of (4.85) is

$$B = \frac{1}{\sqrt{M}} \sum_{p=0}^{\infty} \delta\omega^p \dot{A}_p \Gamma_p \tag{4.86}$$

where the $\dot{A}_p$ and Γ_p applicable to the example scenarios are of the form (2.68) and (2.59) with $M = 6$. It is straightforwardly verified for matrix B of (4.86) that

- Condition **C1** is sufficient for B to satisfy Condition I
- Condition **C2** is sufficient for B to satisfy Condition II
- Conditions **C1-C3** are sufficient for B to satisfy Conditions I-III

with $\tilde{m} = m$.

The limiting and exact SVD for the three example scenarios of Examples 2.3-2.5 are compared numerically in the following.

Example 4.1 : For this example, the array and source geometries are defined as in Example 2.3. That is,

Array: Sensors in a sparse grid per Figure 2-4A,

Sources: Sources clustered around broadside in a "double chevron" configuration per Figure 2-5A.

As shown in Example 2.3, this scenario satisfies Conditions **C1-C3** with $m = 2$. Consequently, matrix B of (4.86) satisfies Conditions I-III with $\tilde{m} = 2$, and the limiting singular matrices of B may be determined using Theorem 4.1.

Figure 4-1 shows the singular values of B for a range of emitter separations $\delta\omega$. Solid curves depict the exact singular values; dashed lines depict the limiting

behavior predicted by our analysis. The horizontal scale denotes spatial frequency separation $\delta\omega$ normalized by the array beamwidth BW, so that unity on the horizontal scale of the graph corresponds to maximum source separation of one beamwidth (i.e. $\delta\omega$/BW= 1). The vertical scale denotes the singular values.

Clearly the limiting expressions capture the essence of the singular values for source separations of less than one beamwidth. As predicted, the limiting singular values are grouped into singular value shells as $\delta\omega \rightarrow 0$, with $n_0 = 1$ having slope of 0 dB/decade, $n_1 = 2$ having slope of 10 dB/decade (i.e. proportional to $\delta\omega$), and $n_2 = 3$ having slope of 20 dB/decade (i.e. proportional to $\delta\omega^2$). In this non-degenerate scenario, the first three singular value shells are full.

Thus the theoretical expressions accurately predict the singular values of B for small source separations $\delta\omega$ for this non-degenerate scenario.

To assess the accuracy of the predicted span of singular vectors, Figure 4-2 shows, for a range of emitter separations $\delta\omega$, the magnitude of the component of each principal left singular vector $\vec{u}_i(\delta\omega)$ of B that is *outside* the column space of the predicted limiting subspace (i.e. the column space of the corresponding $B_{k,0}$). Specifically, the curves depict the vector norms

$$\alpha_i \;=\; \left\| P_{[B_{k,0}]} \vec{u}_i(\delta\omega) \right\| \tag{4.87}$$

for $i = 1, \cdots M$, where $P_{[B_{k,0}]}$ denotes the projection onto the column nullspace of $B_{k,0}$, and $\vec{u}_i(\delta\omega)$ is the left singular vector of B associated with singular value $\sigma_i(\delta\omega)$ proportional to $\delta\omega^k$ as $\delta\omega \rightarrow 0$. Since $\vec{u}_i(\delta\omega)$ is predicted to converge to the column space of $B_{k,0}$, we expect $\alpha_i \rightarrow 0$ as $\delta\omega \rightarrow 0$.

The horizontal scale in Figure 4-2 again denotes spatial frequency separation $\delta\omega$ normalized to the array beamwidth BW. The vertical scale denotes the α_i for $i = 1 \cdots 6$, corresponding to the principal singular values. Clearly, $\alpha_i \rightarrow 0$ as $\delta\omega \rightarrow 0$; thus the column space of limiting singular matrix $B_{k,0}$ accurately describes the span of the left singular vectors for small $\delta\omega$.

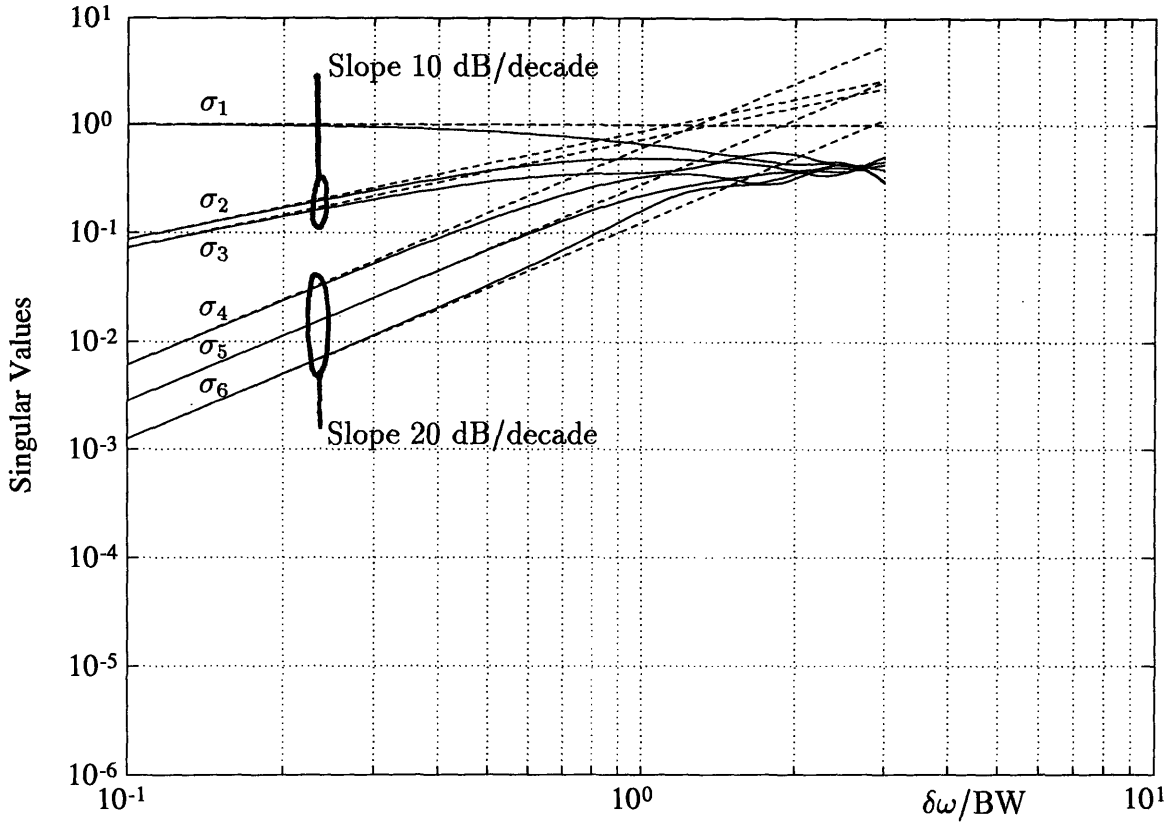

Figure 4-1: Limiting Singular Values for Non-Degenerate Matrix

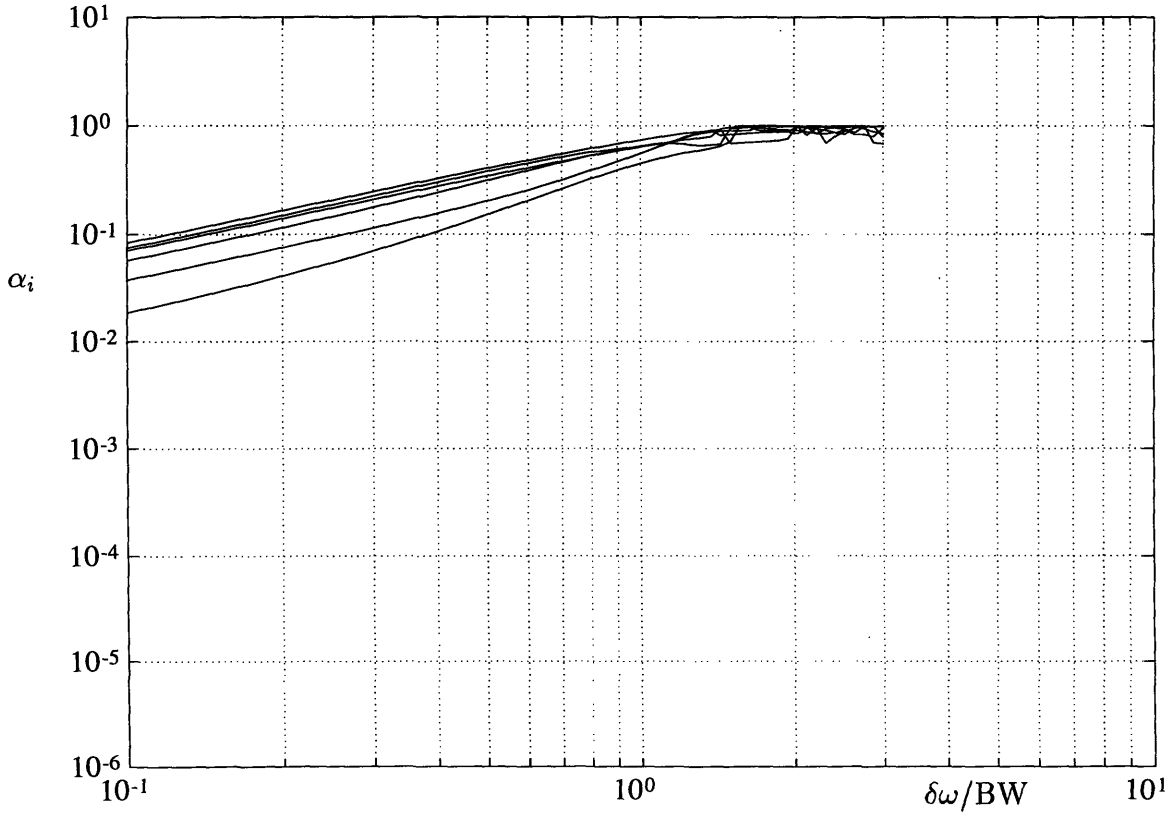

Figure 4-2: Convergence of Left Singular Vectors for Non-Degenerate Matrix

We now consider two partially degenerate examples.

Example 4.2 : For this example, the array and source geometries are defined as in Example 2.4. That is,

Array: Sensors in a sparse grid per Figure 2-4A,

Sources: Sources clustered around broadside in a circular configuration per Figure 2-5B.

As shown in Example 2.4, this scenario satisfies Condition **C1** with $m = 3$. It can straightforwardly be shown that matrix B of (4.86) satisfies Conditions I and IIIr with $\tilde{m} = 3$, and thus the limiting singular matrices of B may be determined using Theorem 4.3.

Figure 4-3 again shows the singular values of B for a range of emitter separations $\delta\omega$. Solid curves depict the exact singular values; dashed lines depict the limiting behavior predicted by our analysis. The horizontal scale denotes spatial frequency separation $\delta\omega$ normalized by the array beamwidth BW, so that unity on the horizontal scale of the graph corresponds to maximum source separation of one beamwidth (i.e. $\delta\omega/\mathrm{BW} = 1$). The vertical scale denotes the singular values.

Clearly the limiting expressions again capture the essence of the singular values for source separations of less than one beamwidth. The limiting singular values are again grouped into singular value shells as $\delta\omega \to 0$, this time with $n_0 = 1$ having slope of 0 dB/decade, $n_1 = 2$ having slope of 10 dB/decade (note that in this scenario the two singular values are exactly equal for all $\delta\omega$), $n_2 = 2$ having slope of 20 dB/decade, $n_3 = 1$ having slope of 30 dB/decade. Thus the $k = 2$ shell is not full for this partially degenerate scenario, and there is one singular value in the $k = 3$ shell.

Thus the theoretical expressions accurately predict the singular values of B for small source separations $\delta\omega$ for this partially degenerate scenario, for which matrix B satisfies Conditions I and IIIr.

Example 4.3 : For this example, the array and source geometries are defined as in Example 2.5. That is,

Array: Sensors in a circular geometry per Figure 2-4B,

Sources: Sources clustered around broadside in a "double chevron" configuration per Figure 2-5A.

As shown in Example 2.5, this scenario satisfies Condition **C2** with $m = 3$. It can straightforwardly be shown that matrix B of (4.86) satisfies Conditions II and IIIc with $\tilde{m} = 3$, and thus the limiting singular matrices of B may be determined using Theorem 4.2.

Figure 4-4 again shows the singular values of B for a range of emitter separations $\delta\omega$. Solid curves depict the exact singular values; dashed lines depict the limiting behavior predicted by our analysis. The horizontal scale denotes spatial frequency separation $\delta\omega$ normalized by the array beamwidth BW, so that unity on the horizontal scale of the graph corresponds to maximum source separation of one beamwidth (i.e. $\delta\omega/\mathrm{BW} = 1$). The vertical scale denotes the singular values.

Clearly the limiting expressions again capture the essence of the singular values for source separations of less than one beamwidth. The limiting singular values are again grouped into singular value shells as $\delta\omega \to 0$, this time with $n_0 = 1$ having slope of 0 dB/decade, $n_1 = 2$ having slope of 10 dB/decade, $n_2 = 2$ having slope of 20 dB/decade, $n_3 = 1$ having slope of 30 dB/decade. Thus the $k = 2$ shell is not full for this partially degenerate scenario, and there is one singular value in the $k = 3$ shell.

Thus the theoretical expressions accurately predict the singular values of B for small source separations $\delta\omega$ for this partially degenerate scenario, for which matrix B satisfies Conditions II and IIIc.

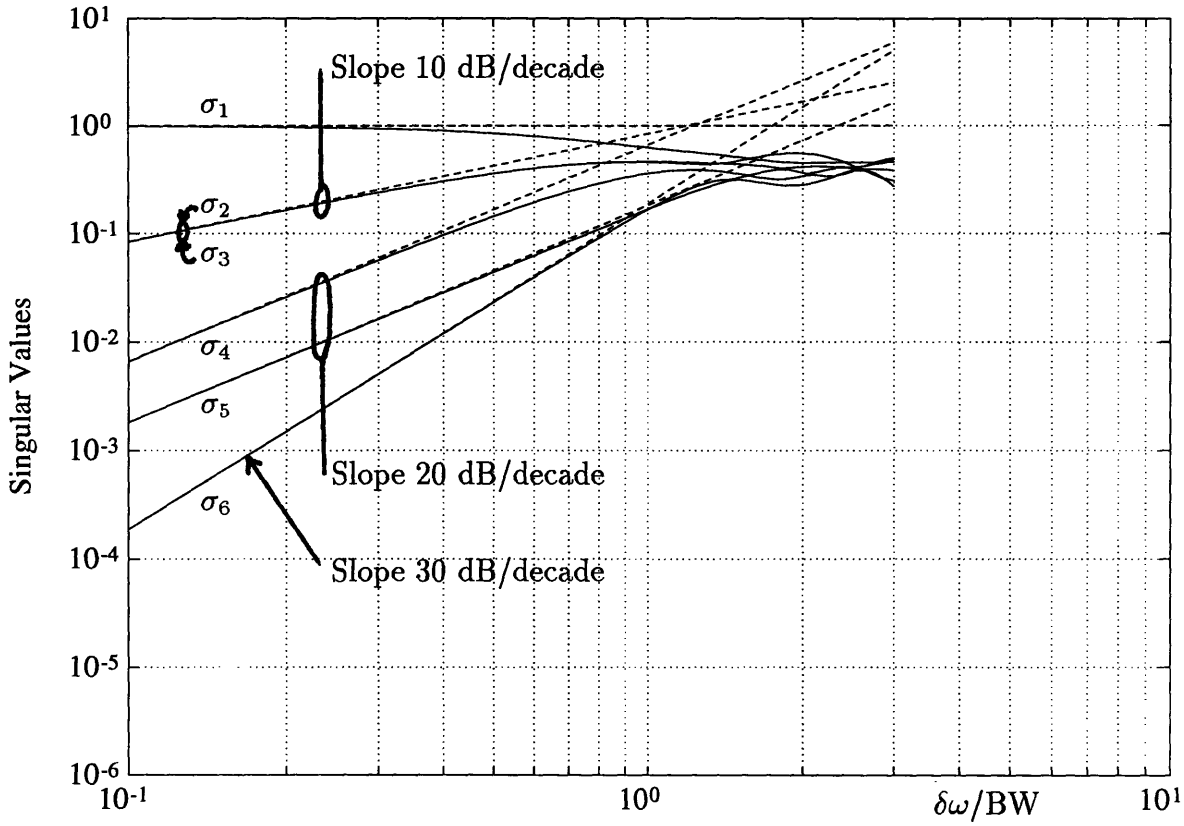

Figure 4-3: Limiting Singular Values for Partially Degenerate Matrix; **C1** Satisfied

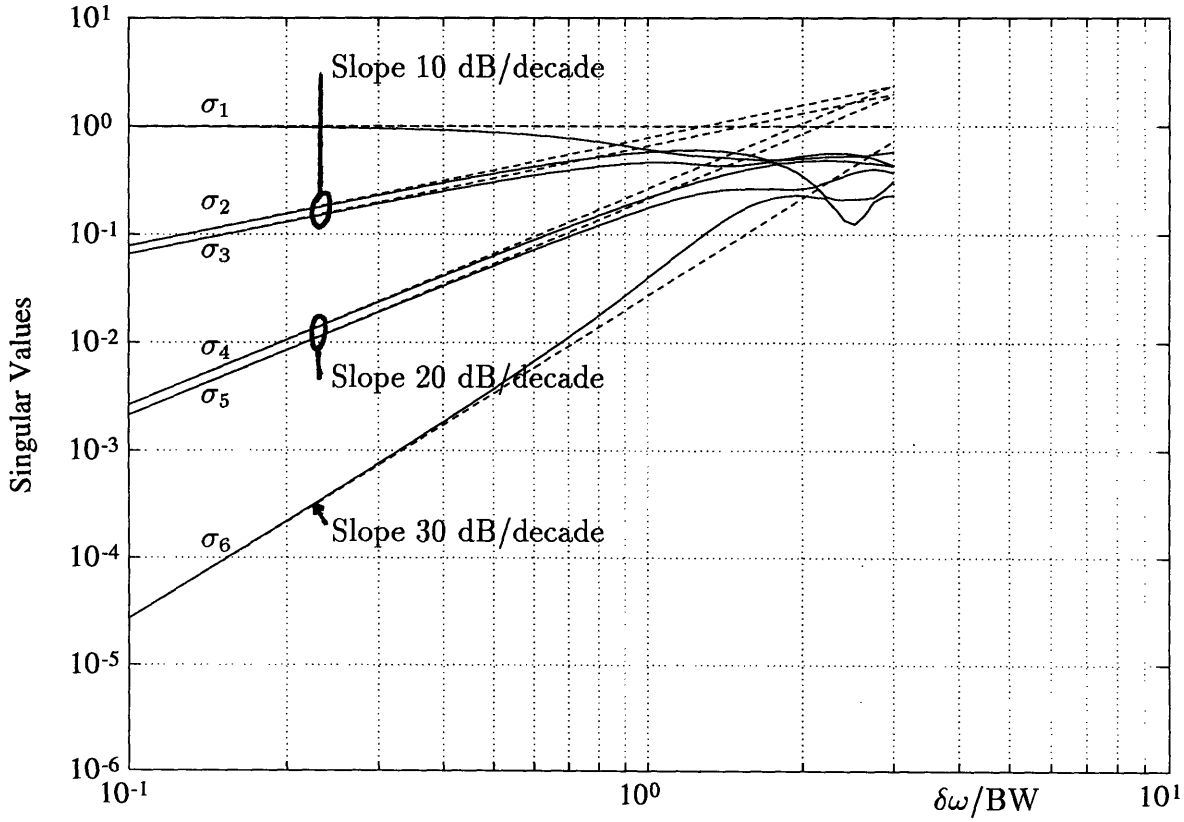

Figure 4-4: Limiting Singular Values for Partially Degenerate Matrix; **C2** Satisfied

Chapter 5

Eigenstructure of R_S for Non-Degenerate Scenarios

This chapter identifies the limiting eigenstructure of the asymptotic signal covariance matrix R_S for closely spaced sources in non-degenerate multi-D direction finding scenarios. The analysis exploits results of Chapter 4 to first identify the limiting SVD of matrix factor B of R_S given by (2.46); the limiting eigenstructure of R_S then follows immediately from the SVD of its factor B.

Recall from Section 2.5.1 that R_S can be factored as

$$R_S = BB^h \tag{5.1}$$

where B is a rectangular matrix with Taylor series (2.60) of the form

$$B = \sum_{p=0}^{\infty} \delta\omega^p \dot{A}_p \Gamma_p \Pi \tag{5.2}$$

Parameter $\delta\omega$ is a scalar measure of the maximum spatial frequency separation between the sources, $\dot{A}_p$ consists of the p^{th} order partial derivatives of the generic arrival vector $\vec{a}(\vec{\omega})$ as in (2.50), Γ_p depends on the normalized source spatial frequency offset vectors $\vec{q}_1, \cdots, \vec{q}_M$ as in (2.58) and Π results from the factorization of source cross-power matrix P in (2.47).

This chapter shows that under the non-degenerate scenario Conditions **C1**, **C2**, and **C3** defined in Section 2.5.3, matrix B *is a non-degenerate matrix.* That is, matrix B satisfies Conditions I, II and III of Chapter 4 applicable to matrix $B_0(\epsilon)$ of the form

$$B_0(\epsilon) = \sum_{p=0}^{\infty} \epsilon^p B_{0,p} \tag{5.3}$$

with the identifications

$$\begin{aligned} B_0(\epsilon) &= B \\ \epsilon &= \delta\omega \\ B_{0,p} &= \dot{A}_p \Gamma_p \Pi \end{aligned} \tag{5.4}$$

Accordingly, the limiting SVD of matrix B for non-degenerate scenarios can be identified using the results of Chapter 4 for non-degenerate scenarios.

The limiting eigenstructure of matrix R_S formed as the outer product of matrix B in (5.1) then follows immediately from the limiting SVD of B. By construction of the SVD, the non-zero eigenvalues of R_S are the squares of the non-zero singular values of B, and the corresponding eigenvectors of R_S are the corresponding left singular vectors of B.

Based upon the limiting eigenstructure of R_S, this chapter presents a reasonably complete characterization of R_S for closely spaced sources. We find that the limiting eigenvalues of R_S are divided into groups proportional to powers of $\delta\omega^2$, for convenience designated as eigenvalue *shells.* The complete eigenstructure problem decomposes into a sequence of shell problems; in multi-D scenarios, a low-rank eigenanalysis is required to identify the limiting eigenvalues and associated eigenvectors in each shell. In 1-D scenarios, the shell problems involve a rank one eigenanalysis, and hence can be solved explicitly as was done by Lee in [12].

Interestingly, a number of useful properties of R_S in multi-D scenarios can be identified without performing the eigenanalyses required to solve the shell problems. For example, the dependence of the numerical conditioning of R_S upon source spac-

ing parameter $\delta\omega$ can be explicitly determined from the number of sources M and scenario dimensionality. As another example, the limiting vector space spanned by the columns of R_S (the signal-space), or its complement (the noise-space), can be explicitly determined from the partial derivatives of the generic signal vector $\vec{a}(\vec{\omega})$ and from the source configuration.

The chapter is organized as follows. Section 5.1 shows that the non-degenerate scenario Conditions **C1-C3** are sufficient for matrix B to satisfy Conditions I-III, and hence identifies the limiting SVD of B from the results of Chapter 4. Section 5.2 then identifies the limiting eigenstructure of R_S and related properties for non-degenerate scenarios. An illustrative numerical example is presented in Section 5.3.

5.1 Limiting SVD of Factor B of R_S for Non-Degenerate Scenarios

This section identifies the limiting SVD of matrix B for non-degenerate scenarios that satisfy Conditions **C1, C2** and **C3**. To do so, we first show that Conditions **C1, C2** and **C3** are sufficient for matrix B to satisfy Conditions I, II and III of Chapter 4.

The sufficient Conditions **C1-C3** for non-degenerate scenarios, defined in Section 2.5.3 are restated here:

C1.
$$\begin{aligned} \text{Rank}\{\dot{A}_0\} &= \bar{n}_0 && \text{for } p = 0 \\ \text{Rank}\{P_{[\dot{A}_0,\cdots\dot{A}_{p-1}]}\,\dot{A}_p\} &= \bar{n}_p && \text{for } p = 1,\cdots m-1 \end{aligned} \tag{5.5}$$

C2.
$$\begin{aligned} \text{Rank}\{\Gamma_0\} &= \bar{n}_0 && \text{for } p = 0 \\ \text{Rank}\{\Gamma_p\,P_{[\Gamma_0,\cdots,\Gamma_{p-1}]}\} &= \bar{n}_p && \text{for } p = 1,\cdots m-1 \end{aligned} \tag{5.6}$$

C3.
$$\text{Rank}\{P_{[\dot{A}_0,\cdots\dot{A}_{m-1}]}\,\dot{A}_m\Gamma_m\,P_{[\Gamma_0,\cdots,\Gamma_{m-1}]}\} = M - \sum_{p=0}^{m-1}\bar{n}_p \tag{5.7}$$

where $\bar{n}_p$ is the number of p^{th} order partial derivatives of $\vec{a}(\vec{\omega})$ with respect to the elements of $\vec{\omega}$, and M is the number of sources. If Conditions **C1-C3** are all satisfied,

then parameter m is given by

$$\sum_{p=0}^{m-1} \bar{n}_p \; < M \; \leq \; \sum_{p=0}^{m} \bar{n}_p \tag{5.8}$$

The sufficient Conditions I-III for non-degenerate matrices $B_0(\epsilon)$ defined in Chapter 4 are also restated here:

$$\textbf{I.} \qquad \text{Rank}\{P_{[C_{p-1}]} B_{0,p}\} \; = \; \text{Rank}\{B_{0,p}\} \qquad \text{for } p = 1, \cdots \tilde{m} - 1 \tag{5.9}$$

$$\textbf{II.} \qquad \text{Rank}\{B_{0,p}\, P_{[R_{p-1}]}\} \; = \; \text{Rank}\{B_{0,p}\} \qquad \text{for } p = 1, \cdots \tilde{m} - 1 \tag{5.10}$$

$$\textbf{III.} \qquad \text{Rank}\{P_{[C_{\tilde{m}-1}]} B_{0,\tilde{m}}\, P_{[R_{\tilde{m}-1}]}\} \; = \; \mathcal{R} - \sum_{p=0}^{\tilde{m}-1} \text{Rank}\{B_{0,p}\} \tag{5.11}$$

Matrices $B_{0,p}$ are the matrix coefficients of the Taylor series for $B_0(\epsilon)$ in (5.3), and C_{p-1}, R_{p-1} respectively aggregate the columns and rows of $B_{0,0} \cdots B_{0,p-1}$ as defined in (4.7), (4.8). If Conditions I-III are all satisfied, then parameter $\tilde{m}$ is given by

$$\sum_{p=0}^{\tilde{m}-1} \text{Rank}\,\{B_{0,p}\} \; < \; \mathcal{R} \; \leq \; \sum_{p=0}^{\tilde{m}} \text{Rank}\,\{B_{0,p}\} \tag{5.12}$$

where $\mathcal{R}$ denotes the rank of $B_0(\epsilon)$ for small, but non-zero ϵ.

Given the identification

$$B_{0,p} \; = \; \dot{A}_p \Gamma_p \Pi \tag{5.13}$$

the rank and span properties of Taylor series coefficient matrix $B_{0,p}$ under Conditions **C1, C2** and **C3** can be identified as follows:

Lemma 5.1 : For $B_{0,p}$ as in (5.13), we have

a) If Condition **C1** is satisfied, then

$$\text{Rank}\{B_{0,p}\} \; = \; \text{Rank}\{\Gamma_p\} \qquad \text{for } p = 0 \cdots m - 1 \tag{5.14}$$

and

$$P_{[R_p]} \; = \; P_{[(\Gamma_0 \Pi)^h, \cdots (\Gamma_p \Pi)^h]} \qquad \text{for } p = 0 \cdots m - 1 \tag{5.15}$$

b) If Condition **C2** is satisfied, then

$$\text{Rank}\{B_{0,p}\} = \text{Rank}\{\dot{A}_p\} \qquad \text{for } p = 0 \cdots m-1 \tag{5.16}$$

and

$$P_{[C_p]} = P_{[\dot{A}_0, \cdots \dot{A}_p]} \qquad \text{for } p = 0 \cdots m-1 \tag{5.17}$$

c) If all Conditions **C1, C2** and **C3** are satisfied, then

$$\text{Rank}\{B_{0,p}\} = \bar{n}_p \qquad \text{for } p = 0 \cdots m-1 \tag{5.18}$$

and

$$\text{Rank}\{P_{[C_{m-1}]} B_{0,m} P_{[R_{m-1}]}\} = M - \sum_{p=0}^{m-1} \bar{n}_p \tag{5.19}$$

Proof: See Appendix G.

The results of Lemma 5.1 imply the following relationship between Conditions **C1, C2** and **C3** and Conditions I, II and III.

Lemma 5.2 : For $B_{0,p}$ as in (5.13), if Conditions **C1, C2** and **C3** are all satisfied, then so are Conditions I, II and III with

$$\tilde{m} = m \tag{5.20}$$

where $\tilde{m}$ is defined by (5.12), and m is defined by (5.8).

Proof: It follows straightforwardly from the results of Lemma 5.1 that Conditions **C1, C2** and **C3** with m in (5.8) are sufficient for Conditions I, II and III with $\tilde{m}$ in (5.12).

Consequently, the limiting SVD of B can be identified for non-degenerate scenarios using the results of Chapter 4, as follows.

Theorem 5.1 : If B has a Taylor series in $\delta\omega$ of the form (5.2), and Conditions **C1, C2** and **C3** are all satisfied, then the limiting singular matrices $B_{k,0}$ of B

are of the form

$$B_{k,0} = \begin{cases} \dot{A}_0\Gamma_0 & k=0 \\ \left(P_{[\dot{A}_0,\cdots\dot{A}_{k-1}]}\dot{A}_k\right)\left(\Gamma_k\Pi\, P_{[(\Gamma_0\Pi)^h,\cdots(\Gamma_{k-1}\Pi)^h]}\right) & k=1,\cdots m \\ 0 & k>m \end{cases} \quad (5.21)$$

Proof: From the result of Lemma 5.2, Theorem 4.1 is applicable to matrix B. The result (5.21) is immediate from Theorem 4.1, using the identifications (5.13), and (5.15), (5.17) of Lemma 5.1. The result $B_{k,0} = 0$ for $k > m$ follows from Corollary 4.1.

Theorem 5.1 presents a remarkably simple characterization of the limiting singular matrices $B_{k,0}$ of matrix B under Conditions **C1-C3** (i.e. for non-degenerate scenarios). The k^{th} order limiting singular matrix $B_{k,0}$ is simply the product of two factors. The first factor is $\dot{A}_k$ minus its projection onto the space spanned by the columns of $\dot{A}_0, \cdots \dot{A}_{k-1}$. The second factor is $\Gamma_k\Pi$ minus its projection onto the space spanned by the rows of $\Gamma_0\Pi, \cdots \Gamma_{k-1}\Pi$.

Results **S1**, **S2** and **S3** of Section 4.2 characterize the limiting SVD of B in terms of the SVD of limiting matrices $B_{k,0}$. Specifically, the SVD of limiting singular matrix $B_{k,0}$ identifies the limiting SVD structure of the k^{th} singular value shell of B as follows:

1. the non-zero singular values of $B_{k,0}$ are the constants σ_i in limiting singular values of B of the form $\sigma_i\delta\omega^k$, and

2. the associated left, right singular vectors of B respectively span the column, row spaces of $B_{k,0}$.

The number of singular values of B in each singular value shell is simply identified using Corollary 4.1 as follows:

Corollary 5.1 : If B has a Taylor series in $\delta\omega$ of the form (5.2), and Conditions **C1**, **C2** and **C3** are all satisfied, then the number n_k of limiting singular values of B proportional to $\delta\omega^k$ is equal to the number $\bar{n}_k$ of k^{th} order partial derivatives

of $\vec{a}(\vec{\omega})$ with respect to the elements of $\vec{\omega}$, for $k = 0, \cdots m-1$. Furthermore the sum of n_k from $k = 0$ to $k = m$ equals M. Specifically

$$n_k = \begin{cases} \bar{n}_k & k = 0, \cdots m-1 \\ M - \sum_{p=0}^{m-1} \bar{n}_p & k = m \end{cases} \tag{5.22}$$

Proof: Immediate from Corollary 4.1, with appropriate identifications from Lemmas 5.1 and 5.2.

The span of the limiting singular vectors associated with each singular value shell is simply identified from Corollary 4.2 as follows:

Corollary 5.2 : If B has a Taylor series in $\delta\omega$ of the form (5.2), and Conditions **C1**, **C2** and **C3** are all satisfied, then

a) the limiting left singular vectors of B associated with limiting singular values proportional to $\delta\omega^k$ span the column space of

   i) $\dot{A}_0$ for $k = 0$,

   ii) $P_{[\dot{A}_0, \cdots \dot{A}_{k-1}]} \dot{A}_k$ for $k = 1, \cdots m-1$,

   iii) $P_{[\dot{A}_0, \cdots \dot{A}_{0,m-1}]} \dot{A}_m \Gamma_m \Pi \; P_{[(\Gamma_0 \Pi)^h, \cdots (\Gamma_{m-1} \Pi)^h]}$ for $k = m$.

b) the limiting right singular vectors of B associated with limiting singular values proportional to $\delta\omega^k$ span the row space of

   i) $\Gamma_0 \Pi$ for $k = 0$,

   ii) $\Gamma_k \Pi \; P_{[(\Gamma_0 \Pi)^h, \cdots (\Gamma_{k-1} \Pi)^h]}$ for $k = 1, \cdots m-1$,

   iii) $P_{[\dot{A}_0, \cdots \dot{A}_{0,m-1}]} \dot{A}_m \Gamma_m \Pi \; P_{[(\Gamma_0 \Pi)^h, \cdots (\Gamma_{m-1} \Pi)^h]}$ for $k = m$.

Proof: Immediate from Corollary 4.2, with appropriate identifications from Lemmas 5.1 and 5.2.

The limiting projections onto the null-space of the columns and rows of B are remarkably easy to express. Paralleling Corollary 4.3, we obtain:

Corollary 5.3 : If B has a Taylor series in $\delta\omega$ of the form (5.2), and Conditions **C1, C2** and **C3** are all satisfied, then

$$\text{a)} \quad \lim_{\delta\omega\to 0} P_{[B]} = \lim_{\delta\omega\to 0} \left(I - BB^{+}\right) = P_{[\overline{B}]} \tag{5.23}$$

where

$$\overline{B} \triangleq \left[\dot{A}_0, \cdots, \dot{A}_{m-1}, (\dot{A}_m \Gamma_m \Pi P_{[(\Gamma_0\Pi)^h, \cdots (\Gamma_{m-1}\Pi)^h]})\right] \tag{5.24}$$

$$\text{b)} \quad \lim_{\delta\omega\to 0} P_{[B^h]} = \lim_{\delta\omega\to 0} \left(I - B^{+}B\right) = P_{[\overline{\overline{B}}]} \tag{5.25}$$

where

$$\overline{\overline{B}} \triangleq \left[(\Gamma_0\Pi)^h, \cdots (\Gamma_{m-1}\Pi)^h, ((\dot{A}_m \Gamma_m \Pi)^h P_{[\dot{A}_0, \cdots \dot{A}_{m-1}]})\right] \tag{5.26}$$

Proof: Immediate from Corollary 4.3, with appropriate identifications from Lemmas 5.1 and 5.2.

The limiting SVD properties of matrix B identified in Theorem 5.1 and associated Corollaries 5.1-5.3 are applied in the next section to identify the limiting eigenstructure properties of covariance matrix R_S for non-degenerate scenarios.

5.2 Limiting Eigenstructure of R_S for Non-Degenerate Scenarios

The eigenstructure of R_S formed as the outer product of factor matrix B as in (5.1) is entirely determined by the SVD of B. Specifically, the non-zero eigenvalues of R_S are the squares of the non-zero singular values of B, and the corresponding eigenvectors of R_S are the corresponding left singular vectors of B. Therefore the limiting eigenstructure of R_S can be determined directly from the limiting SVD of matrix B identified in Section 5.1.

Alternately, the limiting eigenstructure of R_S can be determined by identifying the limiting eigenmatrices of R_S. By construction of the SVD, the limiting eigenmatrices of R_S are simply the outer products of the limiting singular matrices of B. We denote as $R_{2k,0}$ the limiting eigenmatrices of R_S corresponding to limiting eigenvalues

proportional to $\delta\omega^{2k}$; hence

$$R_{2k,0} \triangleq B_{k,0}B_{k,0}^h \tag{5.27}$$

where $B_{k,0}$ are the limiting singular matrices of B corresponding to the limiting singular values proportional to $\delta\omega^k$. Note that, consistent with Lemma 4.1, there are no eigenvalues of R_S proportional to odd powers of $\delta\omega$.

Using the results of Theorem 5.1, we express $R_{2k,0}$ directly in terms of the factors $\dot{A}_p$, Γ_p and Π of the Taylor series coefficients of B. That is,

Theorem 5.2 : If R_S is formed as the outer product of matrix B with Taylor series in $\delta\omega$ of the form (5.2), and Conditions **C1**, **C2** and **C3** are all satisfied, then the limiting eigenmatrices $R_{2k,0}$ of R_S are of the form

$$R_{2k,0} \triangleq \begin{cases} \dot{A}_0\ \Gamma_0\Pi\ \Pi^h\Gamma_0^h\ \dot{A}_0^h & k=0 \\ (P_{[\dot{A}_0,\cdots\dot{A}_{p-1}]}\dot{A}_k)\ (\Gamma_k\Pi P_{[(\Gamma_0\Pi)^h,\cdots(\Gamma_{k-1}\Pi)^h]}) & \\ \cdot\ (P_{[(\Gamma_0\Pi)^h,\cdots(\Gamma_{k-1}\Pi)^h]}\Pi^h\Gamma_k^h)\ (\dot{A}_k^h P_{[\dot{A}_0,\cdots\dot{A}_{p-1}]}) & k=1,\cdots m \\ 0 & k>m \end{cases} \tag{5.28}$$

Proof: Immediate from (5.27) and Theorem 5.1.

Theorem 5.2 presents a remarkably simple characterization of the limiting eigenmatrices of R_S for non-degenerate scenarios. The limiting eigenmatrices are decomposed into factors which consist of $\dot{A}_k$ minus its projection onto the space spanned by the columns of $\dot{A}_0,\cdots\dot{A}_{k-1}$, and of $\Gamma_k\Pi$ minus its projection onto the space spanned by the rows of $\Gamma_0\Pi,\cdots\Gamma_{k-1}\Pi$.

Note that Theorem 5.2 takes the following particularly simple form for 1-D scenarios.

$$R_{2k,0} = \vec{\alpha}_k\vec{\beta}_k^h\vec{\beta}_k\vec{\alpha}_k^h \tag{5.29}$$

where

$$\vec{\alpha}_k = \begin{cases} \dot{A}_0 & k = 0 \\ P_{[\dot{A}_0, \cdots \dot{A}_{p-1}]} \dot{A}_k & k = 1, \cdots m \end{cases} \tag{5.30}$$

$$\vec{\beta}_k = \begin{cases} \Pi^h \Gamma_0^h & k = 0 \\ P_{[(\Gamma_0 \Pi)^h, \cdots (\Gamma_{k-1} \Pi)^h]} \Pi^h \Gamma_k^h & k = 1, \cdots m \end{cases} \tag{5.31}$$

These results are identical to those of Lee [12] cited in Section 3.1. Specifically $R_{2k,0}$ in (5.29) has unity rank, hence only one eigenvalue of R_S is proportional to $\delta\omega^{2k}$, as per result **E1** of Section 3.1. The principal eigenvector of $R_{2k,0}$ is equal to the suitably normalized vector $\vec{\alpha}_k$, as per result **E2** of Section 3.1. Finally, the principal eigenvalue η of $R_{2k,0}$ is equal to

$$\eta = (\vec{\alpha}^h \vec{\alpha}) \cdot (\vec{\beta}^h \vec{\beta}) \tag{5.32}$$

which can be shown, using well-known determinant properties [21], to be equal to the limiting eigenvalue expression (3.9) identified in [12].

Thus for 1-D scenarios the results of Theorem 5.2 reduce to those of Lee [12].

5.2.1 Limiting R_S Eigenstructure Properties for Non-Degenerate Scenarios

Results **R1**, **R2** and **R3** of Section 3.1 characterize the limiting eigenstructure of R_S in terms of the limiting eigenmatrices $R_{2k,0}$. Specifically, the eigenstructure of $R_{2k,0}$ identifies the limiting eigenstructure of the k^{th} eigenvalue shell of R_S as follows:

1. the non-zero eigenvalues of $R_{2k,0}$ are the constants λ_i in limiting eigenvalues of R_S of the form $\lambda_i \delta\omega^{2k}$, and

2. the associated eigenvectors of R_S span the column space of $R_{2k,0}$.

The number of eigenvalues in each eigenvalue shell is simply identified using Corollary 5.1 as follows:

Corollary 5.4 : If matrix R_S is formed as the outer product of matrix B with Taylor series in $\delta\omega$ of the form (5.2), and Conditions **C1**, **C2** and **C3** are all satisfied, then the number n_k of limiting eigenvalues of R_S proportional to $\delta\omega^{2k}$ is equal to the number $\bar{n}_k$ of k^{th} order partial derivatives of $\vec{a}(\vec{\omega})$ with respect to the elements of $\vec{\omega}$, for $k = 0, \cdots m-1$; furthermore, the sum of n_k from $k = 0$ to $k = m$ equals M. Specifically

$$n_k = \begin{cases} \bar{n}_k & k = 0, \cdots m-1 \\ M - \sum_{p=0}^{m-1} \bar{n}_p & k = m \end{cases} \tag{5.33}$$

Proof: Immediate from Corollary 5.1, since the limiting eigenvalues of R_S proportional to $\delta\omega^2$ are simply the squares of the limiting singular values of B proportional to $\delta\omega$.

The span of the limiting eigenvectors associated with each eigenvalue shell is simply identified from Corollary 5.2 as follows:

Corollary 5.5 : If matrix R_S is formed as the outer product of matrix B with Taylor series in $\delta\omega$ of the form (5.2), and Conditions **C1**, **C2** and **C3** are all satisfied, then the limiting eigenvectors of R_S associated with limiting eigenvalues proportional to $\delta\omega^{2k}$ span the column space of

i) $\dot{A}_0$ for $k = 0$,

ii) $P_{[\dot{A}_0, \cdots \dot{A}_{k-1}]} \dot{A}_k$ for $k = 1, \cdots m-1$,

iii) $P_{[\dot{A}_0, \cdots \dot{A}_{0,m-1}]} \dot{A}_m \Gamma_m \Pi \; P_{[(\Gamma_0 \Pi)^h, \cdots (\Gamma_{m-1} \Pi)^h]}$ for $k = m$.

Proof: Immediate from Corollary 5.2a) since the eigenvectors of R_S are simply the left singular vectors of B.

The limiting projection onto the nullspace of R_S is also easily identified from Corollary 5.3 as follows.

Corollary 5.6 : If matrix R_S is formed as the outer product of matrix B with Taylor series in $\delta\omega$ of the form (5.2), and Conditions **C1**, **C2** and **C3** are all satisfied, then

$$\lim_{\delta\omega\to 0} P_{[R_S]} = P_{[\overline{B}]} \tag{5.34}$$

where $\overline{B}$ is defined in (5.24).

Proof: Immediate from Corollary 5.3a) since the column space of R_S is equal to the column space of B.

The numerical conditioning of a matrix is typically characterized by the condition number ρ defined as

$$\rho \triangleq \frac{\lambda_1(\delta\omega)}{\lambda_M(\delta\omega)} \tag{5.35}$$

where eigenvalues are ordered as $\lambda_1(\delta\omega) \geq \cdots \geq \lambda_M(\delta\omega) \neq 0$. As $\delta\omega \to 0$, the condition number ρ of R_S can be characterized as follows.

Corollary 5.7 : If matrix R_S is formed as the outer product of matrix B with Taylor series in $\delta\omega$ of the form (5.2), and Conditions **C1**, **C2** and **C3** are all satisfied, then

$$\lim_{\delta\omega\to 0} \left\{ \frac{\rho}{\frac{\lambda_1}{\lambda_M \delta\omega^{2m}}} \right\} = 1 \tag{5.36}$$

where λ_1 is the largest eigenvalue of $R_{0,0}$, and λ_M is the smallest non-zero eigenvalue of $R_{2m,0}$.

Proof: Immediate from result **R1**, **R2** and Theorem 5.2.

Corollary 5.7 shows that ρ is proportional to $\delta\omega^{-2m}$ as $\delta\omega \to 0$. Hence m can be interpreted as a *numerical conditioning parameter.*

We recall from (5.8) that parameter m satisfies

$$\sum_{p=0}^{m-1} \bar{n}_p \; < \; M \; \leq \; \sum_{p=0}^{m} \bar{n}_p \tag{5.37}$$

where M is the number of sources, and $\bar{n}_p \geq 1$. Clearly for two or more sources ($M \geq 2$), we have $m \geq 1$ so that $\rho \rightarrow 0$ as $\delta\omega \rightarrow 0$. Moreover, the larger the m the faster $\rho \rightarrow 0$. This circumstance reflects the fact that factor A which appears in R_S as defined in (2.44), approaches unit rank as $\delta\omega \rightarrow 0$.

In multi-D DF scenarios $\bar{n}_p > 1$ for all $p > 0$, and therefore parameter m satisfies

$$m \; < \; M - 1 \tag{5.38}$$

In 1-D scenarios $\bar{n}_p = 1$ for all p, and therefore $m = M - 1$. Consequently, for a given number M of sources, *matrix conditioning parameter m is smaller in multi-D than in 1-D scenarios.*

5.2.2 Summary of R_S Eigenstructure Results

Thesis results so far have identified the following R_S eigenstructure properties for closely-spaced sources whenever Conditions **C1**, **C2** and **C3** are all satisfied:

Shell Structure: The non-zero eigenvalues of R_S can be grouped according to their $\delta\omega$ dependence into sets, or *shells.* Eigenvalues in the k^{th} shell, $k = 0, \cdots m$, are proportional to $\delta\omega^{2k}$ as $\delta\omega \rightarrow 0$. Thus eigenvalue energy decreases rapidly with shell number k.

Shell Size: In non-degenerate cases, the number of eigenvalues in the k^{th} shell equals the number $\bar{n}_k$ of k^{th} order partial derivatives in the Taylor series, except for the last shell, which may not be full. For 1-D scenarios, there is only one eigenvalue per shell, $\bar{n}_k = 1$, as noted in [12].

Shell Problems: The eigenanalysis of R_S can be decomposed into a set of *shell problems*, consisting of the eigenanalyses of a set of $m + 1$ constant low-rank

matrices $R_{2k,0}$ specified by (5.28). For 1-D scenarios, each shell problem consists of an eigenanalysis of a rank 1 matrix, hence solving a characteristic equation is not required, as noted in [12].

Limiting Eigenvalues: Limiting eigenvalues of R_S converge to the non-zero eigenvalues of $R_{2k,0}$ scaled by $\delta\omega^{2k}$.

Limiting Eigenvectors: The eigenvectors associated with limiting eigenvalues of R_S proportional to $\delta\omega^{2k}$ converge as $\delta\omega \rightarrow 0$ to the column space of $R_{2k,0}$ which, except for the last shell, is the space spanned by k^{th} order spatial derivatives of the generic signal vector, suitably orthogonalized from spatial derivatives of lower order.

Condition Number: Limiting condition number ρ of R_S is proportional to $\delta\omega^{-2m}$, and $m < M-1$ for non-degenerate multi-D scenarios. For 1-D, $m = M-1$. Thus for a given number of sources, R_S is typically better conditioned in multi-D than in 1-D settings.

Degenerate Cases: In degenerate cases the shells are not full. Conditions **C1**, **C2** and **C3** are sufficient to prevent degeneracy, and are related to sensor array geometry and source configuration (See Chapter 7).

The foregoing R_S eigenstructure properties provide a reasonably complete characterization of the eigenstructure of R_S for closely-spaced sources, which we expect will facilitate the performance analysis of candidate DF techniques in multi-D scenarios. Analysis of specific techniques is not pursued in this thesis.

5.3 Example Non-Degenerate R_S Eigenstructure

To illustrate the accuracy of the foregoing limiting eigenstructure theoretical expressions, we compare the predicted limiting and exact eigenvalues and eigenvectors for matrix R_S for the non-degenerate 2-D direction finding scenario of Example 2.3 of Section 2.6.

The example involves a planar array of $W = 16$ unit-gain, isotropic sensors, and $M = 6$ far-field sources clustered near to the array broadside.

We assume that the sources are *correlated* and equal power. Total source power is taken to be unity. Specifically, the source cross-power matrix P is taken to be

$$P = 1/M \cdot \begin{bmatrix} 1 & p_{12} & \cdots & p_{12}^{n-1} \\ p_{12}^* & 1 & p_{12} & \vdots \\ \vdots & \ddots & \ddots & \ddots \\ (p_{12}^{n-1})^* & \cdots & p_{12}^* & 1 \end{bmatrix} \tag{5.39}$$

with $p_{12} = 0.4 + j0.6$.

The matrix factor B of R_S in such scenarios is of the form (2.46)

$$B = A\Pi \tag{5.40}$$

where Π is taken to be the Cholesky factor of the cross-power matrix P, and A is the matrix of source generic arrival vectors. The Taylor series of B is

$$B = \sum_{p=0}^{\infty} \delta\omega^p \dot{A}_p \Gamma_p \Pi \tag{5.41}$$

where the $\dot{A}_p$ and Γ_p applicable to the example scenarios are of the form (2.68) and (2.59) with $M = 6$.

The limiting and exact eigenvalues and eigenvectors of R_S for this scenario are compared numerically in the following.

Example 5.1 : For this example, the array and source geometries are defined as in Example 2.3. That is,

Array: Sensors in a sparse grid per Figure 2-4A,

Sources: Sources clustered around broadside in a "double chevron" configuration per Figure 2-5A.

As shown in Example 2.3, this scenario satisfies Conditions **C1-C3** with $m = 2$.

Consequently, the limiting eigenmatrices $R_{2k,0}$ of R_S may be determined using Theorem 5.2.

Figure 5-1 shows the eigenvalues of R_S for a range of emitter separations $\delta\omega$. Solid curves depict the exact eigenvalues; dashed lines depict the limiting behavior predicted by our analysis. The horizontal scale denotes spatial frequency separation $\delta\omega$ normalized by the array beamwidth BW, so that unity on the horizontal scale of the graph corresponds to maximum source separation of one beamwidth (i.e. $\delta\omega/\mathrm{BW}= 1$). The vertical scale denotes the eigenvalues.

Clearly the limiting expressions capture the essence of the eigenvalues for source separations of less than one beamwidth. As predicted, the limiting eigenvalues are grouped into eigenvalue shells as $\delta\omega \rightarrow 0$, with $n_0 = 1$ having slope of 0 dB/decade, $n_1 = 2$ having slope of 20 dB/decade (i.e. proportional to $\delta\omega^2$), and $n_2 = 3$ having slope of 40 dB/decade (i.e. proportional to $\delta\omega^4$). In this non-degenerate scenario, the first three eigenvalue shells are full.

Thus the theoretical expressions accurately predict the eigenvalues of R_S for small source separations $\delta\omega$ for this non-degenerate scenario.

To assess the accuracy of the predicted span of eigenvectors, Figure 5-2 shows, for a range of emitter separations $\delta\omega$, the magnitude of the component of the principal eigenvectors $\vec{e}_i(\delta\omega)$ of R_S that is *outside* the column space of the predicted limiting subspace (i.e. the column space of the corresponding $R_{2k,0}$). Specifically, the curves depict the vector norms

$$\alpha_i \;=\; \left\| P_{[P_{[\dot{A}_0 \cdots \dot{A}_{k-1}]}\dot{A}_k]} \vec{e}_i(\delta\omega) \right\| \tag{5.42}$$

for $i = 1, \cdots M$, where $P_{[P_{[\dot{A}_0 \cdots \dot{A}_{k-1}]}\dot{A}_k]}$ denotes the projection onto the column nullspace of $R_{2k,0}$ per Corollary 5.5, and $\vec{e}_i(\delta\omega)$ is the eigenvector of R_S associated with eigenvalue $\lambda_i(\delta\omega)$ proportional to $\delta\omega^k$ as $\delta\omega \rightarrow 0$. Since $\vec{e}_i(\delta\omega)$ is predicted to converge to the column space of $R_{2k,0}$, we expect $\alpha_i \rightarrow 0$ as $\delta\omega \rightarrow 0$.

The horizontal scale in Figure 5-2 again denotes spatial frequency separation

$\delta\omega$ normalized to the array beamwidth BW. The vertical scale denotes the α_i for $i = 1 \cdots 6$, corresponding to the principal eigenvalues. Clearly, $\alpha_i \rightarrow 0$ as $\delta\omega \rightarrow 0$; thus the column space of limiting eigenmatrix $R_{2k,0}$ accurately describes the span of the eigenvectors for small $\delta\omega$.

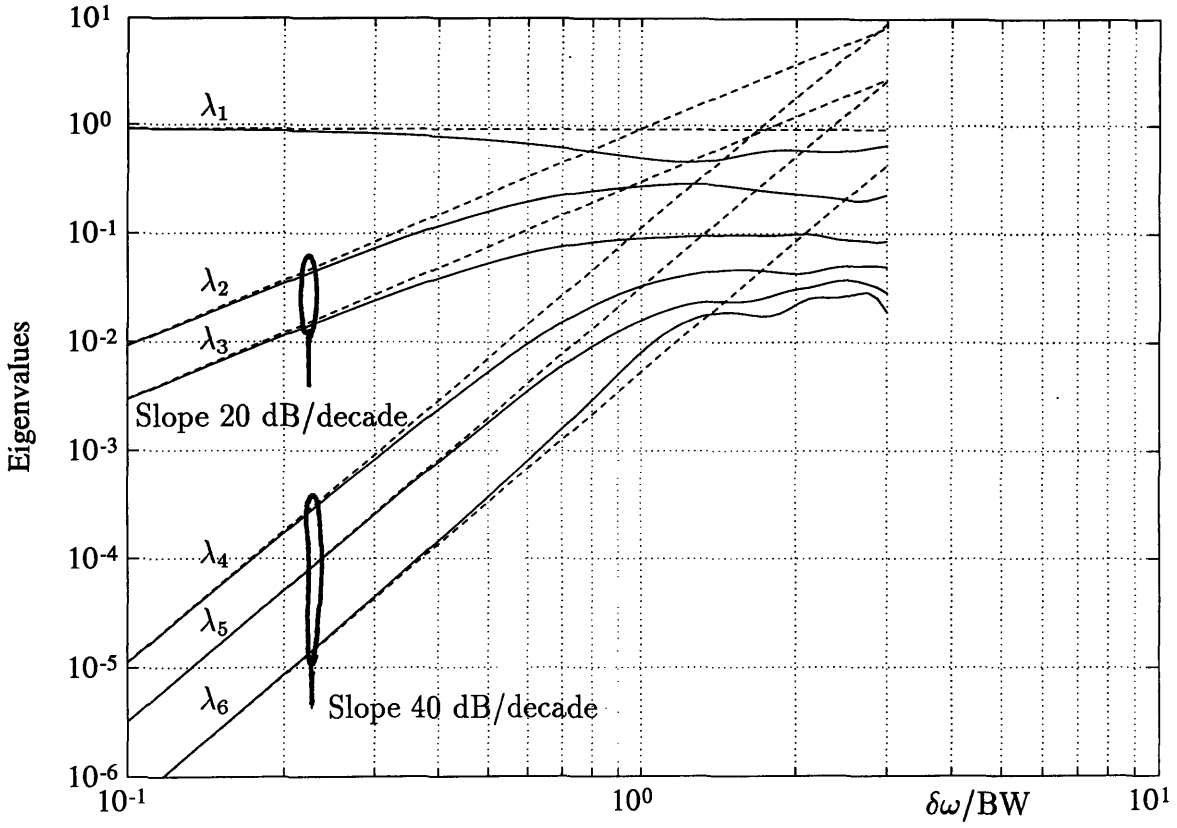

Figure 5-1: Limiting Eigenvalues for Non-Degenerate Scenario

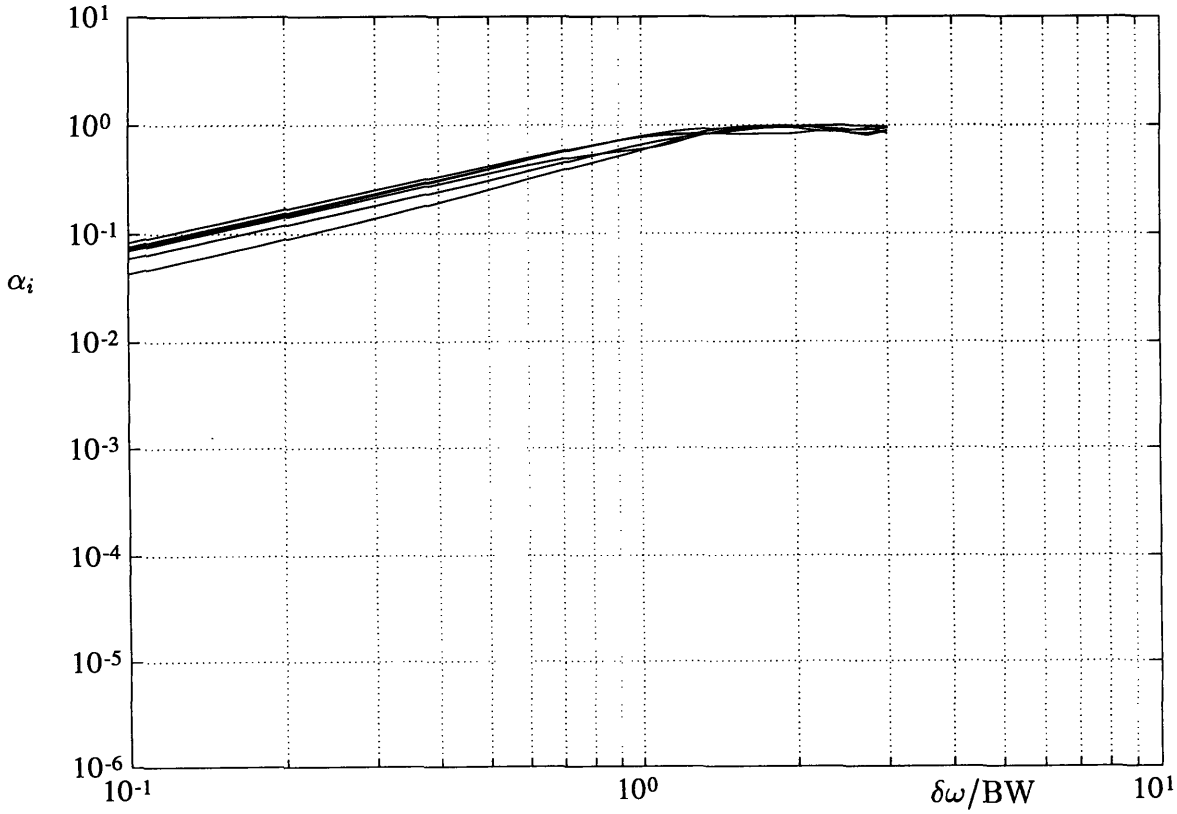

Figure 5-2: Convergence of Eigenvectors for Non-Degenerate Scenario

Chapter 6

Detection Thresholds

A fundamental problem in DF applications is to determine the number of sources; indeed many eigenvector-based DF algorithms such as MUSIC and MinNorm require a priori knowledge of the source number for proper operation.

Accordingly a set of algorithms have been developed the objective of which is to correctly *detect* or estimate the source number M. These algorithms are called *detection algorithms.* Example algorithms are Akaike Information Criteria (AIC) [22], and Minimum Descriptive Length (MDL) [23].

One useful performance measure for a detection algorithm is the signal-to-noise ratio (SNR) threshold $\mathcal{E}_D$ at which the algorithm can reliably estimate source number for a given source-array configuration, and a given number N of data snapshots. An alternative performance measure is the data set size N threshold $\mathcal{N}_D$ at which the algorithm can reliably estimate source number for a given source-array configuration, and a given SNR. These threshold values also can be regarded respectively as the minimum SNR and N at which "one can see" the full eigenstructure of the spatial covariance matrix R.

An obvious approach to detection is to examine the eigenvalues of a sample covariance matrix, and to attempt separation of the sample eigenvalues into signal-space and noise-space eigenvalues (in the sense of MUSIC). If successful, one takes the number of signal-space eigenvalues to be the estimate of source number M. This approach can be implemented by introducing a metric that effectively separates eigenvalues

into groups, and counts the number of signal space eigenvalues. Indeed both AIC and MDL employ (differing) metrics of this type.

This chapter draws upon the limiting eigenstructure results of Chapter 5 to elucidate the (SNR) threshold $\mathcal{E}_D$ and the data set size threshold $\mathcal{N}_D$ at which, based upon the consideration of sample eigenvalues, one can reliably detect M closely spaced sources in non-degenerate multi-D scenarios. The threshold expressions to be derived assume asymptotic conditions (i.e. large N or SNR) so that classical perturbation formulae apply to the eigenvalues of the sample covariance matrix $\hat{R}$. The results are:

$$\mathcal{E}_D \simeq \frac{K'_D}{\sqrt{N}} \cdot \delta\omega^{-2m} \tag{6.1}$$

$$\mathcal{N}_D \simeq \left(\frac{1}{f} + \frac{K'_D}{\mathrm{SNR}} \cdot \delta\omega^{-2m}\right)^2 \tag{6.2}$$

for large N, and

$$\mathcal{N}_D \simeq \left(\frac{K'_D}{\mathrm{SNR}}\right)^2 \cdot \delta\omega^{-4m} \tag{6.3}$$

for sufficiently small $\delta\omega$, where $\delta\omega$ is the maximum source separation parameter, m is the R_S conditioning parameter defined in (2.62), and K'_D and f are constants defined in Section 6.4.

The result (6.1) extends results of Lee and Li [13] which analyzed the SNR detection threshold $\mathcal{E}_D$ for closely spaced sources in 1-D scenarios. The authors argued that $\mathcal{E}_D$ at which so-called Normal Algorithms can reliably estimate the number of sources in 1-D scenarios is proportional to $\delta\omega^{-2(M-1)}$. That is

$$\mathcal{E}_D \simeq K_D \cdot \delta\omega^{-2(M-1)} \tag{6.4}$$

where K_D is constant with $\delta\omega$.

Since parameter $m < M - 1$ for typical multi-D scenarios, comparison of (6.4) and (6.1) leads to the conclusion that for small $\delta\omega$, the SNR detection threshold is typically much smaller (more favorable) in multi-D than in 1-D scenarios.

The analysis approach in this chapter is to use classical eigenstructure perturbation formulas and the asymptotic eigenvalues identified in Chapter 5 to formulate statistical models for the eigenvalues of the sample correlation matrix $\widehat{R}$ for M closely spaced sources in multi-D. It is then argued that any detection algorithm based upon consideration of sample eigenvalues can succeed with useful probability only if the difference between the mean of the smallest signal-space eigenvalue and the mean of the noise-space eigenvalues is substantially greater than the standard deviation of each. First order identification of the threshold SNR and N values required to satisfy the above condition result in expressions (6.1)-(6.3).

The chapter is organized as follows. The eigenvalue approach to detecting the number of sources is reviewed in Section 6.1. Section 6.2 then reviews the prior results of [13]. Section 6.3 postulates necessary conditions for successful sample eigenvalue based detection, and Sections 6.4, 6.5 develop the expressions (6.1)-(6.3) for the detection threshold SNR and N. Section 6.6 summarizes the detection threshold results.

6.1 Eigenvalue-Based Detection Algorithms

The problem addressed is that of determining which of the eigenvalues of the sample covariance matrix $\widehat{R}$ include a signal component, and which eigenvalues are noise-only.

Recall from Section 2.3 that under the data model assumptions, the sample covariance matrix $\widehat{R}$ converges for large N with probability one to the asymptotic covariance matrix R of the form

$$R \;=\; R_S + \sigma^2 I \qquad\qquad W \times W \qquad\qquad (6.5)$$

where R_S is the signal covariance matrix of rank $M < W$, and $\sigma^2 I$ is the additive white noise component.

Following the previously used notation,

$\widehat{\lambda}_1 \geq \cdots \geq \widehat{\lambda}_W$ denote the ordered eigenvalues of $\widehat{R}$,

$\bar{\lambda}_1 \geq \cdots \geq \bar{\lambda}_W$ denote the ordered eigenvalues of R,

$\lambda_1(\delta\omega) \geq \cdots \geq \lambda_M(\delta\omega)$ denote the ordered non-zero eigenvalues of R_S,

$\lambda_1 \geq \cdots \geq \lambda_M \delta\omega^{2m}$ denote the ordered non-zero limiting eigenvalues of R_S.

It follows from (6.5) that the eigenvalues of asymptotic covariance matrices R and R_S are related by

$$\begin{aligned} \bar{\lambda}_i &= \lambda_i(\delta\omega) + \sigma^2 && \text{for } i = 1 \cdots M \\ \bar{\lambda}_i &= \sigma^2 && \text{for } i = M \cdots W \end{aligned} \tag{6.6}$$

Thus the eigenvalues of R can be divided into two groups: the "signal-space eigenvalues" $\bar{\lambda}_1 \geq \cdots \geq \bar{\lambda}_M$ which are larger than σ^2, and the "noise-space eigenvalues" $\bar{\lambda}_M = \cdots = \bar{\lambda}_W$ which are equal to σ^2. Therefore the detection problem would be easy if the asymptotic matrix R were available; one could simply identify the number of sources as the largest M for which

$$\bar{\lambda}_M \neq \sigma^2 \tag{6.7}$$

The asymptotic covariance matrix is not available in practice, since only the sample covariance matrix $\hat{R}$ can be computed using a finite number N of snapshots. However, for asymptotic conditions (i.e. large SNR and/or N), $\hat{R}$ closely approximates R. Under these conditions, the eigenvalues of $\hat{R}$ can be related to those of R using the perturbation model of Section 2.3. Specifically, the sample eigenvalues $\hat{\lambda}_i$ can be expressed as the sum of the asymptotic eigenvalues $\bar{\lambda}_i$ and random perturbations μ_i as follows

$$\hat{\lambda}_i = \bar{\lambda}_i + \mu_i \tag{6.8}$$

For asymptotic conditions, and with Gaussian statistical assumptions, the first and second order statistics of μ_i are available from classical perturbation theory, and show

that

$$E\{\mu_i\} = o(1/N) \tag{6.9}$$

$$E\{\mu_i\mu_j\} = \frac{\bar{\lambda}_i^2}{N}\delta_{ij} + o(1/N) \tag{6.10}$$

where N is data set size, δ_{ij} is the Kronecker delta and $o(1/N)$ denotes terms of order $1/N^q$ with $q > 1$ [9].

For detection algorithms which estimate source number based upon consideration of the sample eigenvalues, the fundamental problem is to decide whether the perturbed eigenvalue $\hat{\lambda}_i$ includes a signal and noise component $\lambda(\delta\omega) + \sigma^2$, or only the noise component σ^2. The critical issue is to reliably detect that the asymptotic eigenvalue $\bar{\lambda}_M$ is larger than $\bar{\lambda}_{M+1}$, as in (6.7), based upon the observation of the sample eigenvalues $\hat{\lambda}_M$, $\hat{\lambda}_{M+1}$.

6.2 Prior Detection Threshold Results

Lee and Li [13] previously have derived expressions for the SNR detection threshold $\mathcal{E}_D$ of so-called Normal Detection Algorithms for 1-D scenarios. The approach and results of [13] are summarized below.

The authors define detection algorithms as Normal if the dominant term of the probability π_e that the algorithm incorrectly estimates the number M of sources depends only upon the number of sources M, the number of sensors W, the data set size N and the ratio

$$\rho_D = \frac{\lambda_M(\delta\omega)}{\sigma^2} \tag{6.11}$$

where $\lambda_M(\delta\omega)$ is the smallest non-zero eigenvalue of R_S, and σ^2 is the noise power. Specifically, π_e does not depend upon the other non-zero eigenvalues $\lambda_1(\delta\omega), \cdots, \lambda_{M-1}(\delta\omega)$ of R_S. Additionally, π_e for Normal algorithms is assumed to decrease monotonically with increasing ρ_D. The authors argue that it is reasonable to assume that any eigenvalue-based detection algorithm is normal, and show that two

popular detection algorithms, the Akaike Information Criteria [22] and the Minimum Descriptive Length [23] algorithms indeed are both normal.

The authors exploit the 1-D eigenvalue results of Lee [12] to show that the smallest eigenvalue of R_S for closely spaced sources is proportional to $\delta\omega^{2(M-1)}$. That is, as $\delta\omega \rightarrow 0$ for 1-D scenarios,

$$\lambda_M(\delta\omega) \simeq \lambda_M \delta\omega^{2(M-1)} \tag{6.12}$$

where λ_M is constant with $\delta\omega$. Using (6.12) in (6.11), the authors argue that SNR threshold $\mathcal{E}_D$ at which Normal Algorithms can reliably estimate the number of sources in 1-D scenarios is proportional to $\delta\omega^{-2(M-1)}$. That is

$$\mathcal{E}_D \simeq \frac{K_D}{\delta\omega^{2(M-1)}} \tag{6.13}$$

where K_D is a positive quantity dependent upon the specific detection algorithm, the source spacing and covariances, the sensor array and the number N of snapshots.

The authors of [13] do not address the corresponding data set size detection threshold $\mathcal{N}_D$. In the following, we extend the results of [13] using classical perturbation theory to identify the expressions for both the detection thresholds $\mathcal{E}_D$ and $\mathcal{N}_D$, for non-degenerate multi-D scenarios.

6.3 "Necessary Conditions" for Reliable Detection

To obtain detection threshold expressions for both SNR and N, we first formulate statistical models for the sample eigenvalues $\hat{\lambda}_i$. It is then argued that any eigenvalue-based detection algorithm can succeed only if the difference between the mean of the smallest signal-space eigenvalue and the mean of the noise-space eigenvalues is substantially greater than the standard deviation of each. The SNR and N values required to satisfy the above condition result are deemed to be the detection threshold

values.

A first order statistical model of the eigenvalues of $\hat{R}$ can be obtained from the perturbation model (6.8) and the classical perturbation statistical models (6.9), (6.10). Specifically, we obtain

$$E\{\hat{\lambda}_i\} = \bar{\lambda}_i + o(1/N) \tag{6.14}$$

$$\text{Cov.}\{\hat{\lambda}_i\hat{\lambda}_j\} = \frac{\bar{\lambda}_i^2}{N}\delta_{ij} + o(1/N) \tag{6.15}$$

$$\text{Std. Dev.}\{\hat{\lambda}_i\} = \frac{\bar{\lambda}_i}{\sqrt{N}} + o(1/N) \tag{6.16}$$

We assume that to detect that there are M sources present, any eigenvalue based detection algorithm needs to detect that the sample eigenvalues $\hat{\lambda}_M$ and $\hat{\lambda}_{M+1}$ have unequal asymptotic values. If the standard deviations of the sample eigenvalues $\hat{\lambda}_M$ and $\hat{\lambda}_{M+1}$ are small relative to the difference between their means, then there is a basis for seeking an algorithm for reliably detecting that there are M sources present. On the other hand, if the standard deviations of $\hat{\lambda}_M$ and $\hat{\lambda}_{M+1}$ exceeds the difference between their means, then it is unlikely that there exists any algorithm that can detect the number of sources with high probability. Accordingly, one strongly suspects that a necessary condition for the existence of an algorithm capable of detecting M closely spaced sources with high probability is that

$$\text{Std. Dev.}\{\hat{\lambda}_M\} \leq f \cdot \left[E\{\hat{\lambda}_M\} - E\{\hat{\lambda}_{M+1}\}\right] \tag{6.17}$$

and

$$\text{Std. Dev.}\{\hat{\lambda}_{M+1}\} \leq f \cdot \left[E\{\hat{\lambda}_M\} - E\{\hat{\lambda}_{M+1}\}\right] \tag{6.18}$$

where f is a suitable fraction (e.g. $f = 1/8$).

For large N, substitution of the statistical model (6.14), (6.16) in (6.17) and (6.18)

gives to first order

$$\frac{\bar{\lambda}_M}{\sqrt{N}} \leq f \cdot \left[\bar{\lambda}_M - \bar{\lambda}_{M+1}\right] \tag{6.19}$$

and

$$\frac{\bar{\lambda}_{M+1}}{\sqrt{N}} \leq f \cdot \left[\bar{\lambda}_M - \bar{\lambda}_{M+1}\right] \tag{6.20}$$

for large N. Note that $\bar{\lambda}_M - \bar{\lambda}_{M+1}$ is the smallest eigenvalue $\lambda_M(\delta\omega)$ of R_S, which was elucidated in Chapter 5. Accordingly the results of Chapter 5 together with (6.19) and (6.20) enable us to make useful statements about the detection thresholds $\mathcal{E}_D$ and $\mathcal{N}_D$.

6.4 SNR Detection Threshold $\mathcal{E}_D$ for Asymptotic Domain

Since the eigenvalues are ordered, $\bar{\lambda}_M \geq \bar{\lambda}_{M+1}$, (6.20) is necessarily satisfied if (6.19) is satisfied. Therefore we focus on condition (6.19), and substitute expressions (6.6) for the asymptotic eigenvalues to obtain

$$\frac{\lambda_M(\delta\omega) + \sigma^2}{\sqrt{N}} \leq f \cdot \lambda_M(\delta\omega) \tag{6.21}$$

or with rearrangement,

$$\frac{\sigma^2}{\sqrt{N}} \leq f \cdot \lambda_M(\delta\omega)\left[1 - \frac{1}{f \cdot \sqrt{N}}\right] \tag{6.22}$$

which for large $f\sqrt{N}$ (e.g. $N \gg 64$ for $f = 1/8$) is equivalent to

$$\frac{\sigma^2}{\sqrt{N}} \leq f \cdot \lambda_M(\delta\omega) \tag{6.23}$$

Thus (6.23) is a first order approximation (for large N) of the postulated necessary conditions (6.17), (6.18) for the detection of M sources.

To define the SNR detection threshold, we extend the approach used in [13]. We represent the source amplitude correlation matrix P as follows

$$P = pP_0 \tag{6.24}$$

where P_0 is a constant matrix the eigenvalues of which sum to unity, and p is a variable scale factor. Note that representation (6.24) retains the correlations between the source powers. We define the signal SNR to be the ratio of the scale factor p to the noise power σ^2. That is

$$\text{SNR} = p/\sigma^2 \tag{6.25}$$

We deem satisfactory detection performance to be possible whenever condition (6.23) is satisfied. We define the detection threshold power to be the smallest value p_{min} of p for which (6.23) is satisfied for a fixed N, and define the detection threshold SNR to be

$$\mathcal{E}_D = p_{min}/\sigma^2 \tag{6.26}$$

Analogously, we define the data set size detection threshold $\mathcal{N}_D$ to be the smallest value of N for which (6.23) is satisfied for a fixed power factor p.

Analysis in Chapter 5 has identified the eigenvalues $\lambda_i(\delta\omega)$ of R_S for closely spaced sources in non-degenerate multi-D scenarios. Specifically for small $\delta\omega$, the smallest eigenvalue of R_S was shown to be

$$\lambda_M(\delta\omega) \simeq p \cdot \lambda_M \, \delta\omega^{2m} \tag{6.27}$$

where parameter m satisfies (2.62) and λ_M is a positive quantity calculable from P_0, the normalized source configuration vectors $\vec{q}_1 \cdots \vec{q}_M$, and the generic arrival vector

$\vec{a}(\vec{\omega})$ and its spatial derivatives of up to m^{th} order. Specifically λ_M is the smallest non-zero eigenvalue of the limiting eigenmatrix $R_{2m,0}$ of the form described by Theorem 5.2, with the identification $P = P_0$.

Substitution of (6.25) and (6.27) in (6.23) and re-arrangement gives

$$\text{SNR} \cdot \sqrt{N} \;\geq\; \frac{1}{f \cdot \lambda_M} \cdot \delta\omega^{-2m} \tag{6.28}$$

Identification of the SNR detection threshold gives

$$\mathcal{E}_D \;\geq\; \frac{K'_D}{\sqrt{N}}\, \delta\omega^{-2m} \tag{6.29}$$

where

$$K'_D \;=\; \frac{1}{f \cdot \lambda_M} \tag{6.30}$$

6.5 Data Set Size Detection Threshold $\mathcal{N}_D$ for Asymptotic Domain

Rearrangement of (6.21) gives

$$\sqrt{N} \;\geq\; \frac{1}{f}\left[1 + \frac{\sigma^2}{\lambda_M(\delta\omega)}\right] \tag{6.31}$$

Substitution of (6.25) and (6.27) in (6.31), followed by squaring and use of (6.30) shows that

$$\begin{aligned} N \;&\geq\; \frac{1}{f^2}\left[1 + \frac{1}{\lambda_M \cdot \text{ SNR } \delta\omega^{2m}}\right]^2 \\ &=\; \left[\frac{1}{f} + \frac{K'_D}{\text{SNR } \delta\omega^{2m}}\right]^2 \end{aligned} \tag{6.32}$$

for small $\delta\omega$. It follows from (6.32) that the minimum data set size $\mathcal{N}_D$ is given by

$$\mathcal{N}_D \simeq \left[\frac{1}{f} + \frac{K'_D}{\text{SNR } \delta\omega^{2m}}\right]^2 \tag{6.33}$$

The following approximations to $\mathcal{N}_D$ follow from (6.33) for the conditions noted:

$$\text{If} \quad (\lambda_M \cdot \text{ SNR } \delta\omega^{2m}) \gg 1 \tag{6.34}$$

$$\mathcal{N}_D \simeq \frac{1}{f^2}\left[1 + \frac{2}{\lambda_M \cdot \text{ SNR } \delta\omega^{2m}}\right] \tag{6.35}$$

$$\text{If} \quad (\lambda_M \cdot \text{ SNR } \delta\omega^{2m}) \ll 1 \tag{6.36}$$

$$\mathcal{N}_D \simeq \left[\frac{K'_D}{\text{SNR } \delta\omega^{2m}}\right]^2 \tag{6.37}$$

Since λ_M is independent of $\delta\omega$, condition (6.36) is satisfied for sufficiently small $\delta\omega$ for any given scenario geometry and SNR. Hence the data set size threshold takes the simple form (6.37) for fixed SNR and sufficiently small $\delta\omega$.

6.6 Summary

The threshold expressions (6.29), (6.33), (6.35) and (6.37) are important since they provide explicit expressions for the minimum SNR and data set size N required to satisfy the "necessary condition" (6.23) for detection using any detection algorithm. The threshold expressions can be used to generate model detection curves for any given scenario, since the constant K'_D can be calculated explicitly given the array geometry, sensor directional response, source configuration and source correlations.

The threshold expressions (6.29), (6.33) (6.35) and (6.37) also clarify the trade-off between SNR, N and maximum source spacing $\delta\omega$ required to maintain source detection performance. For example, if noise power is doubled in a given scenario with $\delta\omega$ small enough to satisfy (6.36), then the size of the data set must increase by a factor of 4 to maintain detection performance. If, on the other hand, the maximum source spacing $\delta\omega$ satisfies (6.36) and is decreased by a factor of 2 in a 2-D non-degenerate scenario with $M = 6$ sources (with $m = 2$), then to maintain detection

performance with a fixed data set size N, the SNR must increase by a factor of $2^4 = 16$. Alternately if the SNR remains fixed, then the data set size N must increase by a factor of $2^8 = 256$!!! Thus the detection threshold data set size $\mathcal{N}_D$ is very sensitive to the maximum source spacing in the asymptotic domain.

By way of comparison, if the maximum source spacing $\delta\omega$ is decreased by a factor of 2 in a 1-D scenario with $M = 6$ sources, then to maintain detection performance with a fixed data set size N the SNR must increase by a factor of $2^{10} = 1024$!!! For small $\delta\omega$ and a given number of sources M, the detection thresholds are typically much smaller (more favorable) in multi-D than in 1-D scenarios.

Chapter 7

Eigenstructure of R_S for Partially Degenerate Scenarios

Analysis in Chapter 5 applied the non-degenerate SVD results of Chapter 4 to derive simple, explicit expressions for the limiting eigenmatrices that characterize the eigenstructure of covariance matrices R_S for small $\delta\omega$ in scenarios for which Conditions **C1-C3** are all satisfied. An important characteristic of the identified eigenstructure is that eigenvalue shells $0 \cdots m-1$ are full, and shell m contains a number of additional eigenvalue results sufficient to account for the rank M of R_S.

This chapter uses the partially degenerate SVD results of Chapter 4 to derive somewhat more complicated expressions for the limiting eigenmatrices of R_S applicable to partially degenerate scenarios for which only one of Conditions **C1** or **C2** are satisfied. Supporting analysis shows that satisfaction of only one of these conditions can produce situations in which one or more eigenvalue shells $0 \cdots m-1$ have vacancies.

Recall from Section 2.5.1 that R_S can be factored as

$$R_S = BB^h \tag{7.1}$$

where B is a rectangular matrix with Taylor series (2.60) of the form

$$B = \sum_{p=0}^{\infty} \delta\omega^p \dot{A}_p \Gamma_p \Pi \tag{7.2}$$

Parameter $\delta\omega$ is a scalar measure of the maximum spatial frequency separation between the sources, $\dot{A}_p$ consists of the p^{th} order partial derivatives of the generic arrival vector $\vec{a}(\vec{\omega})$ as in (2.50), Γ_p depends on the normalized source spatial frequency vectors $\vec{q}_1, \cdots, \vec{q}_M$ as in (2.58) and Π results from the factorization of source cross-power matrix P in (2.47).

This chapter shows that for partially degenerate scenarios matrices B are partially degenerate. Specifically, that Condition **C1** is sufficient for matrix B to satisfy Condition I, and that Condition **C2** is sufficient for matrix B to satisfy for Condition II. Conditions I and II are defined in Chapter 4 in terms of matrix $B_0(\epsilon)$ of the form

$$B_0(\epsilon) = \sum_{p=0}^{\infty} B_{0,p} \epsilon^p \tag{7.3}$$

To characterize the limiting singular matrices of the factor B of R_S, we make the identifications

$$\begin{aligned} B_0(\epsilon) &= B \\ \epsilon &= \delta\omega \\ B_{0,p} &= \dot{A}_p \Gamma_p \Pi \end{aligned} \tag{7.4}$$

Accordingly, the limiting SVD of B is identified using the expressions of Theorems 4.2 and 4.3 for the limiting singular matrices of partially degenerate matrices. The limiting eigenstructure of R_S then follows immediately from the limiting SVD of B.

A geometrical interpretation for scenario degeneracy is introduced, which relates Condition **C1** to array geometry, and Condition **C2** to source configuration. For example, in a 2-D DF scenario scenario with a planar array of isotropic sensors and $M = 6$ far-field sources clustered near array broadside, Condition **C1** is violated if all the sensors lie on a conic section curve (e.g. a circular sensor array). Similarly,

Condition **C2** is violated if all the sources lie on a conic section curve in spatial frequency (e.g. circular source configuration).

The chapter is organized as follows. Section 7.1 identifies the limiting SVD of B if only one of Conditions **C1** or **C2** are satisfied. Section 7.2 then identifies the limiting eigenstructure of R_S for such partially degenerate scenarios. Section 7.3 introduces a geometrical interpretation of Conditions **C1, C2** in terms of array geometry and source configuration. Section 7.4 presents numerical simulations that illustrate the limiting eigenstructure of R_S in partially degenerate scenarios.

7.1 Limiting SVD of B for Partially Degenerate Scenarios

In this section, we characterize the limiting SVD of the factor matrix B of R_S for degenerate scenarios that satisfy only one of Conditions **C1**, or **C2**.

Recall from Section 2.5.3 the non-degenerate scenario Conditions **C1, C2**:

$$\begin{aligned}
\textbf{C1.} \quad & \text{Rank}\{\dot{A}_0\} = \bar{n}_0 && \text{for } p = 0 \\
& \text{Rank}\{P_{[\dot{A}_0,\cdots\dot{A}_{p-1}]}\,\dot{A}_p\} = \bar{n}_p && \text{for } p = 1,\cdots m-1 \qquad (7.5) \\
\textbf{C2.} \quad & \text{Rank}\{\Gamma_0\} = \bar{n}_0 && \text{for } p = 0 \\
& \text{Rank}\{\Gamma_p\, P_{[\Gamma_0,\cdots,\Gamma_{p-1}]}\} = \bar{n}_p && \text{for } p = 1,\cdots m-1 \qquad (7.6)
\end{aligned}$$

where $\bar{n}_p$ is the number of p^{th} order partial derivatives of $\vec{a}(\vec{\omega})$ with respect to the elements of $\vec{\omega}$, and M is the number of sources.

Recall from Section 2.5.3 that integer parameter m is defined as the smallest number of successive leading terms of the Taylor series (2.61) of matrix A that must be included in a partial sum for the partial sum to have full rank. For degenerate scenarios for which Conditions **C1-C3** *are not all satisfied* parameter m is *not necessarily given by* (2.62). For partially degenerate scenarios, we identify m as follows:

C1 satisfied: Provided Conditions **C1** and **C3**$_\Gamma$ (detailed subsequently) are satisfied

$m = m_\Gamma$, where m_Γ satisfies

$$\text{Rank}\left\{\left[\Gamma_0^h, \cdots, \Gamma_{(m_\Gamma-1)}^h\right]\right\} < M \leq \text{Rank}\left\{\left[\Gamma_0^h, \cdots, \Gamma_{m_\Gamma}^h\right]\right\} \tag{7.7}$$

C2 satisfied: Provided Conditions **C2** and $\mathbf{C3}_{\dot{A}}$ (detailed subsequently) are satisfied

$m = m_{\dot{A}}$, where $m_{\dot{A}}$ satisfies

$$\text{Rank}\left\{\left[\dot{A}_0, \cdots, \dot{A}_{(m_{\dot{A}}-1)}\right]\right\} < M \leq \text{Rank}\left\{\left[\dot{A}_0, \cdots, \dot{A}_{m_{\dot{A}}}\right]\right\} \tag{7.8}$$

Conditions **C1** and **C2** are central to the simplified SVD analysis of partially degenerate matrices B. Conditions $\mathbf{C3}_\Gamma$, $\mathbf{C3}_{\dot{A}}$ are modified versions of Condition **C3** defined as follows.

$$\mathbf{C3}_\Gamma\text{:} \quad \text{Rank}\{P_{[\dot{A}_0,\cdots\dot{A}_{m-1}]}\,\dot{A}_m\Gamma_m\,P_{[\Gamma_0^h,\cdots,\Gamma_{m-1}^h]}\} = \mathcal{R} - \text{Rank}\left\{\left[\Gamma_0^h, \cdots, \Gamma_{(m_\Gamma-1)}^h\right]\right\} \tag{7.9}$$

$$\mathbf{C3}_{\dot{A}}\text{:} \quad \text{Rank}\{P_{[\dot{A}_0,\cdots\dot{A}_{m-1}]}\,\dot{A}_m\Gamma_m\,P_{[\Gamma_0^h,\cdots,\Gamma_{m-1}^h]}\} = \mathcal{R} - \text{Rank}\left\{\left[\dot{A}_0, \cdots, \dot{A}_{m_{\dot{A}}-1}\right]\right\} \tag{7.10}$$

Conditions $\mathbf{C3}_\Gamma$ or $\mathbf{C3}_{\dot{A}}$ are sufficient to guarantee that m determined by (7.7) or (7.8) is such that the partial Taylor series of matrix A consisting of terms of order $p = 0$ through $p = m$, does in fact have rank M. We will find that whenever Conditions **C1** and $\mathbf{C3}_\Gamma$, or **C2** and $\mathbf{C3}_{\dot{A}}$ are satisfied, the limiting SVD of B as $\delta\omega \to 0$ is entirely determined by the $p = 0 \cdots m$ terms of (7.2); subsequent terms only add higher order effects.

Next recall from Chapter 4 the Conditions I, II, IIIr and IIIc defined for matrices $B_0(\epsilon)$.

$$\textbf{I.} \quad \text{Rank}\{P_{[C_{p-1}]}B_{0,p}\} = \text{Rank}\{B_{0,p}\} \qquad \text{for } p = 1, \cdots \tilde{m} - 1 \tag{7.11}$$

$$\textbf{II.} \quad \text{Rank}\{B_{0,p}\,P_{[R_{p-1}]}\} = \text{Rank}\{B_{0,p}\} \qquad \text{for } p = 1, \cdots \tilde{m} - 1 \tag{7.12}$$

$$\textbf{IIIr.} \quad \text{Rank}\{P_{[C_{\tilde{m}-1}]}B_{0,\tilde{m}}\,P_{[R_{\tilde{m}-1}]}\} = \mathcal{R} - \text{Rank}\left\{\left[B_{0,0}^h, \cdots, B_{0,\tilde{m}_r-1}^h\right]\right\} \tag{7.13}$$

$$\textbf{IIIc.} \quad \text{Rank}\{P_{[C_{\tilde{m}-1}]}B_{0,\tilde{m}}\,P_{[R_{\tilde{m}-1}]}\} = \mathcal{R} - \text{Rank}\left\{[B_{0,0}, \cdots, B_{0,\tilde{m}_c-1}]\right\} \tag{7.14}$$

Matrices $B_{0,p}$ are the matrix coefficients of the Taylor series for $B_0(\epsilon)$ in (7.3), and C_{p-1}, R_{p-1} respectively aggregate the columns and rows of $B_{0,0} \cdots B_{0,p-1}$ as defined in (4.7), (4.8).

Recall from Chapter 4 that integer parameter $\tilde{m}$ is defined as the smallest number of successive leading terms of the Taylor series (7.3) of matrix $B_0(\epsilon)$ that must be included in a partial sum for the partial sum to have rank equal to that of $B_0(\epsilon)$. For degenerate scenarios for which Conditions I-III *are not all satisfied* parameter $\tilde{m}$ is *not necessarily given by* (4.6).

To relate the non-degenerate scenario Conditions **C1**, **C2** to the non-degenerate matrix Conditions I, II, and identify the associated parameter $\tilde{m}$ for partially degenerate cases, we develop the following result.

Lemma 7.1 : If B and $B_0(\epsilon)$ have Taylor series as in (7.2) and (7.3), and given identifications (7.4) then

a) if Conditions **C1** and $\mathbf{C3}_\Gamma$ are satisfied with $m = m_\Gamma$, then so are Conditions I and IIIr with $\tilde{m} = m_\Gamma$,

b) if Condition **C2** and $\mathbf{C3}_{\dot{A}}$ are satisfied with $m = m_{\dot{A}}$, then so are Conditions II and IIIc with $\tilde{m} = m_{\dot{A}}$.

where m_Γ and $m_{\dot{A}}$ are respectively defined by relations (7.7) and (7.8).

Proof: See Appendix H.

Consequently, the limiting singular matrices of matrix B for the two types of degenerate scenarios addressed can be identified using Theorems 4.2 or 4.3, as follows.

Theorem 7.1 : If B has Taylor series in $\delta\omega$ of the form (7.2), and Conditions **C1** and $\mathbf{C3}_\Gamma$ are satisfied, then

$$\text{1)}\quad P_{[B_{0,0},\cdots B_{k-1,0}]} \;=\; P_{[C''_{k-1}]} \qquad\qquad k = 0 \cdots m_\Gamma \qquad (7.15)$$

where

$$C''_{k-1} \;=\; \left[\dot{A}_0\Gamma_0\Pi,\; (\dot{A}_1\Gamma_1\Pi P_{[(\Gamma_0\Pi)^h]}),\; \cdots\; (\dot{A}_{k-1}\Gamma_{k-1}\Pi P_{[(\Gamma_0\Pi)^h,\cdots(\Gamma_{k-2}\Pi)^h]})\right] \qquad (7.16)$$

$$\textbf{2)}\quad P_{[B^h_{0,0},\cdots B^h_{k-1,0}]} = P_{[(\Gamma_0\Pi)^h,\cdots(\Gamma_{k-1}\Pi)^h]} \qquad k=0\cdots m_\Gamma \tag{7.17}$$

$$\textbf{3)}\quad B_{k,0} = \begin{cases} \dot{A}_0\Gamma_0\Pi & k=0 \\ (P_{[C''_{k-1}]}\dot{A}_k)\,(\Gamma_k\Pi P_{[(\Gamma_0\Pi)^h,\cdots(\Gamma_{k-1}\Pi)^h]}) & k=1,\cdots m_\Gamma \end{cases} \tag{7.18}$$

Proof: From the result of Lemma 7.1, Theorem 4.3 is applicable to B with $\tilde{m} = m_\Gamma$ when Conditions **C1** and $\mathbf{C3}_\Gamma$ are satisfied. The results (7.15)-(7.18) are immediate from Theorem 4.3, using (7.4) and identification (5.15) of Lemma 5.1.

Theorem 7.2 : If B has Taylor series in $\delta\omega$ of the form (7.2), and Conditions **C2** and $\mathbf{C3}_{\dot{A}}$ are satisfied, then

$$\textbf{1)}\quad P_{[B_{0,0},\cdots B_{k-1,0}]} = P_{[\dot{A}_0,\cdots\dot{A}_{k-1}]} \qquad k=0\cdots m_{\dot{A}} \tag{7.19}$$

$$\textbf{2)}\quad P_{[B^h_{0,0},\cdots B^h_{k-1,0}]} = P_{[R''_{k-1}]} \qquad k=0\cdots m_{\dot{A}} \tag{7.20}$$

where

$$R''_{k-1} = \left[(\dot{A}_0\Gamma_0\Pi)^h,\ ((\dot{A}_1\Gamma_1\Pi)^h P_{[\dot{A}_0]}),\ \cdots\ ((\dot{A}_{k-1}\Gamma_{k-1}\Pi)^h P_{[\dot{A}_0,\cdots\dot{A}_{k-2}]})\right] \tag{7.21}$$

$$\textbf{3)}\quad B_{k,0} = \begin{cases} \dot{A}_0\Gamma_0\Pi & k=0 \\ (P_{[\dot{A}_0,\cdots\dot{A}_{k-1}]}\dot{A}_k)\,(\Gamma_k\Pi P_{[R''_{k-1}]}) & k=1,\cdots m_{\dot{A}} \end{cases} \tag{7.22}$$

Proof: From the result of Lemma 7.1, Theorem 4.2 is applicable to B with $\tilde{m} = m_{\dot{A}}$ when Conditions **C2** and $\mathbf{C3}_{\dot{A}}$ satisfied. The results (7.19)-(7.22) are immediate from Theorem 4.2, using (7.4) and identification (5.17) of Lemma 5.1.

Theorems 7.1, 7.2 express the $B_{k,0}$ explicitly in terms of factor matrices $\dot{A}_p$, Γ_p and Π of the Taylor series of B. The expressions are more complicated than those obtained for non-degenerate scenarios in Theorem 5.1, due to the structure of C'' in (7.16) or of R'' in (7.21). Nevertheless, with m_Γ and $m_{\dot{A}}$ respectively defined in (7.7) and (7.8), Theorems 7.1, 7.2 identify all the non-trivial $B_{k,0}$.

The expressions for the limiting singular matrices of B identified above are applied in the next section to identify expressions for the limiting eigenmatrices of R_S.

7.2 Limiting Eigenstructure of R_S for Partially Degenerate Scenarios

This section characterizes the limiting eigenstructure of R_S for partially degenerate scenarios by identifying expressions for the limiting eigenmatrices of R_S.

By construction of the SVD, the limiting eigenmatrices of R_S are simply the outer products of the limiting singular matrices of B. Hence the limiting eigenmatrices $R_{2k,0}$ of R_S corresponding to limiting eigenvalues proportional to $\delta\omega^{2k}$ are

$$R_{2k,0} \triangleq B_{k,0}B_{k,0}^h \tag{7.23}$$

where $B_{k,0}$ are the limiting singular matrices of B corresponding to the limiting singular values proportional to $\delta\omega^k$.

The limiting eigenmatrices $R_{2k,0}$ of R_S can be straightforwardly identified for the two types of partially degenerate scenarios addressed as follows.

Theorem 7.3 : If R_S is formed as the outer product of matrix B with Taylor series in $\delta\omega$ of the form (7.2), and Conditions **C1** and $\mathbf{C3}_\Gamma$ are satisfied, then

$$R_{2k,0} \triangleq \begin{cases} \dot{A}_0\Gamma_0\Pi\ \Pi^h\Gamma_0^h\dot{A}_0^h & k=0 \\ (P_{[C''_{k-1}]}\dot{A}_k)\ (\Gamma_k\Pi P_{[(\Gamma_0\Pi)^h,\cdots(\Gamma_{k-1}\Pi)^h]}) & \\ \quad \cdot\ (P_{[(\Gamma_0\Pi)^h,\cdots(\Gamma_{k-1}\Pi)^h]}\Pi^h\Gamma_k^h)\ (\dot{A}_k^h P_{[C''_{k-1}]}) & k=1,\cdots m_\Gamma \\ 0 & k>m_\Gamma \end{cases} \tag{7.24}$$

where C''_{k-1} is as defined in (7.16).

Proof: Immediate from (7.23) and Theorem 7.1.

Theorem 7.4 : If R_S is formed as the outer product of matrix B with Taylor series

in $\delta\omega$ of the form (7.2), and Conditions **C2** and $\mathbf{C3}_{\dot{A}}$ are satisfied, then

$$R_{2k,0} \triangleq \begin{cases} \dot{A}_0\Gamma_0\Pi\ \Pi^h\Gamma_0^h\dot{A}_0^h & k=0 \\ (P_{[\dot{A}_0,\cdots\dot{A}_{k-1}]}\dot{A}_k)\ (\Gamma_k\Pi P_{[R''_{k-1}]}) & \\ \quad \cdot\ (P_{[R''_{k-1}]}\Pi^h\Gamma_k^h)\ (\dot{A}_k^h P_{[\dot{A}_0,\cdots\dot{A}_{k-1}]}) & k=1,\cdots m_{\dot{A}} \\ 0 & k > m_{\dot{A}} \end{cases} \tag{7.25}$$

where R''_{k-1} is as defined in (7.21).

Proof: Immediate from (7.23) and Theorem 7.2.

Theorems 7.3, 7.4, express the $R_{2k,0}$ explicitly in terms of factor matrices $\dot{A}_p$, Γ_p and Π of the Taylor series of B. The expressions are more complicated than those obtained for non-degenerate scenarios in Theorem 5.2, due to the structure of C'' in (7.16) or of R'' in (7.21).

In the non-degenerate case, Corollary 5.4 explicitly identified the number n_k of limiting eigenvalues in each eigenvalue shell of R_S. We now develop a bounding relation for n_k applicable to partially degenerate scenarios.

Corollary 7.1 : If R_S is formed as the outer product of matrix B with Taylor series in $\delta\omega$ of the form (7.2), and either set of Conditions **C1** and $\mathbf{C3}_\Gamma$ or **C2** and $\mathbf{C3}_{\dot{A}}$ is satisfied, then the number n_k of limiting eigenvalues of R_S proportional to $\delta\omega^{2k}$ is less than or equal to the number $\bar{n}_k$ of k^{th} order partial derivatives of $\vec{a}(\vec{\omega})$ with respect to the elements of $\vec{\omega}$, for $k = 0,\cdots m$. That is,

$$\begin{aligned} n_0 &= \bar{n}_0 & k=0 \\ n_k &\leq \bar{n}_k & k=1,\cdots m \end{aligned} \tag{7.26}$$

where $m = m_\Gamma$ if Conditions **C1** and $\mathbf{C3}_\Gamma$ are satisfied, and $m = m_{\dot{A}}$ if Conditions **C2** and $\mathbf{C3}_{\dot{A}}$ are satisfied.

Proof: Immediate from the applicable Theorem 7.3 or Theorem 7.4, since $\dot{A}_k$ is at most rank $\bar{n}_k$, and the rank of a product is at most the rank of any of its factors.

For partially degenerate scenarios **Corollary 7.1** shows that $\bar{n}_k$ provides an upper

bound on the number n_k of limiting eigenvalues of R_S proportional to $\delta\omega^{2k}$ as $\delta\omega \rightarrow 0$. We note from Corollary 5.4 that the bound is satisfied with equality for $k = 0 \cdots m-1$ in non-degenerate scenarios.

7.3 Geometric Interpretation of Degeneracy

To help clarify the two types of partially degenerate scenarios, this section provides a physical interpretation for Conditions **C1** and **C2** in terms of sensor array geometry and source configuration, respectively, in the context of a 2-D scenario with a planar array of isotropic sensors and far-field sources clustered near array broadside.

Conditions **C1** and **C2** are respectively defined in terms of matrices $\dot{A}_p$ and Γ_p. For a 2-D scenario with a planar array of isotropic sensors and far-field sources clustered at array broadside, the applicable forms of $\dot{A}_p$, Γ_p for $p = 0, 1, 2$ are restated here from (2.68), (2.59):

- For 2-D scenarios where $\vec{r}_i = [r_{xi}, r_{yi}]^t$ is the location of the i^{th} sensor in sensor plane, and the reference parameter vector $\vec{\omega}_0$ is taken to be at array broadside $\vec{\omega}_0 = [0,\ 0]^t$, we have

$$\dot{A}_0 = \begin{bmatrix} 1 \\ \vdots \\ 1 \end{bmatrix}, \ \dot{A}_1 = j \cdot \begin{bmatrix} r_{x1} & r_{y1} \\ \vdots & \vdots \\ r_{xW} & r_{yW} \end{bmatrix}, \ \dot{A}_2 = -1 \cdot \begin{bmatrix} r_{x1}^2 & r_{x1}r_{y1} & r_{y1}^2 \\ \vdots & \vdots & \vdots \\ r_{xW}^2 & r_{xW}r_{yW} & r_{yW}^2 \end{bmatrix} \quad (7.27)$$

- For 2-D scenarios, with $\vec{q}_j = [q_{xj}, q_{yj}]^t$

$$\begin{aligned} \Gamma_0 &= [1, \quad \cdots \quad 1] \\ \Gamma_1 &= \begin{bmatrix} q_{x1}, & \cdots & q_{xM} \\ q_{y1}, & \cdots & q_{yM} \end{bmatrix} \\ \Gamma_2 &= \begin{bmatrix} q_{x1}^2/2, & \cdots & q_{xM}^2/2 \\ q_{x1}q_{y1}, & \cdots & q_{xM}q_{yM} \\ q_{y1}^2/2, & \cdots & q_{yM}^2/2 \end{bmatrix} \end{aligned} \quad (7.28)$$

Consider Condition **C1** with $m = 3$. The linear independence of the columns of $\dot{A}_0, \dot{A}_1$ and $\dot{A}_2$ required by Condition **C1** implies that

$$\vec{0} = \left[\dot{A}_0, \dot{A}_1, \dot{A}_2\right] \vec{\alpha} \tag{7.29}$$

is satisfied only iff $\vec{\alpha} = 0$.

Now suppose that there exists a $\vec{\alpha} \neq 0$ that satisfies (7.29), and hence that Condition **C1** is not satisfied for $p = 0, 1, 2$. In that case, the i^{th} row of (7.29) is of the form

$$\begin{aligned} 0 &= \alpha_1 + j \cdot \alpha_2 r_{xi} + j \cdot \alpha_3 r_{yi} - \alpha_4 r_{xi}^2 - \alpha_5 r_{xi} r_{yi} - \alpha_6 r_{yi}^2 \\ &= f(\vec{r}_i) \end{aligned} \tag{7.30}$$

where $f(\vec{r}_i)$ denotes a suitable 2nd order polynomial function of the elements of $\vec{r}_i$. Eq. (7.29) can only be satisfied with $\vec{\alpha} \neq 0$ if Eq. (7.30) is satisfied for each $\vec{r}_1 \cdots \vec{r}_W$ for some $\vec{\alpha} \neq 0$. Therefore Condition **C1** is violated for $p = 0, 1, 2$ if the sensor coordinates $\vec{r}_1 \cdots \vec{r}_W$ all satisfy a (non-trivial) second order polynomial function (i.e. conic section equation). In terms of the geometry the sensor array, Condition **C1** is violated for $p = 0, 1, 2$ if *all* the sensors are located on a conic section curve (i.e. circle, ellipse, parabola, hyperbola, line).

A parallel argument shows that Condition **C1** is violated for $p = 0, 1$ if the sensor coordinates $\vec{r}_1 \cdots \vec{r}_W$ all satisfy a first order polynomial function (i.e. the sensors are co-linear). Extension of the argument to arbitrary m gives:

Geometric Interpretation of Violation of Condition C1: For a 2-D scenario with a planar array of isotropic sensors, and far-field sources near array broadside, Condition **C1** is violated for $p = 0 \cdots m - 1$ if the sensors are located on a curve described by a $(m-1)^{th}$ order polynomial equation.

An analogous argument applied to the source configuration establishes that Condition **C2** is violated for $p = 0, 1, 2$ if *all* the source spatial frequency offset vectors $\vec{q}_1, \cdots \vec{q}_M$ are located on a conic section curve (i.e. lie on a circle, ellipse, parabola,

hyperbola, line). Similarly, a co-linear source configuration violates Condition **C2** for $p = 0, 1$. Extending to arbitrary m, we have

Geometric Interpretation of Violation of Condition C2: In 2-D scenarios, Condition **C2** is violated for $p = 0 \cdots m-1$ if the sources are located on a curve described by a $(m-1)^{th}$ order polynomial equation in spatial frequency space.

Illustrative examples of scenarios with circular source configurations, and with circular sensor arrays, are presented in the next section.

7.4 Example Partially Degenerate R_S Eigenstructures

To illustrate the accuracy of the foregoing limiting eigenstructure theoretical expressions for partially degenerate scenarios, we compare the predicted limiting and exact eigenvalues for matrix R_S for the two partially degenerate 2-D direction finding scenarios of Examples 2.4 and 2.5 of Section 2.6.

The examples involve a planar array of $W = 16$ unit-gain, isotropic sensors, and $M = 6$ far-field sources clustered near to the array broadside.

We assume that the sources are *correlated* and have equal powers. Total source power is taken to be unity. Specifically, the source cross-power matrix P is taken to be (5.39). The matrix factor B of R_S in such scenarios is of the form (5.40), with Taylor series of the form (5.41).

The limiting and exact eigenvalues of R_S for two partially degenerate scenarios are compared numerically in the following.

Example 7.1 : For this example, the array and source geometries are defined as in Example 2.4. That is,

Array: Sensors in a sparse grid per Figure 2-4A,

Sources: Sources clustered around broadside in a circular configuration per Figure 2-5B.

As shown in Example 2.4, this scenario satisfies Conditions **C1** and $\mathbf{C3}_\Gamma$ with $m = m_\Gamma = 3$. Consequently, the limiting eigenmatrices of R_S may be determined using Theorem 7.3.

Figure 7-1 shows the eigenvalues of R_S for a range of emitter separations $\delta\omega$. Solid curves depict the exact eigenvalues; dashed lines depict the limiting behavior predicted by our analysis. The horizontal scale denotes spatial frequency separation $\delta\omega$ normalized by the array beamwidth BW, so that unity on the horizontal scale of the graph corresponds to maximum source separation of one beamwidth (i.e. $\delta\omega/\text{BW}= 1$). The vertical scale denotes the eigenvalues.

Clearly the limiting expressions again capture the essence of the eigenvalues for source separations of less than one beamwidth. The limiting eigenvalues are grouped into eigenvalue shells as $\delta\omega \rightarrow 0$, with $n_0 = 1$ having slope of 0 dB/decade, $n_1 = 2$ having slope of 20 dB/decade, $n_2 = 2$ having slope of 40 dB/decade, $n_3 = 1$ having slope of 60 dB/decade. Thus the $k = 2$ shell is not full for this partially degenerate scenario, and there is one eigenvalue in the $k = 3$ shell.

The theoretical expressions accurately predict the eigenvalues of R_S for small source separations $\delta\omega$ for this partially degenerate scenario which satisfies Conditions **C1** and $\mathbf{C3}_\Gamma$.

Example 7.2 : For this example, the array and source geometries are defined as in Example 2.5. That is,

Array: Sensors in a circular geometry per Figure 2-4B,

Sources: Sources clustered around broadside in a "double chevron" configuration per Figure 2-5A.

As shown in Example 2.5, this scenario satisfies Conditions **C2** and $\mathbf{C3}_{\dot{A}}$, with

$m = m_{\hat{A}} = 3$. Consequently the limiting eigenmatrices of R_S may be determined using Theorem 7.4.

Figure 7-2 again shows the eigenvalues of R_S for a range of emitter separations $\delta\omega$. Solid curves depict the exact eigenvalues; dashed lines depict the limiting behavior predicted by our analysis. The horizontal scale denotes spatial frequency separation $\delta\omega$ normalized by the array beamwidth BW, so that unity on the horizontal scale of the graph corresponds to maximum source separation of one beamwidth (i.e. $\delta\omega$/BW= 1). The vertical scale denotes the eigenvalues.

Clearly the limiting expressions again capture the essence of the eigenvalues for source separations of less than one beamwidth. The limiting eigenvalues are again grouped into eigenvalue shells as $\delta\omega \rightarrow 0$, with $n_0 = 1$ having slope of 0 dB/decade, $n_1 = 2$ having slope of 20 dB/decade, $n_2 = 2$ having slope of 40 dB/decade, $n_3 = 1$ having slope of 60 dB/decade. Thus the $k = 2$ shell is not full for this partially degenerate scenario, and there is one eigenvalue in the $k = 3$ shell.

The theoretical expressions again accurately predict the eigenvalues of R_S for small source separations $\delta\omega$ for this partially degenerate scenario which satisfies Conditions **C2** and $\mathbf{C3}_{\hat{A}}$.

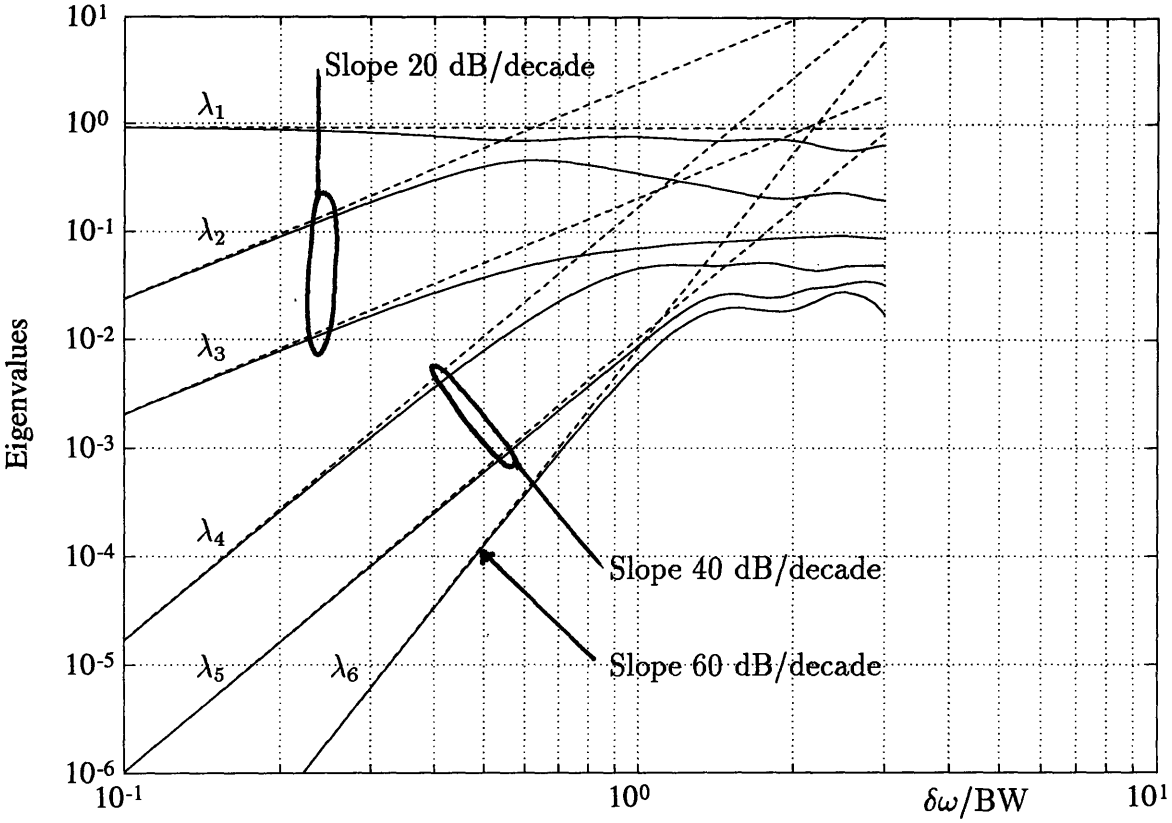

Figure 7-1: Limiting Eigenvalues for Partially Degenerate Scenario; **C1** Satisfied

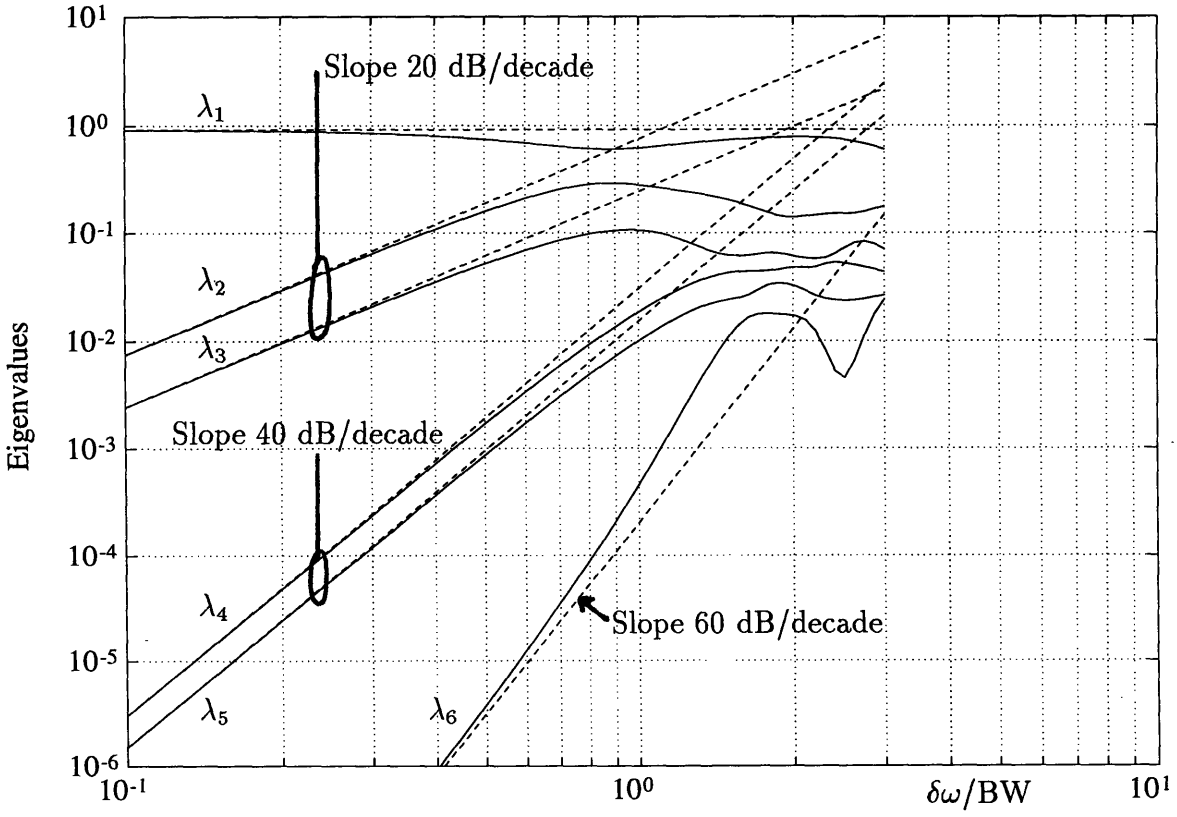

Figure 7-2: Limiting Eigenvalues for Partially Degenerate Scenario; **C2** Satisfied

Chapter 8

Cramér-Rao Bounds: Background

The Cramér-Rao (CR) lower bound on the variance of unbiased parameter estimates is a commonly used yardstick for assessing the estimation accuracy of direction finding algorithms [15]. The CR bound is of interest since it is not algorithm specific, but rather characterizes the optimum performance of any unbiased algorithm. The CR bound can also provide insight into the individual impact of scenario parameters such as sensor array geometry, source powers and correlations, source configuration, and maximum source spacing. Such insight has been developed by Lee [11] for closely-spaced sources in 1-D scenarios. The thesis results pertaining to CR bounds develop analogous insight for closely-spaced sources in multi-D scenarios.

This chapter lays a foundation for the subsequent CR bound analysis, and is organized as follows. Section 8.1 reviews the data model assumptions, and introduces the assumptions required for finite CR bounds. Section 8.2 summarizes prior CR bound expressions which serve as the point of departure for our analysis. Section 8.3 clarifies the CR bound expressions by reference to the MUSIC null spectrum. Section 8.4 reviews the analysis approach for closely-spaced sources in multi-D. Section 8.5 details conditions which simplify the multi-D CR bound analysis, and defines three cases with distinct CR bound structure. Illustrative examples of each case for scenarios that satisfy the simplifying conditions are presented in Section 8.6.

8.1 Data Model

Recall from Section 2.2 that the data model of interest is

$$\vec{y}(t) \;=\; A\vec{x}(t) + \vec{\epsilon}(t) \qquad\qquad t = 1, \cdots N \tag{8.1}$$

where

$$A \;\triangleq\; [\vec{a}(\vec{\omega}_1), \vec{a}(\vec{\omega}_2), \cdots \vec{a}(\vec{\omega}_M)] \tag{8.2}$$

$\vec{a}(\vec{\omega})$ is a generic arrival vector for signals with spatial frequency $\vec{\omega}$, $\vec{x}(t)$ is a vector of signal complex amplitudes and $\vec{\epsilon}(t)$ is a vector of additive noise signals the t^{th} sampling index. For 1-D DF problems, $\vec{\omega} = \omega$ is a scalar. For multi-D DF problems, $\vec{\omega}$ is a vector of spatial frequency parameters which are related by transformation to the source direction parameters (ex. azimuth, elevation, (2-D) and possibly also range (3-D)).

The vectors $\vec{a}(\vec{\omega})$, $\vec{x}(t)$ and $\vec{\epsilon}(t)$ in data model (8.1), (8.2) are assumed to satisfy assumptions **A1-A4, X1-X3** and **E1** of Section 2.2.1. The data model (8.1), (8.2) with the foregoing assumptions corresponds to the Conditional Model [15], [11] for which the sequence $\vec{x}(1)$, $\vec{x}(2), \cdots \vec{x}(N)$ of source signal vectors is fixed (frozen), whereas the additive noise vector $\vec{\epsilon}(t)$ varies randomly over the ensemble of sample values.

Two additional assumptions used in our CR bound analysis are

A5. the number of sensors exceeds the number of sources by at least the scenario dimensionality $\mathcal{D}$

$$W \;\geq\; M + \mathcal{D} \tag{8.3}$$

A6. the $\mathcal{D}$ first order partial derivatives of $\vec{a}(\vec{\omega})$ with respect to the elements of $\vec{\omega}$, at each source direction $\vec{\omega} = \vec{\omega}_j$, $(j = 1 \cdots M)$ are linearly independent from the source arrival vectors $\vec{a}(\vec{\omega}_1), \cdots \vec{a}(\vec{\omega}_M)$.

Our analysis will show that Assumption **A6** is required for the existence of finite CR bounds; Assumption **A5** is an enabling condition for **A6**. For 1-D scenarios, **A5** simplifies to the well known relation

$$W \geq M+1 \tag{8.4}$$

which states that the number of sensors is greater than the number of sources.

8.2 Referenced CR Bound Expressions

The point of departure of our CR bound analysis are compact expressions for the submatrix of the inverse Fisher Information matrix applicable to the spatial frequency parameters (See discussion in Section 2.4). Such compact expressions have been developed by Stoica and Nehorai for 1-D scenarios [15], and served as the basis for the development by Lee [11] of simple explicit CR bound expressions for the case of closely-spaced sources in 1-D scenarios.

The compact expressions developed by Stoica and Nehorai have been extended to multi-D scenarios by Yau and Bresler [16]. The latter results serve as the basis of our analysis of closely-spaced sources in multi-D scenarios. The referenced expressions of [15], [11] and [16] are summarized below.

8.2.1 Compact Expression for CR Bound in 1-D Frequency [15]

For 1-D scenarios, the CR bound on sample frequency covariances takes the form [15],

$$E\left\{\left(\hat{\vec{\Omega}}-\vec{\Omega}\right)\left(\hat{\vec{\Omega}}-\vec{\Omega}\right)^{h}\right\} \geq B_C \tag{8.5}$$

where

$$\vec{\Omega} \triangleq [\omega_1, \omega_2, \cdots, \omega_M]^t \tag{8.6}$$

$$\vec{\hat{\Omega}} \triangleq [\hat{\omega}_1, \hat{\omega}_2, \cdots, \hat{\omega}_M]^t \tag{8.7}$$

and $\hat{\omega}_j$ denotes an unbiased estimate of ω_j ($j = 1 \cdots M$). B_C is the $M \times M$ submatrix of the inverse Fisher Information matrix corresponding to the elements of $\vec{\Omega}$.

Stoica and Nehorai [15] have shown that this submatrix can be expressed as follows

$$B_C = \frac{\sigma^2}{2N} \left\{ \mathrm{Re}\left[H \odot \hat{P}^t \right] \right\}^{-1} \tag{8.8}$$

where $\odot$ denotes the Hadamard element-by-element matrix product, and

$$H \triangleq D^h \left[I - A(A^h A)^{-1} A^h \right] D \tag{8.9}$$

$$D \triangleq \left[\vec{d}(\omega_1), \vec{d}(\omega_2), \cdots \vec{d}(\omega_M) \right] \tag{8.10}$$

$$\vec{d}(\omega_j) \triangleq \frac{d}{d\omega} \vec{a}(\omega) \Big|_{\omega=\omega_j} \tag{8.11}$$

$$\hat{P} \triangleq \frac{1}{N} \sum_{t=1}^{N} \vec{x}(t) \vec{x}(t)^h \tag{8.12}$$

The formulation (8.8)-(8.12) is very useful for both analytical and numerical work in that it bypasses the tedious calculation associated with calculating and inverting the (large) Fisher Information Matrix. However, a shortcoming to the formulation (8.8) is that the dependence of B_C upon scenario parameters such as array geometry, source configuration, and source powers and correlations remains implicit.

8.2.2 Limiting Form of B_C for M Signals Closely-Spaced in 1-D [11]

A recent paper by Lee [11] analyzed the bound (8.8) for the case of M signals closely-spaced in 1-D frequency. The signal frequencies were represented by scalar frequency parameters $\omega_1 \cdots \omega_M$ as follows:

$$\omega_j = \omega_0 + q_j \delta\omega \tag{8.13}$$

$j = 1 \cdots M$. Here ω_0 denotes a fixed reference frequency, the q_j are normalized offsets such that $q_1 < q_2 < \cdots q_M$ with $q_1 = -1/2$ and $q_M = +1/2$, and $\delta\omega$ is a variable scale parameter corresponding to the separation of the extreme frequencies. The paper analyzed the bound (8.8) as the multiplier $\delta\omega \to 0$. Representation (8.13) facilitates analysis of the bound (8.8) since the problem is reduced to one with a single variable parameter $\delta\omega$. The condition $\delta\omega \to 0$ corresponds to coalescing the signal frequencies about the reference frequency ω_0.

The approach of [11] is to identify the dominant term of H for small $\delta\omega$ as follows

$$H = \frac{(\delta\omega)^{2(M-1)}}{(M!)^2}(\vec{\epsilon}_M^h \vec{\epsilon}_M)\dot{\Psi}U\dot{\Psi} + \mathcal{O}\left\{(\delta\omega)^{2(n-1)+1}\right\} \tag{8.14}$$

where

$$\vec{\epsilon}_M \triangleq \left[I - \dot{A}(\dot{A}^h\dot{A})^{-1}\dot{A}^h\right]\vec{a}^{(M)}(\omega_0) \tag{8.15}$$

$$\dot{A} \triangleq \left[\vec{a}(\omega_0), \vec{a}^{(1)}, \cdots, \vec{a}^{(M-1)}\right] \tag{8.16}$$

$$\vec{a}^{(k)} \triangleq \frac{d^k}{d\omega^k}\vec{a}(\omega)\Big|_{\omega=\omega_0} \tag{8.17}$$

$$\dot{\Psi} \triangleq \text{Diag.}\left[\psi'(q_1), \psi'(q_2), \cdots \psi'(q_M)\right] \tag{8.18}$$

$$\psi(q) \triangleq \prod_{l=1}^{M}(q - q_l) \tag{8.19}$$

$$\psi'(q) \triangleq \frac{d\psi(q)}{dq} \tag{8.20}$$

$$U \triangleq \vec{u}\vec{u}^t \tag{8.21}$$

$$\vec{u} \triangleq [1, 1, \cdots 1]^t \tag{8.22}$$

Eq. (8.14) is then substituted into (8.8) to obtain the following first order representation of B_C for small $\delta\omega$,

$$B_C = (\delta\omega)^{-2(M-1)}K + \mathcal{O}\left\{(\delta\omega)^{-2(M-1)+1}\right\} \tag{8.23}$$

where

$$K = \frac{\sigma^2 (M!)^2}{2N} \frac{1}{\vec{\epsilon}_M^h \vec{\epsilon}_M} \dot{\Psi}^{-1} \left[\mathrm{Re}\left\{ \hat{P} \right\} \right]^{-1} \dot{\Psi}^{-1} \tag{8.24}$$

The result (8.23), (8.24) is quite useful in that it is applicable to a broad range of scenarios, and it makes explicit tradeoffs among scenario parameters such as frequency separations, signal powers and correlations, and the sampling grid. Specifically these quantities are represented in (8.23), (8.24) as follows

$$\begin{aligned} \text{frequency separations} &\iff \psi'(q_j) \cdot (\delta\omega)^{M-1} \\ \text{signal powers and correlations} &\iff \left[\mathrm{Re}\left\{ \hat{P} \right\} \right]^{-1} \\ \text{sampling grid} &\iff \|\vec{\epsilon}_M\|^2 \end{aligned}$$

Thus, for example, it is immediately clear from (8.23) for *any* one-dimensional scenario that reducing the frequency separation factor $\delta\omega$ by a factor of 10 in a $M = 3$ signal scenario requires that the source powers be increased by $2(M-1) \cdot 10\text{dB} = 40\text{dB}$ for an unbiased estimator to maintain the same frequency standard deviation. By requiring the standard deviation of frequency estimates to be smaller than the separation of adjacent frequencies, it also was argued that the threshold Signal-to-Noise ratio $\mathcal{E}_R$ at which an unbiased estimator can resolve M signals closely-spaced in 1-D frequency satisfies

$$\mathcal{E}_R \simeq K_R/(N \cdot \delta\omega^{2M}) \tag{8.25}$$

where N is sample size and K_R is a (positive) function of relative frequency separations, signal powers and covariances and array geometry. See [11].

8.2.3 Compact Expression for CR Bound in Multi-D [16]

Yau and Bresler [16] have extended the result (8.8)-(8.12) to multi-D scenarios with parameter vectors $\vec{\omega}_1 \cdots \vec{\omega}_M$. For the multi-D case,

$$\vec{\Omega} \triangleq [\omega_{11} \cdots \omega_{\mathcal{D}1} \cdots \omega_{1M} \cdots \omega_{\mathcal{D}M}]^t \tag{8.26}$$

$$\hat{\vec{\Omega}} \triangleq [\hat{\omega}_{11} \cdots \hat{\omega}_{\mathcal{D}1} \cdots \hat{\omega}_{1M} \cdots \hat{\omega}_{\mathcal{D}M}]^t \tag{8.27}$$

$\hat{\omega}_{ij}$ denotes an unbiased estimate of i^{th} element of $\vec{\omega}_j$, $(i = 1 \cdots \mathcal{D}, j = 1 \cdots M)$. In the multi-D case, B_C is an $M\mathcal{D} \times M\mathcal{D}$ matrix with the compact form [16],

$$B_C = \frac{\sigma^2}{2N} \left\{ \mathrm{Re}\left[H \odot \hat{P}_+^t \right] \right\}^{-1} \tag{8.28}$$

with

$$H \triangleq D^h \left[I - A(A^h A)^{-1} A^h \right] D \tag{8.29}$$

$$D \triangleq \left[\dot{D}(\vec{\omega}_1), \cdots \dot{D}(\vec{\omega}_M) \right] \tag{8.30}$$

$$\dot{D}(\vec{\omega}_j) \triangleq \left[\frac{\partial}{\partial \omega_1} \vec{a}(\vec{\omega}), \cdots \frac{\partial}{\partial \omega_{\mathcal{D}}} \vec{a}(\vec{\omega}) \right]_{\vec{\omega}=\vec{\omega}_j} \tag{8.31}$$

$$\begin{aligned} \hat{P}_+ &\triangleq \hat{P} \otimes 1_{\mathcal{D}\times\mathcal{D}} \\ &= \begin{bmatrix} 1_{\mathcal{D}\times\mathcal{D}} \cdot \hat{p}_{11} & \cdots & 1_{\mathcal{D}\times\mathcal{D}} \cdot \hat{p}_{M1} \\ \vdots & & \vdots \\ 1_{\mathcal{D}\times\mathcal{D}} \cdot \hat{p}_{1M} & \cdots & 1_{\mathcal{D}\times\mathcal{D}} \cdot \hat{p}_{MM} \end{bmatrix} \quad (M\mathcal{D} \times M\mathcal{D}) \end{aligned} \tag{8.32}$$

where $\hat{p}_{ij}$ is the i,j^{th} scalar element of the sample cross power matrix $\hat{P}$ of (8.12), $\otimes$ denotes Kronecker product, and $1_{\mathcal{D}\times\mathcal{D}}$ denotes the $\mathcal{D} \times \mathcal{D}$ matrix of ones.

The thesis objective with respect to the CR bounds is to derive expressions for B_C for closely-spaced sources in multi-D scenarios which are analogous to those of Lee [11] for 1-D scenarios. Specifically, we would like to explicitly identify the dependence of B_C upon scenario parameters such as maximum spatial frequency separation $\delta\omega$, source configuration, source powers and correlations, and array geometry.

8.2.4 2-D DF Example

To illustrate the structure of the CR bound expressions (8.28)-(8.32) for a multi-D DF scenario, consider an example two-dimensional $\mathcal{D} = 2$ scenario with $M = 3$ sources. The spatial frequency vector has two elements $\vec{\omega} = [\omega_x, \omega_y]$. The DF problem is to estimate the spatial frequency vector for each of the three sources, namely $\vec{\omega}_1, \vec{\omega}_2, \vec{\omega}_3$.

Let $\hat{p}_{ij}$ denote the i,j^{th} element of sample source amplitude covariance matrix $\hat{P}$, for $i = 1,2,3$ and $j = 1,2,3$. The expanded and transposed matrix $\hat{P}_+^t$ then takes the form

$$\hat{P}_+^t = \begin{bmatrix} \hat{p}_{11} & \hat{p}_{11} & \hat{p}_{21} & \hat{p}_{21} & \hat{p}_{31} & \hat{p}_{31} \\ \hat{p}_{11} & \hat{p}_{11} & \hat{p}_{21} & \hat{p}_{21} & \hat{p}_{31} & \hat{p}_{31} \\ \hat{p}_{12} & \hat{p}_{12} & \hat{p}_{22} & \hat{p}_{22} & \hat{p}_{32} & \hat{p}_{32} \\ \hat{p}_{12} & \hat{p}_{12} & \hat{p}_{22} & \hat{p}_{22} & \hat{p}_{32} & \hat{p}_{32} \\ \hat{p}_{13} & \hat{p}_{13} & \hat{p}_{23} & \hat{p}_{23} & \hat{p}_{33} & \hat{p}_{33} \\ \hat{p}_{13} & \hat{p}_{13} & \hat{p}_{23} & \hat{p}_{23} & \hat{p}_{33} & \hat{p}_{33} \end{bmatrix} \tag{8.33}$$

and matrix B_C takes the form

$$B_C = \frac{\sigma^2}{2N} \left[\mathrm{Re} \left\{ \begin{matrix} \hat{p}_{11} \cdot Z_{11} & \hat{p}_{21} \cdot Z_{12} & \hat{p}_{31} \cdot Z_{13} \\ \hat{p}_{12} \cdot Z_{21} & \hat{p}_{22} \cdot Z_{22} & \hat{p}_{32} \cdot Z_{23} \\ \hat{p}_{13} \cdot Z_{31} & \hat{p}_{23} \cdot Z_{32} & \hat{p}_{33} \cdot Z_{33} \end{matrix} \right\} \right]^{-1} \tag{8.34}$$

where

$$Z_{ij} = \dot{D}(\vec{\omega}_i)^h [I - A(A^h A)^{-1} A^h] \dot{D}(\vec{\omega}_j) \qquad 2 \times 2 \tag{8.35}$$

8.3 Relationship to the MUSIC Null Spectrum

The formulation (8.28) for the multi-D CR bound on $\mathrm{Cov}\{\hat{\vec{\Omega}}\}$ can be clarified by reference to the MUSIC null spectrum.

The null spectrum $\Delta(\vec{\omega})$ for the MUSIC algorithm for an arbitrary direction $\vec{\omega}$ is

defined as follows:

$$\Delta(\vec{\omega}) \triangleq \frac{\vec{a}(\vec{\omega})^h \left[I - A(A^hA)^{-1}A^h\right] \vec{a}(\vec{\omega})}{\|\vec{a}(\vec{\omega})\|^2} \tag{8.36}$$

where A denotes the matrix (8.2) of source arrival vectors. This scalar function has the useful property that it equals zero whenever $\vec{\omega}$ coincides with a source spatial frequency $\vec{\omega}_j$. The MUSIC algorithm uses this property as a basis for estimating source directions. The spectrum function $S_{MUSIC}(\vec{\omega})$ of Table 1.1 is asymptotically equal to the inverse of the null spectrum $\Delta(\vec{\omega})$, for large data set size N. Thus the values of spatial frequency at the maxima of the spectrum function, used as the MUSIC estimates of source spatial frequencies, are asymptotically equal to the values of spatial frequency at the minima of the null spectrum.

Straightforward differentiation of (8.36) shows that the Hessian matrix $\mathcal{H}_j$ of $\Delta(\vec{\omega})$ at $\vec{\omega} = \vec{\omega}_j$ is

$$\mathcal{H}_j = \frac{2 \cdot \mathrm{Re}\left\{\dot{D}(\vec{\omega}_j)^h \left[I - A(A^hA)^{-1}A^h\right] \dot{D}(\vec{\omega}_j)\right\}}{\|\vec{a}(\vec{\omega}_j)\|^2} \tag{8.37}$$

Thus the real part of the block of H corresponding to the j^{th} source in (8.28) simply is equal to $\|\vec{a}(\vec{\omega}_j)\|^2\mathcal{H}_j/2$.

Additionally, the block of B_C^{-1} corresponding the j^{th} source is

$$\left(B_C^{-1}\right)_{[jj]} = \frac{N \cdot \hat{p}_{jj} \cdot \|\vec{a}(\vec{\omega}_j)\|^2}{\sigma^2}\mathcal{H}_j \tag{8.38}$$

where subscript $_{[jj]}$ denotes the j^{th} block of $\mathcal{D} \times \mathcal{D}$ elements along the main diagonal, and $\hat{p}_{jj}$ denotes the sample power of the j^{th} source.

For uncorrelated sources, matrix $\hat{P}$ is diagonal, hence matrices $\hat{P}_+$ and B_C are block diagonal. Therefore from (8.38), the block of B_C corresponding the j^{th} source is

$$(B_C)_{[jj]} = \frac{\sigma^2}{N \cdot \hat{p}_{jj} \cdot \|\vec{a}(\vec{\omega}_j)\|^2}\mathcal{H}_j^{-1} \tag{8.39}$$

For correlated sources, a lower limit on the $(B_C)_{[jj]}$ can be established as follows. From the identity for the inverse of any partitioned matrix Z,

$$\left(Z^{-1}\right)_{[j,j]} \geq \left[Z_{[jj]}\right]^{-1} \tag{8.40}$$

Use of (8.40) with $Z = B_C^{-1}$, and (8.38) gives

$$(B_C)_{[jj]} \geq \frac{\sigma^2}{N \cdot \hat{p}_{jj} \cdot \|\vec{a}(\vec{\omega}_j)\|^2} \mathcal{H}_j^{-1} \tag{8.41}$$

We note from (8.39) and (8.41) that for given source powers, the Cramér-Rao variance bound for correlated sources is lower bounded by the CR bound for uncorrelated sources.

It is well known that the Hessian describes the curvature of a quadratic surface. Eqs. (8.38), (8.41) indicate that the CR bound can be expected to be favorable for the i^{th} element of $\vec{\omega}_j$ corresponding to a large i^{th} diagonal element of $\mathcal{H}_j$ or, equivalently, corresponding to large curvature of the spectrum $\Delta(\vec{\omega})$ along the i^{th} spatial frequency coordinate. Similarly the CR bound can be expected to be unfavorable for the l^{th} element of $\vec{\omega}$ corresponding to a small curvature of the spectrum $\Delta(\vec{\omega})$ along the l^{th} coordinate.

8.4 Analysis Approach

The main CR bound results of this thesis are obtained by identifying explicit expressions for the multi-D CR bound (8.28) for the case of M signals closely-spaced in multi-dimensional frequency. The analysis approach is an extension to multi-D of the approach used by Lee [11] for 1-D scenarios.

As introduced in Section 2.5, our approach is to express the spatial frequency vector for the j^{th} source as

$$\vec{\omega}_j = \vec{\omega}_0 + \vec{q}_j \delta\omega \tag{8.42}$$

$j = 1 \cdots M$, where $\vec{\omega}_0$ denotes the fixed reference frequency vector, $\vec{q}_j$ the normalized vector offsets such that $\max_{i,j} \|\vec{q}_i - \vec{q}_j\| = 1$, and $\delta\omega$ the variable scale parameter corresponding to the separation of the extreme frequency vectors. Paralleling the approach of [11], we analyze the bound (8.28) as the multiplier $\delta\omega \rightarrow 0$. Representation (8.42) facilitates analysis of the bound (8.28) since the problem is reduced to one with a single variable parameter $\delta\omega$. The condition $\delta\omega \rightarrow 0$ corresponds to coalescing the signal frequencies about the reference frequency vector $\vec{\omega}_0$.

Taylor series representations are central to our CR bound analysis. We recall from Section 2.5.2 that the generic arrival vector $\vec{a}(\vec{\omega})$ has a Taylor series about $\delta\omega = 0$ of the form

$$\vec{a}(\vec{\omega}) \;=\; \sum_{p=0}^{\infty} \delta\omega^p \dot{A}_p \vec{\gamma}_p(\vec{q}) \qquad (W \times 1) \tag{8.43}$$

where the columns of $\dot{A}_p$ are the p^{th} order spatial derivatives of $\vec{a}(\vec{\omega})$ at $\vec{\omega}_0$,

$$\dot{A}_p \;\triangleq\; \left[\frac{\partial^p \vec{a}(\vec{\omega})}{\partial \omega_1^p}, \frac{\partial^p \vec{a}(\vec{\omega})}{\partial \omega_1^{p-1} \partial \omega_2}, \cdots, \frac{\partial^p \vec{a}(\vec{\omega})}{\partial \omega_D^p} \right]_{\vec{\omega}=\vec{\omega}_0} \qquad (W \times \bar{n}_p) \tag{8.44}$$

where $\bar{n}_p$ is the number of p^{th} order spatial derivatives. Vector $\vec{\gamma}_p(\vec{q})$ is $\bar{n}_p \times 1$, real, constant with $\delta\omega$ and depends only on the normalized direction offset vector $\vec{q}$. For 2-D applications with $\vec{q} = [q_x, q_y]^t$ the vectors $\vec{\gamma}_p(\vec{q})$ are

$$\vec{\gamma}_0(\vec{q}) = [1], \quad \vec{\gamma}_1(\vec{q}) = \begin{bmatrix} q_x \\ q_y \end{bmatrix}, \quad \vec{\gamma}_2(\vec{q}) = \begin{bmatrix} q_x^2/2 \\ q_x q_y \\ q_y^2/2 \end{bmatrix}, \quad \vec{\gamma}_3(\vec{q}) = \begin{bmatrix} q_x^3/6 \\ q_x^2 q_y/2 \\ q_x q_y^2/2 \\ q_y^3/6 \end{bmatrix} \tag{8.45}$$

Vector $\vec{\gamma}_p(\vec{q})$ has the general form (2.55) for 2-D scenarios. Expressions analogous to (8.44), (8.45) can be written for Taylor series of any dimensionality.

The CR bound B_C is expressed in (8.28)-(8.32) in terms of matrices A and $\dot{D}(\vec{\omega}_j)$.

It follows from (8.43) that matrix A in (8.2) has Taylor series of the form

$$\begin{aligned} A &= [\vec{a}(\vec{\omega}_1), \cdots \vec{a}(\vec{\omega}_M)] \\ &= \sum_{p=0}^{\infty} \delta\omega^p \dot{A}_p \Gamma_p \end{aligned} \tag{8.46}$$

with matrix $\dot{A}_p$ as in (8.44), and Γ_p is a constant real $\bar{n}_p \times M$ matrix of the form

$$\Gamma_p \triangleq [\vec{\gamma}_p(\vec{q}_1), \cdots \vec{\gamma}_p(\vec{q}_M)] \tag{8.47}$$

A Taylor series characterization of $\dot{D}(\vec{\omega}_j)$ is likewise straightforwardly identified from the Taylor series (8.43) of $\vec{a}(\vec{\omega})$. As defined in (8.31), each column $\vec{d}_i(\vec{\omega}_j)$ of $\dot{D}(\vec{\omega}_j)$ is a partial derivative of the generic arrival vector $\vec{a}(\vec{\omega})$ at $\vec{\omega}_j$, hence

$$\vec{d}_i(\vec{\omega}_j) = \left[\frac{\partial}{\partial\omega_i}\vec{a}(\vec{\omega})\right]_{\vec{\omega}=\vec{\omega}_j} = \frac{1}{\delta\omega}\left[\frac{\partial}{\partial q_i}\vec{a}(\vec{\omega}_0 + \delta\omega\vec{q})\right]_{\vec{q}=\vec{q}_i} \tag{8.48}$$

since $\vec{\omega} = \vec{\omega}_0 + \delta\omega\vec{q}$. Hence from (8.31) and (8.48) we obtain

$$\dot{D}(\vec{\omega}_j) = \sum_{p=0}^{\infty} \delta\omega^{p-1} \dot{A}_p \dot{\Gamma}_p(\vec{q}_j) \tag{8.49}$$

where

$$\dot{\Gamma}_p(\vec{q}_j) \triangleq \left[\frac{\partial\vec{\gamma}_p(\vec{q})}{\partial q_1}, \frac{\partial\vec{\gamma}_p(\vec{q})}{\partial q_2}, \ldots, \frac{\partial\vec{\gamma}_p(\vec{q})}{\partial q_{\mathcal{D}}}\right]_{\vec{q}=\vec{q}_j} \tag{8.50}$$

and $\dot{A}_p$, $\vec{\gamma}_p(\vec{q})$ are as in (8.44), (8.45). Note that $\dot{\Gamma}_0(\vec{q}_j) = 0$ since $\vec{\gamma}_0(\vec{q}) = 1$, and that the $\dot{A}_p$ and $\dot{\Gamma}_p(\vec{q}_j)$ are constant with $\delta\omega$, so that (8.49) is a Taylor series in $\delta\omega$.

8.5 Sufficient Conditions for Non-Degenerate CR Bounds

The CR bound analysis presented in Chapter 9 is simplified by identification of structural conditions satisfied in many DF scenarios; we refer to such scenarios as characterized by *non-degenerate CR bounds.*

Analysis will show that the behavior of the CR bound for small $\delta\omega$ depends fundamentally upon the interaction between the columns of matrix A and of the matrix $\dot{D}(\vec{\omega}_j)$ of first spatial derivatives of $\vec{a}(\vec{\omega})$ at $\vec{\omega}_j$, for each $j = 1 \cdots M$. For convenience, we define the *augmented matrices*

$$\Xi_j \triangleq \left[\delta\omega \cdot \dot{D}(\vec{\omega}_j) \ , \ A\right] \qquad W \times (M + \mathcal{D}) \qquad (8.51)$$

for $j = 1 \cdots M$, which aggregate the columns of $\dot{D}(\vec{\omega}_j)$, scaled by $\delta\omega$, and the columns of A. We note that Ξ_j has full rank $M + \mathcal{D}$ by Assumption **A6.**

Since the constituent matrices have Taylor series (8.49) and (8.46), each Ξ_j also has Taylor series of the form

$$\Xi_j = \sum_{p=0}^{\infty} \delta\omega^p \dot{A}_p \Gamma'_p(\vec{q}_j) \qquad (8.52)$$

where $\dot{A}_p$ is as in (8.44) and

$$\Gamma'_p(\vec{q}_j) \triangleq \left[\dot{\Gamma}_p(\vec{q}_j) \ , \ \Gamma_p\right] \qquad \bar{n}_p \times (M + \mathcal{D}) \qquad (8.53)$$

with $\dot{\Gamma}_p(\vec{q}_j)$ as in (8.50) and Γ_p as in (8.47).

The sufficient conditions for non-degenerate CR bounds are simply stated as:

Scenarios with non-degenerate CR bounds are scenarios which satisfy Conditions **C1-C3** that specify a non-degenerate matrix A, *and* additional scenario Conditions **CR1-CR2** (detailed subsequently) that specify non-degenerate augmented matrices Ξ_j, for $j = 0 \cdots M$.

The sufficient conditions **C1-C3** are restated here from Section 2.5.3:

$$\textbf{C1.} \qquad \begin{aligned} \text{Rank}\{\dot{A}_0\} &= \bar{n}_0 && \text{for } p = 0 \\ \text{Rank}\{P_{[\dot{A}_0,\cdots\dot{A}_{p-1}]}\,\dot{A}_p\} &= \bar{n}_p && \text{for } p = 1,\cdots m-1 \end{aligned} \tag{8.54}$$

$$\textbf{C2.} \qquad \begin{aligned} \text{Rank}\{\Gamma_0\} &= \bar{n}_0 && \text{for } p = 0 \\ \text{Rank}\{\Gamma_p\,P_{[\Gamma_0^h,\cdots,\Gamma_{p-1}^h]}\} &= \bar{n}_p && \text{for } p = 1,\cdots m-1 \end{aligned} \tag{8.55}$$

$$\textbf{C3.} \qquad \text{Rank}\{P_{[\dot{A}_0,\cdots\dot{A}_{m-1}]}\,\dot{A}_m\Gamma_m\,P_{[\Gamma_0^h,\cdots,\Gamma_{m-1}^h]}\} = M - \sum_{p=0}^{m-1}\bar{n}_p \tag{8.56}$$

where M is the number of sources and m is the minimum number such that the sum of terms $p = 0\cdots m$ of the Taylor series of matrix A is full rank. If Conditions **C1-C3** are all satisfied, then m is determined by

$$\sum_{p=0}^{m-1}\bar{n}_p \;< M \;\leq \sum_{p=0}^{m}\bar{n}_p \tag{8.57}$$

We define the additional scenario conditions analogously, using the component matrices of the Taylor series (8.52) for augmented matrices:

$$\textbf{CR1.} \qquad \begin{aligned} \text{Rank}\{\dot{A}_0\} &= \bar{n}_0 && \text{for } p = 0 \\ \text{Rank}\{P_{[\dot{A}_0,\cdots\dot{A}_{p-1}]}\,\dot{A}_p\} &= \bar{n}_p && \text{for } p = 1,\cdots \chi-1 \end{aligned} \tag{8.58}$$

$$\textbf{CR2.}\ \text{For } j = 1\cdots M, \qquad \begin{aligned} \text{Rank}\{\Gamma'_0(\vec{q}_j)\} &= \bar{n}_0 && \text{for } p = 0 \\ \text{Rank}\{\Gamma'_p(\vec{q}_j)\,P_{[\Gamma'_0(\vec{q}_j)^h,\cdots,\Gamma'_{p-1}(\vec{q}_j)^h]}\} &= \bar{n}_p && \text{for } p = 1,\cdots \chi-1 \end{aligned} \tag{8.59}$$

$$\textbf{CR3.}\ \text{For } j = 1\cdots M,$$

$$\text{Rank}\{P_{[\dot{A}_0,\cdots\dot{A}_{\chi-1}]}\,\dot{A}_\chi\Gamma'_\chi(\vec{q}_j)\,P_{[\Gamma'_0(\vec{q}_j)^h,\cdots,\Gamma'_{\chi-1}(\vec{q}_j)^h]}\} = M + \mathcal{D} - \sum_{p=0}^{\chi-1}\bar{n}_p \tag{8.60}$$

where $M+\mathcal{D}$ is the number of columns in augmented matrix Ξ_j, and χ is the minimum number such that the sum of terms $p = 0\cdots\chi$ of Taylor series (8.52) of matrix Ξ is full rank. If Conditions **CR1-CR3** are satisfied, then χ is determined by

$$\sum_{p=0}^{\chi-1}\bar{n}_p \;< M+\mathcal{D} \;\leq \sum_{p=0}^{\chi}\bar{n}_p \tag{8.61}$$

8.5.1 Definition of Cases I, II and III

Subsequent analysis will show that the small $\delta\omega$ behavior of the CR bound in multi-D scenarios depends fundamentally upon a parameter ν, defined as

$$\nu \triangleq \sum_{p=0}^{m} \bar{n}_p - M \tag{8.62}$$

Referring to definition (8.57) of m, we see that ν reflects the number by which M can be augmented without changing the value of m. We designate ν as the number of "vacancies" the m^{th} SVD shell of matrix A. Parameter ν depends only upon the number M of sources, and the dimensionality $\mathcal{D}$ of the scenario, which determines the values of $\bar{n}_p$.

Referring to definition (8.61) of χ, we see that χ is simply the value of m if M is augmented by $\mathcal{D}$. Thus we relate χ to the number of vacancies by

$$\chi = \begin{cases} m & \nu \geq \mathcal{D} \\ m+1 & \nu < \mathcal{D} \end{cases} \tag{8.63}$$

For convenience, we define three distinct cases based upon the value of vacancy parameter ν:

Case I. ($\nu = 0$) In this "full shell" case there are no vacancies in the m^{th} shell, and $\chi = m + 1$.

Case II. ($\nu \geq \mathcal{D}$) In this case there are at least $\mathcal{D}$ vacancies in the m^{th} shell, hence $\chi = m$.

Case III. ($0 < \nu < \mathcal{D}$) In this case there are some, but fewer than $\mathcal{D}$, vacancies in the m^{th} shell, hence $\chi = m + 1$.

Subsequent analysis will be simplified by separate consideration of each Case.

Examples in the following section illustrate the three Cases I, II and III, and show that the CR bound simplifying Conditions **C1-C3**, and **CR1-CR3**, are satisfied for typical direction finding scenarios.

8.6 Example Scenarios for CR Bounds

This section introduces the direction finding scenarios which will be used in numerical simulations to illustrate CR bound thesis results. The four scenarios are derived from the non-degenerate scenario of Example 2.3. The scenarios differ only in the number M of sources present, and illustrate the occurrence of Cases I, II and III for $M = 3, 4, 5, 6$.

Each example involves a planar array of $W = 16$ unit-gain, isotropic sensors, and far-field sources clustered near to the array broadside.

We recall from (2.68) that for this scenario the matrices $\dot{A}_0$, $\dot{A}_1$, $\dot{A}_2$ and $\dot{A}_3$ are

$$\dot{A}_0 = \begin{bmatrix} 1 \\ \vdots \\ 1 \end{bmatrix}, \dot{A}_1 = j \cdot \begin{bmatrix} r_{x1} & r_{y1} \\ \vdots & \vdots \\ r_{xW} & r_{yW} \end{bmatrix}, \dot{A}_2 = -1 \cdot \begin{bmatrix} r_{x1}^2 & r_{x1}r_{y1} & r_{y1}^2 \\ \vdots & \vdots & \vdots \\ r_{xW}^2 & r_{xW}r_{yW} & r_{yW}^2 \end{bmatrix}$$

$$\dot{A}_3 = -j \cdot \begin{bmatrix} r_{x1}^3 & r_{x1}^2 r_{y1} & r_{x1}r_{y1}^2 & r_{y1}^3 \\ \vdots & \vdots & \vdots & \vdots \\ r_{xW}^3 & r_{xW}^2 r_{yW} & r_{xW}r_{yW}^2 & r_{yW}^3 \end{bmatrix} \tag{8.64}$$

From (2.59), we recall for this scenario that

$$\begin{aligned} \Gamma_0 &= [1, \quad \cdots \quad 1] \\ \Gamma_1 &= \begin{bmatrix} q_{x1}, & \cdots & q_{xM} \\ q_{y1}, & \cdots & q_{yM} \end{bmatrix} \\ \Gamma_2 &= \begin{bmatrix} q_{x1}^2/2, & \cdots & q_{xM}^2/2 \\ q_{x1}q_{y1}, & \cdots & q_{xM}q_{yM} \\ q_{y1}^2/2, & \cdots & q_{yM}^2/2 \end{bmatrix} \\ \Gamma_3 &= \begin{bmatrix} q_{x1}^3/6, & \cdots & q_{xM}^3/6 \\ q_{x1}^2 q_{y1}/2, & \cdots & q_{xM}^2 q_{yM}/2 \\ q_{x1}q_{y1}^2/2, & \cdots & q_{xM}q_{yM}^2/2 \\ q_{y1}^3/6, & \cdots & q_{yM}^3/6 \end{bmatrix} \end{aligned} \tag{8.65}$$

Therefore the partial derivative matrices $\dot{\Gamma}_p(\vec{q}_j)$ in (8.50) take the form

$$\begin{aligned}
\dot{\Gamma}_0(\vec{q}_j) &= \begin{bmatrix} 0 & , & 0 \end{bmatrix} \\
\dot{\Gamma}_1(\vec{q}_j) &= \begin{bmatrix} 1 & , & 0 \\ 0 & , & 1 \end{bmatrix} \\
\dot{\Gamma}_2(\vec{q}_j) &= \begin{bmatrix} q_{xj} & , & 0 \\ q_{yj} & , & q_{xj} \\ 0 & , & q_{yj} \end{bmatrix} \\
\dot{\Gamma}_3(\vec{q}_j) &= \begin{bmatrix} q_{xj}^2/2 & , & 0 \\ q_{xj}q_{yj} & , & q_{xj}^2/2 \\ q_{yj}^2/2 & , & q_{xj}q_{yj} \\ 0 & , & q_{yj}^2/2 \end{bmatrix}
\end{aligned} \tag{8.66}$$

The four example scenarios differ in the number M of sources which are active out of the 6 sources in the "double chevron" source configuration of Figure 8-1. The scenarios are defined as follows:

Example 8.1 : For this example $M = 3$ and the array and source geometries are as follows.

Array: Sensors in a sparse grid per Figure 2-4A,

Sources: Sources SC1, SC2, SC3 clustered around broadside in a triangular configuration per Figure 8-1.

Per Example 2.3, the columns of $\dot{A}_0$, $\dot{A}_1$, $\dot{A}_2$, $\dot{A}_3$ in (8.64) are all linearly independent for this sensor array. It can be verified that the rows of Γ_0, Γ_1, given by (8.65) with $M = 3$ are all linearly independent for this source configuration. Thus the partial Taylor sum of A with terms $p = 0, 1$ has full rank $M = 3$, and thus $m = 1$. Consequently, Conditions **C1-C3** are all satisfied with $m = 1$.

Similarly, the rows of $\Gamma_0'(\vec{q}_j)$, $\Gamma_1'(\vec{q}_j)$ given by (8.53) with (8.65) and (8.66) are all linearly independent for this source configuration, and $\Gamma_0'(\vec{q}_j)$, $\Gamma_1'(\vec{q}_j)$ and $\Gamma_2'(\vec{q}_j)$ have $M + \mathcal{D} = 5$ linearly independent rows. Thus the partial Taylor sum

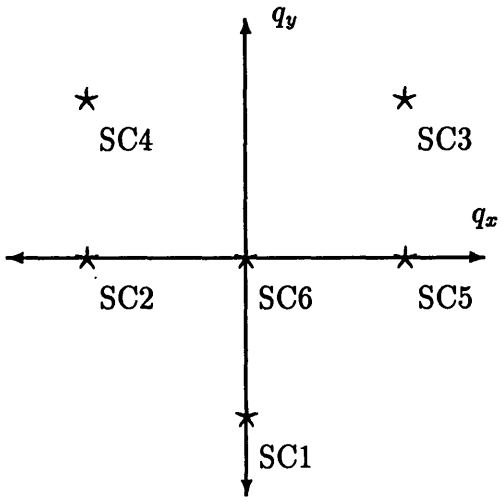

A. Double Chevron

Figure 8-1: Normalized Source Configuration for CR Bound Simulations

of Ξ with terms $p = 0, 1, 2$ has full rank $M = 5$, and thus $\chi = 2$. Consequently, Conditions **CR1-CR3** are all satisfied with $\chi = 2$.

Since $\nu = 0$, this is an example of a Case I scenario with non-degenerate CR bounds.

Example 8.2 : For this example $M = 4$ and the array and source geometries are as follows.

Array: Sensors in a sparse grid per Figure 2-4A,

Sources: Sources SC1, SC2, SC3, SC4 clustered around broadside as in Figure 8-1.

Paralleling the arguments of Example 8.1, Conditions **C1-C3** are all satisfied with $m = 2$, and Conditions **CR1-CR3** are all satisfied with $\chi = 2$ and $\nu = 2$. This is an example of a Case II scenario with non-degenerate CR bounds.

Example 8.3 : For this example $M = 5$ and the array and source geometries are as follows.

Array: Sensors in a sparse grid per Figure 2-4A,

Sources: Sources SC1, SC2, SC3, SC4, SC5 clustered around broadside as in Figure 8-1.

Paralleling the arguments of Example 8.1, Conditions **C1-C3** are all satisfied with $m = 2$, and Conditions **CR1-CR3** are all satisfied with $\chi = 3$ and $\nu = 1$. This is an example of a Case III scenario with non-degenerate CR bounds.

Example 8.4 : For this example $M = 6$ and the array and source geometries are as follows.

Array: Sensors in a sparse grid per Figure 2-4A,

Sources: Sources SC1-SC6 clustered around broadside as in Figure 8-1.

Paralleling the arguments of Example 8.1, Conditions **C1-C3** are all satisfied with $m = 3$, and Conditions **CR1-CR3** are all satisfied with $\chi = 4$ and $\nu = 0$. This is another example of a Case I scenario with non-degenerate CR bounds.

Chapter 9

Cramér-Rao Bounds: New Multi-D Results

The principal results of this chapter are simple expressions for the multi-D CR bound (8.28), valid for the case of M closely spaced sources. The expressions make explicit the individual contributions of scenario parameters such as maximum source separation $\delta\omega$, source configuration, source powers and correlations, and sensor array geometry. These results can be regarded as extensions of those of Lee [11] to the multi-D case.

It is shown for typical multi-D scenarios that the expression for B_C for small $\delta\omega$ is

$$B_C = (\delta\omega)^{-2(\chi-1)} K_\chi + \mathcal{O}\left(\delta\omega^{-2(\chi-1)+1}\right) \tag{9.1}$$

where χ is the integer that satisfies (8.61) for scenarios which satisfy Conditions **C1-C3** and **CR1-CR3**, and matrix K_χ is identified in Section 9.4. The parameter χ determines the sensitivity of the bound to the maximum source spacing $\delta\omega$ for closely spaced sources. Matrix K_χ is constant with $\delta\omega$ and depends upon the normalized source configuration, the array geometry and cross-power matrix $\hat{P}$. Expressions for K_χ are identified in the following sections for each Case I, II and III defined in Section 8.5, with the general properties listed in Table 9.1.

Table 9.1: Properties of (9.1) for Cases I-III

Case	χ	Rank$\{K_\chi\}$
I	$m+1$	full
II	m	full
III	$m+1$	partial

The corresponding bound on the variance of $\hat{\omega}_{ij}$, the estimate of the i^{th} component of the j^{th} source parameter vector $\vec{\omega}_j$, is identified to be

$$\text{Var}\{\hat{\omega}_{ij}\} \geq \frac{1}{N \cdot \text{SNR}_j} \frac{b_{ij}}{\delta\omega^{2(\chi-1)}} + \mathcal{O}(\delta\omega^{-2(\chi-1)+1}) \tag{9.2}$$

for small $\delta\omega$, where SNR_j denotes the signal-to-noise ratio for the j^{th} source, and b_{ij} is constant with $\delta\omega$ and is identified in Section 9.4.1. In the case that K_χ is not full rank (Case III), we identify "preferred" coordinate directions for which the leading term of (9.2) vanishes, and show that along those coordinates Var$\{\hat{\omega}_{ij}\}$ has the more favorable (smaller) $\delta\omega^{-2(\chi-2)}$ dependence for small $\delta\omega$.

In order to identify the small $\delta\omega$ behavior of B_C, we begin with the prior expressions (8.28)-(8.32). Since the matrix $\hat{P}_+$ in (8.28) is constant, the $\delta\omega$ dependence of B_C has its origins in the $\delta\omega$ dependence of the matrix H. Thus this chapter first identifies the (distinct) small $\delta\omega$ expressions for H in each Case I, II and III. These expressions are then transformed into small $\delta\omega$ expressions for B_C^{-1}, and finally for B_C.

The chapter is organized as follows. Section 9.1 identifies explicit small $\delta\omega$ expressions for matrix H in each Case I, II and III for scenarios that satisfy the non-degenerate conditions **C1-C3** and **CR1-CR3**. Section 9.2 then develops explicit small $\delta\omega$ expressions that identify B_C^{-1} in each of the three cases. Finally Section 9.3 derives small $\delta\omega$ expressions for B_C in each of the three cases. A summary of CR bound results is presented in Section 9.4, including expressions (9.1) and (9.2), and a characterization of the CR bound along preferred frequency coordinates. Illustrative simulation examples are presented in Section 9.5.

9.1 Small $\delta\omega$ Behavior of H

The $\delta\omega$ dependence of B_C has its origins in the $\delta\omega$ dependence of matrix H. To clarify the $\delta\omega$ dependence of H, we rewrite (8.29) as follows

$$H = Z(\delta\omega)^h Z(\delta\omega) \tag{9.3}$$

where

$$Z(\delta\omega) \triangleq \left[I - A(A^hA)^{-1}A^h\right]\left[\dot{D}(\vec{\omega}_1), \cdots, \dot{D}(\vec{\omega}_M)\right] \tag{9.4}$$

with

$$\dot{D}(\vec{\omega}_j) \triangleq \left[\frac{\partial}{\partial\omega_1}\vec{a}(\vec{\omega}), \cdots \frac{\partial}{\partial\omega_{\mathcal{D}}}\vec{a}(\vec{\omega})\right]_{\vec{\omega}=\vec{\omega}_j} \tag{9.5}$$

The factor $\left[I - A(A^hA)^{-1}A^h\right]$ is a projection matrix onto columns of $W \times M$ matrix A, and hence 1) has constant non-zero rank $W - M$ for all $\delta\omega \neq 0$ from Assumptions **A1, A3**, and 2) has unity non-zero eigenvalues for all $\delta\omega$. Therefore, $\left[I - A(A^hA)^{-1}A^h\right]$ does not approach zero as $\delta\omega \to 0$. Similarly the typical column $\vec{d}_i(\vec{\omega}_j)$ of $\dot{D}(\vec{\omega}_j)$ approaches the constant vector $\vec{d}_i(\vec{\omega}_0)$ as $\delta\omega \to 0$. However, numerical examples show that the product (9.4) is such that $Z(\delta\omega) \to 0$ as $\delta\omega \to 0$. Consequently, the essential properties of $Z(\delta\omega)$ and, therefore of H, for $\delta\omega \to 0$ derive from the *interaction* of the factors $\left[I - A(A^hA)^{-1}A^h\right]$ and $\dot{D}(\vec{\omega}_j)$.

To clarify the small $\delta\omega$ behavior of H, it is desirable to obtain appropriate small $\delta\omega$ characterizations of $\left[I - A(A^hA)^{-1}A^h\right]$ and $\dot{D}(\vec{\omega}_j)$, and then of the product $\left[I - A(A^hA)^{-1}A^h\right]\dot{D}(\vec{\omega}_j)$. Such characterizations are developed below.

9.1.1 Small $\delta\omega$ Behavior of $\left[I - A(A^hA)^{-1}A^h\right]$

Subject to Conditions **C1-C3**, prior thesis results show that

$$\begin{aligned}\left[I - A(A^hA)^{-1}A^h\right] &= \left[I - \left[\dot{A}_0, \cdots, \dot{A}_{m-1}, \dot{A}_m\Gamma_m P_{[\Gamma_0^h,\cdots,\Gamma_{m-1}^h]}\right]\right. \\ &\qquad \left. \cdot \left[\dot{A}_0, \cdots, \dot{A}_{m-1}, \dot{A}_m\Gamma_m P_{[\Gamma_0^h,\cdots,\Gamma_{m-1}^h]}\right]^+\right] + \mathcal{O}(\delta\omega) \\ &= \left[I - \bar{A}\bar{A}^+\right] + \mathcal{O}(\delta\omega) \qquad (9.6)\end{aligned}$$

(see Corollary 5.3a with the specialization $\Pi = I$), where $\dot{A}_p$ and Γ_p are as in (8.44) and (8.47), and where we define

$$\bar{A} \triangleq \left[\dot{A}_0, \cdots, \dot{A}_{m-1}, \dot{A}_m T_m\right] \qquad (9.7)$$

$$T_m \triangleq \Gamma_m P_{[\Gamma_0^h,\cdots,\Gamma_{m-1}^h]} \left(\Gamma_m P_{[\Gamma_0^h,\cdots,\Gamma_{m-1}^h]}\right)^+ \qquad \bar{n}_m \times \bar{n}_m \qquad (9.8)$$

The second equality in (9.6) is a consequence of the equality of the column spaces of $\dot{A}_m\Gamma_m P_{[\Gamma_0^h,\cdots,\Gamma_{m-1}^h]}$ and of $\dot{A}_m\Gamma_m P_{[\Gamma_0^h,\cdots,\Gamma_{m-1}^h]}(\Gamma_m P_{[\Gamma_0^h,\cdots,\Gamma_{m-1}^h]})^+$.

For convenience, we define

$$\bar{n}_{\{0\cdots k\}} \triangleq \sum_{p=0}^{k} \bar{n}_p \qquad (9.9)$$

As a consequence of Condition **C1**, all the column spaces of submatrices $\dot{A}_0$, $\cdots$ $\dot{A}_{m-1}$ of $\bar{A}$ are linearly independent, and make a rank contribution of $\bar{n}_{\{0,\cdots m-1\}}$ to (9.7). As a consequence of Condition **C3**, the final matrix $\dot{A}_m T_m$ contributes additional independent columns to complete the column space of $\bar{A}$. The role of the post-factor T_m of $\dot{A}_m$ in (9.7) is to select a subspace of that defined by the columns of $\dot{A}_m$ to produce the result

$$\text{Rank}\{\bar{A}\} = M \qquad (9.10)$$

As a consequence of Condition **C2**, the columns of matrices $\Gamma_0^h, \cdots, \Gamma_{m-1}^h$ are linearly independent, and thus the $(M \times M)$ nullspace projection $P_{[\Gamma_0^h,\cdots,\Gamma_{m-1}^h]}$ has

$M - \bar{n}_{\{0,\cdots m-1\}}$. Since $P_{[\Gamma_0^h,\cdots,\Gamma_{m-1}^h]}$ appears as a factor in (9.8), T_m can have rank *at most* $M - \bar{n}_{\{0,\cdots m-1\}}$. As argued above, $\dot{A}_m T_m$ must have rank *at least* $M - \bar{n}_{\{0,\cdots m-1\}}$. Therefore it must be that

$$\text{Rank}\{T_m\} \;=\; M - \bar{n}_{\{0,\cdots m-1\}} \tag{9.11}$$

From (9.8) it is clear that T_m is defined by $\vec{q}_1, \cdots, \vec{q}_M$ and, therefore, by the relative geometry of the sources. We note specifically that projection T_m is independent of $\delta\omega$ or of the sensor array geometry.

9.1.2 Small $\delta\omega$ Behavior of $\left[I - A(A^hA)^{-1}A^h\right]\dot{D}(\vec{\omega}_j)$

The small $\delta\omega$ behavior of $\dot{D}(\vec{\omega}_j)$ is described by the Taylor series (8.49), for convenience restated here,

$$\dot{D}(\vec{\omega}_j) \;=\; \sum_{p=0}^{\infty} \delta\omega^{p-1} \dot{A}_p \dot{\Gamma}_p(\vec{q}_j) \qquad\qquad W \times \mathcal{D} \tag{9.12}$$

where $\dot{\Gamma}_p(\vec{q}_j)$ is defined in (8.50).

It is evident that the pre-factor $[I - A(A^hA)^{-1}A^h]$ in (9.4) acts to annihilate all components of the columns of $\dot{D}(\vec{\omega}_j)$ which lie in the subspace defined by the columns of A; the residual matrix then specifies the behavior of $Z(\delta\omega)$ and, therefore, of H. Therefore it is desirable to decompose $\dot{D}(\vec{\omega}_j)$ as

$$\dot{D}(\vec{\omega}_j) \;=\; A\beta + \dot{F}(\vec{\omega}_j) \tag{9.13}$$

where matrix β specifies a linear interpolation of the columns of A, and matrix $\dot{F}(\vec{\omega}_j)$ is the interpolation residual. Pre-multiplication of (9.13) by $\left[I - A(A^hA)^{-1}A^h\right]$ shows that

$$\left[I - A(A^hA)^{-1}A^h\right]\dot{D}(\vec{\omega}_j) = \left[I - A(A^hA)^{-1}A^h\right]\dot{F}(\vec{\omega}_j) \tag{9.14}$$

regardless of the choice of matrix β. Representation (9.13) facilitates analysis if matrix

β is selected to clarify the small $\delta\omega$ properties of the product $\left[I - A(A^hA)^{-1}A^h\right]\dot{F}(\vec{\omega}_j)$.

It is convenient to express the residual matrix $\dot{F}(\vec{\omega}_j)$ in terms of the augmented matrix Ξ_j defined in (8.51). Specifically

$$\begin{aligned}\dot{F}(\vec{\omega}_j) &= \dot{D}(\vec{\omega}_j) - A\beta \\ &= \frac{1}{\delta\omega}\left[\delta\omega\cdot\dot{D}(\vec{\omega}_j)\ ,\ A\right]\begin{bmatrix} I \\ -\delta\omega\beta \end{bmatrix} \\ &= \frac{1}{\delta\omega}\Xi_j\begin{bmatrix} I \\ -\delta\omega\beta \end{bmatrix}\end{aligned} \tag{9.15}$$

Since matrix Ξ_j has Taylor series (8.52) in $\delta\omega$, the residual matrix $\dot{F}(\vec{\omega}_j)$ has series expansion in $\delta\omega$ of the form

$$\dot{F}(\vec{\omega}_j) = \sum_{p=0}^{\infty}\delta\omega^{p-1}\dot{A}_p\left[\dot{\Gamma}_p(\vec{q}_j)\ ,\ \Gamma_p\right]\begin{bmatrix} I \\ -\delta\omega\beta \end{bmatrix} \qquad W\times\mathcal{D} \tag{9.16}$$

Note that decomposition (9.16) may or may not be a Taylor series, depending on how β depends on $\delta\omega$.

As $\delta\omega\to 0$, reference to (9.6) shows that the dominant term of $\left[I - A(A^hA)^{-1}A^h\right]$ in (9.14) acts to annihilate the components of the columns of $\dot{F}(\vec{\omega}_j)$ which lie in the subspace defined by the columns of $\bar{A}$. Reference to (9.16) shows that indeed the $p = 0\cdots m-1$ series terms of $\dot{F}(\vec{\omega}_j)$ are *entirely contained* in the space spanned by the columns of $\bar{A}$, as are the components of the $p = m$ series term that are spanned by the columns of $\dot{A}_mT_m$. Consequently, it is desirable to select matrix β so that the *dominant components* of the residual matrix $\dot{F}(\vec{\omega}_j)$ for small $\delta\omega$ are *linearly independent* from the (doomed for small $\delta\omega$) components which lie in the column space of $\bar{A}$.

To obtain a residual with a linearly independent dominant term, we select β to annihilate entirely the $p = 0,\cdots m-1$ terms of (9.16), and also annihilate the $\dot{A}_mT_m$

component of the $p = m$ term. Specifically, a "desirable" β would satisfy

$$\begin{aligned} 0 &= \begin{bmatrix} \dot{\Gamma}_0(\vec{q}_j) & , & \Gamma_0 \\ \vdots & & \vdots \\ \dot{\Gamma}_{m-1}(\vec{q}_j) & , & \Gamma_{m-1} \\ T_m\dot{\Gamma}_m(\vec{q}_j) & , & T_m\Gamma_m \end{bmatrix} \begin{bmatrix} I \\ -\delta\omega\beta \end{bmatrix} \\ &= \left[\dot{\Gamma}(\vec{q}_j) \ , \ \Gamma\right] \begin{bmatrix} I \\ -\delta\omega\beta \end{bmatrix} \end{aligned} \tag{9.17}$$

where we define the shorthand

$$\Gamma \triangleq \begin{bmatrix} \Gamma_0 \\ \vdots \\ \Gamma_{m-1} \\ T_m\Gamma_m \end{bmatrix} \qquad \bar{n}_{\{0,\cdots m\}} \times M \tag{9.18}$$

$$\dot{\Gamma}(\vec{q}) \triangleq \begin{bmatrix} \dot{\Gamma}_0(\vec{q}) \\ \vdots \\ \dot{\Gamma}_{m-1}(\vec{q}) \\ T_m\dot{\Gamma}_m(\vec{q}) \end{bmatrix} \qquad \bar{n}_{\{0,\cdots m\}} \times \mathcal{D} \tag{9.19}$$

As a consequence of Conditions **C2** and **C3**, matrix Γ has full column rank M. The projection onto the columns of Γ is of the form

$$\Gamma\Gamma^{+} = \begin{bmatrix} I_{\bar{n}_{\{0,\cdots m-1\}} \times \bar{n}_{\{0,\cdots m-1\}}} & 0 \\ 0 & T_m \end{bmatrix} \tag{9.20}$$

since the projection identified in (9.20) is a pre-factor of Γ in (9.18) and, from (9.11), is of rank M equal to that of Γ.

Therefore we select a "desirable" β to be

$$\beta \triangleq \delta\omega^{-1}\,\Gamma^{+}\,\dot{\Gamma}(\vec{q}_j) \tag{9.21}$$

Straightforward substitution with use of (9.20) shows that (9.21) satisfies (9.17).

Substitution of (9.21) in (9.16) results in

$$\begin{aligned}\dot{F}(\vec{\omega}_j) &= \sum_{p=0}^{\infty} \delta\omega^{p-1} \dot{A}_p \left[\dot{\Gamma}_p(\vec{q}_j)\ ,\ \Gamma_p\right] \begin{bmatrix} I \\ -\Gamma^{+}\dot{\Gamma}(\vec{q}_j) \end{bmatrix} \\ &= \sum_{p=m}^{\infty} \delta\omega^{p-1} \dot{A}_p \dot{\Psi}_p(\vec{q}_j) \end{aligned} \tag{9.22}$$

where we define the shorthand

$$\dot{\Psi}_p(\vec{q}_j) \triangleq \left[\dot{\Gamma}_p(\vec{q}_j)\ ,\ \Gamma_p\right] \begin{bmatrix} I \\ -\Gamma^{+}\dot{\Gamma}(\vec{q}_j) \end{bmatrix} \tag{9.23}$$

Note that $\dot{\Psi}_p(\vec{q}_j)$ is real, and constant with $\delta\omega$, so that (9.22) is a Taylor series in $\delta\omega$. From (9.17), we see that

$$\dot{\Psi}_p(\vec{q}_j) = 0 \qquad p = 0, \cdots m-1 \tag{9.24}$$

$$T_m \dot{\Psi}_m(\vec{q}_j) = 0 \tag{9.25}$$

To clarify further analysis of the product $\left[I - A(A^hA)^{-1}A^h\right]\dot{F}(\vec{\omega}_j)$ and consequently, of matrix H, for the small $\delta\omega$, the following subsections address each Case I, II, and III individually.

9.1.3 Small $\delta\omega$ Expressions for H in Case I

As defined in Section 8.5, Case I is the "full-shell" case for which there are no vacancies in the m^{th} shell ($\nu = 0$), that is

$$\bar{n}_{\{0,\cdots,m\}} = M \tag{9.26}$$

We consider scenarios with non-degenerate CR bounds for which conditions **C1-C3** and **CR1-CR3** are satisfied.

Reference to (9.26), (9.8) and (9.11) shows that in Case I, projection T_m has full rank and hence

$$T_m = I \tag{9.27}$$

Therefore the columns of matrix $\bar{A}$ in (9.7) span the entire column space of $\dot{A}_m$. Specifically, we have

$$\bar{A} = \dot{A} \tag{9.28}$$

where

$$\dot{A} \triangleq \left[\dot{A}_0,\ \dot{A}_1,\ \cdots,\ \dot{A}_{m-1},\ \dot{A}_m\right] \tag{9.29}$$

Furthermore, use of (9.27) in (9.25) shows that for Case I

$$\dot{\Psi}_m(\vec{q}_j) = 0 \tag{9.30}$$

Therefore the $p = m$ term of Taylor series (9.22) of $\dot{F}(\vec{\omega}_j)$ is zero for Case I, as are the $p = 0 \cdots m-1$ terms from (9.24). Thus the leading (possibly) non-zero term of (9.22) is identified as

$$\dot{F}(\vec{\omega}_j) = \delta\omega^m \dot{A}_{m+1} \dot{\Psi}_{m+1}(\vec{q}_j) + \mathcal{O}(\delta\omega^{m+1}) \tag{9.31}$$

Substitution of (9.31), (9.6) and (9.28) in (9.14) gives

$$\begin{aligned}
&\left[I - A(A^hA)^{-1}A^h\right]\dot{D}(\vec{\omega}_j) \\
&\quad = \left[I - A(A^hA)^{-1}A^h\right]\dot{F}(\vec{\omega}_j) \\
&\quad = \left\{\left[I - \dot{A}\dot{A}^+\right] + \mathcal{O}(\delta\omega)\right\}\left\{\delta\omega^m \dot{A}_{m+1}\dot{\Psi}_{m+1}(\vec{q}_j) + \mathcal{O}(\delta\omega^{m+1})\right\} \\
&\quad = \delta\omega^m \mathcal{E}_{m+1}\dot{\Psi}_{m+1}(\vec{q}_j) + \mathcal{O}(\delta\omega^{m+1})
\end{aligned} \tag{9.32}$$

where we define the constant matrix

$$\mathcal{E}_{m+1} \triangleq \left[I - \dot{A}\dot{A}^{+}\right] \dot{A}_{m+1} \tag{9.33}$$

and from (9.23) we have

$$\dot{\Psi}_{m+1}(\vec{q}_j) \triangleq \left[\dot{\Gamma}_{m+1}(\vec{q}_j)\ ,\ \Gamma_{m+1}\right] \begin{bmatrix} I \\ -\Gamma^{+}\dot{\Gamma}(\vec{q}_j) \end{bmatrix} \tag{9.34}$$

(Note that Γ^{+} may be specialized to Γ^{-1} for Case I, since reference to (9.18) and (9.26) shows that Γ is square, and full rank subject to Conditions **C2, C3.**

Equation (9.32) together with (9.33) and (9.34), identify the dominant term of $\left[I - A(A^{h}A)^{-1}A^{h}\right] \dot{D}(\vec{\omega}_j)$ for small $\delta\omega$ in Case I.

The question arises as to whether the identified dominant term of (9.32) constitutes a complete first order representation of the entire span of (9.32). For scenarios with non-degenerate CR bounds, the leading term of (9.32) is indeed full rank, as shown by the following result.

Lemma 9.1 : In Case I with $\nu = 0$, if Conditions **C1-C3** and **CR1-CR3** are satisfied, then the leading term of (9.32) has full column rank. That is

$$\text{Rank}\left\{\mathcal{E}_{m+1}\dot{\Psi}_{m+1}(\vec{q}_j)\right\} = \mathcal{D} \tag{9.35}$$

for $j = 1 \cdots M$.

Proof: See Appendix I.

Therefore subject to Conditions **C1-C3, CR1-CR3,** a complete first order characterization of the product $\left[I - A(A^{h}A)^{-1}A^{h}\right] \dot{D}(\vec{\omega}_j)$ for Case I is given by (9.32) with (9.33) and (9.34).

Substitution of (9.32) in (9.4) gives

$$Z(\delta\omega) = \delta\omega^{m}\mathcal{E}_{m+1}\left[\dot{\Psi}_{m+1}(\vec{q}_1), \cdots \dot{\Psi}_{m+1}(\vec{q}_M)\right] + \mathcal{O}(\delta\omega^{m+1}) \tag{9.36}$$

and then (9.3) yields

$$H = \delta\omega^{2m} H_{2(m+1)} + \mathcal{O}(\delta\omega^{2m+1}) \tag{9.37}$$

where

$$H_{2(m+1)} = \left[\dot{\Psi}_{m+1}(\vec{q}_1), \cdots \dot{\Psi}_{m+1}(\vec{q}_M)\right]^h \mathcal{E}_{m+1}^h \mathcal{E}_{m+1} \left[\dot{\Psi}_{m+1}(\vec{q}_1), \cdots \dot{\Psi}_{m+1}(\vec{q}_M)\right] \tag{9.38}$$

Eqs. (9.37), (9.38), with (9.33), (9.34), characterize the small $\delta\omega$ behavior of H for Case I in scenarios with non-degenerate CR bounds. Note that $H_{2(m+1)}$ may not be full rank. Nevertheless, analysis in Section 9.2 will show that $H_{2(m+1)}$ and the result of Lemma 9.1 are sufficient to identify a full rank first order representation of B_C^{-1} for small $\delta\omega$ in Case I.

9.1.4 Small $\delta\omega$ Expressions for H in Case II

Next we address Case II of Section 8.5 for which there are at least $\mathcal{D}$ vacancies in the m^{th} shell ($\nu \geq \mathcal{D}$), that is

$$\bar{n}_{\{0,\cdots,m\}} \geq M + \mathcal{D} \tag{9.39}$$

We again consider scenarios with non-degenerate CR bounds, for which conditions **C1-C3** and **CR1-CR3** are satisfied.

Reference to (9.39), (9.8) and (9.11) shows that in Case II, projection T_m has only partial rank. Therefore columns of matrix $\bar{A}$ *may not* span the entire column space of $\dot{A}_m$. Consequently, unlike Case I, it is possible that the dominant term of $\left[I - A(A^hA)^{-1}A^h\right]$ in (9.14) does not entirely annihilate the $p = m$ term of $\dot{F}(\vec{\omega}_j)$ in (9.22).

Directly from (9.22) we identify the (possibly) non-zero leading term as

$$\dot{F}(\vec{\omega}_j) = \delta\omega^{m-1} \dot{A}_m \dot{\Psi}_m(\vec{q}_j) + \mathcal{O}(\delta\omega^m) \tag{9.40}$$

Substitution of (9.40) and (9.6) in (9.14) gives

$$\begin{aligned}\left[I - A(A^hA)^{-1}A^h\right]\dot{D}(\vec{\omega}_j) &= \left[I - A(A^hA)^{-1}A^h\right]\dot{F}(\vec{\omega}_j) \\ &= \left\{\left[I - \bar{A}\bar{A}^+\right] + \mathcal{O}(\delta\omega)\right\}\left\{\delta\omega^{m-1}\dot{A}_m\dot{\Psi}_m(\vec{q}_j) + \mathcal{O}(\delta\omega^m)\right\} \\ &= \delta\omega^{m-1}\mathcal{E}_m\dot{\Psi}_m(\vec{q}_j) + \mathcal{O}(\delta\omega^m) \qquad (9.41)\end{aligned}$$

where we define the constant matrix

$$\mathcal{E}_m \triangleq \left[I - \bar{A}\bar{A}^+\right]\dot{A}_m \qquad (9.42)$$

and from (9.23) we have

$$\dot{\Psi}_m(\vec{q}_j) \triangleq \left[\dot{\Gamma}_m(\vec{q}_j)\ ,\ \Gamma_m\right]\begin{bmatrix} I \\ -\Gamma^+\dot{\Gamma}(\vec{q}_j)\end{bmatrix} \qquad (9.43)$$

Equation (9.41) together with (9.42) and (9.43) identify a candidate dominant term of $\left[I - A(A^hA)^{-1}A^h\right]\dot{D}(\vec{\omega}_j)$ for small $\delta\omega$ in Case II.

The identified term of (9.41) is non-zero, and in fact is full rank, for Case II scenarios with non-degenerate CR bounds, as shown by the following result.

Lemma 9.2 : In Case II with $\nu \geq \mathcal{D}$, if Conditions **C1-C3** and **CR1-CR3** are satisfied, then the leading term of (9.41) has full column rank. That is,

$$\text{Rank}\left\{\mathcal{E}_m\dot{\Psi}_m(\vec{q}_j)\right\} = \mathcal{D} \qquad (9.44)$$

for $j = 1 \cdots M$.

Proof: See Appendix J.

Therefore subject to Conditions **C1-C3**, **CR1-CR3**, a complete first order characterization of the product $\left[I - A(A^hA)^{-1}A^h\right]\dot{D}(\vec{\omega}_j)$ for Case II is given by (9.41) with (9.42) and (9.43).

Substitution of (9.41) in (9.4) gives

$$Z(\delta\omega) \;=\; \delta\omega^{m-1}\mathcal{E}_m\left[\dot{\Psi}_m(\vec{q}_1),\cdots\dot{\Psi}_m(\vec{q}_M)\right]+\mathcal{O}(\delta\omega^m) \tag{9.45}$$

and then (9.3) yields

$$H \;=\; \delta\omega^{2(m-1)}H_{2m}+\mathcal{O}(\delta\omega^{2(m-1)+1}) \tag{9.46}$$

where

$$H_{2m} \;=\; \left[\dot{\Psi}_m(\vec{q}_1),\cdots\dot{\Psi}_m(\vec{q}_j)\right]^h\mathcal{E}_m^h\mathcal{E}_m\left[\dot{\Psi}_m(\vec{q}_1),\cdots\dot{\Psi}_m(\vec{q}_j)\right] \tag{9.47}$$

Eqs. (9.46), (9.47), with (9.42), (9.43), characterize the small $\delta\omega$ behavior of H for Case II in scenarios with non-degenerate CR bounds. Again note that H_{2m} may not be full rank, but that analysis will show that H_{2m} and the result of Lemma 9.2 are sufficient to identify a full rank first order representation of B_C^{-1} for small $\delta\omega$ in Case II.

9.1.5 Small $\delta\omega$ Expressions for H in Case III

Finally we consider Case III, for which there are some, but fewer than $\mathcal{D}$, vacancies in the m^{th} shell ($0<\nu<\mathcal{D}$), that is

$$\bar{n}_{\{0,\cdots,m\}} \;<\; M+\mathcal{D} \tag{9.48}$$

We again consider scenarios with non-degenerate CR bounds, for which conditions **C1-C3** and **CR1-CR3** are satisfied.

Reference to (9.48), (9.8) and (9.11) shows that in Case III, as in Case II, projection T_m has only partial rank. Therefore columns of matrix $\bar{A}$ *may not* span the entire column space of $\dot{A}_m$. Consequently, as in Case II, it is possible that the dominant term of $\left[I-A(A^hA)^{-1}A^h\right]$ in (9.14) does not entirely annihilate the $p=m$ term of $\dot{F}(\vec{\omega}_j)$ in (9.22).

Directly from (9.22) we identify the (possibly) non-zero leading term as

$$\dot{F}(\vec{\omega}_j) \;=\; \delta\omega^{m-1}\dot{A}_m\dot{\Psi}_m(\vec{q}_j) + \mathcal{O}(\delta\omega^m) \tag{9.49}$$

Substitution of (9.49) and (9.6) in (9.14) gives

$$\begin{aligned}\left[I - A(A^hA)^{-1}A^h\right]\dot{D}(\vec{\omega}_j) &= \left[I - A(A^hA)^{-1}A^h\right]\dot{F}(\vec{\omega}_j) \\ &= \left\{\left[I - \bar{A}\bar{A}^+\right] + \mathcal{O}(\delta\omega)\right\}\left\{\delta\omega^{m-1}\dot{A}_m\dot{\Psi}_m(\vec{q}_j) + \mathcal{O}(\delta\omega^m)\right\} \\ &= \delta\omega^{m-1}\mathcal{E}_m\dot{\Psi}_m(\vec{q}_j) + \mathcal{O}(\delta\omega^m) \end{aligned} \tag{9.50}$$

where $\mathcal{E}_m$, $\dot{\Psi}_m(\vec{q}_j)$ are as in (9.42), (9.43).

Case III differs from Case I and II in that the identified term of (9.50) is *not full rank* $\mathcal{D}$. Specifically $\mathcal{E}_m\dot{\Psi}_m(\vec{q}_j)$ is non-zero, but has only partial rank ν ($\nu < \mathcal{D}$) for Case III scenarios for which Conditions **C1-C3** and **CR1-CR3** are satisfied, as shown by the following.

Lemma 9.3 : In Case III with $0 < \nu < \mathcal{D}$, if Conditions **C1-C3** and **CR1-CR3** are satisfied, then

$$\text{Rank}\left\{\mathcal{E}_m\dot{\Psi}_m(\vec{q}_j)\right\} \;=\; \text{Rank}\left\{\mathcal{E}_m\right\} \;=\; \text{Rank}\left\{\dot{\Psi}_m(\vec{q}_j)\right\} \;=\; \nu \tag{9.51}$$

for $j = 1 \cdots M$, with the property

$$\mathcal{E}_m^+\mathcal{E}_m \;=\; \dot{\Psi}_m(\vec{q}_j)\dot{\Psi}_m(\vec{q}_j)^+ \tag{9.52}$$

Proof: See Appendix K.

Consideration of only the single leading term of (9.22) is thus insufficient to identify a full rank first order representation of $\left[I - A(A^hA)^{-1}A^h\right]\dot{D}(\vec{\omega}_j)$ in Case III.

Accordingly, from (9.22) we identify two leading terms as

$$\dot{F}(\vec{\omega}_j) \;=\; \delta\omega^{m-1}\dot{A}_m\dot{\Psi}_m(\vec{q}_j) + \delta\omega^m\dot{A}_{m+1}\dot{\Psi}_{m+1}(\vec{q}_j) + \mathcal{O}(\delta\omega^{m+1}) \tag{9.53}$$

Substitution of (9.53) in (9.14) gives

$$\begin{aligned}\left[I - A(A^hA)^{-1}A^h\right]\dot{D}(\vec{\omega}_j) &= \delta\omega^{m-1}\mathcal{E}_m(\delta\omega)\dot{\Psi}_m(\vec{q}_j) \\ &\quad +\delta\omega^m\left[I - A(A^hA)^{-1}A^h\right]\dot{A}_{m+1}\dot{\Psi}_{m+1}(\vec{q}_j) \\ &\quad +\mathcal{O}(\delta\omega^{m+1}) \qquad (9.54)\end{aligned}$$

where making use of (9.52) we define

$$\begin{aligned}\mathcal{E}_m(\delta\omega) &\triangleq \left[I - A(A^hA)^{-1}A^h\right]\dot{A}_m\dot{\Psi}_m(\vec{q}_j)\dot{\Psi}_m(\vec{q}_j)^+ \\ &= \left[I - A(A^hA)^{-1}A^h\right]\dot{A}_m\mathcal{E}_m^+\mathcal{E}_m \\ &= \mathcal{E}_m + \mathcal{O}(\delta\omega) \qquad (9.55)\end{aligned}$$

Since $\mathcal{E}_m$ is a factor of $\mathcal{E}_m(\delta\omega)$, the rank of $\mathcal{E}_m(\delta\omega)$ is at most that of $\mathcal{E}_m$. For small $\delta\omega$, the rank of $\mathcal{E}_m(\delta\omega)$ is at least that of its leading term $\mathcal{E}_m$, since the $\mathcal{O}(\delta\omega)$ term cannot reduce the rank of the constant term for sufficiently small $\delta\omega$. It follows that for sufficiently small $\delta\omega$,

$$\text{Rank}\{\mathcal{E}_m(\delta\omega)\} = \text{Rank}\{\mathcal{E}_m\} \qquad (9.56)$$

To facilitate analysis, we rearrange expression (9.54) to be the sum of orthogonal projections onto the column space, and column nullspace, of the leading term factor $\mathcal{E}_m(\delta\omega)$. That is, we express (9.54) as

$$\begin{aligned}&\left[I - A(A^hA)^{-1}A^h\right]\dot{D}(\vec{\omega}_j) \\ &= \left(\mathcal{E}_m(\delta\omega)\mathcal{E}_m(\delta\omega)^+ + \left[I - \mathcal{E}_m(\delta\omega)\mathcal{E}_m(\delta\omega)^+\right]\right) \\ &\quad \cdot\left(\delta\omega^{m-1}\mathcal{E}_m(\delta\omega)\dot{\Psi}_m(\vec{q}_j) + \delta\omega^m\left[I - A(A^hA)^{-1}A^h\right]\dot{A}_{m+1}\dot{\Psi}_{m+1}(\vec{q}_j) + \mathcal{O}(\delta\omega^{m+1})\right) \\ &= \delta\omega^{m-1}\tilde{Z}_m(\vec{q}_j) + \delta\omega^m\tilde{Z}_{m+1}(\vec{q}_j) \qquad (9.57)\end{aligned}$$

where we define

$$\tilde{Z}_m(\vec{q}_j) \triangleq \mathcal{E}_m(\delta\omega)\mathcal{E}_m(\delta\omega)^+ \left[\mathcal{E}_m(\delta\omega)\dot{\Psi}_m(\vec{q}_j) + \mathcal{O}(\delta\omega)\right] \tag{9.58}$$

$$\begin{aligned}\tilde{Z}_{m+1}(\vec{q}_j) \triangleq & \left[I - \mathcal{E}_m(\delta\omega)\mathcal{E}_m(\delta\omega)^+\right] \\ & \cdot \left[\left[I - A(A^hA)^{-1}A^h\right]\dot{A}_{m+1}\dot{\Psi}_{m+1}(\vec{q}_j) + \mathcal{O}(\delta\omega)\right]\end{aligned} \tag{9.59}$$

Noting from (9.55) and (9.56) that

$$\mathcal{E}_m(\delta\omega)\mathcal{E}_m(\delta\omega)^+ = \mathcal{E}_m\mathcal{E}_m^+ + \mathcal{O}(\delta\omega) \tag{9.60}$$

and that

$$\begin{aligned}&\left[I - \mathcal{E}_m\mathcal{E}_m^+\right]\left[I - \bar{A}\bar{A}^+\right]\dot{A}_{m+1} \\ &\quad = \left\{\left[I - \bar{A}\bar{A}^+\right] - \left[I - \bar{A}\bar{A}^+\right]\dot{A}_m\left(\left[I - \bar{A}\bar{A}^+\right]\dot{A}_m\right)^+\right\}\dot{A}_{m+1} \\ &\quad = \left[I - \dot{A}\dot{A}^+\right]\dot{A}_{m+1} \\ &\quad = \mathcal{E}_{m+1}\end{aligned} \tag{9.61}$$

we identify the dominant terms of (9.58), (9.59) for small $\delta\omega$ as

$$\tilde{Z}_m(\vec{q}_j) = \mathcal{E}_m\dot{\Psi}_m(\vec{q}_j) + \mathcal{O}(\delta\omega) \tag{9.62}$$

$$\tilde{Z}_{m+1}(\vec{q}_j) = \mathcal{E}_{m+1}\dot{\Psi}_{m+1}(\vec{q}_j) + \mathcal{O}(\delta\omega) \tag{9.63}$$

From Lemma 9.3, the dominant term of $\tilde{Z}_m(\vec{q}_j)$ satisfies

$$\text{Rank}\{\mathcal{E}_m\dot{\Psi}_m(\vec{q}_j)\} = \nu \tag{9.64}$$

for all $j = 1 \cdots M$, and therefore that the rank of $\tilde{Z}_m(\vec{q}_j)$ is at least ν for sufficiently small $\delta\omega$. From (9.56) and (9.51), we see that the rank of factor $\mathcal{E}_m(\delta\omega)$ of $\tilde{Z}_m(\vec{q}_j)$ in (9.58) is ν. Therefore it must be that

$$\text{Rank}\{\tilde{Z}_m(\vec{q}_j)\} = \nu \tag{9.65}$$

for sufficiently small $\delta\omega$, and all $j = 1 \cdots M$.

Substitution of (9.54) in (9.4) yields

$$Z(\delta\omega) = \delta\omega^{m-1}\tilde{Z}_m + \delta\omega^m \tilde{Z}_{m+1} \tag{9.66}$$

where

$$\begin{aligned}
\tilde{Z}_m &\triangleq \left[\tilde{Z}_m(\vec{q}_1),\ \cdots \tilde{Z}_m(\vec{q}_M)\right] \\
&= \mathcal{E}_m(\delta\omega)\mathcal{E}_m(\delta\omega)^+ \left\{\mathcal{E}_m(\delta\omega)\left[\dot{\Psi}_m(\vec{q}_1), \cdots \dot{\Psi}_m(\vec{q}_M)\right] + \mathcal{O}(\delta\omega)\right\} \qquad (9.67) \\
\tilde{Z}_{m+1} &= \left[\tilde{Z}_{m+1}(\vec{q}_1),\ \cdots \tilde{Z}_{m+1}(\vec{q}_M)\right] \\
&= \left[I - \mathcal{E}_m(\delta\omega)\mathcal{E}_m(\delta\omega)^+\right] \\
&\quad \cdot \left\{\left[I - A(A^hA)^{-1}A^h\right]\dot{A}_{m+1}\left[\dot{\Psi}_{m+1}(\vec{q}_1), \cdots \dot{\Psi}_{m+1}(\vec{q}_M)\right] + \mathcal{O}(\delta\omega)\right\} \qquad (9.68)
\end{aligned}$$

Finally, substitution of (9.66) in (9.3) and use of the orthogonality of the columns of $\tilde{Z}_m$ and $\tilde{Z}_{m+1}$ gives

$$H = \delta\omega^{2(m-1)}H_{2m}(\delta\omega) + \delta\omega^{2m}H_{2(m+1)}(\delta\omega) \tag{9.69}$$

where

$$\begin{aligned}
H_{2m}(\delta\omega) &= \tilde{Z}_m^h \tilde{Z}_m \\
H_{2(m+1)}(\delta\omega) &= \tilde{Z}_{m+1}^h \tilde{Z}_{m+1} \qquad (9.70)
\end{aligned}$$

and for small $\delta\omega$

$$\begin{aligned}
H_{2m}(\delta\omega) &= \left[\dot{\Psi}_m(\vec{q}_1),\ \cdots\ \dot{\Psi}_m(\vec{q}_M)\right]^h \mathcal{E}_m^h \mathcal{E}_m \left[\dot{\Psi}_m(\vec{q}_1),\ \cdots\ \dot{\Psi}_m(\vec{q}_M)\right] \\
&\quad + \mathcal{O}(\delta\omega) \qquad (9.71) \\
H_{2(m+1)}(\delta\omega) &= \left[\dot{\Psi}_{m+1}(\vec{q}_1),\ \cdots\ \dot{\Psi}_{m+1}(\vec{q}_M)\right]^h \mathcal{E}_{m+1}^h \mathcal{E}_{m+1} \left[\dot{\Psi}_{m+1}(\vec{q}_1),\ \cdots\ \dot{\Psi}_{m+1}(\vec{q}_M)\right] \\
&\quad + \mathcal{O}(\delta\omega) \qquad (9.72)
\end{aligned}$$

with $\mathcal{E}_m$, $\dot{\Psi}_m(\vec{q}_j)$ as in (9.42), (9.43), and $\boldsymbol{\mathcal{E}}_{m+1}$, $\dot{\boldsymbol{\Psi}}_{m+1}(\vec{q}_j)$ as in (9.33), (9.34).

Eqs. (9.69)-(9.72) characterize the small $\delta\omega$ behavior of H for Case III in scenarios with non-degenerate CR bounds. We note that by suitably specializing Eqs. (9.69)-(9.72), we can obtain Eqs. (9.37), (9.38) for Case I and Eqs. (9.46), (9.47) for Case II. Analysis in the subsequent Sections shows that Eqs. (9.69)-(9.72), together with the rank properties (9.64) and (9.65), are sufficient to identify a complete small $\delta\omega$ representation of B_C in Case III.

9.2 Small $\delta\omega$ Behavior of B_C^{-1}

This section exploits the representations of H developed in Section 9.1 to identify small $\delta\omega$ representations for the inverse of the CR bound matrix B_C for each Case I, II and III. The B_C^{-1} expressions serve as the basis for identifying expressions for B_C in Section 9.3.

Reference to (8.28) shows that

$$B_C^{-1} = \frac{2N}{\sigma^2} \cdot \mathrm{Re}\left\{H \odot \hat{P}_+^t\right\} \tag{9.73}$$

where from (9.3)

$$H = Z(\delta\omega)^h Z(\delta\omega) \tag{9.74}$$

and

$$Z(\delta\omega) = \left[I - A(A^hA)^{-1}A^h\right]\left[\dot{D}(\vec{\omega}_1), \cdots, \dot{D}(\vec{\omega}_M)\right] \tag{9.75}$$

For each Case I, II and III, the small $\delta\omega$ behavior of H has been identified respectively in (9.37), (9.46) and (9.69), and that of $\left[I - A(A^hA)^{-1}A^h\right] D(\vec{\omega}_j)$ $(j = 1 \cdots M)$ respectively in (9.32), (9.41) and (9.54).

To identify a complete small $\delta\omega$ representation of B_C^{-1} suitable for computation B_C, it is desirable to identify the contribution to the rank of B_C^{-1} of series terms of $\left[I - A(A^hA)^{-1}A^h\right] \dot{D}(\vec{q}_j)$ of either full or partial rank. To this end, we develop the

following two enabling results.

Lemma 9.4 : Let G be a $M\mathcal{D} \times M\mathcal{D}$ matrix of the form

$$G = \mathrm{Re}\Big\{\Big([\Phi_1, \cdots, \Phi_M]^h [\Phi_1, \cdots, \Phi_M]\Big) \odot \hat{P}_+^t\Big\} \tag{9.76}$$

If Φ_j has full rank ($= \mathcal{D}$) for $j = 1 \cdots M$, and $\hat{P}$ is Hermitian positive definite, then G is Hermitian positive definite. That is

$$\mathrm{Rank}\{G\} = M\mathcal{D} \tag{9.77}$$

Proof: See Appendix L.

If each Φ_j has only partial rank, we obtain the following parallel result.

Lemma 9.5 : Let

$$G = \mathrm{Re}\Big\{\Big([\Phi_1, \cdots, \Phi_M]^h [\Phi_1, \cdots, \Phi_M]\Big) \odot \hat{P}_+^t\Big\} \tag{9.78}$$

If Φ_j has partial rank r ($< \mathcal{D}$) for each $j = 1 \cdots M$, and $\hat{P}$ is Hermitian positive definite, then G is Hermitian non-negative definite with

$$\mathrm{Rank}\{G\} = M \cdot r \tag{9.79}$$

Proof: See Appendix M.

The following sections identify a complete first order representation of B_C^{-1} for each of Cases I, II and III.

9.2.1 Small $\delta\omega$ Behavior of B_C^{-1} in Case I

Substitution of (9.37) in (9.73) gives

$$\begin{aligned} B_C^{-1} &= \delta\omega^{2m} \frac{2N}{\sigma^2} \cdot \mathrm{Re}\Big\{H_{2(m+1)} \odot \hat{P}_+^t\Big\} + \mathcal{O}(\delta\omega^{2m+1}) \\ &= \delta\omega^{2m} \frac{2N}{\sigma^2} G_{2(m+1)} + \mathcal{O}(\delta\omega^{2m+1}) \end{aligned} \tag{9.80}$$

where we define

$$\begin{aligned} G_{2(m+1)} &\triangleq \mathrm{Re}\left\{H_{2(m+1)} \odot \widehat{P}_+^t\right\} \\ &= \mathrm{Re}\Big\{\Big(\left[\dot{\Psi}_{m+1}(\vec{q}_1), \cdots \dot{\Psi}_{m+1}(\vec{q}_M)\right]^h \mathcal{E}_{m+1}^h \\ &\qquad \cdot \mathcal{E}_{m+1}\left[\dot{\Psi}_{m+1}(\vec{q}_1), \cdots \dot{\Psi}_{m+1}(\vec{q}_M)\right]\Big) \odot \widehat{P}_+^t\Big\} \end{aligned} \tag{9.81}$$

where use is made of (9.38) to expand $H_{2(m+1)}$. Use of the block constant property of $\widehat{P}_+$, and of the real property of $\dot{\Psi}_k(\vec{q}_j)$ $(j = 1, \cdots M)$, results in

$$G_{2(m+1)} = \dot{\Psi}_{m+1}^t \mathrm{Re}\left\{\left([I, \cdots, I]^h \mathcal{E}_{m+1}^h \mathcal{E}_{m+1} [I, \cdots, I]\right) \odot \widehat{P}_+^t\right\} \dot{\Psi}_{m+1} \tag{9.82}$$

where we define the real, constant, block diagonal matrix

$$\dot{\Psi}_{m+1} \triangleq \text{Block Diag.}\left\{\dot{\Psi}_{m+1}(\vec{q}_1), \cdots \dot{\Psi}_{m+1}(\vec{q}_M)\right\} \tag{9.83}$$

To further simplify (9.82), the Hadamard product $\odot$ with the enlarged matrix $\widehat{P}_+^t$ may be replaced by the Kronecker product $\otimes$ with the non-enlarged cross-power matrix $\widehat{P}^t$, with the result

$$G_{2(m+1)} = \dot{\Psi}_{m+1}^t \mathrm{Re}\left[\widehat{P}^t \otimes \mathcal{E}_{m+1}^h \mathcal{E}_{m+1}\right] \dot{\Psi}_{m+1} \tag{9.84}$$

Matrix $G_{2(m+1)}$ is Hermitian positive definite with

$$\mathrm{Rank}\{G_{2(m+1)}\} = M \cdot \mathcal{D} \tag{9.85}$$

as seen by application of Lemma 9.4 to (9.81) with identifications

$$\begin{aligned} G &= G_{2(m+1)} \\ \Phi_j &= \mathcal{E}_{m+1} \dot{\Psi}_{m+1}(\vec{q}_M) \end{aligned} \tag{9.86}$$

and use of the full rank $(= \mathcal{D})$ property of $\mathcal{E}_{m+1} \dot{\Psi}_{m+1}(\vec{q}_M)$ in Case I identified in Lemma 9.1.

Therefore, the identified leading term of (9.80) is a complete small $\delta\omega$ representation of B_C^{-1} for Case I.

9.2.2 Small $\delta\omega$ Behavior of B_C^{-1} in Case II

Identification of the behavior of B_C^{-1} for Case II parallels that of Section 9.2.1 for Case I. For Case II, substitution of (9.46) in (9.73) gives

$$\begin{aligned} B_C^{-1} &= \delta\omega^{2(m-1)}\frac{2N}{\sigma^2}\cdot \mathrm{Re}\left\{H_{2m}\odot \hat{P}_+^t\right\} + \mathcal{O}(\delta\omega^{2(m-1)+1}) \\ &= \delta\omega^{2(m-1)}\frac{2N}{\sigma^2}G_{2m} + \mathcal{O}(\delta\omega^{2(m-1)+1}) \end{aligned} \tag{9.87}$$

Using (9.47) to expand H_{2m}, and by rearrangement parallel to that of (9.81)-(9.84), we define

$$\begin{aligned} G_{2m} &\triangleq \mathrm{Re}\left\{H_{2m}\odot \hat{P}_+^t\right\} \\ &= \dot{\Psi}_m^t \mathrm{Re}\left[\hat{P}^t \otimes \mathcal{E}_m^h \mathcal{E}_m\right]\dot{\Psi}_m \end{aligned} \tag{9.88}$$

with the real, constant, block diagonal matrix

$$\dot{\Psi}_m \triangleq \text{Block Diag.}\left\{\dot{\Psi}_m(\vec{q}_1),\ \cdots\ \dot{\Psi}_m(\vec{q}_M)\right\} \tag{9.89}$$

Matrix G_{2m} is Hermitian positive definite with

$$\mathrm{Rank}\{G_{2m}\} = M\cdot\mathcal{D} \tag{9.90}$$

as seen by application of Lemma 9.4 with identifications

$$\begin{aligned} G &= G_{2m} \\ \Phi_j &= \mathcal{E}_m\dot{\Psi}_m(\vec{q}_j) \end{aligned} \tag{9.91}$$

and use of the full rank ($=\mathcal{D}$) property of $\mathcal{E}_m\dot{\Psi}_m(\vec{q}_M)$ in Case II identified in Lemma 9.2.

Therefore, the identified leading term of (9.87) is a complete small $\delta\omega$ representation of B_C^{-1} for Case II.

9.2.3 Small $\delta\omega$ Behavior of B_C^{-1} in Case III

Identification of the small $\delta\omega$ behavior of B_C^{-1} for Case III scenarios is complicated by the $\delta\omega$ dependence of the small $\delta\omega$ representation of H in (9.69).

Substitution of (9.69) in (9.73) gives

$$\begin{aligned} B_C^{-1} &= \delta\omega^{2(m-1)}\frac{2N}{\sigma^2}\cdot \mathrm{Re}\left\{\left(H_{2m}(\delta\omega)+\delta\omega^2 H_{2(m+1)}(\delta\omega)\right)\odot \hat{P}_+^t\right\} \\ &= \delta\omega^{2(m-1)}\frac{2N}{\sigma^2}\left[G_{2m}(\delta\omega)+\delta\omega^2 G_{2(m+1)}(\delta\omega)\right] \end{aligned} \tag{9.92}$$

where using (9.70) we define

$$\begin{aligned} G_{2m}(\delta\omega) &\triangleq \mathrm{Re}\left\{H_{2m}(\delta\omega)\odot \hat{P}_+^t\right\} \\ &= \mathrm{Re}\left\{\left(\tilde{Z}_m^h \tilde{Z}_m\right)\odot \hat{P}_+^t\right\} \end{aligned} \tag{9.93}$$

$$\begin{aligned} G_{2(m+1)}(\delta\omega) &\triangleq \mathrm{Re}\left\{H_{2(m+1)}(\delta\omega)\odot \hat{P}_+^t\right\} \\ &= \mathrm{Re}\left\{\left(\tilde{Z}_{m+1}^h \tilde{Z}_{m+1}\right)\odot \hat{P}_+^t\right\} \end{aligned} \tag{9.94}$$

For small $\delta\omega$, we identify the dominant terms of (9.93), (9.94) by a development parallel to that of (9.84), (9.88) to be

$$G_{2m}(\delta\omega) = G_{2m}+\mathcal{O}(\delta\omega) \tag{9.95}$$

$$G_{2(m+1)}(\delta\omega) = G_{2(m+1)}+\mathcal{O}(\delta\omega) \tag{9.96}$$

where G_{2m} is as in (9.88) and $G_{2(m+1)}$ is as in (9.84).

Matrix $G_{2m}(\delta\omega)$ and its leading constant term G_{2m} are Hermitian non-negative with equal but partial rank $M\nu$ for small $\delta\omega$ in Case III, with

$$\mathrm{Rank}\{G_{2m}(\delta\omega)\} = \mathbf{Rank}\{G_{2m}\} = M\cdot\nu \tag{9.97}$$

for small $\delta\omega$, as seen by application of Lemma 9.5 first with identifications

$$\begin{aligned} G &= G_{2m}(\delta\omega) \\ \Phi_j &= \tilde{Z}_m(\vec{q}_j) \end{aligned} \tag{9.98}$$

and use of the rank ν property of $\tilde{Z}_m(\vec{q}_j)$ for small $\delta\omega$ identified in (9.65), and then with identifications

$$\begin{aligned} G &= G_{2m} \\ \Phi_j &= \mathcal{E}_m \dot{\Psi}_k(\vec{q}_j) \end{aligned} \tag{9.99}$$

and use of the rank ν property of $\mathcal{E}_m \dot{\Psi}_k(\vec{q}_j)$ identified in Lemma 9.3.

Finally, matrix B_C^{-1} is Hermitian positive definite with

$$\text{Rank}\{B_C^{-1}\} = M \cdot \mathcal{D} \tag{9.100}$$

for small $\delta\omega$ in scenarios with non-degenerate CR bounds, as seen by application of Lemma 9.4 with identifications

$$\begin{aligned} G &= G_{2m}(\delta\omega) + \delta\omega^2 G_{2(m+1)}(\delta\omega) \\ \Phi_j &= \tilde{Z}_m(\vec{q}_j) + \delta\omega^2 \tilde{Z}_{m+1}(\vec{q}_j) \\ &= \left[I - A(A^h A)^{-1} A^h\right] \dot{D}(\vec{\omega}_j) \end{aligned} \tag{9.101}$$

since $\left[I - A(A^h A)^{-1} A^h\right] \dot{D}(\vec{\omega}_j)$ is full rank $(= \mathcal{D})$ by the linear independence assumption **A6** of Chapter 8.

The small $\delta\omega$ representation of B_C^{-1} in (9.92)-(9.96), together with foregoing rank properties, are sufficient to identify a complete small $\delta\omega$ representation of B_C for Case III, as shown in the next section.

9.3 Expressions for B_C

This section transforms the small $\delta\omega$ expressions for B_C^{-1} identified in the previous section for each Case I, II and III into small $\delta\omega$ expressions for B_C.

To elucidate the inverse of B_C^{-1}, we make use of the following inverse and pseudo-inverse properties.

PI1. Let matrix $X(\delta\omega)$ be of the form

$$X(\delta\omega) = X_0 + \mathcal{O}(\delta\omega) \tag{9.102}$$

where

$$\text{Rank}\{X(\delta\omega)\} = \text{Rank}\{X_0\} \tag{9.103}$$

for sufficiently small $\delta\omega$. It is well known [21] that

$$X(\delta\omega)^+ = X_0^+ + \mathcal{O}(\delta\omega) \tag{9.104}$$

and if X_0 is full rank then (9.104) specializes to

$$X(\delta\omega)^{-1} = X_0^{-1} + \mathcal{O}(\delta\omega) \tag{9.105}$$

PI2. Let $X(\delta\omega)$ be Hermitian non-negative definite and of the form (9.102), with rank property (9.103), but not full rank. Let $G(\delta\omega)$ be Hermitian positive definite (thus full rank) of the form

$$G(\delta\omega) = X(\delta\omega) + \delta\omega^2 Y(\delta\omega) \tag{9.106}$$

where $Y(\delta\omega)$ is Hermitian non-negative definite of the form

$$Y(\delta\omega) = Y_0 + \mathcal{O}(\delta\omega) \tag{9.107}$$

It is shown in Appendix N that the inverse of $G(\delta\omega)$ in (9.106) is of the form

$$\begin{aligned} G(\delta\omega)^{-1} &= \delta\omega^{-2}\, W(\delta\omega)^{+} \\ &\quad + \left[I - W(\delta\omega)^{+}Y(\delta\omega)\right]\, X(\delta\omega)^{+}\, \left[I - Y(\delta\omega)W(\delta\omega)^{+}\right] \\ &\quad + \mathcal{O}(\delta\omega^{2}) \end{aligned} \tag{9.108}$$

where

$$W(\delta\omega) = P_{[X(\delta\omega)]}Y(\delta\omega)P_{[X(\delta\omega)]} \tag{9.109}$$

$$P_{[X(\delta\omega)]} = I - X(\delta\omega)X(\delta\omega)^{+} \tag{9.110}$$

The foregoing inverse properties are applied in the following to identify the small $\delta\omega$ behavior of B_C in each Case I, II and III.

9.3.1 Small $\delta\omega$ Behavior of B_C in Case I

We rearrange the Case I expression (9.80) for B_C^{-1} to the form

$$B_C^{-1} = \delta\omega^{2m}\left[\frac{2N}{\sigma^2}G_{2(m+1)} + \mathcal{O}(\delta\omega^{1})\right] \tag{9.111}$$

where $G_{2(m+1)}$ is the constant matrix (9.84), full rank by (9.85). Clearly the bracketed expression in (9.111) is of the form (9.102), and satisfies rank property (9.103) with full rank. Accordingly, the inverse of the bracketed expression in (9.111) is of the form (9.105), and the inverse of (9.111) is

$$\begin{aligned} B_C &= \delta\omega^{-2m}\frac{\sigma^2}{2N}G_{2(m+1)}^{-1} + \mathcal{O}(\delta\omega^{-2m+1}) \\ &= \delta\omega^{-2m}\frac{\sigma^2}{2N}\left[\dot{\Psi}_{m+1}^{t}\mathrm{Re}\left\{\widehat{P}^{t}\otimes\mathcal{E}_{m+1}^{h}\mathcal{E}_{m+1}\right\}\dot{\Psi}_{m+1}\right]^{-1} + \mathcal{O}(\delta\omega^{-2m+1}) \end{aligned} \tag{9.112}$$

where use is made of expansion (9.84) of $G_{2(m+1)}$. Expression (9.112) provides a complete first order representation of B_C for Case I for small $\delta\omega$, since the dominant term is full rank.

9.3.2 Small $\delta\omega$ Behavior of B_C in Case II

A parallel argument elucidates the behavior of B_C for Case II. We rearrange expression (9.87) for B_C^{-1} for Case II to the form

$$B_C^{-1} = \delta\omega^{2(m-1)}\left[\frac{2N}{\sigma^2}G_{2m} + \mathcal{O}(\delta\omega^1)\right] \tag{9.113}$$

where G_{2m} is the constant matrix (9.88), full rank by (9.90). Clearly the bracketed expression in (9.113) is of the form (9.102), and satisfies rank property (9.103) with full rank. Accordingly, the inverse of (9.113) is

$$\begin{aligned} B_C &= \delta\omega^{-2(m-1)}\frac{\sigma^2}{2N}G_{2m}^{-1} + \mathcal{O}(\delta\omega^{-2(m-1)+1}) \\ &= \delta\omega^{-2(m-1)}\frac{\sigma^2}{2N}\left[\dot{\Psi}_m^t \mathrm{Re}\left\{\hat{P}^t \otimes \mathcal{E}_m^h \mathcal{E}_m\right\}\dot{\Psi}_m\right]^{-1} + \mathcal{O}(\delta\omega^{-2(m-1)+1}) \end{aligned} \tag{9.114}$$

where use is made of expansion (9.88) of G_{2m}. Expression (9.114) provides a complete first order representation of B_C for Case II for small $\delta\omega$, since the dominant term is full rank.

9.3.3 Small $\delta\omega$ Behavior of B_C in Case III

The structure of B_C for small $\delta\omega$ is complicated in Case III by the non-full rank nature of the leading term of B_C^{-1}. We recall expression (9.92) for B_C^{-1} for Case III to be

$$B_C^{-1} = \delta\omega^{2(m-1)}\frac{2N}{\sigma^2}\left[G_{2m}(\delta\omega) + \delta\omega^2 G_{2(m+1)}(\delta\omega)\right] \tag{9.115}$$

where $G_{2m}(\delta\omega)$, $G_{2(m+1)}(\delta\omega)$ are the matrices (9.93), (9.94) non-constant with $\delta\omega$. Clearly the bracketed expression of (9.115) is of the form (9.106) and is Hermitian positive definite by (9.100). The term $G_{2m}(\delta\omega)$ as in (9.95) is of the form (9.102), is Hermitian non-negative definite and satisfies rank property (9.103) with partial rank $M\nu$ from (9.97).

Accordingly, the inverse of the bracketed expression in (9.115) is of the form

(9.108) and therefore

$$\begin{aligned} B_C &= \delta\omega^{-2(m-1)}\frac{\sigma^2}{2N}\Big[\delta\omega^{-2}\,W(\delta\omega)^+ \\ &\quad + \Big[I - W(\delta\omega)^+ G_{2(m+1)}(\delta\omega)\Big]\, G_{2m}(\delta\omega)^+\, \Big[I - G_{2(m+1)}(\delta\omega)\, W(\delta\omega)^+\Big] \\ &\quad + \mathcal{O}(\delta\omega^2)\Big] \end{aligned} \tag{9.116}$$

where

$$W(\delta\omega) = P_{[G_{2m}(\delta\omega)]} G_{2(m+1)}(\delta\omega) P_{[G_{2m}(\delta\omega)]} \tag{9.117}$$

$$P_{[G_{2m}(\delta\omega)]} = I - G_{2m}(\delta\omega) G_{2m}(\delta\omega)^+ \tag{9.118}$$

To identify the dominant term of (9.116) for small $\delta\omega$, we note from (9.95), (9.97), and (9.104) that

$$\begin{aligned} G_{2m}(\delta\omega) &= G_{2m} + \mathcal{O}(\delta\omega) \\ G_{2m}(\delta\omega)^+ &= G_{2m}^+ + \mathcal{O}(\delta\omega) \end{aligned} \tag{9.119}$$

and therefore

$$P_{[G_{2m}(\delta\omega)]} = I - G_{2m} G_{2m}^+ + \mathcal{O}(\delta\omega) \tag{9.120}$$

From (9.88) $\dot{\Psi}_m^t$ is the leading term of G_{2m}. By construction (9.89) and Lemma 9.3, $\dot{\Psi}_m$ has the same rank $M\nu$ as G_{2m}, hence the projection onto the column space of G_{2m} is simply

$$G_{2m} G_{2m}^+ = \dot{\Psi}_m^t (\dot{\Psi}_m^t)^+ = \dot{\Psi}_m^+ \dot{\Psi}_m \tag{9.121}$$

Using (9.121), we simplify (9.120) to

$$\begin{aligned} P_{[G_{2m}(\delta\omega)]} &= I - \dot{\Psi}_m^+ \dot{\Psi}_m + \mathcal{O}(\delta\omega) \\ &= P_{[\dot{\Psi}_m^t]} + \mathcal{O}(\delta\omega) \end{aligned} \tag{9.122}$$

Substitution of (9.122), (9.96) and (9.88) in (9.117) identifies the constant dominant term of $W(\delta\omega)$ for small $\delta\omega$ as

$$W(\delta\omega) = P_{[\dot{\Psi}_m^t]}\dot{\Psi}_{m+1}^t \mathrm{Re}\left\{\widehat{P}^t \otimes \mathcal{E}_{m+1}^h \mathcal{E}_{m+1}\right\} \dot{\Psi}_{m+1} P_{[\dot{\Psi}_m^t]} + \mathcal{O}(\delta\omega) \quad (9.123)$$

Using the block diagonal and real properties of $\dot{\Psi}_{m+1}$ and $P_{[\dot{\Psi}_m^t]}$, we express

$$\begin{aligned} & P_{[\dot{\Psi}_m^t]}\dot{\Psi}_{m+1}^t \mathrm{Re}\left\{\widehat{P}^t \otimes \mathcal{E}_{m+1}^h \mathcal{E}_{m+1}\right\} \dot{\Psi}_{m+1} P_{[\dot{\Psi}_m^t]} \\ &= \mathrm{Re}\left\{\left[\dot{\Psi}_{m+1}(\vec{q}_1)P_{[\dot{\Psi}_m(\vec{q}_1)^t]}, \cdots, \dot{\Psi}_{m+1}(\vec{q}_M)P_{[\dot{\Psi}_m(\vec{q}_M)^t]}\right]^h \mathcal{E}_{m+1}^h \right. \\ &\quad \left. \cdot\ \mathcal{E}_{m+1}\left[\dot{\Psi}_{m+1}(\vec{q}_1)P_{[\dot{\Psi}_m(\vec{q}_1)^t]}, \cdots, \dot{\Psi}_{m+1}(\vec{q}_M)P_{[\dot{\Psi}_m(\vec{q}_M)^t]}\right]\right\} \end{aligned} \quad (9.124)$$

and therefore

$$\mathrm{Rank}\{P_{[\dot{\Psi}_m^t]}\dot{\Psi}_{m+1}^t \mathrm{Re}\left\{\widehat{P}^t \otimes \mathcal{E}_{m+1}^h \mathcal{E}_{m+1}\right\} \dot{\Psi}_{m+1} P_{[\dot{\Psi}_m^t]}\} = M(\mathcal{D}-\nu) \quad (9.125)$$

as seen by application of Lemma 9.5 with identifications

$$\begin{aligned} G &= P_{[\dot{\Psi}_m^t]}\dot{\Psi}_{m+1}^t \mathrm{Re}\left\{\widehat{P}^t \otimes \mathcal{E}_{m+1}^h \mathcal{E}_{m+1}\right\} \dot{\Psi}_{m+1} P_{[\dot{\Psi}_m^t]} \\ \Phi_j &= \mathcal{E}_{m+1}\dot{\Psi}_{m+1}(\vec{q}_j)P_{[\dot{\Psi}_m(\vec{q}_j)^t]} \end{aligned} \quad (9.126)$$

and use of the following result:

Lemma 9.6 : In Case III with $0 < \nu < \mathcal{D}$, if Conditions **C1-C3** and **CR1-CR3** are satisfied, then

$$\mathrm{Rank}\left\{\mathcal{E}_{m+1}\dot{\Psi}_{m+1}(\vec{q}_j)P_{[\dot{\Psi}_m(\vec{q}_j)^t]}\right\} = \mathcal{D}-\nu \quad (9.127)$$

for $j = 1 \cdots M$.

Proof: See Appendix O.

Since the factor $P_{[G_{2m}(\delta\omega)]}$ of $W(\delta\omega)$ in (9.117) also has rank $M(\mathcal{D}-\nu)$ by (9.97),

it follows from (9.125) that

$$\text{Rank}\{W(\delta\omega)\} \;=\; M(\mathcal{D}-\nu) \tag{9.128}$$

for sufficiently small $\delta\omega$.

Reference to (9.125) and (9.128) shows that $W(\delta\omega)$ satisfies rank property (9.103) with rank $M(\mathcal{D}-\nu)$ and therefore the pseudo-inverse is of the form (9.104), namely

$$W(\delta\omega)^{+} \;=\; \left[P_{[\dot{\Psi}_m^t]}\dot{\Psi}_{m+1}^t \text{Re}\left\{\hat{P}^t \otimes \mathcal{E}_{m+1}^h \mathcal{E}_{m+1}\right\}\dot{\Psi}_{m+1}P_{[\dot{\Psi}_m^t]}\right]^{+} + \mathcal{O}(\delta\omega) \tag{9.129}$$

Substitution in (9.116) shows that the dominant term of B_C for small $\delta\omega$ is

$$B_C \;=\; \delta\omega^{-2m}\frac{\sigma^2}{2N}\left[P_{[\dot{\Psi}_m^t]}\dot{\Psi}_{m+1}^t \text{Re}\left\{\hat{P}^t \otimes \mathcal{E}_{m+1}^h \mathcal{E}_{m+1}\right\}\dot{\Psi}_{m+1}P_{[\dot{\Psi}_m^t]}\right]^{+} + \mathcal{O}(\delta\omega^{-2m+1}) \tag{9.130}$$

In contrast to Cases I and II, the dominant term in expression (9.130) of B_C for Case III is not full rank. Specifically, the leading term of (9.130) which identifies the components of B_C with a $\delta\omega^{-2m}$ dependence for small $\delta\omega$, is shown in (9.125) to have only partial rank $M(\mathcal{D}-\nu)$. A complete small $\delta\omega$ representation of B_C is provided by (9.116), which identifies additional components of B_C with a (more favorable) $\delta\omega^{-2m+2}$ dependence for small $\delta\omega$. The effect of these additional components is addressed in Section 9.4.2.

9.4 Summary of Results

The expressions (9.112), (9.114), and (9.130) for B_C for small $\delta\omega$ can be compactly expressed as follows

$$B_C \;=\; \delta\omega^{-2(x-1)}K_x + \mathcal{O}(\delta\omega^{-2(x-1)+1}) \tag{9.131}$$

where parameter χ defined in (8.61) takes the values

$$\chi = \begin{cases} m & \text{Case II} \\ m+1 & \text{Cases I and III} \end{cases} \tag{9.132}$$

and the constant matrix K_χ is defined as

$$K_\chi \triangleq \frac{\sigma^2}{2N}\left(P_{[\dot{\Psi}^t_{\chi-1}]}\dot{\Psi}^t_\chi \mathrm{Re}\left[\hat{P}^t \otimes \mathcal{E}^h_\chi \mathcal{E}_\chi\right]\dot{\Psi}_\chi P_{[\dot{\Psi}^t_{\chi-1}]}\right)^+ \tag{9.133}$$

where

$$P_{[\dot{\Psi}^t_{\chi-1}]} = \begin{cases} I & \text{Cases I and II} \\ I - \dot{\Psi}^+_m \dot{\Psi}_m & \text{Case III} \end{cases} \tag{9.134}$$

The general expression (9.133) for K_χ can be specialized for each of the cases as follows

$$K_\chi = \begin{cases} \frac{\sigma^2}{2N}\left(\dot{\Psi}^t_{m+1}\mathrm{Re}\left[\hat{P}^t \otimes \mathcal{E}^h_{m+1}\mathcal{E}_{m+1}\right]\dot{\Psi}_{m+1}\right)^{-1} & \text{Case I} \\ \frac{\sigma^2}{2N}\left(\dot{\Psi}^t_m \mathrm{Re}\left[\hat{P}^t \otimes \mathcal{E}^h_m \mathcal{E}_m\right]\dot{\Psi}_m\right)^{-1} & \text{Case II} \\ \frac{\sigma^2}{2N}\left(P_{[\dot{\Psi}^t_m]}\dot{\Psi}^t_{m+1}\mathrm{Re}\left[\hat{P}^t \otimes \mathcal{E}^h_{m+1}\mathcal{E}_{m+1}\right]\dot{\Psi}_{m+1}P_{[\dot{\Psi}^t_m]}\right)^+ & \text{Case III} \end{cases} \tag{9.135}$$

for $k = m, m+1$, with

$$\mathcal{E}_m = \left[I - \bar{A}\bar{A}^+\right]\dot{A}_m \tag{9.136}$$

$$\mathcal{E}_{m+1} = \left[I - \dot{A}\dot{A}^+\right]\dot{A}_{m+1} \tag{9.137}$$

$$\bar{A} = \left[\dot{A}_0,\ \dot{A}_1,\ \cdots,\ \dot{A}_{m-1},\ \dot{A}_m T_m\right] \tag{9.138}$$

$$\dot{A} = \left[\dot{A}_0,\ \dot{A}_1,\ \cdots,\ \dot{A}_{m-1},\ \dot{A}_m\right] \tag{9.139}$$

$$\dot{\Psi}_p = \text{Block Diag.}\left\{\dot{\Psi}_p(\vec{q}_1), \dot{\Psi}_p(\vec{q}_2), \cdots \dot{\Psi}_p(\vec{q}_M)\right\} \qquad p = m, m+1 \tag{9.140}$$

We interpret the terms in (9.136)-(9.140) as follows. Matrix $\mathcal{E}_m$ consists of the m^{th} order spatial derivatives of $\vec{a}(\vec{\omega})$ at $\vec{\omega}_0$, less their projection onto the limiting column space of A as $\delta\omega \to 0$. Similarly, matrix $\mathcal{E}_{m+1}$ consists of the $(m+1)^{th}$ order spatial

derivatives of $\vec{a}(\vec{\omega})$ at $\vec{\omega}_0$, less their projection onto the column space spanned by all the spatial derivatives of lower order. Note that the matrix $\mathcal{E}_{m+1}$ specializes to the vector $\vec{\epsilon}_M$ used in the 1-D small $\delta\omega$ CR bound expressions (8.14)-(8.24) previously developed by Lee [11].

To interpret $\dot{\Psi}_p(\vec{q}_j)$, we express (9.23) as

$$\begin{aligned}\dot{\Psi}_p(\vec{q}_j) &= \dot{\Gamma}_p(\vec{q}_j) - \Gamma_p\Gamma^+\dot{\Gamma}(\vec{q}_j) \\ &= \left[\frac{\partial\vec{\psi}_p(\vec{q})}{\partial q_1}, \frac{\partial\vec{\psi}_p(\vec{q})}{\partial q_2}, \cdots, \frac{\partial\vec{\psi}_p(\vec{q})}{\partial q_D}\right]_{\vec{q}=\vec{q}_j}\end{aligned} \tag{9.141}$$

with vector function

$$\vec{\psi}_p(\vec{q}) \triangleq \left[\vec{\gamma}_p(\vec{q}) - \Gamma_p\Gamma^+\vec{\gamma}(\vec{q})\right] \tag{9.142}$$

where the vector $\vec{\gamma}(\vec{q})$ is defined as

$$\vec{\gamma}(\vec{q}) \triangleq \begin{bmatrix} \vec{\gamma}_0(\vec{q}) \\ \vdots \\ \vec{\gamma}_{m-1}(\vec{q}) \\ T_m\vec{\gamma}_m(\vec{q}) \end{bmatrix} \tag{9.143}$$

The vector function $\vec{\psi}_p(\vec{q})$ has zeros at each of the normalized source directions $\vec{q} = \vec{q}_j$, $j = 1 \cdots M$, since $\vec{\gamma}(\vec{q}_j)$ is simply the j^{th} column Γ so that

$$\Gamma^+\vec{\gamma}(q_j) = \vec{u}_j \tag{9.144}$$

where $\vec{u}_j$ is a vector of zeros except for element j which is 1.

Thus the j^{th} matrix element $\dot{\Psi}_p(\vec{q}_j)$ along the diagonal of $\dot{\Psi}_p$ consists of the partial derivatives with respect to the elements of $\vec{q}$ of vector function $\vec{\psi}_p(\vec{q})$ at the zero crossing $\vec{q} = \vec{q}_j$. Note that the block diagonal matrix $\dot{\Psi}_p$ generalizes to multi-D the diagonal matrix $\dot{\Psi}$ used in the 1-D small $\delta\omega$ CR bound expressions (8.14)-(8.24) previously developed by Lee [11]; recall that the j^{th} scalar diagonal element $\psi'(q_j)$ of

$\dot{\Psi}$ is the derivative of scalar polynomial $\psi(q)$ at the zero crossing $q = q_j$.

Given the above interpretations, we obtain the following insight on the small $\delta\omega$ behavior of the CR bound. The bound B_C will have a small norm (i.e. be favorable) if

1. the χ^{th} order partial derivatives of the generic arrival vector $\vec{a}(\vec{\omega})$ are well-separated from the vector space spanned by the partial derivatives of lower order (i.e. $\mathcal{E}_\chi$ has large norm), and

2. the scalar functions that make up the vector function $\vec{\psi}_\chi(\vec{q})$ have steep slope at the zero-crossings $\vec{q} = \vec{q}_j$. (i.e. $\dot{\Psi}_\chi(\vec{q}_j)$ has large norm)

9.4.1 CR Bound on Var$(\hat{\omega}_{ij})$

The corresponding bound on the variance of $\hat{\omega}_{ij}$, the estimate of the i^{th} component of the j^{th} source parameter vector $\vec{\omega}_j$, is by definition given by the diagonal entries of B_C. For small $\delta\omega$, we have from (9.131)

$$\text{Var}\{\hat{\omega}_{ij}\} \;\geq\; (B_C)_{ll} \;=\; \frac{1}{N \cdot \text{SNR}_j} \frac{b_{ij}}{\delta\omega^{2(\chi-1)}} + \mathcal{O}(\delta\omega^{-2(\chi-1)+1}) \qquad (9.145)$$

where $l = \mathcal{D}(j-1) + i$ and

$$b_{ij} \;\triangleq\; \frac{1}{2}\left(\left[P_{[\dot{\Psi}^t_{\chi-1}]}\dot{\Psi}^t_\chi \text{Re}\left\{\rho \otimes \mathcal{E}^h_\chi \mathcal{E}_\chi\right\}\dot{\Psi}_\chi P_{[\dot{\Psi}^t_{\chi-1}]}\right]^+\right)_{\mathcal{D}(j-1)+i,\mathcal{D}(j-1)+i} \qquad (9.146)$$

SNR_j denotes the signal-to-noise ratio for the j^{th} source,

$$\text{SNR}_j \;=\; \left(\hat{P}\right)_{jj} \Big/ \sigma^2 \qquad (9.147)$$

and ρ denotes the matrix of (complex) signal correlation coefficients

$$\begin{aligned} \rho &= \hat{P}_D^{-1/2}\hat{P}\hat{P}_D^{-1/2} \\ \hat{P}_D &= \text{diag}\left[(\hat{P})_{11}, (\hat{P})_{22}, \cdots (\hat{P})_{MM}\right] \end{aligned} \qquad (9.148)$$

The result (9.145), (9.146) is quite useful in that it makes explicit tradeoffs among scenario parameters such as frequency separations, signal powers and correlations, and the sampling grid. Specifically these quantities are represented in (9.145), (9.146) as follows

$$\begin{aligned} \text{frequency separations} &\iff \dot{\Psi}_\chi(q_j),\ \dot{\Psi}_{\chi-1}(q_j),\ (\delta\omega)^{-2(\chi-1)} \\ \text{signal powers and correlations} &\iff \rho,\ \mathrm{SNR}_j \\ \text{sampling grid} &\iff \mathcal{E}_\chi \end{aligned}$$

Thus, for example, it is immediately clear from (9.131) for a 2-dimensional scenario with non-degenerate CR bounds, that reducing the frequency separation factor $\delta\omega$ by a factor of 10 in a $M = 3$, $(\chi = 2)$ signal scenario requires that the source powers be increased by $2(\chi - 1) \cdot 10\text{dB} = 20\text{dB}$ for an unbiased estimator to maintain the same frequency standard deviation. Note that the same conditions require a 40dB SNR increase in 1-D scenarios.

9.4.2 CR Bound in Preferred Directions

Expression (9.131) showed that for Case III scenarios the dominant term of B_C for small $\delta\omega$ is $\delta\omega^{-2(\chi-1)}K_{\chi-1}$ with $\chi = m + 1$. Matrix K_m was found in (9.125) to have only partial rank $(= M(\mathcal{D} - \nu))$ for Case III scenarios for which $0 < \nu < \mathcal{D}$. Consequently, in Case III scenarios, there exist coordinate directions for which the coefficient b_{ij} of the $\delta\omega^{-2m}$ term of the variance bound (9.145) vanishes, and for which the small $\delta\omega$ CR bound is more favorable (smaller). This section identifies the preferred directions and the dominant term of the CR bound in those directions.

In order to identify the CR bound in preferred directions, we note from (9.116), (9.117) that

$$Q_{[G_{2m}(\delta\omega)]}B_C Q_{[G_{2m}(\delta\omega)]} = \delta\omega^{-2(m-1)}\frac{\sigma^2}{2N}\left[G_{2m}(\delta\omega)^+ + \mathcal{O}(\delta\omega^2)\right] \qquad (9.149)$$

where projection

$$Q_{[G_{2m}(\delta\omega)]} = G_{2m}(\delta\omega)G_{2m}(\delta\omega)^{+} \tag{9.150}$$

is orthogonal to $W(\delta\omega)$.

Therefore the dominant term of (9.149) for small $\delta\omega$ is identified using (9.119), (9.88) to be

$$\begin{aligned} Q_{[G_{2m}(\delta\omega)]}B_C Q_{[G_{2m}(\delta\omega)]} &= \delta\omega^{-2(m-1)}\frac{\sigma^2}{2N}\left[G_{2m}^{+} + \mathcal{O}(\delta\omega^1)\right] \\ &= \delta\omega^{-2(m-1)}\frac{\sigma^2}{2N}\left[\dot{\Psi}_m^t \mathrm{Re}\left\{\hat{P}^t \otimes \mathcal{E}_m^h \mathcal{E}_m\right\}\dot{\Psi}_m\right]^{+} \\ &\quad + \mathcal{O}(\delta\omega^{-2(m-1)+1}) \end{aligned} \tag{9.151}$$

Furthermore,

$$\begin{aligned} Q_{[G_{2m}(\delta\omega)]} &= G_{2m}\,(G_{2m})^{+} + \mathcal{O}(\delta\omega) \\ &= \dot{\Psi}_m^{+}\dot{\Psi}_m + \mathcal{O}(\delta\omega) \\ &= Q_{[\dot{\Psi}_m^t]} + \mathcal{O}(\delta\omega) \end{aligned} \tag{9.152}$$

where use is made of (9.121). Since $\dot{\Psi}_m$ has block diagonal structure, it follows that the

Preferred Coordinate Directions at the j^{th} source for small $\delta\omega$ are specified by coordinate vectors $\hat{\imath}_p$ that lie in the row space of $\dot{\Psi}_m(\vec{q}_j)$.

The CR bound along preferred coordinate for small $\delta\omega$ is proportional to $\delta\omega^{2(m-1)} = \delta\omega^{2(\chi-2)}$ from (9.149).

A geometric interpretation of preferred coordinate directions in terms of emitter configuration can be derived straightforwardly for 2-D scenarios. The results are

Geometric Interpretation of Preferred Directions in 2-D: For small $\delta\omega$, the preferred directions are normal to the unique $(\chi-1)^{th}$ order polynomial curve specified by the M source locations $\vec{q}_1, \cdots \vec{q}_M$.

Two simple examples of Case III scenarios are

1. $M = 2$ source 2-D scenario for which the preferred direction is normal to line between through the two source locations specified by $\vec{q}_1, \vec{q}_2$.

2. $M = 5$ source 2-D scenario with non-degenerate CR bounds for which the preferred directions are normal to the unique conic section curve specified by the $\vec{q}_1, \cdots \vec{q}_5$.

The latter example is illustrated in the simulation examples in the following section.

The practical effect of preferred directions in Case III is that for these types of multi-D scenarios, the resolution ability of any unbiased DF algorithm is likely to be much more severely challenged in certain spectral directions than in others. In a 2-D example with $M = 5$ sources in a circular configuration, it is likely to be much more difficult to accurately estimate the tangential than the radial spectral parameter of each source. Note that preferred directions do not arise in 1-D scenarios, for which there is only one spectral coordinate.

9.5 CR Bound Examples

To illustrate the accuracy of the foregoing limiting theoretical expressions for directional CR bounds as $\delta\omega \to 0$, we compare the small $\delta\omega$ representations to the exact CR bounds for the 2-D direction finding scenarios of Examples 8.1-8.4.

Each example involves a planar array of $W = 16$ unit-gain, isotropic sensors, and far-field sources clustered near to the array broadside.

We assume that the sources are *correlated* and equal power. The source cross-correlation matrix ρ is taken to be of the form (5.39).

The exact CR bounds computed using (8.28) are compared to the asymptotic values for small $\delta\omega$ predicted by the result (9.131) of our analysis in the following numerical examples.

Example 9.1 : For this example $M = 3$ and the array and source geometries are as follows.

Array: Sensors in a sparse grid per Figure 2-4A,

Sources: Sources SC1, SC2, SC3 clustered around broadside in a triangular configuration per Figure 8-1.

As shown in Example 8.1, this is a Case I scenario with non-degenerate CR bounds. Consequently the directional variance CR bounds for small $\delta\omega$ may be determined using (9.145).

Figure 9-1 shows the values of the CR bounds for parameter estimates along the x and y spectral frequency axes for one of the sources, specifically SC1 in Figure 8-1. The solid curves depict the exact CR bounds; the dashed lines depict the asymptotic behavior predicted by Eq. (9.145). The horizontal scale denotes spatial frequency separation $\delta\omega$ normalized by the array beamwidth BW, so that unity on the horizontal scale of the graph corresponds to maximum source separation of one beamwidth. The vertical scale depicts the value of the normalized bound

$$N \cdot \mathrm{SNR}_1 \cdot (B_C)_{ll} \tag{9.153}$$

where $(B_C)_{ll}$ is as in (9.145).

Clearly the simplified asymptotic expressions capture the essence of the bounds for emitter separation less than one beamwidth. As predicted, the CR bounds exhibit a $\delta\omega^{-2}$ behavior for small $\delta\omega$, with a slope of 20 dB/decade. Thus the theoretical expressions accurately predict the CR bounds for small separations $\delta\omega$ for this Case I scenario with non-degenerate CR bounds.

Example 9.2 : For this example $M = 4$ and the array and source geometries are as follows.

Array: Sensors in a sparse grid per Figure 2-4A,

Sources: Sources SC1, SC2, SC3, SC4 clustered around broadside as in Figure 8-1.

$$\Upsilon' = \begin{bmatrix} 0 \\ P_{[\Gamma_0^h,\cdots,\Gamma_{m-1}^h]} \end{bmatrix} \qquad (M+\mathcal{D}) \times M \tag{J.17}$$

The columns of Υ are by construction linearly independent, and form a rank $\mathcal{D}$ subspace of the nullspace of the columns of $\Gamma_0'(\vec{q}_j)^h$, $\cdots$ $\Gamma_{m-1}'(\vec{q}_j)^h$, since Υ satisfies

$$\begin{aligned} \left[\Gamma_0'(\vec{q}_j)^h, \cdots \Gamma_{m-1}'(\vec{q}_j)^h\right]\Upsilon &= \begin{bmatrix} \dot{\Gamma}_0(\vec{q}_j), & \Gamma_0 \\ \dot{\Gamma}_1(\vec{q}_j), & \Gamma_1 \\ \vdots & \vdots \\ \dot{\Gamma}_{m-1}(\vec{q}_j), & \Gamma_{m-1} \end{bmatrix} \begin{bmatrix} I \\ -\Gamma^{-1}\dot{\Gamma}(\vec{q}_j) \end{bmatrix} \\ &= 0 \end{aligned} \tag{J.18}$$

since the rows of Γ_p, $(p = 0 \cdots m-1)$ are equal to rows of Γ.

The columns of Υ' are by construction linearly independent from those of Υ and also lie in the nullspace of the columns of $\Gamma_0'(\vec{q}_j)^h$, $\cdots$ $\Gamma_{m-1}'(\vec{q}_j)^h$, since Υ' satisfies

$$\begin{aligned} \left[\Gamma_0'(\vec{q}_j)^h, \cdots \Gamma_{m-1}'(\vec{q}_j)^h\right]\Upsilon' &= \begin{bmatrix} \dot{\Gamma}_0(\vec{q}_j), & \Gamma_0 \\ \dot{\Gamma}_1(\vec{q}_j), & \Gamma_1 \\ \vdots & \vdots \\ \dot{\Gamma}_{m-1}(\vec{q}_j), & \Gamma_{m-1} \end{bmatrix} \begin{bmatrix} 0 \\ P_{[\Gamma_0^h,\cdots\Gamma_{m-1}^h]} \end{bmatrix} \\ &= 0 \end{aligned} \tag{J.19}$$

As a consequence of Conditions **C2**, the $\bar{n}_{\{0\cdots m-1\}}$ columns of $\Gamma_0^h, \cdots \Gamma_{m-1}^h$ are linearly independent, and thus

$$\text{Rank}\{\Upsilon'\} = \text{Rank}\left\{P_{[\Gamma_0^h,\cdots\Gamma_{m-1}^h]}\right\} = M - \bar{n}_{\{0\cdots m-1\}} \tag{J.20}$$

Thus the columns of Υ and Υ' together span the rank $M + \mathcal{D} - \bar{n}_{\{0\cdots m-1\}}$ column nullspace of $\Gamma_0'(\vec{q}_j)^h$, $\cdots$ $\Gamma_{m-1}'(\vec{q}_j)^h$, that is

$$P_{[\Gamma_0'(\vec{q}_j)^h,\cdots,\Gamma_{m-1}'(\vec{q}_j)^h]} = [\Upsilon\ ,\ \Upsilon'][\Upsilon\ ,\ \Upsilon']^+ \tag{J.21}$$

$$+ \text{ Rank}\left\{Q_{[P_{[\dot{A}_0,\cdots\dot{A}_{m-1}]}\dot{A}_m T_m]}\Gamma'_m(\vec{q}_j)\, P_{[\Gamma'_0(\vec{q}_j)^h,\cdots,\Gamma'_m(\vec{q}_j)^h]}\right\} \quad \text{(J.12)}$$

since $\text{Rank}\{X+Y\} = \text{Rank}\{X\} + \text{Rank}\{Y\}$ for matrices X, Y with orthogonal column spaces.

Using definition (J.6) of T_m we note that

$$\begin{aligned}
&\text{Rank}\left\{P_{[\dot{A}_0,\cdots\dot{A}_{m-1}]}\dot{A}_m T_m\right\} \\
&\quad = \text{Rank}\left\{P_{[\dot{A}_0,\cdots\dot{A}_{m-1}]}\dot{A}_m\Gamma_m P_{[\Gamma_0^h,\cdots,\Gamma_{m-1}^h]}\left(\Gamma_m P_{[\Gamma_0^h,\cdots,\Gamma_{m-1}^h]}\right)^+\right\} \\
&\quad = \text{Rank}\left\{P_{[\dot{A}_0,\cdots\dot{A}_{m-1}]}\dot{A}_m\Gamma_m P_{[\Gamma_0^h,\cdots,\Gamma_{m-1}^h]}\right\} \\
&\quad = M - \bar{n}_{\{0\cdots m-1\}} \qquad \text{(J.13)}
\end{aligned}$$

since removal of the post-factor Y^+ does not change the rank of the product XYY^+ for any X, Y, and the last equality follows from (J.8). Consequently, the rank of $Q_{[P_{[\dot{A}_0,\cdots\dot{A}_{m-1}]}\dot{A}_m T_m]}$ is $M - \bar{n}_{\{0\cdots m-1\}}$, and the second term in (J.12) is at most $M - \bar{n}_{\{0\cdots m-1\}}$. Rearrangement of (J.12) yields

$$\begin{aligned}
\text{Rank}\left\{\mathcal{E}_m\Gamma'_m(\vec{q}_j)\, P_{[\Gamma'_0(\vec{q}_j)^h,\cdots,\Gamma'_{m-1}(\vec{q}_j)^h]}\right\} &\geq (M + \mathcal{D} - \bar{n}_{\{0\cdots m-1\}}) - (M - \bar{n}_{\{0\cdots m-1\}}) \\
&= \mathcal{D} \qquad \text{(J.14)}
\end{aligned}$$

As a consequence of Condition **CR2**, all the $\bar{n}_{\{0\cdots m-1\}}$ columns of $\Gamma'_0(\vec{q}_j)^h, \cdots, \Gamma'_{m-1}(\vec{q}_j)^h$ are linearly independent, and thus the post-factor projection in (J.14) has rank

$$\text{Rank}\left\{P_{[\Gamma'_0(\vec{q}_j)^h,\cdots,\Gamma'_{m-1}(\vec{q}_j)^h]}\right\} = (M + \mathcal{D}) - \bar{n}_{\{0\cdots m-1\}} \qquad \text{(J.15)}$$

Now consider matrices

$$\Upsilon = \begin{bmatrix} I \\ -\Gamma^{-1}\dot{\Gamma}(\vec{q}_j) \end{bmatrix} \qquad (M + \mathcal{D}) \times \mathcal{D} \qquad \text{(J.16)}$$

Proof: For scenarios with non-degenerate CR bounds, reference to Condition **C3** shows that

$$\text{Rank}\{P_{[\dot{A}_0,\cdots\dot{A}_{m-1}]}\,\dot{A}_m\Gamma_m\,P_{[\Gamma_0^h,\cdots,\Gamma_{m-1}^h]}\} \;=\; M-\bar{n}_{\{0\cdots m-1\}} \tag{J.8}$$

and reference to Condition **CR3** with $\chi = m$ for Case II shows that

$$\text{Rank}\{P_{[\dot{A}_0,\cdots\dot{A}_{m-1}]}\,\dot{A}_m\Gamma'_m(\vec{q}_j)\,P_{[\Gamma'_0(\vec{q}_j)^h,\cdots,\Gamma'_{m-1}(\vec{q}_j)^h]}\} \;=\; M+\mathcal{D}-\bar{n}_{\{0\cdots m-1\}} \tag{J.9}$$

for $j = 1\cdots M$, where

$$\Gamma'_p(\vec{q}_j) \;=\; \left[\dot{\Gamma}_p(\vec{q}_j)\;,\;\Gamma_p\right] \tag{J.10}$$

We now show that (J.1) can be inferred from (J.8) and (J.9). Specifically, we decompose the matrix product in (J.9) into the sum of the matrix product in (J.1), and an orthogonal term of rank $M-\bar{n}_{\{0\cdots m-1\}}$, as follows.

First we rearrange the pre-factor projection matrix in (J.9) to be the sum

$$\begin{aligned}
P_{[\dot{A}_0,\cdots\dot{A}_{m-1}]} &= I-\left[\dot{A}_0,\;\cdots,\;\dot{A}_{m-1},\right]\left[\dot{A}_0,\;\cdots,\;\dot{A}_{m-1},\right]^+ \\
&\quad -\left[P_{[\dot{A}_0,\cdots\dot{A}_{m-1}]}\dot{A}_mT_m\right]\left[P_{[\dot{A}_0,\cdots\dot{A}_{m-1}]}\dot{A}_mT_m\right]^+ \\
&\quad +\left[P_{[\dot{A}_0,\cdots\dot{A}_{m-1}]}\dot{A}_mT_m\right]\left[P_{[\dot{A}_0,\cdots\dot{A}_{m-1}]}\dot{A}_mT_m\right]^+ \\
&= I-\left[\dot{A}_0,\;\cdots,\;\dot{A}_{m-1},\;\dot{A}_mT_m\right]\left[\dot{A}_0,\;\cdots,\;\dot{A}_{m-1},\;\dot{A}_mT_m\right]^+ \\
&\quad +\left[P_{[\dot{A}_0,\cdots\dot{A}_{m-1}]}\dot{A}_mT_m\right]\left[P_{[\dot{A}_0,\cdots\dot{A}_{m-1}]}\dot{A}_mT_m\right]^+ \\
&= \left[I-\bar{A}\bar{A}^+\right]+Q_{[P_{[\dot{A}_0,\cdots\dot{A}_{m-1}]}\dot{A}_mT_m]}
\end{aligned} \tag{J.11}$$

where $Q_{[P_{[\dot{A}_0,\cdots\dot{A}_{m-1}]}\dot{A}_mT_m]}$ is the projection onto the column space of $P_{[\dot{A}_0,\cdots\dot{A}_{m-1}]}\dot{A}_mT_m$. The two terms in (J.11) have orthogonal column spaces, since the columns of matrix $P_{[\dot{A}_0,\cdots\dot{A}_{m-1}]}\dot{A}_mT_m$ are contained in the space spanned by the columns of $\bar{A}$.

Substitution of (J.11) in (J.9), and use of (J.2) gives

$$M+\mathcal{D}-\bar{n}_{\{0\cdots m-1\}} \;=\; \text{Rank}\left\{\mathcal{E}_m\Gamma'_m(\vec{q}_j)\,P_{[\Gamma'_0(\vec{q}_j)^h,\cdots,\Gamma'_m(\vec{q}_j)^h]}\right\}$$

Appendix J

Proof of Lemma 9.2

This appendix establishes the result:

Lemma 9.2: In Case II with $\nu \geq \mathcal{D}$, if Conditions **C1-C3** and **CR1-CR3** are satisfied, then

$$\text{Rank}\left\{\mathcal{E}_m \dot{\Psi}_m(\vec{q}_j)\right\} = \mathcal{D} \tag{J.1}$$

for $j = 1 \cdots M$, where

$$\mathcal{E}_m = \left[I - \bar{A}\bar{A}^+\right] \dot{A}_m \tag{J.2}$$

$$\bar{A} = \left[\dot{A}_0, \cdots, \dot{A}_{m-1}, \dot{A}_m T_m\right] \tag{J.3}$$

$$\dot{\Psi}_m(\vec{q}_j) = \left[\dot{\Gamma}_m(\vec{q}_j)\ ,\ \Gamma_m\right] \begin{bmatrix} I \\ -\Gamma^{-1}\dot{\Gamma}(\vec{q}_j) \end{bmatrix} \tag{J.4}$$

$$\Gamma = \begin{bmatrix} \Gamma_0 \\ \vdots \\ \Gamma_{m-1} \\ T_m\Gamma_m \end{bmatrix} \bar{n}_{\{0,\cdots m\}} \times M, \qquad \dot{\Gamma}(\vec{q}) = \begin{bmatrix} \dot{\Gamma}_0(\vec{q}) \\ \vdots \\ \dot{\Gamma}_{m-1}(\vec{q}) \\ T_m\dot{\Gamma}_m(\vec{q}) \end{bmatrix} \bar{n}_{\{0,\cdots m\}} \times \mathcal{D} \tag{J.5}$$

$$T_m = \Gamma_m P_{[\Gamma_0^h,\cdots,\Gamma_{m-1}^h]} \left(\Gamma_m P_{[\Gamma_0^h,\cdots,\Gamma_{m-1}^h]}\right)^+ \tag{J.6}$$

$$\nu = \bar{n}_{\{0,\cdots m\}} - M \geq \mathcal{D} \tag{J.7}$$

where the last equality follows from (I.7).

Now consider matrix

$$\Upsilon = \begin{bmatrix} I \\ -\Gamma^{-1}\dot{\Gamma}(\vec{q}_j) \end{bmatrix} \qquad (M+\mathcal{D}) \times \mathcal{D} \qquad \text{(I.15)}$$

with $\mathcal{D}$ linearly independent columns and the property

$$\left[\dot{\Gamma}(\vec{q}_j),\ \Gamma\right] \Upsilon = \left[\dot{\Gamma}(\vec{q}_j),\ \Gamma\right] \begin{bmatrix} I \\ -\Gamma^{-1}\dot{\Gamma}(\vec{q}_j) \end{bmatrix} = 0 \qquad \text{(I.16)}$$

Hence the columns of Υ form a complete spanning set for the rank $\mathcal{D}$ nullspace of the columns of (I.12). Thus we express nullspace projection (I.13) as

$$P_{[\Gamma'_0(\vec{q}_j)^h, \cdots, \Gamma'_m(\vec{q}_j)^h]} = \Upsilon\Upsilon^+ \qquad \text{(I.17)}$$

Substitution of (I.17) into (I.11) gives

$$\begin{aligned} \mathcal{D} &= \text{Rank}\{\mathcal{E}_{m+1}\, \Gamma'_{m+1}(\vec{q}_j)\, \Upsilon\Upsilon^+\} \\ &= \text{Rank}\{\mathcal{E}_{m+1}\, \Gamma'_{m+1}(\vec{q}_j)\, \Upsilon\} \end{aligned} \qquad \text{(I.18)}$$

since removal of the post-factor Y^+ does not change the rank of the product XYY^+ for any X, Y. From (I.4), (I.9) and (I.15) we note that

$$\dot{\Psi}_{m+1}(\vec{q}_j) = \Gamma'_{m+1}(\vec{q}_j)\, \Upsilon \qquad \text{(I.19)}$$

Assertion (I.1) of the lemma is established by substitution of (I.19) in (I.18).

Proof: For scenarios with non-degenerate CR bounds, reference to Condition **CR3** with $\chi = m+1$ in Case I shows that

$$\begin{aligned} \text{Rank}\left\{P_{[\dot{A}_0,\cdots\dot{A}_m]}\,\dot{A}_{m+1}\Gamma'_{m+1}(\vec{q}_j)\,P_{[\Gamma'_0(\vec{q}_j)^h,\cdots,\Gamma'_m(\vec{q}_j)^h]}\right\} &= M+\mathcal{D}-\bar{n}_{\{0,\cdots m\}} \\ &= \mathcal{D} \end{aligned} \tag{I.8}$$

for all $j = 1\cdots M$, where the last equality follows from (I.7), and

$$\Gamma'_p(\vec{q}_j) \;=\; \left[\dot{\Gamma}_p(\vec{q}_j)\;,\;\Gamma_p\right] \tag{I.9}$$

We now show that (I.1) follows directly from (I.8). From (I.3) we note that

$$P_{[\dot{A}_0,\cdots\dot{A}_m]} \;=\; I - \dot{A}\dot{A}^+ \tag{I.10}$$

Substitution in (I.8), and use of (I.2) gives

$$\text{Rank}\left\{\mathcal{E}_{m+1}\Gamma'_{m+1}(\vec{q}_j)\,P_{[\Gamma'_0(\vec{q}_j)^h,\cdots,\Gamma'_m(\vec{q}_j)^h]}\right\} \;=\; \mathcal{D} \tag{I.11}$$

From (I.5), (I.6) and (I.9) we note that

$$\left[\Gamma'_0(\vec{q}_j)^h,\cdots,\Gamma'_m(\vec{q}_j)^h\right] = \left[\dot{\Gamma}(\vec{q}_j)\;,\;\Gamma\right]^h \qquad\qquad (M+\mathcal{D})\times\bar{n}_{\{0\cdots m\}} \tag{I.12}$$

Thus the post-factor in (I.11) can be expressed as

$$P_{[\Gamma'_0(\vec{q}_j)^h,\cdots,\Gamma'_m(\vec{q}_j)^h]} \;=\; I - \left[\dot{\Gamma}(\vec{q}_j),\;\Gamma\right]^+\left[\dot{\Gamma}(\vec{q}_j),\;\Gamma\right] \qquad (M+\mathcal{D})\times(M+\mathcal{D}) \tag{I.13}$$

As a consequence of Condition **CR2**, the $\bar{n}_{\{0\cdots m\}}$ columns of (I.12) are linearly independent, and thus the projection (I.13) onto the nullspace of the columns of (I.12) has rank

$$\text{Rank}\{P_{[\Gamma'_0(\vec{q}_j)^h,\cdots,\Gamma'_m(\vec{q}_j)^h]}\} \;=\; (M+\mathcal{D})-\bar{n}_{\{0\cdots m\}} \;=\; \mathcal{D} \tag{I.14}$$

Appendix I

Proof of Lemma 9.1

This appendix establishes the result:

Lemma 9.1: In Case I with $\nu = 0$, if Conditions **C1-C3** and **CR1-CR3** are satisfied, then

$$\text{Rank}\left\{\mathcal{E}_{m+1}\dot{\Psi}_{m+1}(\vec{q}_j)\right\} \;=\; \mathcal{D} \tag{I.1}$$

for $j = 1 \cdots M$, where

$$\mathcal{E}_{m+1} \;=\; \left[I - \dot{A}\dot{A}^{+}\right]\dot{A}_{m+1} \tag{I.2}$$

$$\dot{A} \;=\; \left[\dot{A}_0,\ \cdots,\ \dot{A}_{m-1},\ \dot{A}_m\right] \tag{I.3}$$

$$\dot{\Psi}_{m+1}(\vec{q}_j) \;=\; \left[\dot{\Gamma}_{m+1}(\vec{q}_j)\ ,\ \Gamma_{m+1}\right]\begin{bmatrix} I \\ -\Gamma^{-1}\dot{\Gamma}(\vec{q}_j) \end{bmatrix} \tag{I.4}$$

$$\Gamma \;=\; \begin{bmatrix} \Gamma_0 \\ \vdots \\ \Gamma_{m-1} \\ T_m\Gamma_m \end{bmatrix} \bar{n}_{\{0,\cdots m\}} \times M, \qquad \dot{\Gamma}(\vec{q}) \;=\; \begin{bmatrix} \dot{\Gamma}_0(\vec{q}) \\ \vdots \\ \dot{\Gamma}_{m-1}(\vec{q}) \\ T_m\dot{\Gamma}_m(\vec{q}) \end{bmatrix} \bar{n}_{\{0,\cdots m\}} \times \mathcal{D} \tag{I.5}$$

$$T_m \;=\; I \tag{I.6}$$

$$\nu \;=\; \bar{n}_{\{0,\cdots m\}} - M \;=\; 0 \tag{I.7}$$

for $p = 0 \cdots m-1$. Pre-multiplication by $\dot{A}_p$ of the matrices in (H.8) does not affect the equality, and hence we have

$$\text{Rank}\{\dot{A}_p \Gamma_p \Pi P_{[B^h_{0,0},\cdots,B^h_{0,p-1}]}\} = \text{Rank}\{\dot{A}_p \Gamma_p \Pi\} \tag{H.9}$$

or equivalently

$$\text{Rank}\{B_{0,p} P_{[B^h_{0,0},\cdots,B^h_{0,p-1}]}\} = \text{Rank}\{B_{0,p}\} \tag{H.10}$$

for $p = 0 \cdots m-1$. Expression (H.10) corresponds to the definition (4.10) of Condition II but over the range of Taylor series terms $p = 0, \cdots m-1$.

To make expression (H.10) equivalent to the definition (4.10) of Condition II, we need to show that $\tilde{m} = m$. We recall that $\tilde{m}$ is defined as the minimum number such that a partial sum of $p = 0 \cdots m$ Taylor series terms of $B_0(\epsilon)$ has rank equal to that of $B_0(\epsilon)$. Similarly, m is defined as the minimum number such that a partial sum of $p = 0 \cdots \tilde{m}$ Taylor series terms of matrix A has full rank. Under identifications (7.4), we have $B_0(\epsilon) = A\Pi$, where Π is a square full rank matrix which does not affect the rank or linear dependence properties of the Taylor series terms, and thus it must be that $\tilde{m} = m$. To complete Assertion b) we note that

$$\tilde{m} = m_{\dot{A}} \tag{H.11}$$

since $m = m_{\dot{A}}$ under Condition **C2**.

The proof of Assertion a) is analogous.

First we establish Assertion b) as follows. By construction Γ_p has $\bar{n}_p$ rows, and hence Condition **C2** implies that Γ_p has full row rank for $p = 0 \cdots m-1$. Therefore

$$\text{Rank}\{\Gamma_p P_{[\Gamma_0^h, \cdots \Gamma_{p-1}^h]}\} \;=\; \text{Rank}\{\Gamma_p\} \qquad \text{for } p = 1 \cdots m-1 \qquad \text{(H.3)}$$

which in turn implies that the rows of Γ_p are linearly independent of the rows of $\Gamma_0 \cdots \Gamma_{p-1}$. Since Π is a square full rank matrix, it follows that the rows of $\Gamma_p\Pi$ are also linearly independent of the rows of $(\Gamma_0\Pi) \cdots (\Gamma_{p-1}\Pi)$. That is

$$\text{Rank}\{\Gamma_p\Pi P_{[(\Gamma_0\Pi)^h, \cdots (\Gamma_{p-1}\Pi)^h]}\} \;=\; \text{Rank}\{\Gamma_p\Pi\} \qquad \text{for } p = 1 \cdots m-1 \quad \text{(H.4)}$$

We note that

$$Q_{[(\Gamma_0\Pi)^h, \cdots (\Gamma_{p-1}\Pi)^h]} \;\geq\; Q_{[(\dot{A}_0\Gamma_0\Pi)^h, \cdots (\dot{A}_{p-1}\Gamma_{p-1}\Pi)^h]} \;=\; Q_{[B_{0,0}^h, \cdots, B_{0,p-1}^h]} \qquad \text{(H.5)}$$

where $B_{0,p}$ is of the form (7.4), since pre-multiplication by $\dot{A}_p$ can only reduce the row space of $\Gamma_p\Pi$. Therefore

$$P_{[(\Gamma_0\Pi)^h, \cdots (\Gamma_{p-1}\Pi)^h]} \;\leq\; P_{[B_{0,0}^h, \cdots, B_{0,p-1}^h]} \qquad \text{(H.6)}$$

Substitution of (H.6) in (H.4) gives

$$\text{Rank}\{\Gamma_p\Pi P_{[B_{0,0}^h, \cdots, B_{0,p-1}^h]}\} \;\geq\; \text{Rank}\{\Gamma_p\Pi P_{[(\Gamma_0\Pi)^h, \cdots (\Gamma_{p-1}\Pi)^h]}\} \;=\; \text{Rank}\{\Gamma_p\Pi\} \quad \text{(H.7)}$$

for $p = 0 \cdots m-1$, which must be satisfied with equality since the rank of a product is at most the rank of any of its factors. Therefore

$$\text{Rank}\{\Gamma_p\Pi P_{[B_{0,0}^h, \cdots, B_{0,p-1}^h]}\} \;=\; \text{Rank}\{\Gamma_p\Pi\} \qquad \text{(H.8)}$$

Appendix H

Proof of Lemma 7.1

This appendix shows that if B and $B_0(\epsilon)$ have Taylor series as in (7.2) and (7.3), and given identifications (7.4), then

a) if Conditions **C1** and $\mathbf{C3}_\Gamma$ are satisfied with $m = m_\Gamma$, then so are Conditions I and IIIr with $\tilde{m} = m_\Gamma$,

b) if Conditions **C2** and $\mathbf{C3}_{\dot{A}}$ are satisfied with $m = m_{\dot{A}}$, then so are Conditions II and IIIc with $\tilde{m} = m_{\dot{A}}$.

where m_Γ and $m_{\dot{A}}$ are respectively defined by relations (7.7) and (7.8).

By definition in Section 2.5.3, Conditions **C1**, **C2** state that

$$\begin{aligned}
\textbf{C1.} \qquad \text{Rank}\{\dot{A}_0\} &= \bar{n}_0 && \text{for } p = 0 \\
\text{Rank}\{P_{[\dot{A}_0,\cdots\dot{A}_{p-1}]}\,\dot{A}_p\} &= \bar{n}_p && \text{for } p = 1,\cdots m-1 \qquad \text{(H.1)} \\
\textbf{C2.} \qquad \text{Rank}\{\Gamma_0\} &= \bar{n}_0 && \text{for } p = 0 \\
\text{Rank}\{\Gamma_p\,P_{[\Gamma_0,\cdots,\Gamma_{p-1}]}\} &= \bar{n}_p && \text{for } p = 1,\cdots m-1 \qquad \text{(H.2)}
\end{aligned}$$

where $m = m_\Gamma$ as defined by (7.7) if Condition **C1** is satisfied, and $m = m_{\dot{A}}$ as defined by (7.8) if Condition **C2** is satisfied.

Using (G.25) in (G.24), we find that it must be that

$$\text{Rank}\left\{P_{[\dot{A}_0,\cdots,\dot{A}_{m-1}]}\dot{A}_m\Gamma_m\Pi P_{[(\Gamma_0\Pi)^h,\cdots,(\Gamma_{m-1}\Pi)^h]}\right\}$$
$$= \text{Rank}\left\{P_{[\dot{A}_0,\cdots,\dot{A}_{m-1}]}\dot{A}_m\Gamma_m P_{[\Gamma_0^h,\cdots\Gamma_{m-1}^h]}\right\} \quad \text{(G.26)}$$

It follows from (G.23), (G.26) and Condition **C3** that

$$\text{Rank}\{P_{[C_{m-1}]}B_{0,m}P_{[R_{m-1}]}\} = M - \sum_{p=0}^{m-1}\bar{n}_p \quad \text{(G.27)}$$

which establishes Assertion (G.7) of the lemma.

$$= P_{[\dot{A}_0,\cdots\dot{A}_p]} \tag{G.22}$$

for $p = 0 \cdots m-1$, which proves Assertion (G.5) of the lemma.

To prove Assertion (G.7), we use (G.1), (G.21), (G.22), to obtain

$$\text{Rank}\{P_{[C_{m-1}]}B_{0,m}P_{[R_{m-1}]}\} = \text{Rank}\{P_{[\dot{A}_0,\cdots,\dot{A}_{m-1}]}\dot{A}_m\Gamma_m\Pi P_{[(\Gamma_0\Pi)^h,\cdots,(\Gamma_{m-1}\Pi)^h]}\} \tag{G.23}$$

We then consider the identity

$$\begin{aligned}
\text{Rank}\left\{\left[\begin{array}{c} \Gamma_0\Pi \\ \vdots \\ \Gamma_{m-1}\Pi \\ P_{[\dot{A}_0,\cdots,\dot{A}_{m-1}]}\dot{A}_m\Gamma_m\Pi P_{[(\Gamma_0\Pi)^h,\cdots,(\Gamma_{m-1}\Pi)^h]} \end{array}\right]\right\} &= \text{Rank}\left\{\left[\begin{array}{c} \Gamma_0\Pi \\ \vdots \\ \Gamma_{m-1}\Pi \\ P_{[\dot{A}_0,\cdots,\dot{A}_{m-1}]}\dot{A}_m\Gamma_m\Pi \end{array}\right]\right\} \\
&= \text{Rank}\left\{\left[\begin{array}{c} \Gamma_0 \\ \vdots \\ \Gamma_{m-1} \\ P_{[\dot{A}_0,\cdots,\dot{A}_{m-1}]}\dot{A}_m\Gamma_m \end{array}\right]\right\} \\
&= \text{Rank}\left\{\left[\begin{array}{c} \Gamma_0 \\ \vdots \\ \Gamma_{m-1} \\ P_{[\dot{A}_0,\cdots,\dot{A}_{m-1}]}\dot{A}_m\Gamma_m P_{[\Gamma_0^h,\cdots\Gamma_{m-1}^h]} \end{array}\right]\right\}
\end{aligned} \tag{G.24}$$

where use is made of property (G.8). Also from property (G.8), we have

$$\text{Rank}\left\{\left[\begin{array}{c} \Gamma_0\Pi \\ \vdots \\ \Gamma_{m-1}\Pi \end{array}\right]\right\} = \text{Rank}\left\{\left[\begin{array}{c} \Gamma_0 \\ \vdots \\ \Gamma_{m-1} \end{array}\right]\right\} \tag{G.25}$$

$$\cdot \text{ Block Diag.} \left\{ (\dot{A}_0^h)^+, \cdots (\dot{A}_p^h)^+ \right\} \Big\}$$

$$= \text{ Rank} \left\{ [(\Gamma_0 \Pi)^h, \cdots, (\Gamma_p \Pi)^h] \right\} \tag{G.18}$$

for $p = 0 \cdots m-1$. Similarly if Condition **C2** is satisfied, then using (G.16), (G.8), and (G.12) we obtain

$$\begin{aligned} \text{Rank} \{C_p\} &= \text{Rank} \Big\{ [\dot{A}_0, \cdots \dot{A}_p] \\ &\qquad \cdot \text{ Block Diag.} \{(\Gamma_0 \Pi), \cdots, (\Gamma_p \Pi)\} \} \\ &= \text{Rank} \Big\{ [\dot{A}_0, \cdots \dot{A}_p] \\ &\qquad \cdot \text{ Block Diag.} \{(\Gamma_0 \Pi), \cdots, (\Gamma_p \Pi)\} \\ &\qquad \cdot \text{ Block Diag.} \left\{ (\Gamma_0 \Pi)^+, \cdots, (\Gamma_p \Pi)^+ \right\} \Big\} \\ &= \text{Rank} \left\{ [\dot{A}_0, \cdots \dot{A}_p] \right\} \end{aligned} \tag{G.19}$$

for $p = 0 \cdots m-1$.

Eqs (G.18) and (G.19) enable us to prove Assertions (G.3), (G.5) and (G.7) as follows. By definition,

$$P_{[Z]} = I - ZZ^+ \tag{G.20}$$

Thus we apply property (G.9) with (G.17) and (G.18) to obtain

$$\begin{aligned} P_{[R_p]} &= I - [B_{0,0}^h, \cdots B_{0,p}^h][B_{0,0}^h, \cdots B_{0,p}^h]^+ \\ &= I - [(\Gamma_0 \Pi)^h, \cdots, (\Gamma_p \Pi)^h][(\Gamma_0 \Pi)^h, \cdots, (\Gamma_p \Pi)^h]^+ \\ &= P_{[(\Gamma_0 \Pi)^h, \cdots, (\Gamma_p \Pi)^h]} \end{aligned} \tag{G.21}$$

for $p = 0 \cdots m-1$, which proves Assertion (G.3) of the lemma.

Similarly, we apply property (G.9) with (G.16) and (G.19) to obtain

$$\begin{aligned} P_{[C_p]} &= I - [B_{0,0}, \cdots B_{0,p}][B_{0,0}, \cdots B_{0,p}]^+ \\ &= I - [\dot{A}_0, \cdots \dot{A}_p][\dot{A}_0, \cdots \dot{A}_p]^+ \end{aligned}$$

for $p = 0 \cdots m-1$.

To prove Assertion (G.4), we use (G.1), (G.8), (G.10) and (G.12) to obtain

$$\begin{aligned} \text{Rank}\{B_{0,p}\} &= \text{Rank}\{\dot{A}_p \Gamma_p \Pi\} \\ &= \text{Rank}\{\dot{A}_p \Gamma_p \Pi \Pi^+\} \\ &= \text{Rank}\{\dot{A}_p \Gamma_p\} \\ &= \text{Rank}\{\dot{A}_p \Gamma_p \Gamma_p^+\} \\ &= \text{Rank}\{\dot{A}_p\} \end{aligned} \tag{G.14}$$

for $p = 0 \cdots m-1$.

To prove Assertion (G.6), we use (G.8) and (G.11) in (G.14) to obtain

$$\begin{aligned} \text{Rank}\{B_{0,p}\} &= \text{Rank}\{\dot{A}_p\} \\ &= \text{Rank}\{\dot{A}_p^+ \dot{A}_p\} \\ &= \text{Rank}\{I_{\bar{n}_p \times \bar{n}_p}\} \\ &= \bar{n}_p \end{aligned} \tag{G.15}$$

for $p = 0 \cdots m-1$.

To show the remaining assertions, we use the identification (G.1) to express

$$C_p = [B_{0,0}, \cdots B_{0,p}] = [\dot{A}_0, \cdots \dot{A}_p] \text{ Block Diag.} \{(\Gamma_0 \Pi), \cdots, (\Gamma_p \Pi)\} \tag{G.16}$$

$$R_p = [B_{0,0}^h, \cdots B_{0,p}^h] = [(\Gamma_0 \Pi)^h, \cdots, (\Gamma_p \Pi)^h] \text{ Block Diag.} \left\{\dot{A}_0^h, \cdots \dot{A}_p^h\right\} \tag{G.17}$$

If Condition **C1** is satisfied, then using (G.17), (G.8), and (G.11) we obtain

$$\begin{aligned} \text{Rank}\{R_p\} &= \text{Rank}\left\{[(\Gamma_0 \Pi)^h, \cdots, (\Gamma_p \Pi)^h] \right. \\ &\qquad \left. \cdot \text{ Block Diag.} \left\{\dot{A}_0^h, \cdots \dot{A}_p^h\right\}\right\} \\ &= \text{Rank}\left\{[(\Gamma_0 \Pi)^h, \cdots, (\Gamma_p \Pi)^h] \right. \\ &\qquad \left. \cdot \text{ Block Diag.} \left\{\dot{A}_0^h, \cdots \dot{A}_p^h\right\}\right. \end{aligned}$$

and

$$\text{Rank}\{P_{[C_{m-1}]}B_{0,m}P_{[R_{m-1}]}\} \;=\; M - \sum_{p=0}^{m-1} \bar{n}_p \tag{G.7}$$

The proof makes use of the following well-known pseudo-inverse properties [21]

$$\text{Rank}\{XY\} \;=\; \text{Rank}\{X^+XY\} \;=\; \text{Rank}\{XYY^+\} \tag{G.8}$$

and

$$XY(XY)^+ \;=\; XX^+ \qquad \text{if} \qquad \text{Rank}\{XY\} \;=\; \text{Rank}\{X\} \tag{G.9}$$

applicable to any suitably sized matrices X, Y.

Since matrix Π is square full rank by construction,

$$\Pi\Pi^+ \;=\; I \tag{G.10}$$

If **C1** is satisfied, then $\dot{A}_p$ has full column rank, and therefore

$$\dot{A}_p^+\dot{A}_p \;=\; I_{\bar{n}_p\times\bar{n}_p} \tag{G.11}$$

for $p = 0\cdots m-1$. If **C2** is satisfied, then Γ_p has full row rank, and therefore

$$\Gamma_p\Gamma_p^+ \;=\; I_{\bar{n}_p\times\bar{n}_p} \tag{G.12}$$

for $p = 0\cdots m-1$.

To prove Assertion (G.2), we use (G.1), (G.8), (G.10) and (G.11) to obtain

$$\begin{aligned}\text{Rank}\{B_{0,p}\} &= \text{Rank}\{\dot{A}_p\Gamma_p\Pi\}\\ &= \text{Rank}\{\dot{A}_p^+\dot{A}_p\Gamma_p\Pi\Pi^+\}\\ &= \text{Rank}\{\Gamma_p\}\end{aligned} \tag{G.13}$$

Appendix G

Proof of Lemma 5.1

This appendix shows that for $B_{0,p}$ defined as

$$B_{0,p} = \dot{A}_p \Gamma_p \Pi \tag{G.1}$$

we have the following results

a) If Condition **C1** is satisfied, then

$$\text{Rank}\{B_{0,p}\} = \text{Rank}\{\Gamma_p\} \qquad \text{for } p = 0 \cdots m-1 \tag{G.2}$$

and

$$P_{[R_p]} = P_{[(\Gamma_0\Pi)^h, \cdots (\Gamma_p\Pi)^h]} \qquad \text{for } p = 0 \cdots m-1 \tag{G.3}$$

b) If Condition **C2** is satisfied, then

$$\text{Rank}\{B_{0,p}\} = \text{Rank}\{\dot{A}_p\} \qquad \text{for } p = 0 \cdots m-1 \tag{G.4}$$

and

$$P_{[C_p]} = P_{[\dot{A}_0, \cdots \dot{A}_p]} \qquad \text{for } p = 0 \cdots m-1 \tag{G.5}$$

c) If all Conditions **C1**, **C2** and **C3** are satisfied, then

$$\text{Rank}\{B_{0,p}\} = \bar{n}_p \qquad \text{for } p = 0 \cdots m-1 \tag{G.6}$$

Matrices $\tilde{B}_j(\epsilon), j = 0, 1 \cdots$, have Taylor series by Lemma 4.3; by definition (4.24), $B_{j,0}$ is the constant term of Taylor series of $\tilde{B}_j(\epsilon)$. Therefore, the row nullspace projection $P_{[\tilde{B}_0(\epsilon)^h, \cdots \tilde{B}_{i-1}(\epsilon)^h]}$ also has Taylor series of the form

$$P_{[\tilde{B}_0(\epsilon)^h, \cdots \tilde{B}_{i-1}(\epsilon)^h]} = P_{[B_{0,0}^h, \cdots B_{i-1,0}^h]} + \sum_{j \geq 1} \epsilon^j W_j \tag{F.5}$$

where the constant term $P_{[B_{0,0}^h, \cdots B_{i-1,0}^h]}$ is the projection onto the row nullspace of $B_{0,0}, \cdots B_{i-1,0}$, and W_j denotes the constant matrix coefficient of the j^{th} order term.

For small ϵ, we identify the dominant term of (F.4) as follows:

$$\begin{aligned} B_0(\epsilon) P_{[\tilde{B}_0(\epsilon)^h, \cdots \tilde{B}_{i-1}(\epsilon)^h]} &= \epsilon^i \tilde{B}_i(\epsilon) + \mathcal{O}(\epsilon^{i+1}) \\ &= \epsilon^i B_{i,0} + \mathcal{O}(\epsilon^{i+1}) \end{aligned} \tag{F.6}$$

Therefore we can express $B_{i,0}$ as

$$B_{i,0} = \lim_{\epsilon \to 0} \frac{1}{\epsilon^i} \beta_i(\epsilon) \tag{F.7}$$

where

$$\beta_i(\epsilon) \triangleq B_0(\epsilon) P_{[\tilde{B}_0(\epsilon)^h, \cdots \tilde{B}_{i-1}(\epsilon)^h]} \tag{F.8}$$

Matrix $\beta_i(\epsilon)$ has a Taylor series since the factor matrices $B_0(\epsilon)$ and $P_{[\tilde{B}_0(\epsilon)^h, \cdots \tilde{B}_{i-1}(\epsilon)^h]}$ have Taylor series. To produce the constant result for $B_{i,0}$ demanded by Lemma 4.3, non-withstanding the division by ϵ^i in (F.7), all Taylor series terms of $\beta_i(\epsilon)$ of order ϵ^j, for $j < i$, must equal zero. Additionally, $B_{i,0}$ must be equal the order ϵ^i term of $\beta_i(\epsilon)$, which is the sum of products of order ϵ^j, $j = 0 \cdots i$ terms of Taylor series of $B_0(\epsilon)$ and of order ϵ^{i-j} terms of Taylor series of $P_{[\tilde{B}_0(\epsilon)^h, \cdots \tilde{B}_{i-1}(\epsilon)^h]}$. That is

$$B_{i,0} = B_{0,i} P_{[B_{0,0}^h, \cdots B_{i-1,0}^h]} + \sum_{j=0}^{i-1} B_{0,j} W_{i-j} \tag{F.9}$$

Assertion (F.1) of the lemma follows from (F.9), with $X_j = W_{i-j}$. Assertion (F.2) follows from a parallel argument involving pre-multiplication of $B_0(\epsilon)$ by $P_{[\tilde{B}_0(\epsilon), \cdots \tilde{B}_{i-1}(\epsilon)]}$.

Appendix F

Proof of Lemma E.1

This appendix establishes the following result:

Lemma E.1: If $B_0(\epsilon)$ has Taylor series in ϵ, then the limiting singular matrix $B_{i,0}$ of $B_0(\epsilon)$ satisfies the relationships

$$B_{i,0} = B_{0,i}P_{[B_{0,0}^h,\cdots B_{i-1,0}^h]} + \sum_{j=0}^{i-1} B_{0,j}X_j \tag{F.1}$$

and

$$B_{i,0} = P_{[B_{0,0},\cdots B_{i-1,0}]}B_{0,k} + \sum_{j=0}^{i-1} Y_j B_{0,j} \tag{F.2}$$

for any $i = 1, 2, \cdots$, where X_j and Y_j are appropriate square matrices.

We begin with the proof of Assertion (F.1) of the lemma. Recall from (4.22) that

$$B_0(\epsilon) = \sum_{i\geq 0} \epsilon^k \tilde{B}_i(\epsilon) \tag{F.3}$$

where the row (and column) spaces of $\tilde{B}_i(\epsilon)$, $\tilde{B}_j(\epsilon)$ are orthogonal for $i \neq j$. Using the row space orthogonality, we write

$$B_0(\epsilon)P_{[\tilde{B}_0(\epsilon)^h,\cdots\tilde{B}_{i-1}(\epsilon)^h]} = \sum_{j\geq i} \epsilon^j \tilde{B}_j(\epsilon) \tag{F.4}$$

where $P_{[\tilde{B}_0(\epsilon)^h,\cdots\tilde{B}_{i-1}(\epsilon)^h]}$ denotes projection onto the row nullspace of $\tilde{B}_0(\epsilon), \cdots \tilde{B}_{i-1}(\epsilon)$.

where Z_i are appropriate matrices. It follows from (E.13) and result (E.2) of Lemma E.1 for $i = 1, \cdots k-1$ that the column space of F_{k-1} is contained within that of $B_{0,0}, B_{0,1}, \cdots, B_{0,k-1}$. Pre-multiplication of (E.13) by $P_{[B_{0,0},\cdots B_{k-1,0}]}$ shows that

$$\begin{aligned} P_{[B_{0,0},\cdots B_{k-1,0}]}F_{k-1} &= P_{[B_{0,0},\cdots B_{k-1,0}]}[P_{[B_{0,0},\cdots B_{k-1,0}]}(\sum_{j=0}^{k-1} B_{0,j}X_j)] \\ &= F_{k-1} \end{aligned} \tag{E.14}$$

since $P_{[B_{0,0},\cdots B_{k-1,0}]}$ is idempotent. Therefore the columns of F_{k-1} are in the nullspace of $B_{0,0}$, and the column space of F_{k-1} satisfies the stricter condition

a) the column space of F_{k-1} is contained in that of Taylor series matrix coefficient sequence $B_{0,1}, \cdots B_{0,k-1}$.

Similarly we find that from (E.12) and (E.11) that

$$F_{k-1} = (\sum_{j=0}^{k-1} Y_j B_{0,j}) P_{[B^h_{0,0},\cdots B^h_{k-1,0}]} \tag{E.15}$$

and

$$\begin{aligned} F_{k-1}P_{[B^h_{0,0},\cdots B^h_{k-1,0}]} &= [(\sum_{j=0}^{k-1} Y_j B_{0,j}) P_{[B^h_{0,0},\cdots B^h_{k-1,0}]}]P_{[B^h_{0,0},\cdots B^h_{k-1,0}]} \\ &= F_{k-1} \end{aligned} \tag{E.16}$$

It follows from (E.15), result (E.3) of Lemma E.1 for $i = 1, \cdots k-1$ and finally from (E.16) that

b) the row space of F_{k-1} is contained in that of Taylor series matrix coefficient sequence $B_{0,1}, \cdots B_{0,k-1}$.

To this point we have established (E.12), and that F_{k-1} has properties **a)** and **b)** of Lemma 4.4. To complete proof of (E.1), we observe from (E.14) and (E.16) that

$$P_{[B_{0,0},\cdots B_{k-1,0}]}F_{k-1}P_{[B^h_{0,0},\cdots B^h_{k-1,0}]} = F_{k-1} \tag{E.17}$$

Use of (E.17) in (E.12) establishes representation (E.1) of $B_{k,0}$ for $k > 1$.

To prove (E.1) for $k > 1$, we begin with expression (E.2) for $i = k$

$$B_{k,0} = B_{0,k} P_{[B^h_{0,0},\cdots B^h_{k-1,0}]} + \sum_{j=0}^{k-1} B_{0,j} X_j \tag{E.8}$$

Pre-multiplication both sides by $P_{[B_{0,0},\cdots B_{k-1,0}]}$ gives

$$P_{[B_{0,0},\cdots B_{k-1,0}]} B_{k,0} = P_{[B_{0,0},\cdots B_{k-1,0}]} B_{0,k} P_{[B^h_{0,0},\cdots B^h_{k-1,0}]} + P_{[B_{0,0},\cdots B_{k-1,0}]} (\sum_{j=0}^{k-1} B_{0,j} X_j) \tag{E.9}$$

Simplification of (E.9) using (E.4) gives

$$B_{k,0} = P_{[B_{0,0},\cdots B_{k-1,0}]} B_{0,k} P_{[B^h_{0,0},\cdots B^h_{k-1,0}]} + P_{[B_{0,0},\cdots B_{k-1,0}]} (\sum_{j=0}^{k-1} B_{0,j} X_j) \tag{E.10}$$

A parallel argument involving post-multiplication of (E.3) by $P_{[B^h_{0,0},\cdots B^h_{k-1,0}]}$ and subsequent simplification using (E.5) gives

$$B_{k,0} = P_{[B_{0,0},\cdots B_{k-1,0}]} B_{0,k} P_{[B^h_{0,0},\cdots B^h_{k-1,0}]} + (\sum_{j=0}^{k-1} Y_j B_{0,j}) P_{[B^h_{0,0},\cdots B^h_{k-1,0}]} \tag{E.11}$$

The remainder of the appendix reconciles the two expressions (E.10) and (E.11) to derive result (E.1) for $k > 1$. Defining

$$B_{k,0} = P_{[B_{0,0},\cdots B_{k-1,0}]} B_{0,k} P_{[B^h_{0,0},\cdots B^h_{k-1,0}]} + F_{k-1} \tag{E.12}$$

we find from (E.10) that

$$\begin{aligned} F_{k-1} &= P_{[B_{0,0},\cdots B_{k-1,0}]} (\sum_{j=0}^{k-1} B_{0,j} X_j) \\ &= (I - [B_{0,0}, \cdots, B_{k-1,0}][B_{0,0}, \cdots, B_{k-1,0}]^+) (\sum_{j=0}^{k-1} B_{0,j} X_j) \\ &= \sum_{j=0}^{k-1} B_{0,j} X_j - \sum_{i=0}^{k-1} B_{i,0} Z_i \end{aligned} \tag{E.13}$$

The lemma is satisfied trivially for $k = 0$.

To establish (E.1) for $k \geq 1$, we first show that the columns, rows of $B_{i,0}$ are contained in the vector spaces spanned respectively by the columns, rows of the Taylor series term sequence $B_{0,0}, \cdots B_{0,i}$. Specifically, we have

Lemma E.1 : If $B_0(\epsilon)$ has Taylor series in ϵ, then

$$B_{i,0} = B_{0,i} P_{[B^h_{0,0}, \cdots B^h_{i-1,0}]} + \sum_{j=0}^{i-1} B_{0,j} X_j \tag{E.2}$$

and

$$B_{i,0} = P_{[B_{0,0}, \cdots B_{i-1,0}]} B_{0,k} + \sum_{j=0}^{i-1} Y_j B_{0,j} \tag{E.3}$$

for any $i = 1, \cdots$, where X_j and Y_j are appropriate square matrices.

Proof: See Appendix F.

Next, we observe that since the columns (and rows) of $B_{k,0}$ are by construction orthogonal to those of $B_{0,0}, \cdots B_{k-1,0}$, it follows that $B_{k,0}$ has the two properties

$$P_{[B_{0,0}, \cdots B_{k-1,0}]} B_{k,0} = B_{k,0} \tag{E.4}$$

$$B_{k,0} P_{[B^h_{0,0}, \cdots B^h_{k-1,0}]} = B_{k,0} \tag{E.5}$$

We make use of Lemma E.1 and properties (E.4), (E.5), to establish (E.1) for $k \geq 1$ as follows.

For $k = 1$, we begin with expression (E.2) for $i = 1$

$$B_{1,0} = B_{0,1} P_{[B^h_{0,0}]} + B_{0,0} X_0 \tag{E.6}$$

Pre-multiplication of both sides by $P_{[B_{0,0}]}$ gives

$$P_{[B_{0,0}]} B_{1,0} = P_{[B_{0,0}]} B_{0,1} P_{[B^h_{0,0}]} \tag{E.7}$$

since the columns of $B_{0,0}$ are in the nullspace of $P_{[B_{0,0}]}$. Simplification of (E.7) using (E.4) establishes (E.1) for $k = 1$.

Appendix E

Proof of Lemma 4.4

This appendix establishes the following result:

Lemma 4.4: For any $B_0(\epsilon)$ with Taylor series in ϵ, limiting singular matrices $B_{k,0}$ have the recursive structure

$$B_{k,0} = \begin{cases} B_{0,0} & k = 0 \\ P_{[B_{0,0}]} B_{0,1} P_{[B^h_{0,0}]} & k = 1 \\ P_{[B_{0,0},\cdots B_{k-1,0}]} \left(B_{0,k} + F_{k-1}\right) P_{[B^h_{0,0},\cdots B^h_{k-1,0}]} & k = 2, \cdots \end{cases} \tag{E.1}$$

where $B_{0,k}$ is the matrix coefficient of the k^{th} order term in the Taylor series of $B_0(\epsilon)$, and $P_{[B_{0,0},\cdots B_{k-1,0}]}$, $P_{[B^h_{0,0},\cdots B^h_{k-1,0}]}$ defined in (4.26), (4.27), respectively, denote projections onto the column, row nullspace of limiting singular matrix sequence $B_{0,0}, \cdots B_{k-1,0}$. Matrix F_{k-1} is a suitable rectangular matrix factor with properties:

a) the column space of F_{k-1} is contained in that of Taylor series matrix coefficient sequence $B_{0,1}, \cdots B_{0,k-1}$.

b) the row space of F_{k-1} is contained in that of Taylor series matrix coefficient sequence $B_{0,1}, \cdots B_{0,k-1}$,

matrix as $\epsilon \to 0$; therefore the singular values of $\tilde{B}_k(\epsilon)$ are proportional to ϵ^0 as $\epsilon \to 0$. It follows that $l = 0$, and that $\tilde{B}_k(\epsilon)$ has a series in non-negative integer powers of ϵ with constant matrix coefficients, hence a Taylor series in ϵ.

Appendix D

Proof of Lemma 4.3

This appendix establishes that if $B_0(\epsilon)$ has Taylor series in ϵ, then the matrices $\tilde{B}_k(\epsilon)$ also have Taylor series in ϵ.

Since column spaces of $\tilde{B}_k(\epsilon)$, $\tilde{B}_j(\epsilon)$ are orthogonal for $k \neq j$, we express $\tilde{B}_k(\epsilon)$ as

$$\tilde{B}_k(\epsilon) = \frac{1}{\epsilon^k} \left(\prod_{j \neq k} P_{[\tilde{B}_j(\epsilon)]} \right) B_0(\epsilon) \tag{D.1}$$

where $P_{[\tilde{B}_j(\epsilon)]}$ denotes the projection onto the nullspace of the columns of $\tilde{B}_j(\epsilon)$.

The columns of $U(\epsilon)$ in (4.23) that span $\tilde{B}_j(\epsilon)$ are by definition eigenvectors of $B_0(\epsilon)B_0(\epsilon)^h$ associated with limiting eigenvalues proportional to ϵ^{2j}. Thus we have

$$P_{[\tilde{B}_j(\epsilon)]} = P_{2j}(\epsilon) \tag{D.2}$$

where $P_{2j}(\epsilon)$ is an eigenprojection matrix as defined in (B.4), with Taylor series (B.8) in ϵ. Since $B_0(\epsilon)$ has Taylor series (4.3), $\tilde{B}_k(\epsilon)$ is expressed in (D.1) as a product of several Taylor series scaled by ϵ^{-k}, hence as a series in integer powers of ϵ, with minimum power $l \geq -k$, and with constant matrix coefficients.

We now show that the power series of $\tilde{B}_k(\epsilon)$ has no terms with negative powers of ϵ (i.e. that the minimum power of ϵ is $l = 0$). As $\epsilon \to 0$, the largest singular value of $\tilde{B}_k(\epsilon)$ must be proportional to ϵ^l. The definition (4.23) of $\tilde{B}_k(\epsilon)$ also identifies the SVD of $\tilde{B}_k(\epsilon)$ for all ϵ. From result **S1**, $\frac{1}{\epsilon^k}\Sigma_k(\epsilon)$ converges to a constant diagonal

Substitution of (C.10) in (C.8) gives a more precise version of result (C.4), namely

$$P_{2k}(\epsilon)A_{2k}(\epsilon) \;=\; \mathcal{O}(\epsilon^2) \tag{C.11}$$

Use of (C.11) in definition (B.3) of matrix $A_{2k+1}(\epsilon)$ shows that

$$\begin{aligned} A_{2k+1}(\epsilon) &= \frac{1}{\epsilon}P_{2k}(\epsilon)A_{2k}(\epsilon) \\ &= \mathcal{O}(\epsilon) \end{aligned} \tag{C.12}$$

As $\epsilon \rightarrow 0$, (C.12) converges to (C.2) which concludes proof of the lemma.

Since P_{2k} is the leading term of the Taylor series (B.8) of $P_{2k}(\epsilon)$, and $A_{2k,0}$ is the leading term of the Taylor series (B.7) of $A_{2k}(\epsilon)$, it follows from (C.3) that

$$P_{2k}(\epsilon)A_{2k}(\epsilon) \;=\; \mathcal{O}(\epsilon) \tag{C.4}$$

Use of property (B.6) gives

$$P_{2k}(\epsilon)A_{2k}(\epsilon) \;=\; P_{2k}(\epsilon)A_{2k}(\epsilon)P_{2k}(\epsilon) \tag{C.5}$$

Use of definition (B.3) of $A_{2k}(\epsilon)$ in (C.5) gives

$$P_{2k}(\epsilon)A_{2k}(\epsilon) \;=\; \frac{1}{\epsilon}P_{2k}(\epsilon)\left[P_{2k-1}(\epsilon)A_{2k-1}(\epsilon)\right]P_{2k}(\epsilon) \tag{C.6}$$

Repeated applications of steps (C.5), (C.6) result in

$$P_{2k}(\epsilon)A_{2k}(\epsilon) = \frac{1}{\epsilon^{2k}}P_{2k}(\epsilon)P_{2k-1}(\epsilon)\cdots P_0(\epsilon)A_0(\epsilon)P_0(\epsilon)\cdots P_{2k-1}(\epsilon)P_{2k}(\epsilon) \tag{C.7}$$

Since $A_0(\epsilon)$ that satisfies Condition IV is the outer product (4.14) of $B_0(\epsilon)$, we rearrange (C.7) as

$$P_{2k}(\epsilon)A_{2k}(\epsilon) = \left(\frac{1}{\epsilon^k}P_{2k}(\epsilon)P_{2k-1}(\epsilon)\cdots P_0(\epsilon)B_0(\epsilon)\right) \left(\frac{1}{\epsilon^k}P_{2k}(\epsilon)P_{2k-1}(\epsilon)\cdots P_0(\epsilon)B_0(\epsilon)\right)^h \tag{C.8}$$

It follows from (C.4) and the product form of $P_{2k}(\epsilon)A_{2k}(\epsilon)$ in (C.8) that

$$\frac{1}{\epsilon^k}P_{2k}(\epsilon)P_{2k-1}(\epsilon)\cdots P_0(\epsilon)B_0(\epsilon) \;=\; \mathcal{O}(\epsilon^{1/2}) \tag{C.9}$$

Since $B_0(\epsilon)$ has Taylor series (4.15) in ϵ, and $P_j(\epsilon)$ $j = 0,\cdots 2k$ have Taylor series (B.8), their product in (C.9) must be a series in integral powers of ϵ. It follows from (C.9) that we must have

$$\frac{1}{\epsilon^k}P_{2k}(\epsilon)P_{2k-1}(\epsilon)\cdots P_0(\epsilon)B_0(\epsilon) \;=\; \mathcal{O}(\epsilon) \tag{C.10}$$

Appendix C

Proof of Lemma 4.1

This appendix establishes the following result:

Lemma 4.1: If matrix $A_0(\epsilon)$ satisfies Condition IV of Chapter 4, then each non-zero eigenvalue $\lambda_i(\epsilon)$ of $A_0(\epsilon)$ is asymptotically (as $\epsilon \to 0$) proportional to non-negative *even* powers of ϵ. That is,

$$\lim_{\epsilon \to 0} \left\{ \frac{\lambda_i(\epsilon)}{\lambda_i \cdot \epsilon^{2k_i}} \right\} = 1 \tag{C.1}$$

for suitable constants λ_i and $k_i \in \{0, 1 \cdots\}$, for all $i = 1, \cdots, \text{rank}\{A_0(\epsilon)\}$.

Whenever $A_0(\epsilon)$ satisfies Condition IV, $A_0(\epsilon)$ is Hermitian and has Taylor series in ϵ. Hence result **R1** states that the limiting eigenvalues of $A_0(\epsilon)$ are proportional to non-negative integer powers of ϵ. Thus to prove the lemma it is sufficient to show that there are no limiting eigenvalues of $A_0(\epsilon)$ proportional to odd powers of ϵ, or equivalently by result **R2**, that the odd order limiting eigenmatrices $A_{2k+1,0}$ satisfy

$$A_{2k+1,0} = 0 \tag{C.2}$$

for all $k \geq 0$.

To show (C.2), we observe from the definition (3.15) of P_{2k} in terms of $A_{2k,0}$ that

$$P_{2k} A_{2k,0} = \left(I - A_{2k,0} A_{2k,0}^{+} \right) A_{2k,0} = 0 \tag{C.3}$$

(See Eq. (2.23) of [18]). In the limit as $\epsilon \to 0$, $A_k(\epsilon)$ converges to limiting eigenmatrix $A_{k,0}$. Therefore eigenprojection $P_k(\epsilon)$ defined by (B.4) converges to *limiting eigenprojection* P_k defined in (3.15) in terms of limiting eigenmatrices.

Note that the characterization (B.2)-(B.8) of the limiting eigenmatrices $A_{k,0}$ as limiting forms of matrices $A_k(\epsilon)$ does not specify the $A_{k,0}$ in terms of the (known) matrix coefficients $A_{0,p}$ in the Taylor series (B.1) for $A_0(\epsilon)$.

To relate the $A_{k,0}$ to the $A_{0,p}$, Reference [17] derives recursive and very complicated expressions in terms of the leading eigenprojection term P_{k-1} and of the Taylor series terms of $A_{k-1}(\epsilon)$ (Eq. (2.18) in Chapter II of [17]). In reference [18], the authors simplify the recursive expressions in [17] to identify the expressions (3.14) for the limiting eigenmatrices $A_{k,0}$ in terms of the known Taylor series terms of $A_0(\epsilon)$.

As evident from (3.14), this approach results in increasingly complex expressions for $A_{k,0}$ as k increases; extension of the approach to $A_{4,0}$ reveals that it involves dozens of terms.

$$A_k(\epsilon) \triangleq \frac{P_{k-1}(\epsilon)A_{k-1}(\epsilon)}{\epsilon} = \frac{P_{k-1}(\epsilon)\cdots P_0(\epsilon)A_0(\epsilon)}{\epsilon^k} \qquad k>1 \qquad \text{(B.3)}$$

where matrices $P_k(\epsilon)$, designated *eigenprojections*, are defined analytically in terms of a contour integral in [17], [18]. (See Eq. (2.22) of [18]). A geometrical interpretation of matrix $P_k(\epsilon)$ for Hermitian $A_0(\epsilon)$ is as a projection onto the space spanned by the eigenvectors associated with the eigenvalues of $A_k(\epsilon)$ that are zero when $\epsilon = 0$. Thus, a convenient definition of $P_k(\epsilon)$ for Hermitian $A_0(\epsilon)$ is

$$P_k(\epsilon) \triangleq I - Q_k(\epsilon) \qquad \text{(B.4)}$$

$$Q_k(\epsilon) \triangleq \{E_k(\epsilon)\}_{\lambda\neq 0\,|\,\epsilon=0}\{E_k(\epsilon)\}^h_{\lambda\neq 0\,|\,\epsilon=0} \qquad \text{(B.5)}$$

for $k = 0, 1\cdots$, where $E_k(\epsilon)$ denotes a complete matrix of eigenvectors of $A_k(\epsilon)$, and operator $\{\ \}_{\lambda\neq 0\,|\,\epsilon=0}$ selects the subset of eigenvectors associated with eigenvalues that remain non-zero when $\epsilon = 0$.

By definition (B.4), (B.5) of $P_k(\epsilon)$, we have the property

$$P_k(\epsilon)A_k(\epsilon) = P_k(\epsilon)A_k(\epsilon)P_k(\epsilon) \qquad \text{(B.6)}$$

for $k = 0, 1\cdots$. Repeated use of property (B.6) in definition (B.3) shows for Hermitian matrices $A_0(\epsilon)$ that matrices $A_k(\epsilon)$ are also Hermitian.

References [17], [18] show that matrices $A_k(\epsilon)$ exist (i.e. remain finite) as $\epsilon \to 0$, non-withstanding the denominator factor ϵ in (B.3). (See Theorem 6.38 Chapter II of [17]). It is further shown that matrices $A_k(\epsilon)$ and eigenprojections $P_k(\epsilon)$ depend on ϵ via Taylor series

$$A_k(\epsilon) = A_{k,0} + \sum_{p=1}^{\infty}\epsilon^p A_{k,p} \qquad \text{(B.7)}$$

where $A_{k,0}$ are the limiting eigenmatrices (See Eq.(4.5) of [18]), and

$$P_k(\epsilon) = P_k + \sum_{p=1}^{\infty}\epsilon^p P_{k,p} \qquad \text{(B.8)}$$

Appendix B

Definition of $A_{k,0}$ in [17], [18]

This appendix states the definition of the limiting eigenmatrices $A_{k,0}$ presented in References [17], [18] and outlines the approach used therein to derive expressions (3.14). The prior results restated in this appendix are used in subsequent appendices to derive the thesis SVD results.

Reference [18] considers a Hermitian matrix $A_0(\epsilon)$ with Taylor series about $\epsilon = 0$

$$A_0(\epsilon) = \sum_{p=0}^{\infty} \epsilon^p A_{0,p} \tag{B.1}$$

where $A_{0,p}$ are known constant matrices, independent of variable parameter ϵ.

The essence of the approach of [17], [18] is to define the constant limiting eigenmatrices $A_{k,0}$ as

$$A_{k,0} \triangleq \lim_{\epsilon \to 0} A_k(\epsilon) \tag{B.2}$$

for $k = 0, 1, \cdots$, where the $A_k(\epsilon)$ are a sequence of matrices non-constant with ϵ whose eigenstructure is related to that of $A_0(\epsilon)$. The $A_k(\epsilon)$ are defined recursively from matrix $A_0(\epsilon)$ as

$$\begin{aligned} A_0(\epsilon) &\triangleq A_0(\epsilon) \\ A_1(\epsilon) &\triangleq \frac{P_0(\epsilon) A_0(\epsilon)}{\epsilon} \end{aligned}$$

Appendix A

Additional Notation

This appendix provides additional notation detail, to explicitly define the Hadamard and Kronecker products.

Hadamard Product:

The Hadamard product of the $I \times J$ matrices A and B is defined as the $I \times J$ matrix

$$A \odot B \triangleq \begin{bmatrix} a_{11}b_{11} & a_{12}b_{12} & \cdots & a_{1J}b_{1J} \\ a_{21}b_{21} & a_{22}b_{22} & \cdots & a_{2J}b_{2J} \\ \vdots & \vdots & \ddots & \vdots \\ a_{I1}b_{I1} & a_{I2}b_{I2} & \cdots & a_{IJ}b_{IJ} \end{bmatrix} \tag{A.1}$$

where a_{ij}, b_{ij} respectively denote the i,j^{th} elements of A, B. The Hadamard product of matrices A and B is simply the element-by-element product of A and B.

Kronecker Product:

The Kronecker product of the $I \times J$ matrix A and the $K \times L$ matrix B is defined as the $IK \times JL$ matrix

$$A \otimes B \triangleq \begin{bmatrix} a_{11}B & a_{12}B & \cdots & a_{1J}B \\ a_{21}B & a_{22}B & \cdots & a_{2J}B \\ \vdots & \vdots & \ddots & \vdots \\ a_{I1}B & a_{I2}B & \cdots & a_{IJ}B \end{bmatrix} \tag{A.2}$$

The multi-D results developed herein in some ways parallel the prior 1-D results, but also differ from the 1-D results in interesting and significant ways. For example, for a given number of sources, we find multi-D scenarios are typically much less sensitive to small source separation $\delta\omega$ than 1-D scenarios. Specifically, for typical multi-D scenarios with closely spaced sources 1) matrix R_S is much better conditioned, 2) the CR directional variance bounds are much lower, and 3) the resolution and detection thresholds are much more favorable than in 1-D scenarios.

Thesis analysis shows that for typical DF scenarios the eigendecomposition of R_S, and the SVD of its rectangular factor matrix B (or A), decompose for small $\delta\omega$ to a series of simpler shell problems, involving decomposition of low rank matrices which are constant with $\delta\omega$. Furthermore, the numerical conditioning and the span of R_S can be determined by simple linear algebra without the need for eigendecomposition or polynomial rooting.

The thesis identifies side conditions that greatly simplify prior results on eigenstructure of perturbed Hermitian matrices of [17], [18]. These side conditions typically are present in DF scenarios. Analysis also develops new results for the SVD of perturbed rectangular matrices, which not only facilitate the eigendecomposition of R_S for closely spaced sources, but may also have use in other applications.

The thesis results show that the direction finding problem imposes challenging requirements on practical systems intended to provide unbiased frequency estimates of closely spaced sources. For example, reducing by a factor of 10 the maximum separation $\delta\omega$ of $M = 6$ sources in a typical 2-D scenario (with $m = 2$ and $\chi = 3$) requires increasing the SNR by $2m \cdot 10\text{dB} = 40\text{dB}$ to maintain constant source detection performance, or increasing the SNR by $2\chi \cdot 10\text{dB} = 60\text{dB}$ to maintain constant source resolution performance.

The thesis provides an analytical framework for the direction finding problem in multi-D scenarios, which should facilitate the performance analyses of candidate DF techniques, help quantify the numerical-accuracy and hardware-alignment issues associated with implementing high-resolution techniques, facilitate beamformer design and provide insight helpful for development of improved DF algorithms in multi-D scenarios.

Chapter 11

Conclusions

The objective of this thesis has been to clarify the multi-dimensional geolocation problem for closely-spaced sources. The principal results are explicit analytical expressions in terms of maximum source separation $\delta\omega$, source configuration, source powers and correlations, and sensor array geometry, that elucidate the following:

- The eigenstructure of covariance matrix R_S that is central to many High Resolution direction finding (DF) algorithms, for closely-spaced sources in non-degenerate and partially degenerate multi-D scenarios (Chapters 5, 7).
- The Cramér Rao (CR) lower bound on the directional variance of any unbiased DF algorithm, for closely-spaced sources in multi-D scenarios with non-degenerate CR bounds (Chapter 9).
- The detection threshold SNR and data set size N at which the number M of closely spaced sources can reliably be determined in typical multi-D scenarios by any eigenvalue based detection algorithm (Chapter 6).
- The resolution threshold SNR and data set size N at which M closely-spaced sources can reliably be resolved in typical multi-D scenarios by any unbiased DF algorithm (Chapter 10).

These results generalize to multi-D the analytical results recently developed for 1-D scenarios [11]-[13]. These results should be useful in identifying fundamental performance limitations and opportunities for multi-dimensional geolocation.

Similarly, identification of the data set size resolution threshold gives

$$\mathcal{N}_R \geq \frac{K'_R}{\mathrm{SNR}} \delta\omega^{-2\chi} \tag{10.15}$$

10.3 Summary

The threshold expressions (10.14) and (10.15) are important since they provide explicit expressions for the minimum SNR and data set size N required to satisfy the "necessary condition" (10.5) for resolution of M closely spaced sources using any unbiased spectral estimation algorithm. The threshold expressions can be used to generate model resolution curves for any given scenario, since the constant K'_R can be calculated explicitly given the array geometry, sensor directional response, source configuration and source correlations.

The threshold expressions (10.14) and (10.15) also clarify the trade-off between SNR, N and maximum source spacing $\delta\omega$ required to maintain resolution performance in multi-D scenarios. For example, if noise power is doubled in a given scenario, then the size of the data set must increase by a factor of 2 to maintain resolution performance. If on the other hand, the maximum source spacing $\delta\omega$ is decreased by a factor of 2 in a 2-D scenario with non-degenerate CR bounds and $M = 6$ sources (with $\chi = 3$), then to maintain resolution performance with a fixed data set size N, the SNR must increase by a factor of $2^6 = 64$. Alternately if $\delta\omega$ is halved while the SNR remains fixed, then the data set size N must increase by a factor of $2^6 = 64$.

By way of comparison, if the maximum source spacing $\delta\omega$ is decreased by a factor of 2 in a 1-D scenario with $M = 6$ sources, then to maintain resolution performance with a fixed data set size N (or fixed SNR), the SNR (or N) must increase by a factor of $2^{12} = 4096$!!! For small $\delta\omega$ and a given number of sources M, the resolution thresholds are typically much smaller (more favorable) in multi-D than in 1-D scenarios.

Analogously, we define the data set size resolution threshold $\mathcal{N}_R$ to be the smallest value of N for which (10.5) is satisfied for a fixed power factor p.

To elucidate the necessary conditions for resolution, we square (10.5) and substitute expression (9.131) to obtain

$$\delta\omega^{-2(\chi-1)}\frac{\sigma^2}{2N}\left(\left[P_{[\dot{\Psi}^t_{\chi-1}]}\dot{\Psi}^t_\chi \mathrm{Re}\left[\widehat{P}^t\otimes\mathcal{E}^h_\chi\mathcal{E}_\chi\right]\dot{\Psi}_\chi P_{[\dot{\Psi}^t_{\chi-1}]}\right]^+\right)_{ll} \leq f^2\cdot\delta\omega^2\cdot\min_{k\neq j}\|\vec{q}_j-\vec{q}_k\|^2 \tag{10.9}$$

for small $\delta\omega$. Rearrangement of (10.9) and use of (10.6) gives the equivalent condition

$$\mathrm{SNR}\cdot N \;\geq\; K'_{R,i,j}\,\delta\omega^{-2\chi} \tag{10.10}$$

where we define

$$K'_{R,i,j}\triangleq\frac{1}{2f^2\cdot\min\limits_{k\neq j}\|\vec{q}_j-\vec{q}_k\|^2}\left(\left[P_{[\dot{\Psi}^t_{\chi-1}]}\dot{\Psi}^t_\chi \mathrm{Re}\left\{\widehat{P}^t_0\otimes\mathcal{E}^h_\chi\mathcal{E}_\chi\right\}\dot{\Psi}_\chi P_{[\dot{\Psi}^t_{\chi-1}]}\right]^+\right)_{ll} \tag{10.11}$$

where $l=\mathcal{D}(j-1)+i$.

We note that an equivalent condition for (10.10) to be satisfied for all $j=1\cdots M$, $i=1\cdots\mathcal{D}$ is the condition

$$\mathrm{SNR}\cdot N \;\geq\; K'_R\,\delta\omega^{-2\chi} \tag{10.12}$$

where we define

$$K'_R \;=\; \max_{i,j}\{K'_{R,i,j}\} \tag{10.13}$$

Thus we deem satisfactory resolution performance to be possible whenever condition (10.12) is satisfied.

Identification of the SNR resolution threshold gives

$$\mathcal{E}_R \;\geq\; \frac{K'_R}{N}\,\delta\omega^{-2\chi} \tag{10.14}$$

is that

$$\sqrt{(B_C)_{ll}} \leq f \cdot \delta\omega_j \tag{10.5}$$

for all $i = 1 \cdots \mathcal{D}$, $j = 1 \cdots M$, with $l = \mathcal{D}(j-1)+i$ and where f is a suitable fraction (e.g. $f = 1/8$).

Note that the structure of the CR bound $(B_C)_{ll}$ was elucidated in Chapter 9. Accordingly the results of Chapter 9 together with (10.5) enable us to make useful statements about the resolution thresholds $\mathcal{E}_R$ and $\mathcal{N}_R$.

10.2 Resolution Thresholds $\mathcal{E}_R$ and $\mathcal{N}_R$

To define the resolution thresholds, we extend the approach used in [13], as in Chapter 6. We represent the source amplitude correlation matrix $\hat{P}$ as follows

$$\hat{P} = p\hat{P}_0 \tag{10.6}$$

where $\hat{P}_0$ is a constant matrix the eigenvalues of which sum to unity, and p is a variable scale factor. Note that representation (10.6) retains the correlations between the source powers. We define the signal SNR to be the ratio of the scale factor p to the noise power σ^2. That is

$$\text{SNR} = p/\sigma^2 \tag{10.7}$$

We deem satisfactory resolution performance to be possible whenever condition (10.5) is satisfied for all i, j, (i.e. for all signals and for all coordinate directions). We define the resolution threshold power to be the smallest value p_{min} of p for which (10.5) is satisfied for a fixed N, and define the resolution threshold SNR to be

$$\mathcal{E}_R = p_{min}/\sigma^2 \tag{10.8}$$

array geometry, normalized source configuration, source powers and correlations.

Since parameter $\chi < M$ for typical multi-D scenarios, comparison of (10.1) and (10.2) leads to the conclusion that for small $\delta\omega$, the resolution thresholds are typically much smaller (more favorable) in multi-D than in 1-D scenarios.

The chapter is organized as follows. Section 10.1 postulates a necessary condition for successful resolution of closely-spaced sources. Section 10.2 then develops the expressions (10.2) and (10.3) for the resolution threshold SNR and N. Section 10.3 summarizes the resolution threshold results.

10.1 "Necessary Conditions" for Reliable Resolution

To obtain resolution threshold expressions for both SNR and N, we follow the argument of Lee [11] that any unbiased estimator can successfully resolve M closely spaced sources only if the standard deviation of the directional estimates is substantially less than the minimum spacing between any two sources. The SNR and N values required to satisfy the above condition result are deemed to be the resolution threshold values.

Thus, consider M closely-spaced signals, and define $\delta\omega_j$ to denote the minimum spacing between the j^{th} and any other source. That is

$$\delta\omega_j \;=\; \delta\omega \cdot \min_{k \neq j} \|\vec{q}_j - \vec{q}_k\| \tag{10.4}$$

where $\vec{q}_1, \cdots \vec{q}_M$ are the normalized spectral frequency offsets. If the root CR bounds $\sqrt{(B_C)_{ll}}$ for all coordinate directions at the j^{th} source ($l = \mathcal{D}(j-1)+i$ and $i = 1 \cdots \mathcal{D}$) are small compared to $\delta\omega_j$ for each source $j = 1 \cdots M$, then there is a basis for seeking an unbiased estimator for resolving the signals. On the other hand, if one or more of the $\sqrt{(B_C)_{ll}}$ are large compared to the associated $\delta\omega_j$, then it is unlikely that there exists an unbiased estimator which can resolve the signals with high probability. Accordingly, one strongly suspects that a necessary condition for the existence of an unbiased estimator capable of resolving M closely spaced sources with high probability

minimum SNR and N at which "one can see" each of the M sources present.

Prior work by Stoica and Nehorai [15] for the 1-D MUSIC algorithm, and by Lee [11] for any unbiased 1-D DF spectral estimation algorithm, has used the CR bound on directional estimate variance to elucidate the dependence on scenario parameters of the SNR resolution threshold $\mathcal{E}_R$, and of the data set size threshold $\mathcal{N}_R$. Specifically, Lee has argued that any unbiased estimator can successfully resolve M closely spaced sources only if the standard deviation of the directional estimates is substantially less than the minimum spacing between any two sources. The CR bound provides a lower bound on the standard deviation of any unbiased estimator, and thus can be used to elucidate the form of the resolution thresholds $\mathcal{E}_R$ and $\mathcal{N}_R$ for any unbiased estimation algorithm.

Lee in [11] identified expressions for the CR bound for closely-spaced sources in 1-D scenarios, and used the results to characterize the SNR resolution threshold $\mathcal{E}_R$ for closely spaced sources in 1-D scenarios. The author argued that the $\mathcal{E}_R$ at which unbiased spectral estimation algorithms can reliably resolve M sources in 1-D scenarios is proportional to $\delta\omega^{-2M}$. That is

$$\mathcal{E}_R \simeq \frac{K_R}{N} \cdot \delta\omega^{-2M} \tag{10.1}$$

where K_R is constant with $\delta\omega$.

This chapter extends the result (10.1) of [11] to multi-D scenarios. Drawing upon the CR bound expressions for multi-D scenarios derived in Chapter 9, we characterize the (SNR) threshold $\mathcal{E}_R$ and the data set size threshold $\mathcal{N}_R$ for M closely spaced sources in multi-D scenarios with non-degenerate CR bounds. The results are:

$$\mathcal{E}_R \simeq \frac{K'_R}{N} \cdot \delta\omega^{-2\chi} \tag{10.2}$$

$$\mathcal{N}_R \simeq \frac{K'_R}{\mathrm{SNR}} \cdot \delta\omega^{-2\chi} \tag{10.3}$$

where $\delta\omega$ is the maximum source separation parameter, χ is the parameter defined in (8.61), and K'_R is a constant defined in Section 10.1, that depends only upon sensor

Chapter 10

Resolution Thresholds

An important aspect of Direction Finding (DF) algorithm performance is the ability to identify distinct direction estimates for each of M closely-spaced sources; if successful, the algorithm is said to have *resolved* the sources. For DF estimators based upon the peaks of a spectrum function $S(\vec{\omega})$, a necessary condition for reliable resolution of M closely spaced sources is the appearance, with high probability, of M distinct peaks in the spectrum function in the vicinity of the sources.

Note that the ability of an algorithm to resolve M sources is different from the ability to determine (detect) the number of sources; indeed many eigenvector-based DF algorithms such as MUSIC and MinNorm require a-priori knowledge of the source number for proper operation. In practice, the number of sources M is typically obtained from side information, or is estimated using detection algorithms. Example detection algorithms are Akaike Information Criteria (AIC) [22], and Minimum Descriptive Length (MDL) [23]. For the purposes of the discussion of resolving ability, we assume that the number M is known or has been correctly estimated.

One useful measure of the "resolving power" of a DF algorithm is the signal-to-noise ratio (SNR) threshold $\mathcal{E}_R$ at which the algorithm can reliably resolve M sources for a given source-array configuration, and a given number N of data snapshots. An alternative performance measure is the data set size N threshold $\mathcal{N}_R$ at which the algorithm can reliably resolve the M sources for a given source-array configuration, and a given SNR. These threshold values also can be regarded respectively as the

normalized bound (9.153).

Clearly the simplified asymptotic expressions again capture the essence of the bounds for emitter separation less than one beamwidth. As predicted, the CR bounds exhibit a $\delta\omega^{-4}$ behavior for small $\delta\omega$, with a slope of 40 dB/decade. Thus the theoretical expressions accurately predict the CR bounds for small separations $\delta\omega$ for this Case I scenario with non-degenerate CR bounds.

depict the asymptotic behavior predicted by Eq. (9.145). The horizontal scale denotes spatial frequency separation $\delta\omega$ normalized by the array beamwidth BW, so that unity on the horizontal scale of the graph corresponds to maximum source separation of one beamwidth. The vertical scale depicts the value of the normalized bound (9.153).

Clearly the simplified asymptotic expressions again capture the essence of the bounds for emitter separation less than one beamwidth. Note that the 5 sensors lie on an ellipse centered at coordinate origin. As predicted, the CR bounds exhibit a preferred $\delta\omega^{-2}$ behavior for small $\delta\omega$, with a slope of 20 dB/decade, along the preferred direction normal to the ellipse curve (y-axis), and exhibit a $\delta\omega^{-4}$ behavior, with a slope of 40 dB/decade, along the tangential direction (x-axis). Thus the theoretical expressions again accurately predict the CR bounds for small separations $\delta\omega$ for this Case III scenario with non-degenerate CR bounds.

Example 9.4 : For this example $M = 6$ and the array and source geometries are as follows.

Array: Sensors in a sparse grid per Figure 2-4A,

Sources: Sources SC1-SC6 clustered around broadside as in Figure 8-1.

As shown in Example 8.4, this is a Case I scenario with non-degenerate CR bounds. Consequently the directional variance CR bounds for small $\delta\omega$ may be determined using (9.145).

Figure 9-4 shows the values of the CR bounds for parameter estimates along the x and y spectral frequency axes for one of the sources, specifically SC1 in Figure 8-1. The solid curves depict the exact CR bounds; the dashed lines depict the asymptotic behavior predicted by Eq. (9.145). The horizontal scale denotes spatial frequency separation $\delta\omega$ normalized by the array beamwidth BW, so that unity on the horizontal scale of the graph corresponds to maximum source separation of one beamwidth. The vertical scale depicts the value of the

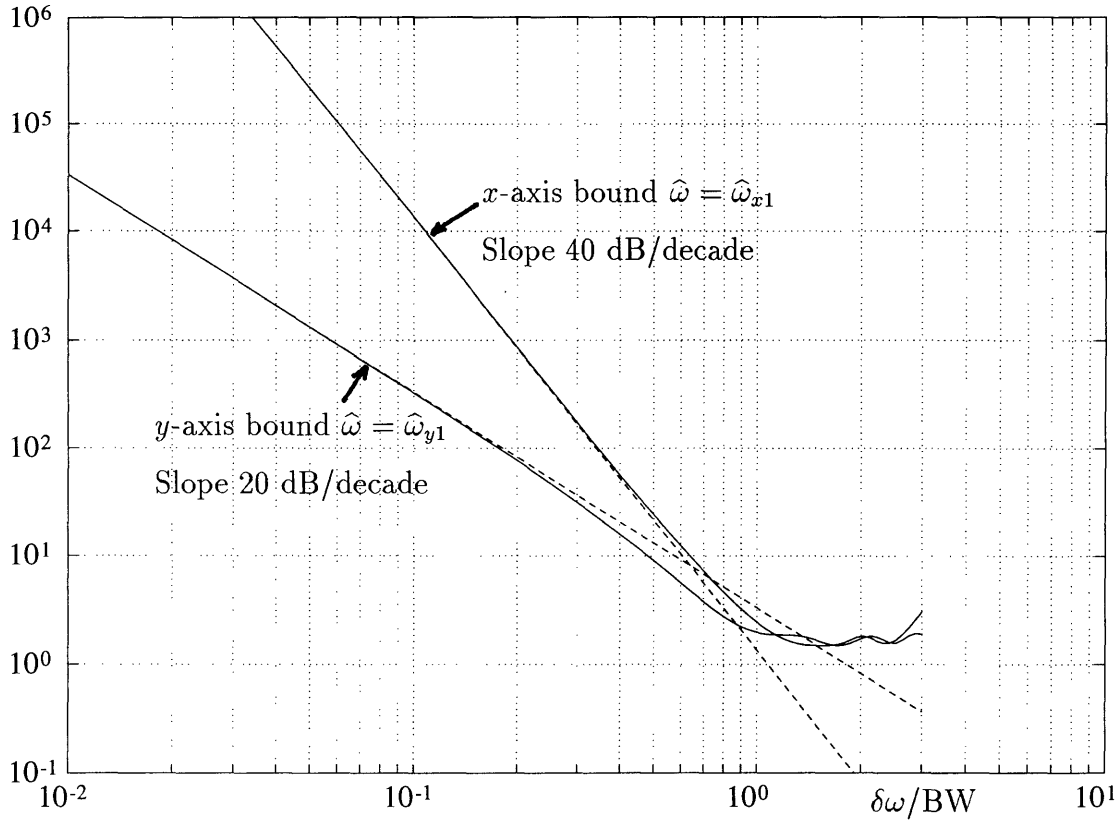

Figure 9-3: Limiting CR Bounds for Source SC1 in $M = 5$ Source Scenario

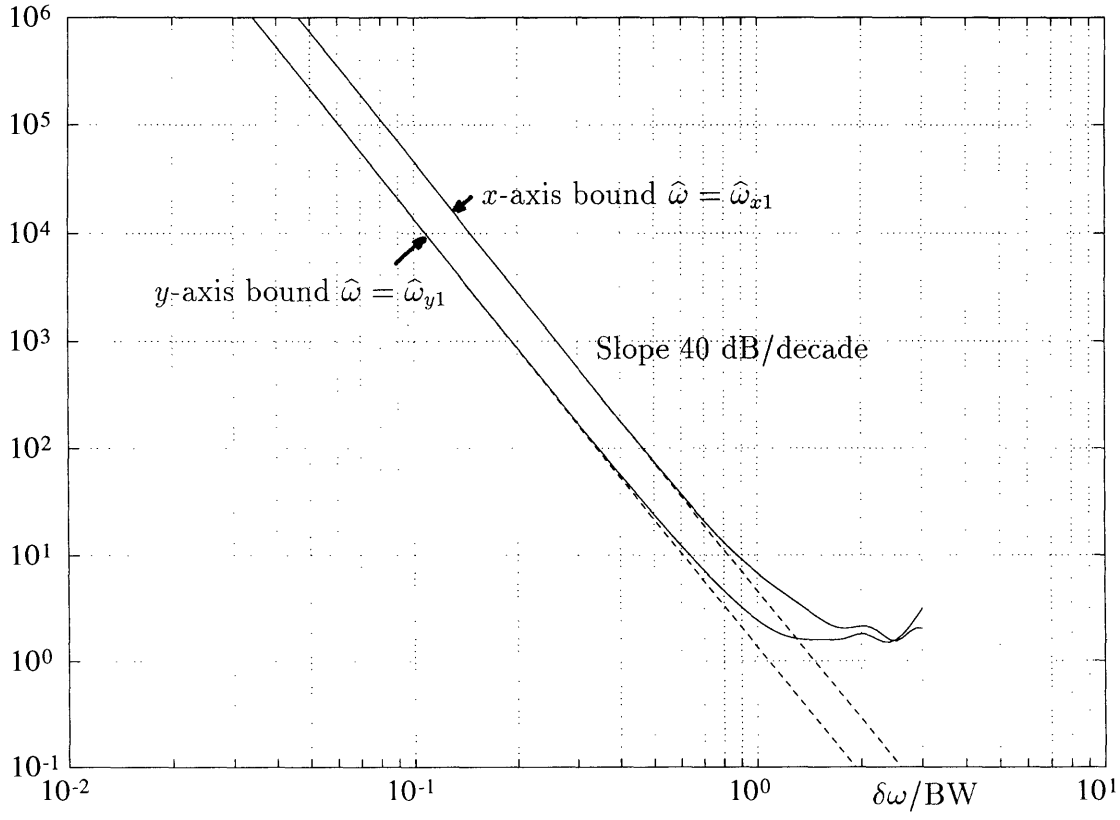

Figure 9-4: Limiting CR Bounds for Source SC1 in $M = 6$ Source Scenario

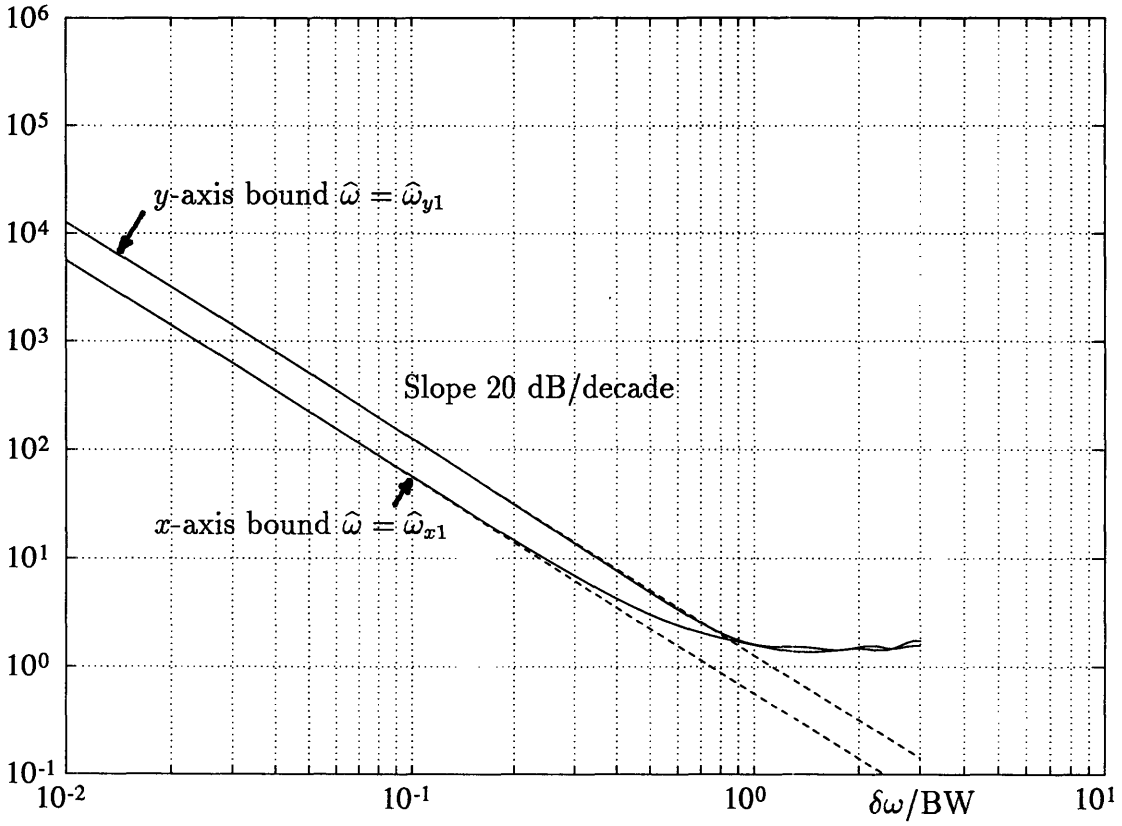

Figure 9-1: Limiting CR Bounds for Source SC1 in $M = 3$ Source Scenario

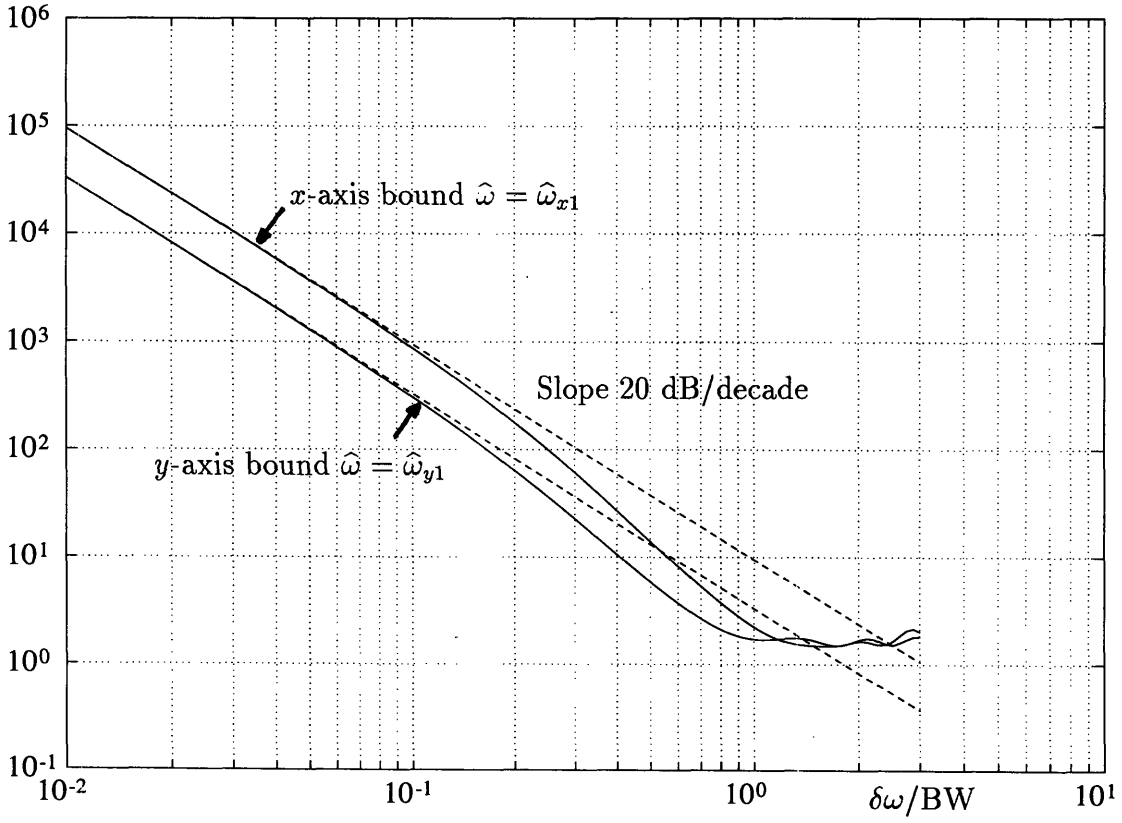

Figure 9-2: Limiting CR Bounds for Source SC1 in $M = 4$ Source Scenario

As shown in Example 8.2, this is a Case II scenario with non-degenerate CR bounds. Consequently the directional variance CR bounds for small $\delta\omega$ may be determined using (9.145).

Figure 9-2 shows the values of the CR bounds for parameter estimates along the x and y spectral frequency axes for one of the sources, specifically SC1 in Figure 8-1. The solid curves depict the exact CR bounds; the dashed lines depict the asymptotic behavior predicted by Eq. (9.145). The horizontal scale denotes spatial frequency separation $\delta\omega$ normalized by the array beamwidth BW, so that unity on the horizontal scale of the graph corresponds to maximum source separation of one beamwidth. The vertical scale depicts the value of the normalized bound (9.153).

Clearly the simplified asymptotic expressions again capture the essence of the bounds for emitter separation less than one beamwidth. As predicted, the CR bounds exhibit a $\delta\omega^{-2}$ behavior for small $\delta\omega$, with a slope of 20 dB/decade. Thus the theoretical expressions again accurately predict the CR bounds for small separations $\delta\omega$ for this Case II scenario with non-degenerate CR bounds.

Example 9.3 : For this example $M = 5$ and the array and source geometries are as follows.

Array: Sensors in a sparse grid per Figure 2-4A,

Sources: Sources SC1, SC2, SC3, SC4, SC5 clustered around broadside as in Figure 8-1.

As shown in Example 8.3, this is a Case III scenario with non-degenerate CR bounds. Consequently the directional variance CR bounds for small $\delta\omega$ may be determined using (9.145).

Figure 9-3 shows the values of the CR bounds for parameter estimates along the x and y spectral frequency axes for one of the sources, specifically SC1 in Figure 8-1. The solid curves depict the exact CR bounds; the dashed lines

Substitution of (J.21) into (J.14) gives

$$\mathcal{D} \leq \text{Rank}\{\mathcal{E}_m \Gamma'_m(\vec{q}_j) [\Upsilon , \Upsilon'][\Upsilon , \Upsilon']^+\} = \text{Rank}\{\mathcal{E}_m \Gamma'_m(\vec{q}_j) [\Upsilon , \Upsilon']\} \quad \text{(J.22)}$$

since removal of the post-factor Y^+ does not change the rank of the product XYY^+ for any X, Y.

From (J.17) we note that

$$\begin{aligned} \mathcal{E}_m \Gamma'_m(\vec{q}_j) \Upsilon' &= \left[I - \bar{A}\bar{A}^+\right] \dot{A}_m \Gamma_m P_{[\Gamma_0^h, \cdots \Gamma_{m-1}^h]} \\ &= 0 \end{aligned} \quad \text{(J.23)}$$

since $\dot{A}_m \Gamma_m P_{[\Gamma_0^h, \cdots \Gamma_{m-1}^h]}$ is in the column space of $\bar{A}$, and is annihilated by $\left[I - \bar{A}\bar{A}^+\right]$. Therefore we simplify (J.22) to

$$\mathcal{D} \leq \text{Rank}\{\mathcal{E}_m \Gamma'_m(\vec{q}_j) \Upsilon\} \quad \text{(J.24)}$$

Since the last factor in (J.24) has only $\mathcal{D}$ columns, (J.24) must be satisfied with equality. From (J.4), (J.10) and (J.16) we note that

$$\dot{\Psi}_m(\vec{q}_j) = \Gamma'_m(\vec{q}_j) \Upsilon \quad \text{(J.25)}$$

Assertion (J.1) of the lemma is established by substitution of (J.25) in (J.24) satisfied with equality.

Appendix K

Proof of Lemma 9.3

This appendix establishes the result:

Lemma 9.3: In Case III with $0 < \nu < \mathcal{D}$, if Conditions **C1-C3** and **CR1-CR3** are satisfied, then

$$\text{Rank}\left\{\mathcal{E}_m \dot{\Psi}_m(\vec{q}_j)\right\} = \text{Rank}\left\{\mathcal{E}_m\right\} = \text{Rank}\left\{\dot{\Psi}_m(\vec{q}_j)\right\} = \nu \quad \text{(K.1)}$$

for $j = 1 \cdots M$, and also

$$\mathcal{E}_m^+ \mathcal{E}_m = \dot{\Psi}_m(\vec{q}_j)\dot{\Psi}_m(\vec{q}_j)^+ \quad \text{(K.2)}$$

where

$$\mathcal{E}_m = \left[I - \bar{A}\bar{A}^+\right]\dot{A}_m \quad \text{(K.3)}$$

$$\bar{A} = \left[\dot{A}_0, \cdots, \dot{A}_{m-1}, \dot{A}_m T_m\right] \quad \text{(K.4)}$$

$$\dot{\Psi}_m(\vec{q}_j) = \left[\dot{\Gamma}_m(\vec{q}_j)\ ,\ \Gamma_m\right]\begin{bmatrix} I \\ -\Gamma^{-1}\dot{\Gamma}(\vec{q}_j) \end{bmatrix} \quad \text{(K.5)}$$

$$\Gamma = \begin{bmatrix} \Gamma_0 \\ \vdots \\ \Gamma_{m-1} \\ T_m\Gamma_m \end{bmatrix} \bar{n}_{\{0,\cdots m\}} \times M, \qquad \dot{\Gamma}(\vec{q}) = \begin{bmatrix} \dot{\Gamma}_0(\vec{q}) \\ \vdots \\ \dot{\Gamma}_{m-1}(\vec{q}) \\ T_m\dot{\Gamma}_m(\vec{q}) \end{bmatrix} \bar{n}_{\{0,\cdots m\}} \times \mathcal{D} \quad \text{(K.6)}$$

$$T_m = \Gamma_m P_{[\Gamma_0^h,\cdots\Gamma_{m-1}^h]}\left(\Gamma_m P_{[\Gamma_0^h,\cdots\Gamma_{m-1}^h]}\right)^+ \quad \text{(K.7)}$$

$$\nu \;=\; \bar{n}_{\{0,\cdots m\}} - M \;<\; \mathcal{D} \tag{K.8}$$

Proof: For scenarios with non-degenerate CR bounds, reference to Condition **C3** shows that

$$\text{Rank}\{P_{[\dot{A}_0,\cdots\dot{A}_{m-1}]}\,\dot{A}_m\Gamma_m\,P_{[\Gamma_0^h,\cdots,\Gamma_{m-1}^h]}\} \;=\; M - \bar{n}_{\{0\cdots m-1\}} \tag{K.9}$$

and reference to Condition **CR2** for $p = \chi - 1$ and $\chi = m+1$ for Case III shows that

$$\text{Rank}\{P_{[\dot{A}_0,\cdots\dot{A}_{m-1}]}\,\dot{A}_m\Gamma'_m(\vec{q}_j)\,P_{[\Gamma'_0(\vec{q}_j)^h,\cdots,\Gamma'_{m-1}(\vec{q}_j)^h]}\} \;=\; \bar{n}_m \tag{K.10}$$

for $j = 1\cdots M$, where

$$\Gamma'_p(\vec{q}_j) \;=\; \left[\dot{\Gamma}_p(\vec{q}_j)\;,\;\Gamma_p\right] \tag{K.11}$$

We first show that (K.1) can be inferred from (K.9) and (K.10). Specifically, a development parallel to that of (J.11)-(J.25) in Appendix J gives

$$\text{Rank}\{\mathcal{E}_m\,\dot{\Psi}_m(\vec{q}_j)\} \;\geq\; \nu \tag{K.12}$$

Recall from (9.25) that

$$T_m\dot{\Psi}_m(\vec{q}_j) \;=\; 0 \tag{K.13}$$

and from (9.11) that

$$\text{Rank}\{T_m\} \;=\; M - \bar{n}_{\{0,\cdots m-1\}} \tag{K.14}$$

Thus the column nullspace of $\dot{\Psi}_m(\vec{q}_j)$ is at least of rank $M - \bar{n}_{\{0,\cdots m-1\}}$, and the maximum rank of $\dot{\Psi}_m(\vec{q}_j)$ is

$$\text{Rank}\{\dot{\Psi}_m(\vec{q}_j)\} \;\leq\; \bar{n}_m - (M - \bar{n}_{\{0,\cdots m\}}) \;=\; \nu \tag{K.15}$$

Similarly, we note that

$$\mathcal{E}_m T_m \;=\; \left[I - \bar{A}\bar{A}^+\right] \dot{A}_m T_m \;=\; 0 \tag{K.16}$$

since $\dot{A}_m T_m$ is contained in the column space of $\bar{A}$. By argument parallel to (K.14)-(K.15), the maximum rank of $\mathcal{E}_m$ is

$$\text{Rank}\,\{\mathcal{E}_m\} \;\leq\; \nu \tag{K.17}$$

Assertion (K.1) follows from (K.12) and (K.15), (K.17).

To show assertion (K.2), we note from (K.13), (K.16) and (K.14) that

$$(I - T_m)\dot{\Psi}_m(\vec{q}_j) \;=\; \dot{\Psi}_m(\vec{q}_j) \tag{K.18}$$

$$\mathcal{E}_m(I - T_m) \;=\; \mathcal{E}_m \tag{K.19}$$

$$\text{Rank}\{(I - T_m)\} \;\leq\; \bar{n}_m - (M - \bar{n}_{\{0,\cdots m\}}) \;=\; \nu \tag{K.20}$$

Since $(I - T_m)$ is a prefactor of $\dot{\Psi}(\vec{q}_j)$ in (K.18), and a post factor of $\mathcal{E}_m$ in (K.19), and the rank of $(I - T_m)$ equals that of $\dot{\Psi}(\vec{q}_j)$ and of $\mathcal{E}_m$ by Assertion (K.1) and (K.19), it must be that $(I - T_m)$ spans the column space of $\dot{\Psi}_m(\vec{q}_j)$ and the row space of $\mathcal{E}_m$. That is,

$$I - T_m \;=\; \mathcal{E}_m^+ \mathcal{E}_m \;=\; \dot{\Psi}_m(\vec{q}_j)\dot{\Psi}_m(\vec{q}_j)^+ \tag{K.21}$$

which establishes Assertion (K.2).

Appendix L

Proof of Lemma 9.4

This appendix establishes the result:

Lemma 9.4: Let G be a $M\mathcal{D} \times M\mathcal{D}$ matrix of the form

$$G = \mathrm{Re}\left\{\left([\Phi_1, \cdots, \Phi_M]^h [\Phi_1, \cdots, \Phi_M]\right) \odot \hat{P}_+^t\right\} \tag{L.1}$$

If Φ_j has full rank ($= \mathcal{D}$) for $j = 1 \cdots M$, and $\hat{P}$ is Hermitian positive definite, then G is Hermitian positive definite. That is

$$\mathrm{Rank}\{G\} = M\mathcal{D} \tag{L.2}$$

Since $\hat{P}$ is positive definite, it can be decomposed as

$$\begin{aligned} \hat{P} &= \Pi\Pi^h \\ &= \vec{\pi}_1\vec{\pi}_1^h + \vec{\pi}_2\vec{\pi}_2^h + \cdots \vec{\pi}_M\vec{\pi}_M^h \end{aligned} \tag{L.3}$$

where

$$\Pi = [\vec{\pi}_1, \vec{\pi}_2, \cdots \vec{\pi}_M] \tag{L.4}$$

is non-singular.

Since G is real, to show that G is positive definite it suffices to show that

$$\vec{v}^t G \vec{v} > 0 \tag{L.5}$$

for all *real* $\vec{v} \neq 0$. Thus let $\vec{v}$ be real, and partition $\vec{v}$ into $\mathcal{D} \times 1$ subvectors as follows

$$\vec{v} = \begin{bmatrix} \vec{v}_1 \\ \vdots \\ \vec{v}_M \end{bmatrix} \tag{L.6}$$

Formation of the product $\vec{v}^t G \vec{v}$ using (L.3) and (L.6), and simplification gives

$$\vec{v}^t G \vec{v} = \sum_{i=1}^{M} \|\vec{u}_i\|^2 \tag{L.7}$$

where

$$\vec{u}_i = Y \vec{\pi}_i \tag{L.8}$$

$i = 1 \cdots M$, and

$$Y = [\vec{y}_1, \cdots \vec{y}_M] \tag{L.9}$$

$$\vec{y}_j = \Phi_j \vec{v}_j \tag{L.10}$$

for $j = 1 \cdots M$.

It follows from (L.7), (L.8) that

$$\vec{v}^t G \vec{v} \geq 0 \tag{L.11}$$

with equality iff

$$\vec{u}_i = Y \vec{\pi}_i = 0 \tag{L.12}$$

for $i = 1 \cdots M$, or equivalently iff

$$Y\Pi \;=\; 0 \tag{L.13}$$

Since Π is non-singular, this requires

$$Y = 0 \tag{L.14}$$

or equivalently

$$\vec{y}_j \;=\; \Phi_j \vec{v}_j \;=\; 0 \tag{L.15}$$

for all $j = 1 \cdots M$. But since Φ_j have full rank by hypothesis, condition (L.12) requires

$$\vec{v}_j \;=\; 0 \tag{L.16}$$

for $j = 1 \cdots M$. Therefore (L.11) is satisfied with equality iff $\vec{v} = 0$. It follows that G is positive definite.

The Hermitian property of G is trivially verified by inspection of (L.1).

Appendix M

Proof of Lemma 9.5

This appendix establishes the result:

Lemma 9.5: Let

$$G \;=\; \mathrm{Re}\Big\{\Big([\Phi_1,\,\cdots\,,\,\Phi_M]^h\,[\Phi_1,\,\cdots\,,\,\Phi_M]\Big)\odot\hat{P}_+^t\Big\} \qquad \text{(M.1)}$$

If Φ_j has partial rank r ($<\mathcal{D}$) for each $j=1\cdots M$, and $\hat{P}$ is Hermitian positive definite, then G is Hermitian non-negative definite with

$$\mathrm{Rank}\{G\} \;=\; M\cdot r \qquad \text{(M.2)}$$

The result (M.2) can be extracted from the proof of Lemma 9.4 as follows. Specifically, the requirement (L.15) is

$$\Phi_j\vec{v}_j \;=\; 0 \qquad \text{(M.3)}$$

for all $j=1\cdots M$. If Φ_j has partial rank r, then there exist $\mathcal{D}-r$ linearly independent real $\vec{v}\neq 0$ which satisfy (M.3). Additionally there exist $M(\mathcal{D}-r)$ linearly independent real $\vec{v}\neq 0$ for which (L.11) is satisfied with equality. It follows that G has rank deficiency of $M(\mathcal{D}-r)$, or has rank

$$\mathrm{Rank}\{G\} \;=\; M\mathcal{D}-M(\mathcal{D}-r) \;=\; M\cdot r \qquad \text{(M.4)}$$

where $M\mathcal{D}$ is the dimension of G.

The Hermitian property of G is trivially verified by inspection of (M.1).

Appendix N

Proof of Property PI2

This appendix derives the result:

PI2. Let

$$G(\delta\omega) = X(\delta\omega) + \delta\omega^2\, Y(\delta\omega) \qquad (L \times L) \qquad \text{(N.1)}$$

where $X(\delta\omega)$, $Y(\delta\omega)$ are non-negative Hermitian matrices having Taylor series valid in the neighborhood of $\delta\omega = 0$. Assume that

1) $X(\delta\omega)$ has constant rank $\mathcal{R}$ for sufficiently small $\delta\omega$, including $\delta\omega = 0$, and

2) the matrix $G(\delta\omega)$ has full rank for sufficiently small $\delta\omega$.

Then for small $\delta\omega$,

$$\begin{aligned} G(\delta\omega)^{-1} &= \delta\omega^{-2} W(\delta\omega)^{+} + \left[I - W(\delta\omega)^{+} Y(\delta\omega)\right] X(\delta\omega)^{+} \left[I - Y(\delta\omega) W(\delta\omega)^{+}\right] \\ &\quad + \mathcal{O}\{\delta\omega^2\} \end{aligned} \qquad \text{(N.2)}$$

where

$$W(\delta\omega) = P_{[X(\delta\omega)]} Y(\delta\omega) P_{[X(\delta\omega)]} \qquad \text{(N.3)}$$

$$P_{[X(\delta\omega)]} = I - X(\delta\omega) X(\delta\omega)^{+} \qquad \text{(N.4)}$$

Proof: This appendix uses the shorthands G, X, Y and W for $G(\delta\omega)$, $X(\delta\omega)$, $Y(\delta\omega)$ and $W(\delta\omega)$.

As a first step, let the eigendecomposition of X be denoted

$$X = E_1 \Lambda E_1^h \tag{N.5}$$

where Λ is an $\mathcal{R} \times \mathcal{R}$ diagonal matrix of positive eigenvalues, E_1 is a $L \times \mathcal{R}$ matrix of corresponding eigenvectors, and both E_1 and Λ depend upon $\delta\omega$ and have a Taylor series in $\delta\omega$.

Consider the matrix

$$\Theta = E^h G E \tag{N.6}$$

where E is a unitary matrix of the form

$$E = [E_1, E_2] \tag{N.7}$$

then

$$G^{-1} = E \Theta^{-1} E^h \tag{N.8}$$

Partition Θ in (N.6) conformally with E in (N.7) as follows

$$\Theta = \begin{bmatrix} \Theta_{11} & \Theta_{12} \\ \Theta_{21} & \Theta_{22} \end{bmatrix} \tag{N.9}$$

with

$$\begin{aligned} \Theta_{11} &= \Lambda + \delta\omega^2 E_1^h Y E_1 \quad , \quad \Theta_{12} = \delta\omega^2 E_1^h Y E_2 \\ \Theta_{21} &= \delta\omega^2 E_2^h Y E_1 \quad , \quad \Theta_{22} = \delta\omega^2 E_2^h Y E_2 \end{aligned} \tag{N.10}$$

Sub-matrix Θ_{11} is $\mathcal{R} \times \mathcal{R}$ and has full rank since Λ is full rank $\mathcal{R}$ and the rank of Θ_{11} is not reduced by the $\mathcal{O}(\delta\omega^2)$ additive term, for sufficiently small $\delta\omega$. Sub-matrix

Θ_{22} is $(L-\mathcal{R}) \times (L-\mathcal{R})$ and likewise has full rank as follows. By construction, the rank of Θ_{22} equals that of the component of the column space of Hermitian matrix Y that is orthogonal to the column space of X. Since by assumption matrix G is full for sufficiently small $\delta\omega$, and column space of Y must have a component of rank $L-\mathcal{R}$ that is orthogonal to the column space of X.

Straightforward calculation shows that

$$\Theta^{-1} = \begin{bmatrix} \left[\Theta_{11} - \Theta_{12}\Theta_{22}^{-1}\Theta_{21}\right]^{-1} & -\left[\Theta_{11} - \Theta_{12}\Theta_{22}^{-1}\Theta_{21}\right]^{-1}\Theta_{12}\Theta_{22}^{-1} \\ -\left[\Theta_{22} - \Theta_{21}\Theta_{11}^{-1}\Theta_{12}\right]^{-1}\Theta_{21}\Theta_{11}^{-1} & \left[\Theta_{22} - \Theta_{21}\Theta_{11}^{-1}\Theta_{12}\right]^{-1} \end{bmatrix} \tag{N.11}$$

Substitution of (N.11) in (N.8) and use of (N.7) gives

$$G^{-1} = T_{11} + T_{12} + T_{21} + T_{22} \tag{N.12}$$

where

$$\begin{aligned} T_{11} &= E_1\left[\Theta_{11} - \Theta_{12}\Theta_{22}^{-1}\Theta_{21}\right]^{-1}E_1^h \\ T_{12} &= -E_1\left[\Theta_{11} - \Theta_{12}\Theta_{22}^{-1}\Theta_{21}\right]^{-1}\Theta_{12}\Theta_{22}^{-1}E_2^h \\ T_{21} &= -E_2\left[\Theta_{22} - \Theta_{21}\Theta_{11}^{-1}\Theta_{12}\right]^{-1}\Theta_{21}\Theta_{11}^{-1}E_1^h \\ T_{22} &= E_2\left[\Theta_{22} - \Theta_{21}\Theta_{11}^{-1}\Theta_{12}\right]^{-1}E_2^h \end{aligned} \tag{N.13}$$

Substitution of (N.10) in (N.13) and simplification gives

$$\begin{aligned} T_{11} &= E_1\left[\Lambda^{-1} + \mathcal{O}\{\delta\omega^2\}\right]E_1^h \\ &= X^+ + \mathcal{O}\{\delta\omega^2\} \qquad \text{(N.14)} \\ T_{12} &= -E_1\left[\Lambda^{-1} + \mathcal{O}\{\delta\omega^2\}\right]E_1^h Y E_2\left[E_2^h Y E_2\right]^{-1}E_2^h \\ &= -X^+ Y W^+ + \mathcal{O}\{\delta\omega^2\} \qquad \text{(N.15)} \\ T_{21} &= -E_2\left[E_2^h Y E_2 + \mathcal{O}\{\delta\omega^2\}\right]^{-1}E_2^h Y E_1\left[\Lambda^{-1} + \mathcal{O}\{\delta\omega^2\}\right]E_1^h \\ &= -W^+ Y X^+ + \mathcal{O}\{\delta\omega^2\} \qquad \text{(N.16)} \end{aligned}$$

$$
\begin{aligned}
T_{22} &= \delta\omega^{-2} E_2 \left[E_2^h Y E_2 - \delta\omega^2 E_2^h Y E_1 \left[\Lambda^{-1} + \mathcal{O}\{\delta\omega^2\} \right] E_1^h Y E_2 \right]^{-1} E_2^h \\
&= \delta\omega^{-2} E_2 \left(E_2^h Y E_2 \right)^{-1/2} \Big[I - \delta\omega^2 \left(E_2^h Y E_2 \right)^{-1/2} E_2^h Y E_1 \left[\Lambda^{-1} + \mathcal{O}\{\delta\omega^2\} \right] \\
&\qquad \cdot E_1^h Y E_2 \left(E_2^h Y E_2 \right)^{-1/2} \Big]^{-1} \left(E_2^h Y E_2 \right)^{-1/2} E_2^h \\
&= \delta\omega^{-2} E_2 \left(E_2^h Y E_2 \right)^{-1/2} \Big[I + \delta\omega^2 \left(E_2^h Y E_2 \right)^{-1/2} E_2^h Y E_1 \left[\Lambda^{-1} + \mathcal{O}\{\delta\omega^2\} \right] \\
&\qquad \cdot E_1^h Y E_2 \left(E_2^h Y E_2 \right)^{-1/2} + \mathcal{O}\{\delta\omega^4\} \Big] \left(E_2^h Y E_2 \right)^{-1/2} E_2^h \\
&= \delta\omega^{-2} W^+ + W^+ Y X^+ Y W^+ + \mathcal{O}\{\delta\omega^2\} \qquad \text{(N.17)}
\end{aligned}
$$

Substitution of (N.14)-(N.17) into (N.12), and rearrangement gives (N.2).

Appendix O

Proof of Lemma 9.6

This appendix establishes the result:

Lemma 9.6: In Case III with $0 < \nu < \mathcal{D}$, if Conditions **C1-C3** and **CR1-CR3** are satisfied, then

$$\text{Rank}\left\{\mathcal{E}_{m+1}\dot{\Psi}_{m+1}(\vec{q}_j)P_{[\dot{\Psi}_m(\vec{q}_j)^t]}\right\} = \mathcal{D} - \nu \tag{O.1}$$

for small $\delta\omega$ and for $j = 1 \cdots M$, where

$$\mathcal{E}_{m+1} = \left[I - \dot{A}\dot{A}^+\right]\dot{A}_{m+1} \tag{O.2}$$

$$\dot{A} = \left[\dot{A}_0, \cdots, \dot{A}_{m-1}, \dot{A}_m\right] \tag{O.3}$$

$$\dot{\Psi}_m(\vec{q}_j) = \left[\dot{\Gamma}_m(\vec{q}_j)\ ,\ \Gamma_m\right]\begin{bmatrix} I \\ -\Gamma^{-1}\dot{\Gamma}(\vec{q}_j) \end{bmatrix} \tag{O.4}$$

$$\dot{\Psi}_{m+1}(\vec{q}_j) = \left[\dot{\Gamma}_{m+1}(\vec{q}_j)\ ,\ \Gamma_{m+1}\right]\begin{bmatrix} I \\ -\Gamma^{-1}\dot{\Gamma}(\vec{q}_j) \end{bmatrix} \tag{O.5}$$

$$\Gamma = \begin{bmatrix} \Gamma_0 \\ \vdots \\ \Gamma_{m-1} \\ T_m\Gamma_m \end{bmatrix} \bar{n}_{\{0,\cdots m\}} \times M, \qquad \dot{\Gamma}(\vec{q}) = \begin{bmatrix} \dot{\Gamma}_0(\vec{q}) \\ \vdots \\ \dot{\Gamma}_{m-1}(\vec{q}) \\ T_m\dot{\Gamma}_m(\vec{q}) \end{bmatrix} \bar{n}_{\{0,\cdots m\}} \times \mathcal{D} \tag{O.6}$$

$$T_m = \Gamma_m P_{[\Gamma_0^h,\cdots\Gamma_{m-1}^h]}\left(\Gamma_m P_{[\Gamma_0^h,\cdots\Gamma_{m-1}^h]}\right)^+ \tag{O.7}$$

$$\nu \;=\; \bar{n}_{\{0,\cdots m\}} - M \;<\; \mathcal{D} \tag{O.8}$$

Proof: For scenarios with non-degenerate CR bounds, reference to Condition **CR3** for Case III with $\chi = m+1$ shows that

$$\begin{aligned} \text{Rank}\{P_{[\dot{A}_0,\cdots\dot{A}_m]}\,\dot{A}_{m+1}\Gamma'_{m+1}(\vec{q}_j)\,P_{[\Gamma'_0(\vec{q}_j)^h,\cdots,\Gamma'_m(\vec{q}_j)^h]}\} &= M + \mathcal{D} - \bar{n}_{\{0,\cdots m\}} \\ &= \mathcal{D} - \nu \end{aligned} \tag{O.9}$$

where the last equality follows from (O.8).

We now show that (O.1) follows directly from (O.9). From (O.3) we note that

$$P_{[\dot{A}_0,\cdots\dot{A}_m]} \;=\; I - \dot{A}\dot{A}^+ \tag{O.10}$$

Substitution in (O.9), and use of (O.2) gives

$$\text{Rank}\left\{\mathcal{E}_{m+1}\Gamma'_{m+1}(\vec{q}_j)\,P_{[\Gamma'_0(\vec{q}_j)^h,\cdots,\Gamma'_m(\vec{q}_j)^h]}\right\} \;=\; \mathcal{D} - \nu \tag{O.11}$$

Further rearrangement shows that

$$\text{Rank}\left\{\mathcal{E}_{m+1}\Gamma'_{m+1}(\vec{q}_j)\,P_{[\Gamma'_0(\vec{q}_j)^h,\cdots,\Gamma'_m(\vec{q}_j)^h]}\right\} = \text{Rank}\left\{\mathcal{E}_{m+1}\dot{\Psi}_{m+1}(\vec{q}_j)P_{[\dot{\Psi}_m(\vec{q}_j)^t]}\right\} \tag{O.12}$$

Assertion (O.1) of the lemma is established by substitution of (O.12) in (O.11).

Bibliography

[1] Burg, J.P., "Maximum Entropy Spectral Analysis", Proc. 37th Annual Meeting of the Society of Exploration Geophysicists, Oklahoma City, Oct. 31, 1967.

[2] Capon, J., "High Resolution Frequency-Wavenumber Spectrum Analysis", *Proc. IEEE*, Vol.57, pp. 1408-1418, Aug. 1969.

[3] Reddi, S.S., "Multiple Source Location - A Digital Approach", *IEEE Trans. Aerosp. Electron. Syst. AES-15*, 1, pp. 95-105 Jan. 1979.

[4] Kumaresan, R. and Tufts, D.W., "Estimating the Angles of Arrival of Multiple Plane Waves", *IEEE Trans. Aerosp. Electron. Syst.*, Vol. AES-19, no. 1, pp. 134-139, Jan. 1983.

[5] Schmidt, R.O., "Multiple Emitter Location and Signal Parameter Estimation" *Proc. RADC Spectral Est. Workshop*, Grifiss AFB, NY, 1979.

[6] Gabriel, W., "Spectral analysis and adaptive array superresolution techniques", *IEEE Proceedings*; June 1980.

[7] Barabell, A.J., Capon, J., Delong, D.F., Johnson, J.R., and Senne, K., "Performance Comparison of Super Resolution Array Processing Algorithms", Technical Report TST-72, MIT Lincoln Laboratory, 1984.

[8] Kay, S.M., Marple, S.T., "Spectrum Analysis – A Modern Perspective", *Proc. of the IEEE*, Vol. 69, No. 11, Nov. 1981.

[9] Kaveh, M. and Barabell, A.J., "The Statistical Performance of the MUSIC and the Minimum-Norm Algorithms in Resolving Plane Waves in Noise," *IEEE Trans. ASSP,* ASSP-34, No. 2, pp. 331-341, 1986.

[10] Lee, H. and Wengrovitz, M. "Statistical Characterization of the MUSIC Null Spectrum" *IEEE Trans. ASSP,* ASSP-39, No. 6, pp. 1333-1347, June 1991.

[11] Lee, H.B., "The Cramér-Rao Bound on Frequency Estimates of Signals Closely Spaced in Frequency", *IEEE Trans. on SP*, June 1992.

[12] Lee, H.B., "Eigenvalues and Eigenvectors of Covariance Matrices for Signals Closely Spaced in Frequency", *IEEE Trans. on SP*, Oct. 1992.

[13] Lee, H.B. and Fu Li, "Quantification of the Difference between Detection and Resolution Thresholds for Multiple Closely-Spaced Emitters" *Proc. Sixth SSAP Workshop on Statistical Signal and Array Processing* Oct. 1992.

[14] Lee, H.B. and Wengrovitz, M., "Resolution threshold of beamspace MUSIC for two closely-spaced emitters", *IEEE Trans. on Acoust., Speech, Signal Processing*; Sept. 1990.

[15] Stoica, P. and Nehorai, A. "MUSIC, Maximum Likelihood, and Cramér-Rao Bound", *IEEE Trans. on Acoustics, Speech and Signal Processing*, Vol 37, no. 5, May 1989.

[16] Yau, S.F. and Bresler, Y. "A Compact Cramér-Rao Bound Expression for Parametric Estimation of Superimposed Signals" *IEEE Trans. on Signal Processing*, Vol 40, no. 5, May 1992.

[17] Kato, T., "A Short Introduction to Perturbation Theory for Linear Operators", Springer-Verlag, New York 1982.

[18] Coderch, M., Willsky, A.S., Sastry, S.S., Castanon, D., "Hierarchical Aggregation of Linear Systems with Multiple Time Scales", *Trans. on Automatic Control*, Vol. AC-28, No. 11, Nov. 1983.

[19] Wilkinson, J. H., "The Algebraic Eigenvalue Problem", New York: Oxford University Press, 1965.

[20] Van Trees, H. L., "Detection, Estimation and Modulation Theory", Part I, New York: Wiley 1968.

[21] Strang, G., "Linear Algebra and its Applications", Harcourt Brace Jovanovich, 1988.

[22] Akaike, H., "A New Look at the Statistical Model Identification", *IEEE Trans. Automat. Contr.,* Vol AC-19, pp.716-723, Dec. 1974.

[23] Rissanen, J., "A Universal Prior for Integers and Estimation by Minimum Descriptive Length". *Ann. Stat.,* Vol 11, no. 2, pp. 431-466, 1983.

[24] Jachner, J., Lee, H., "Eigenvalues and Eigenvectors of Covariance Matrices for Closely-Spaced Signals in Multi-Dimensional Direction Finding", *ICASSP-93*, April 1993.

[25] Jachner, J., Lee, H., "Cramér Rao Bounds on Direction Estimates for Closely Spaced Emitters in Multi-Dimensional Applications", *ICASSP-92*, Vol II, pp 513-516, March 1992.